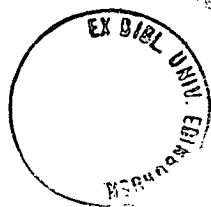


**Glacial dynamics  
of the Fennoscandian Ice Sheet:  
a remote-sensing study**

**Pieter Dongelmans**

**PhD  
The University of Edinburgh  
1996**



Amsterdam, 1 December 1996

Hereby I declare that all the work presented in thesis is my own.

Pieter Dongelmans

## Contents

### List of figures and tables

### Acknowledgements

**Abstract** 1

<b>Chapter 1</b>	<b>Introduction</b>	
	1.1 Objective	3
	1.2 Use of remote sensing in ice-sheet reconstruction	5
	1.3 Organisation of this thesis	7
<b>Chapter 2</b>	<b>Geology, glacial stratigraphy and deglaciation history of Fennoscandia</b>	
	2.1 Geology and topography of northwest Europe	9
	2.1.1 Geology	9
	2.1.2 Topography	13
	2.2 Weichselian glacial stratigraphy	16
	2.2.1 Finland	18
	2.2.2 Norway	21
	2.2.3 Sweden	22
	2.2.4 Problems associated with stratigraphic correlation and interpretation	24
	2.3 Deglaciation and palaeo-geographic reconstructions	26
	2.3.1 Introduction	26
	2.3.2 Relative sea-level data	28
	2.3.3 Palaeo-geographic reconstructions	31
<b>Chapter 3</b>	<b>Remote sensing and geomorphology</b>	
	3.1 Introduction	44
	3.2 Spectral sensitivity of different remote-sensing systems	44
	3.3 Resolution versus Instantaneous Working Area	46
	3.4 Imagery used	48
<b>Chapter 4</b>	<b>Subglacial streamlined bedforms</b>	
	4.1 Introduction	59
	4.2 Subglacial processes	63
	4.3 Superimposed linear bedforms	66
<b>Chapter 5</b>	<b>Methodology and case studies</b>	
	5.1 Introduction	71
	5.2 Methodology	71
	5.3 Case studies	74
	5.3.1 Introduction	74
	5.3.2 Sheet F4	76
	5.3.3 Sheet F6	81
	5.3.4 Sheet F13b	84
	5.3.5 Sheet F15	87
	5.3.6 Sheet F19	90

<b>Chapter 6</b>	<b>Reconstruction of ice-flow patterns in Fennoscandia using remotely sensed lineation data</b>	
6.1	Introduction	93
6.2	Southern Baltic Lowlands	96
6.3	Central and south Sweden	100
	6.3.1 Introduction	100
	6.3.2 Deglaciation flow patterns of central and south Sweden	100
	6.3.3 Ice-flow patterns prior to 13 ka BP	105
	6.3.4 Deglaciation of central and north Sweden	106
	6.3.5 Summary	108
6.4	Central and south Finland and Russian Karelia	109
	6.4.1 Introduction	109
	6.4.2 Deglaciation flow systems	112
	6.4.3 Quantitative analysis of lineations	115
	6.4.4 Summary	118
6.5	North Scandinavia	119
	6.5.1 Introduction	119
	6.5.2 Deglaciation flow systems	122
	6.5.3 Pre-glacial weathered bedrock	125
6.6	Comparison of different palaeo- ice-flow indicators	126
	6.6.1 Introduction	126
	6.6.2 Striae and till-fabric data compared to lineation data	128
	6.6.3 Interpretation	132
	6.6.4 Summary	139
<b>Chapter 7</b>	<b>Advance phase flow</b>	
7.1	Introduction	140
7.2	Pre-deglaciation flow patterns	141
7.3	Initiation and growth	144
	7.3.1 North Scandinavia	144
	7.3.2 South Scandinavia	146
7.4	Summary	147
<b>Chapter 8</b>	<b>Ice-sheet dynamics</b>	
8.1	Introduction	149
8.2	Glaciological theory and ice-sheet reconstruction	150
8.3	Modern ice streams	152
8.4	Fennoscandian ice streams	153
	8.4.1 Topographically controlled ice streams	155
	8.4.2 Non-topographically controlled ice streams	157
8.5	Reconstruction of deglaciation flow dynamics	164
<b>Chapter 9</b>	<b>Conclusions and future perspective</b>	
9.1	Conclusions	173
9.2	Future perspective	177

<b>Appendix A</b>	<b>Isostasy and relative sea level</b>	178
A.1	Introduction	179
A.2	Reconstruction of relative-sea-level history: methods and problems	180
A.3	The earth's response to changes in surface loading	183
	A.3.1 Different components of response	183
	A.3.2 Zonal distribution of response	186
A.4	Relative-sea-level curves used in this study	188
<b>Appendix B</b>	<b>First- and second-order interpretations of Landsat MSS images</b>	197
	<b>References</b>	232

## List of figures and tables

### Figures

Chapter 2		
2.1	Location map of Northwest Europe	10
2.2	Geological map of Northwest Europe	11
2.3	Geological map of Fennoscandia	11
2.4	Contour map of Northwest Europe	14
2.5	Bathymetric map of Northwest Europe	14
2.6	Flow stage II, Finland	19
2.7	Flow stage III, Finland	19
2.8	Location map of stratigraphic sites	25
2.9	Proposed glaciation curve for Weichselian in Fennoscandia	25
2.10	Ice-recession lines in Fennoscandia	27
2.11	Location map of relative sea-level curves	29
2.12	RSL curves of Oslo, South Vestfold and Kragero	30
2.13	RSL curves of Stette, Sula, Leinøy and Borgundvåg	30
2.14	RSL curves of Kiel and Groningen	32
2.15	RSL curve of Helsinki area	32
2.16	Geographic reconstruction and uplift pattern of Northwest Europe at 12,000 yr BP.	34
2.17	Geographic reconstruction and uplift pattern of Northwest Europe at 10,500 yr BP.	35
2.18	Geographic reconstruction and uplift pattern of Northwest Europe at 10,000 yr BP.	36
2.19	Geographic reconstruction and uplift pattern of Northwest Europe at 9,500 yr BP.	37
2.20	Geographic reconstruction and uplift pattern of Northwest Europe at 9,000 yr BP.	38
2.21	Geographic reconstruction and uplift pattern of Northwest Europe at 7,000 yr BP.	39
Chapter 3		
3.1	Spectral sensitivity of remote-sensing systems	45
3.2	Reflectance characteristics of earth-surface materials	45
3.3	Comparison of the resolution and areal coverage of remote-sensing systems with the dimensions of glacially streamlined landforms	47
3.4	Remote-sensing imagery used in this study	49
3.5	Locations of Landsat MSS and TM images in Finland	50
3.6	Locations of images shown in Figs 3.7- 3.11, 4.2 and 4.3	51
3.7a,b	Landsat mosaic of north Scandinavia and enlarged area	53
3.8a,b	Landsat TM image and enlarged area	54
3.9a,b	Detail of Landsat TM image and enlarged area	55
3.10a,b	Landsat MSS image of north Norway and enlarged area	57
3.11a,b	Landsat MSS image of central Finland and enlarged area	58

<b>Chapter 4</b>		
4.1	Different types of drumlins	62
4.2	The Kuusamo drumlin field	68
4.3	Aerial photograph of fluted moraine surface and drumlins at Utsjoki	69
<b>Chapter 5</b>		
5.1	Cartoon of the interpretation of flow patterns from lineation data	72
5.2	Cartoon of large-scale organisation of flow systems	72
5.3	Cartoon of lineation pattern produced by a retreating fan	72
5.4	Legend used for interpretation of satellite images	75
5.5a,b	Satellite image (sheet F4) and first-order interpretation	77
5.6a,b	Interpretation of glacial linear features and ice-flow directions (sheet F4)	78
5.7a,b	Satellite image (sheet F6) and first-order interpretation	82
5.8a,b	Interpretation of glacial linear features and ice-flow directions (sheet F6)	83
5.9a,b	Satellite image (sheet F13b) and first-order interpretation	85
5.10a,b	Interpretation of glacial linear features and ice-flow directions (sheet F13b)	86
5.11a,b	Satellite image (sheet F15) and first-order interpretation	88
5.12a,b	Interpretation of glacial linear features and ice-flow directions (sheet F15)	89
5.13a,b	Satellite image (sheet F19) and first-order interpretation	91
5.14a,b	Interpretation of glacial linear features and ice-flow directions (sheet F19)	92
<b>Chapter 6</b>		
6.1	Isochrons of ice margin retreat during deglaciation	94
6.2	Simplified lineation map of Scandinavia	95
6.3	Weichselian flow stages in Denmark and south Sweden	97
6.4	Late Weichselian flow stages south of the Baltic Sea	99
6.5	Lineation map of central and south Sweden	101
6.6a-d	Interpreted flow stages in central and south Sweden	102
6.6e-h	Interpreted flow stages in central and south Sweden	103
6.7	Lineation map and ice-flow directions in north Sweden	107
6.8	Simplified lineation map of Finland and Russian Karelia	110
6.9	Deglaciation and associated ice-flow patterns in Finland and Russian Karelia	111
6.10a	Spatial distribution of deglaciation lineations in central and south Finland	116
6.10b	Percentage of pre-deglaciation lineations on total number of lineations in central and south Finland.	116
6.11	Lineation map of north Scandinavia	120
6.12	Deglaciation and associated ice-flow patterns of north Scandinavia	121
6.13	Bathymetry of the Barents Sea	123
6.14	Striae measurements in north Scandinavia	129
6.15	Till-fabric measurements in north Scandinavia	130
6.16	Striae measurements in north Scandinavia, younger flow directions	133
6.17	Till-fabric measurements in north Scandinavia, younger flow directions	134
6.18	Dominant deglaciation ice-flow directions in north Scandinavia (lineations)	135

6.19	Striae measurements in north Scandinavia, older flow directions	136
6.20	Till-fabric measurements in north Scandinavia, older flow directions	137
6.21	Dominant pre-deglaciation ice-flow directions in north Scandinavia (lineations)	138
<b>Chapter 7</b>		
7.1	Simplified pre-deglaciation lineation map of Scandinavia	142
7.2	Positions of the ice margin during growth phase	145
<b>Chapter 8</b>		
8.1	Centre lines of ice streams during deglaciation of the Late Weichselian Fennoscandian Ice Sheet	154
8.2	Eskers and fluvio-glacial deposits in Finland	159
8.3	Cartoon of flow geometry in ice-stream/interstream system	162
8.4	Reconstruction of ice-flow dynamics at 11 ka BP	165
8.5	Reconstruction of ice-flow dynamics at 10 ka BP	166
8.6	Reconstruction of ice-flow dynamics at 9.5 ka BP	167
8.7	Spatial patterns of deglaciation and pre-deglaciation lineations in Scandinavia	171
<b>Appendix A</b>		
A.1	Eustatic sea-level curves	184
A.2	Zonal distribution of sea-level response	184

### **Tables**

<b>Chapter 2</b>		
2.1	Chronostratigraphic correlations	17
<b>Chapter 3</b>		
3.1	Areal coverage and resolution of several remote-sensing systems	47
3.2	Dimensions of glacially streamlined landforms	47
<b>Chapter 4</b>		
4.1	Classification of morainic landforms	60

## **Acknowledgements**

I would like to thank sincerely all the people that have helped me with my work on this thesis, through their assistance and encouragement.

I am especially grateful to Mikko Punkari who provided me with satellite images of Finland without which this study could not have been done. The discussions we had on the development of the Fennoscandian Ice Sheet were very stimulating and were crucial for the development of my ideas.

Also I would like to thank Tony Payne with whom I shared an office for several years. The discussions we had on ice-sheet modelling were enlightening. He is also thanked for critically reading my thesis and for his friendship over these years.

I am grateful to Geoffrey Boulton, my supervisor, who gave me the possibility to work and live in Edinburgh.

The many heated discussions I had with Dan Praeg are fondly remembered, he is also thanked for reading my thesis. Johan Kleman was very important in helping to start my research. I enjoyed the co-operation with Marianne Broadgate in the analysis of lineation data using GIS. I also want to thank Ned Pegler for digitising the lineation data.

Finally, I am indebted to Roos Bots for her support and patience during these years.

**Glacial dynamics of the Fennoscandian Ice Sheet:  
a remote-sensing study**

**P. Dongelmans**

**Abstract**

In this study, the extensive terrestrial record of glacial streamlined landforms in Fennoscandia is used to analyse and reconstruct the internal organisation of the Late Weichselian Scandinavian Ice Sheet and its evolution during the deglaciation.

Glacial lineations have been mapped over an ice-sheet-wide area using remote-sensing techniques. The remote-sensing systems used include Landsat mosaics, Landsat MSS and TM images and aerial photographs. Together they provide complete coverage of the Baltic Shield area. The analyses involve identification of coherent sets of lineations which can be linked to flow systems within the ice sheet. The presence of superimposed sets of glacial lineations makes it possible establish relative ages for different coherent lineation patterns. In a number of cases, absolute dating is possible because lineation patterns can be linked to dated positions of the ice margin.

The ice-sheet organisation in Fennoscandia was dominated by the presence of a number of ice streams. In many areas these zones of fast flow are to a large extent controlled by the presence of valleys and troughs. In the case of central and south Finland and Russian Karelia, however, a persistent system of ice streams/ice lobes developed which was not topographically controlled. The scale of these ice streams was at least an order of magnitude larger than the scale of the underlying topographic variations, both in vertical and horizontal dimensions. The regular distribution of these ice streams, their persistence during the Late Weichselian deglaciation and their independence of local topography and geology implies that they are the result of internal dynamic processes within the ice sheet and reflect the internal organisation of the ice sheet.

The landform distribution reflects these lateral variations in ice velocity. Ice-stream areas are dominated by streamlined bedforms, whereas in the interstream areas, hummocky fluvio-glacial deposition is more important. As a result of the limited ice activity in the interstream areas, landforms pre-dating deglaciation have been preserved here. During deglaciation diachronous, superimposed patterns of diverging glacial lineations developed in the ice stream areas.

During the later stages of deglaciation ice-stream activity diminished. As a result north Sweden, where the ice sheet remained longest, is dominated by landforms that are older than the Late Weichselian deglaciation and possibly reflect ice flow during the advance phase of the ice sheet.

## Chapter 1

### Introduction

#### 1.1 Objective

Many studies have been undertaken to reconstruct the flow dynamics of the former mid-latitude ice sheets from the landforms they left behind (*e.g.* Ljunger, 1949; Prest, 1969; Sugden, 1977; Boulton *et al.*, 1985, Dyke and Prest, 1987). The existence of extensive superimposed lineation patterns in North America (Boulton and Clark, 1990) and evidence of structural spatial variability in ice-sheet activity in Finland (Punkari, 1980, 1985) have shown that the organisation of ice sheets does not conform to the simple concentric pattern predicted by many numerical models (Sugden, 1977; Huybrechts and T'siobbel, 1995).

In recent years interest in modern and former ice sheets, and their effects on global climate and sea level has greatly increased. This interest focuses on the organisation of flow dynamics within ice sheets and the role that ice streams play (Shabtaie and Bentley, 1987; Alley *et al.*, 1987a,b; Huybrechts and Oerlemans, 1990). In Antarctica, the potential effects of future warming and sea-level change on the stability of the West Antarctic Ice Sheet and more specific the Siple Coast Ice Streams have attracted a lot of attention (Huybrechts and Oerlemans, 1990). The stability of the former mid-latitude ice sheets has also been questioned in recent years. In the North Atlantic, layers rich in ice-rafted carbonate detritus that were deposited during distinct periods between 65,000 and 14,000 years before present (BP) were identified by Heinrich (1988). These Heinrich layers are attributed to short-lived but massive influxes of icebergs from the Laurentide Ice Sheet. It has been suggested that the influx of meltwater could seriously disrupt North Atlantic ocean circulation and lead to a change in climate (Bond *et al.*, 1993). Age relations in this study refer to  $C^{14}$  years before present (BP), unless stated differently.

In this discussion the term "ice stream" is used to describe a zone in which ice-flow velocity is considerably higher than in normal sheet flow. The ice

streams have substantial upstream drainage areas and play an important role in the total mass transfer from accumulation area to ablation area. In Finland the ice streams fan out in the marginal area and form broad ice lobes which display radial flow patterns. Perpendicular to the ice-flow direction the size of the lobes can be up to 250 km. From snout to apex the length of a lobe can be 200/250 km. The term inter-lobate area refers to the area between two ice streams in the marginal zone. Interstream area refers to the entire zone between two ice streams, both in the accumulation zone and the ablation zone.

In the present study the extensive terrestrial record of glacial landforms in Fennoscandia is used to analyse and reconstruct the overall setting and internal organisation of the Late Weichselian Fennoscandian Ice Sheet and its evolution during deglaciation. A better knowledge of the dynamics of the Weichselian ice sheets leads to an increased understanding of landform organisation in formerly glaciated areas. It also helps to improve our insight into the complex ice sheet/climate interactions both in the past and the present.

Interaction between the Weichselian Ice Sheets and their subsurface has substantially reshaped the land surface of formerly glaciated areas. Glacial deposits and landforms dominate the surface topography to a very large extent (Sugden and John, 1976). Of the wide variety of glacial landforms that occur in these areas, subglacially streamlined landforms are of most interest to this study. Subglacially streamlined landforms exhibit a wide variety of shapes, sizes and internal composition. But, irrespective of these differences, most authors agree that the features share a number of important characteristics. Their long axes are parallel to the ice flow directions during their formation. They are the result of differential movement between the sole of the ice sheet and the subsurface. The last condition implies that subglacially streamlined bedforms develop only underneath warm and wet based ice (Menzies and Rose, 1987).

Formerly glaciated areas thus provide a time-integrated picture of the ice flow directions of former ice sheets. Successive ice-sheet geometries have left superimposed sets of landforms. This superimposition enables relative dating of individual lineations. In order to draw conclusions about the basal thermal

regime and the organisation of ice flow it is important to reconstruct ice-sheet dynamics during one period. In other words it is necessary to try and work out which lineations formed contemporaneously. The way this was done is to use dated positions of the ice margin and identify coherent lineation patterns that are related to these ice-marginal geometries.

The best way for mapping and analysing the palaeo- ice-flow record is by using remote sensing. This method enables a single person to study lineations on an ice-sheet-wide scale, and analyse them using clear and consistent criteria. The Scandinavian mountains were not included in the study because in that mountainous area ice flow is completely topographically controlled and the strong relief makes interpretation very difficult. The area studied was therefore restricted to the Baltic Shield. Sweden was covered by 1:1,000,000 Landsat mosaics and 1:150,000 aerial photographs of areas of specific interest. North Scandinavia, Finland and Russian Karelia were covered by 1:400,000 Landsat TM and MSS images.

## 1.2 Use of remote sensing in ice-sheet reconstruction

The reconstructions of the former mid-latitude ice sheets focus on two major topics. First, the pattern and timing of deglaciation and, second, the reconstruction and evolution of the ice-flow dynamics. To determine the first, ice-marginal deposits have been mapped and dated using radio-carbon methods or varve-chronology (Denton and Hughes, 1981; Lundqvist, 1986). The second is deduced from palaeo-ice-flow indicators such as drumlins, striae, till-fabrics and eskers (Glückert, 1974; Nordkalott Project, 1986).

Remote-sensing techniques offered a major improvement in the reconstruction of the flow dynamics of former ice sheets (Prest, 1969; Punkari, 1984). The possibility of mapping subglacial bedforms over large areas in a relatively short time has greatly improved our knowledge of the glacio-dynamic behaviour of ice sheets (Punkari, 1984, 1985; Boulton *et al.* 1985; Dyke and Prest, 1987; Boulton and Clark, 1990)

Punkari (1980, 1982) used satellite images to map lineations and glacio-fluvial landforms in Finland. He concluded that ice flow in Finland was dominated by large active ice lobes separated from each other by zones of slower moving ice. He concluded that the lineations in Finland formed time-transgressively during deglaciation.

Boulton *et al.* (1985) used satellite images and aerial photographs to establish a detailed reconstruction of the deglaciation and flow dynamics of the Fennoscandian and North American Ice Sheets. Lineations were assumed to have formed in a narrow marginal zone where the ice was at pressure melting. On the basis of this assumption they argued that the long axes of lineations were perpendicular to the ice-sheet margin and that therefore the lineations could be used to reconstruct the positions of the ice margin during deglaciation. In other words, they assumed that lineations always formed right at the ice margin.

Boulton & Clark (1990) interpreted the formation of lineations differently. Using satellite pictures, they recognised extensive sets of superimposed lineations in the Canadian Shield area. This led them to formulate a model in which successive ice-sheet geometries had produced ice-sheet-wide, coherent patterns of lineations which reflected contemporaneous ice-flow configurations. The entire ice sheet was thought to have a warm base and was believed to be active throughout. The changes of ice-sheet geometry (as reconstructed from the successive sets of lineations) were used to explain the movement of the major ice divides in response to climatic forcing.

The above shows that different remote-sensing studies of lineations have arrived at different conclusions with respect to ice-sheet behaviour. The main problem with the interpretation of lineations, and indeed all palaeo-ice-flow indicators on ice-sheet-wide scales, is the difficulty in considering both spatial and temporal variability of ice-sheet activity. Boulton *et al.* (1985) assumed a simple concentric ice-sheet model and argued that the lineation patterns found in Scandinavia formed time-transgressively. Boulton and Clark (1990), on the other hand, claimed that lineation patterns reflected contemporaneous ice-sheet-wide flow events. The time factor is reduced to a number of discrete

time steps in this case, the time-transgressive operation of processes is not considered.

Punkari presented different models of ice-sheet behaviour. In his 1980 and 1982 studies on Finland, local ice streaming was recognised, but flow patterns were assumed to have formed ice-sheet-wide. Moreover, lineations were considered to have formed during deglaciation, no older lineations were recognised. In his later work (1985, 1989) more emphasis was put on the relationship between the spatial variability of ice-sheet dynamics and its effect on the organisation of glacial landforms. He also emphasised the diachronous nature in which lineations were formed during retreat. In these later studies different palaeo-ice-flow indicators were used in combination with lineation data.

The present study builds on the ideas outlined in the studies mentioned above. The possibility of establishing relative ages from the intersection of lineations and the grouping of individual lineations into coherent flow patterns are central also to this study. However, an important extra tool is used here to relate the flow patterns to the dated positions of ice margins. This enables absolute dating of flow patterns. This helped to establish a detailed reconstruction of the ice-flow evolution and enabled spatial correlation of different flow patterns, which is necessary to describe flow dynamics on an ice-sheet-wide scale. The development of ice streaming over Finland and the time-transgressive nature of lineation formation, as was first suggested by Punkari (1980, 1985, 1989) is confirmed in the present study. The methodology used in the present study enables a more detailed reconstruction of the deglaciation ice-flow evolution. In addition the sometimes contrasting glacio-dynamic behaviour in different parts of the ice sheet can be explained because the entire Baltic Shield was studied.

### 1.3 Organisation of this thesis

Chapter 2 gives a description of the bedrock geology and glacial stratigraphy of Northwest Europe. In section 2.3 the changing pro-glacial environment during deglaciation is reconstructed using of relative-sea-level data. In Chapter 3, the available remote-sensing systems are described and their use for this

study is discussed. Chapter 4 lists the prerequisites for the development of streamlined landforms. The methods of satellite interpretation and analyses used in this study, are described in five case studies in Chapter 5.

The lineation patterns and interpreted ice-flow patterns are described in Chapter 6. The deglaciation flow in Scandinavia is discussed for separate regions: the southern Baltic Lowlands (section 6.2); central and south Sweden (section 6.3); central and south Finland and Russian Karelia (section 6.4); and finally north Scandinavia (section 6.5). The final section of this chapter (6.6) compares the lineation data used in this study with other palaeo-ice-flow indicators from north Finland and north Sweden (Nordkalott, 1986b). The contrasts between the conclusions concerning ice-sheet conditions reached in this study and those found in the literature are discussed. In Chapter 7, a possible advance phase flow pattern is described. Conclusions concerning ice-sheet dynamics and the role of ice streaming are discussed in Chapter 8. In Appendix A problems concerning the collection of relative-sea-level data and the global effects of crustal loading are discussed. Finally, all interpreted Landsat MSS images are included in Appendix B.

## Chapter 2

### **Geology, glacial stratigraphy and deglaciation history of Fennoscandia**

#### 2.1 Geology and topography of Northwest Europe

##### 2.1.1 Geology

Locations and areas referred to in the text of this thesis can be found in Fig. 2.1. Figure 2.2 shows a map of the geology of Northwest Europe. Geologically, Northwest Europe can be divided into two regions: Fennoscandia, (the Baltic Shield and the Scandinavian Caledonides) which consist mainly of metamorphic and plutonic rocks; and the fringing sedimentary areas to the south and east where the basement rocks are covered by thick, undisturbed, sedimentary sequences. The literature sources used in this section are: Simonen, 1980 "The Precambrian of Finland" ; Ager, 1980 "The Geology of Europe" ; and Ziegler, 1990 "Geological Atlas of Western and Central Europe".

##### *The Baltic Shield*

The Baltic Shield is the uplifted part of a wide basement area that dips towards the south and east, upon which the sediments of the North and East European platform have been deposited. To the west and the north, the shield area is bordered by the Paleozoic Caledonidic mountain chain. The bedrock of the Baltic Shield is formed by the strongly eroded and fractured remnants of successive Precambrian orogenic phases. The oldest part of the Shield area is the broad basement area in the east (see Fig. 2.3), which consists of the Saamides and Belomorides regions. The Belomoridic gneiss belt represents an area that underwent intense reworking and recrystallization during the younger Svecokarelidic orogeny.

The central area of the Baltic Shield consists of rocks formed during the Svecokarelidic orogeny. Geosynclinal belts developed into which turbidites and basalts with a total thickness of many kilometres were deposited. After the orogenic phase followed a long period of erosion and cratonization. Many generations of faulting, jointing and shearing produced a mosaic structure in

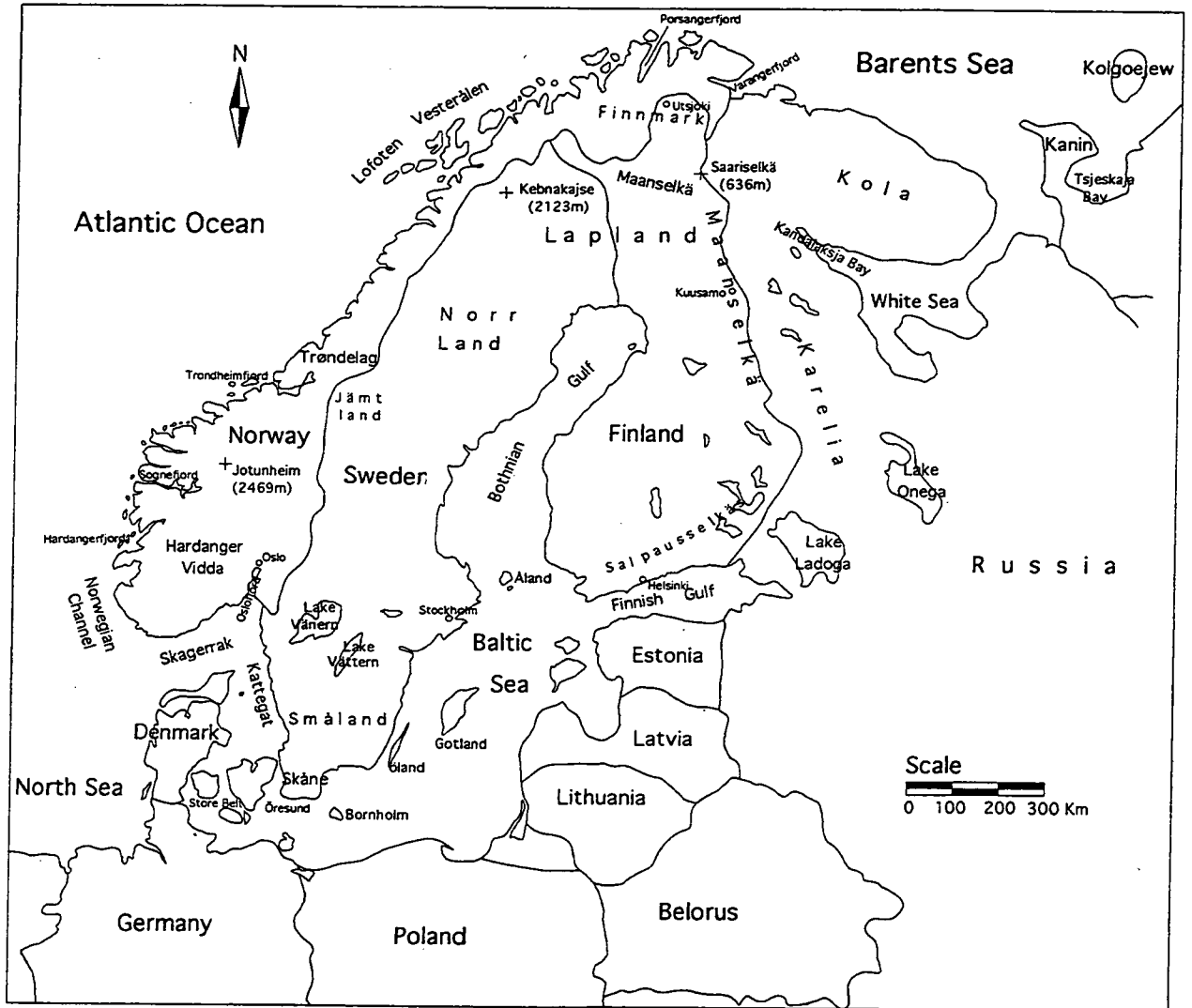


Fig. 2.1 Location map of Northwest Europe.

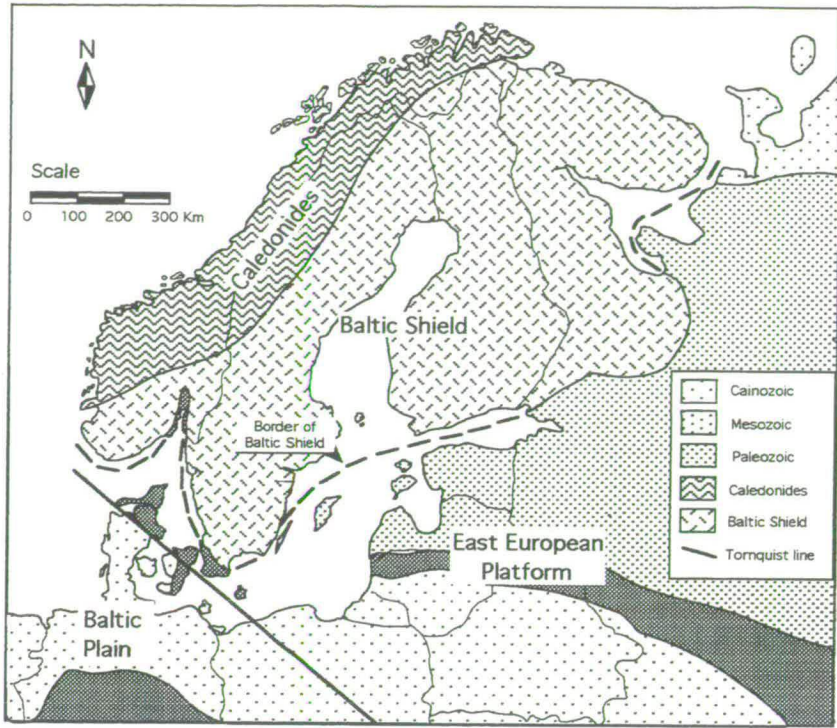


Fig. 2.2 Geological map of Northwest Europe (Modified from Ziegler, 1990).

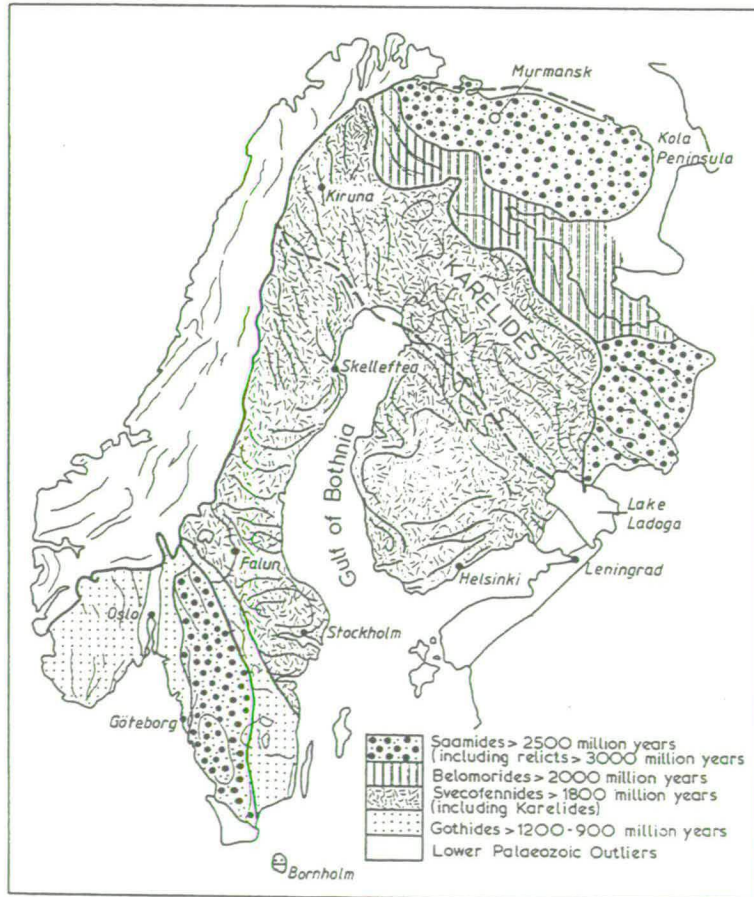


Fig. 2.3 Geological map of Fennoscandia. (From Ager, 1980).

the bedrock. Plutonic intrusions occurred on a large scale. Sedimentation over the Svecokarelidic crust continued, with interruptions, into the Paleozoic.

The Baltic Shield has undergone a long period of erosion. In combination with uplifting of the area this has led to the removal of most of the platform cover. Remnants of the Paleozoic platform cover of the Baltic Shield are present mainly in the southern part. They are preserved in graben-like structures formed during the Caledonian and Hercynian movements. Only in southernmost Sweden did sedimentation continue after the Paleozoic. On Skåne and the islands of Gotland and Öland, Cretaceous sediments, mainly chinks, were deposited. During the Alpine orogeny, the edges of the Baltic Shield in Norway and Finland were uplifted, while the central shield area subsided. As a consequence of these differential tectonic movements the Bothnian Gulf and the Baltic Sea were formed.

The Pleistocene glaciations have strongly modified the existing relief. As a result of glacial erosion pre-existing valleys became U-shaped. Most of the loose materials were removed from the mountains and the old peneplain. Bedrock became striated and polished and numerous roches moutonnées were formed. Tills, morainic and fluvial-glacial deposits are wide-spread in Fennoscandia and are by far the most important source of unconsolidated material. Upon deglaciation most of Finland, large areas of Sweden and some parts of Norway became submerged as a result of isostatic depression of the crust by the ice. Marine and lacustrine deposits are widespread in these formerly submerged areas.

### *Caledonides*

The Scandinavian Caledonides were formed during the Silurian by the Caledonian orogeny. The mountain chain contains two belts of Precambrian rocks, the Western Gneiss Complex, which are in part older than the Baltic Shield basement gneisses. Geosynclinal sedimentary and plutonic rocks, deposited from the Late Precambrian until the Silurian, also form an important part of the mountain chain. During the orogeny, large nappes were overthrust from west to east. The associated folding and thrusting metamorphosed most rocks.

### *The North European Plain*

The Baltic Shield is bordered to the east and south by unfolded, un-metamorphosed, epicontinental deposits of the East European Platform (see Fig. 2.2). After the Late Precambrian the East European Platform was no longer subjected to orogenic activity and the basement rock became covered by sediments. Most deposits are of Paleozoic age, but to the southwest sedimentation continued into the Cainozoic.

Southwest of the Baltic Shield lies the Baltic Plain, also an area of subsidence and sedimentation. It is separated from the East European Platform by the Tornquist line, south of which a Precambrian basement is not proven. To the south, the Baltic Plain is bordered by the Variscan massifs of the Ardennes, the Eifel, Schiefergebirge and Harz. To the west the subsidence area extends into the North Sea Basin. Subsidence of the Baltic Plain continues into the present and thick sequences of Tertiary and Quaternary age overlie Late Mesozoic sediments.

### 2.1.2 Topography

#### *Fennoscandia*

The Fennoscandian topography is dominated by the Caledonides mountain range which forms a barrier between the Baltic Shield and the Atlantic Ocean (Figs 2.4 and 2.5). The Caledonides form a continuous ridge from the Skagerrak in the south to Finnmark in the north. The highest areas are the Hardanger Vidda in south Norway (Jotunheimen, 2469m) and the Kebnekaise Group (Kebnekaise, 2123m ) in north Sweden. Wide U-shaped valleys and fjords have been cut into the mountain range by glacial erosion. The mountain range has a considerable effect on the precipitation distribution over Fennoscandia. On the western side of the Caledonides precipitation rates of 2000 mm/y are common, especially in south Norway. In middle and north Sweden and in Finland precipitation rates are in the order of 400-600 mm/y. North Finland is also mountainous. The highest peak of the Maanselkä mountains is the Pallastunturi (821 m). On the Kola peninsula more isolated peaks reach up to 1191 m (Chibiny Mountains). The Bothnian Gulf is thus

Fig. 2.4  
Contour map of  
Northwest Europe

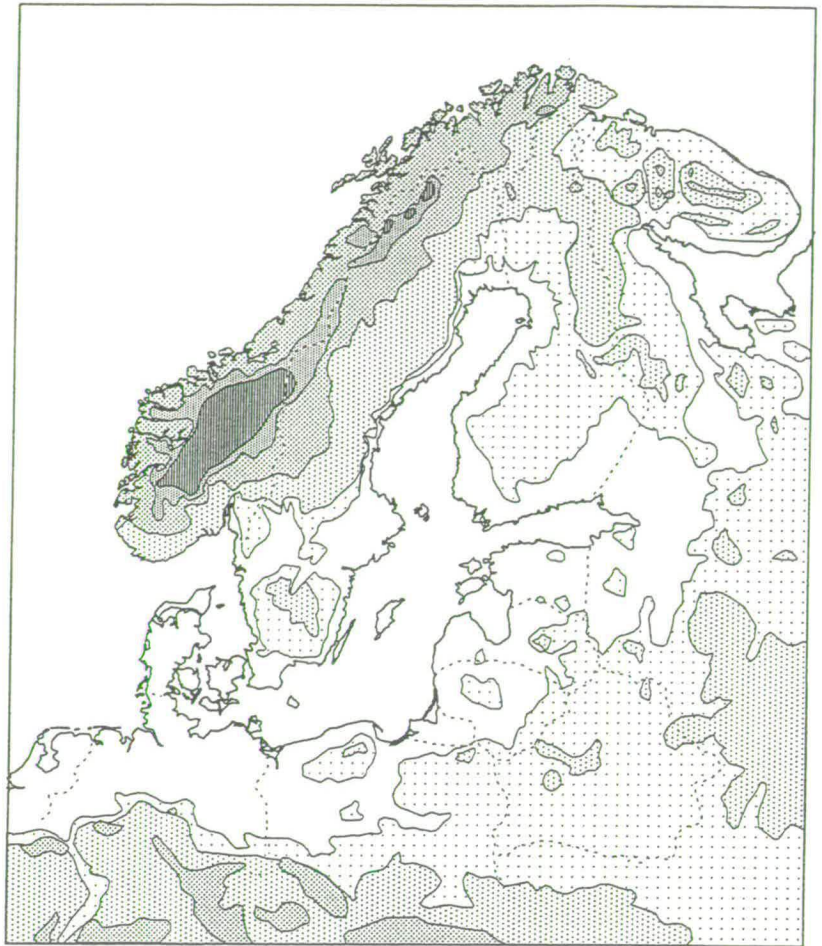
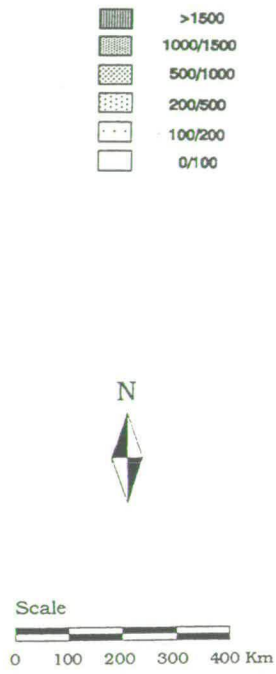
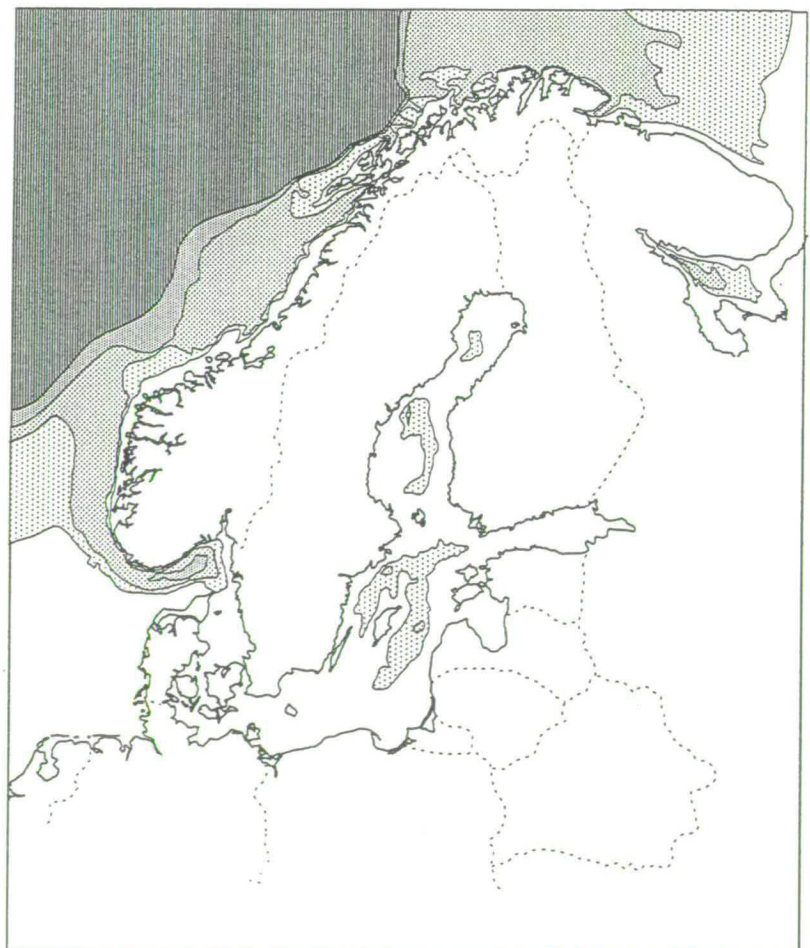
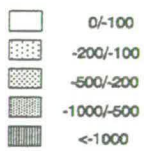


Fig. 2.5  
Bathymetric map of  
Northwest Europe



surrounded on three sides by higher areas that slope towards the centre of the Baltic Shield.

East of the Caledonides Fennoscandia is for the largest part a low-lying, gently inclined peneplain. Strong fracturing during earlier geological history produced a mosaic structure in the bedrock with numerous small, isolated bedrock knobs. Glacial erosion also strongly influenced the local topography. Roches moutonnées are scattered in the landscape and exposed bedrock is commonly polished by the abrasive action of the ice. The sediment cover in most parts of Fennoscandia is thin and often discontinuous. Okko (1964) estimated that the median thickness of overburden in Finland is 6.7 m. The sediments are unevenly distributed over the shield area. The sediment cover is thickest in Lapland, where bedrock exposures are relatively rare (Nordkalott Project, 1986a) and constitute approximately 5% of the total area below 500m asl. Further to the south the overburden thickness decreases. In the southern half of Finland bare bedrock forms approximately 40% of the surface area. The bulk of the sediments consist of tills and fluvio-glacial deposits. However, in the southern half of the Shield, subaqueous sediments form a substantial part of the overburden. These sediments have been deposited after deglaciation in water at the margin of the ice. Subaqueous sediments often form shallow drapes of silty sediment on top of the bedrock.

Outside Lapland a substantial part of the Shield area consists of bedrock which has a high-frequency, low-amplitude relief. The bedrock is partly exposed, partly covered by often thin deposits. Continuous sediment covers are found in the intervening low-lying areas and in places where glacial sedimentation was abundant such as morainic belts. Sediment thickness increases to the north.

### *Sedimentary Lowlands*

Whereas on the Baltic Shield bedrock lies at or very close to the surface, the situation in the sedimentary basins to the south and east is completely different. Here thick sequences of undisturbed, unconsolidated deposits occur at the surface. They form a continuous lowland area, from Lake Onega in the east, to the North Sea in the west. The relief in this sedimentary belt is below 200 m above sea level (asl). To the south the sedimentary sequences wedge out

against the Variscan massifs. These mountainous areas rise to heights well above 1000 m.

In the southwest the Baltic Shield is separated from the shallow North Sea Basin by the Skagerrak and the Norwegian Channel, where water depths exceed 300m in many parts. Along the west coast of Norway water depths increase rapidly towards the shelf break. To the north Fennoscandia gives way to the Barents Sea. Water depth of the central Barents Sea is between 100 and 200m, towards the west the depth increases to over 400m.

## 2.2 Weichselian glacial stratigraphy

In section 1.2 the different techniques were described that are used for the analysis of the glacio-dynamic evolution of the ice sheet. Cross-cutting relationships enable relative dating, identification of coherent flow patterns and correlation of these patterns with dated positions of the ice margin. Another strategy that might be used to obtain absolute ages for lineations and flow patterns, is correlation with the Weichselian glacial stratigraphy. A close correspondence between orientations of lineations and till fabrics can be used to correlate geomorphology and stratigraphy. Once the glacial stratigraphy is well established and dates for different units are available this is potentially a powerful method to establish the absolute ages of separate flow systems that could otherwise only be known relatively and only if cross cutting occurred.

In this section an overview will be given of some stratigraphic studies that have been done in Scandinavia. Locations referred to in this section are shown in Fig. 2.8. Table 2.1 shows the chronostratigraphic correlation of stadial and interstadial development in various regions of Scandinavia. Considerable uncertainty about regional correlation of different units and events exists. Moreover there are good reasons to doubt the chronostratigraphic frameworks that were proposed by different authors (Lundqvist, 1986, Mangerud, 1991). For that reason it was decided not to incorporate stratigraphic correlations in this study. In fact lineation analysis may be used to correlate spatially separated stratigraphic exposures.

Time (ka BP)	Isotope Stage	Chronostratigraphy	Stadial/ Interstadial	north Finland	Norrbotten (N Sweden)	central Sweden	southwest Norway	south Sweden
10	1	Holocene						
20	2	Late Weichselian		Till bed 1			Rogne Till	
30	3	Middle Weichselian	Denekamp	Till bed 11			Ålesund	Gärslöv
40			Hengelo					
50			Moershoofd					
60	4						Karmøy Diamicton	
80	5a	Early Weichselian	Odderade		Tärändö		Torvastad	O. Dösebacka ?
90	5b		Rederstall				Bones Till	
100	5c		Brørup	Peräpohjola	(Peräpohjola)	Jämtland	Fana	
110	5d		Herning	Till bed 111				
120	5e		Eemian		Leveäntemi			Fjøsangerian

Table 2.1 Chronostratigraphic correlation of the stadial and interstadial development of various regions in Scandinavia. Ages for isotope stage boundaries from Martinsson *et al.* (1987). The stadial/interstadial division is according to Behre & Lade (1986), interstadials are dotted. Chronostratigraphy of north Finland according to Hirvas & Nenonen (1987) and Hirvas (1991), northeast Norrbotten according to Lagerbäck and Robertsson (1988), central Sweden according to Lundqvist (1981) and (1986), southwest Norway according to Mangerud (1991), south Sweden according to Ringberg (1988).

After discussing stratigraphic work from Finland, Norway and Sweden some attention will be given to the problems of stratigraphic interpretation and correlation.

### 2.2.1 Finland

Till stratigraphy in north Finland is based on the stages of flow of the ice sheet, representing the various stages of glaciation. Till beds at different locations are correlated on the basis of corresponding till fabrics (Kujansuu 1976; Hirvas *et al.*, 1981; Hirvas & Nenonen, 1987). The argument being that till beds with similar till fabrics probably belong to the same flow stage of the ice sheet.

In central Finnish Lapland five glaciation stages have been distinguished on the basis of different flow directions (Hirvas, 1991). In central Lapland where, according to some authors, the ice divide was located during the late Weichselian maximum (Lundqvist, 1986; Hirvas *et al.*, 1981; Kleman, 1990) all five till beds are found. To the north and south of this zone the thickness of the youngest till beds (I, II & III) increases whereas the oldest tills (IV & V) disappear (Hirvas, 1991). Till beds IV & V are considered to be of pre-Weichselian age and will be further ignored. Layers of well-sorted material and occasionally peat or gyttja have been found intercalated between the till beds. Till beds I and II have been interpreted as having been deposited during the Middle/Late Weichselian glaciation. Organogenic deposits have not been found between Till beds I and II, but have been found underlying Till bed II. No organogenic deposits younger than the Peräpohjola (see below) have been found in Finland. At present, only one interstadial has been recognised in Finland, the Peräpohjola Interstadial, which has been correlated with the Brørup Interstadial (see Table 2.1) (Hirvas & Nenonen 1987).

Till bed I, deposited during deglaciation, has been interpreted as being the result of oscillations of the ice margin. Broadly speaking the flow pattern of stage I is conformable to flow during stage II (Fig. 2.6). During stage II (Middle and Late Weichselian) the ice-flow direction was from west to east in south and central Lapland and to the northeast in northern Lapland. The ice in the more peripheral zone was thought to be very active and most of the striae and

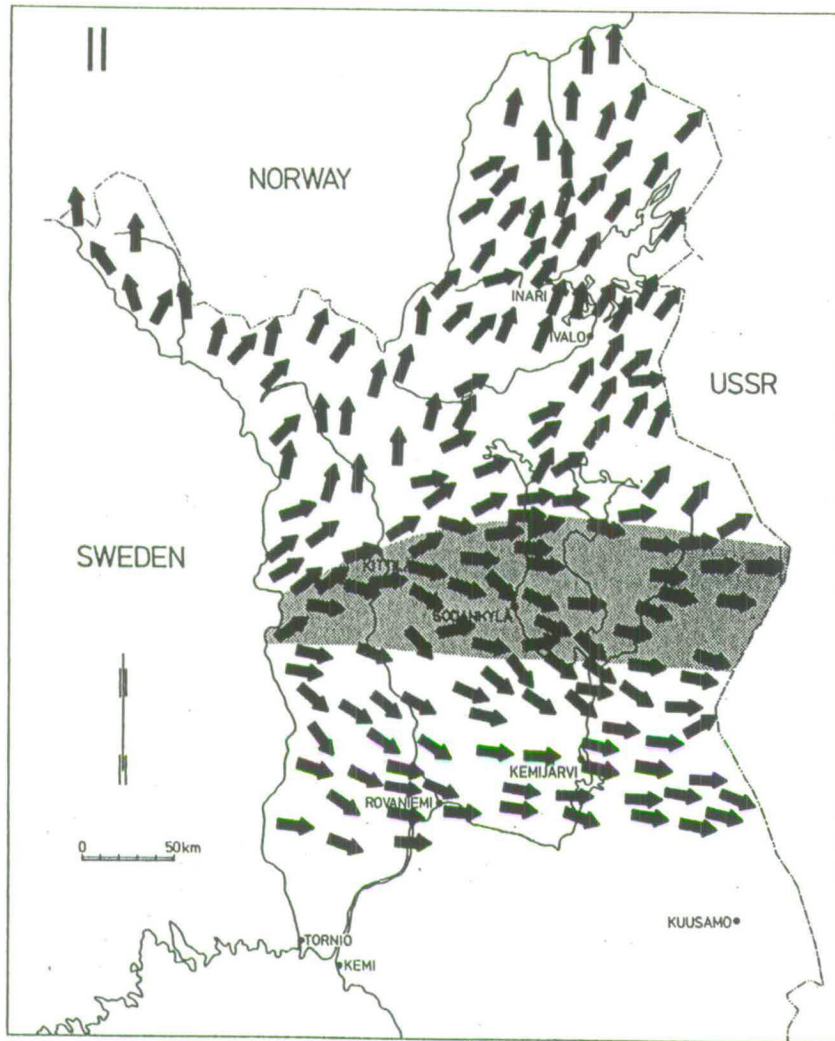


Fig. 2.6 Flow stage II, Finland. Interpreted by Hirvas (1991) to reflect ice flow during the Middle/Late Weichselian glaciation. Hatched area shows inferred position of ice divide (From Hirvas, 1991).

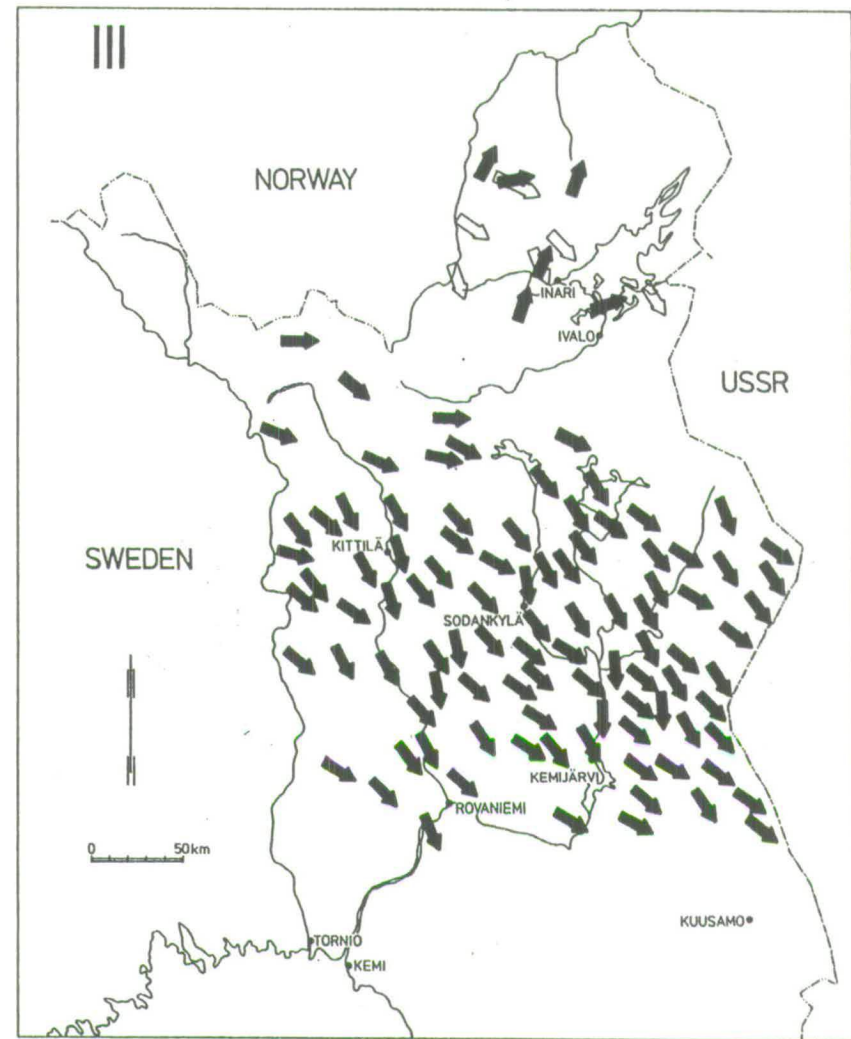


Fig. 2.7 Flow stage III, Finland, Interpreted by Hirvas (1991) to reflect ice flow during the Early Weichselian glaciation. Open arrows in northern Lapland show ice flow during initial stage of the glaciation (From Hirvas, 1991).

glacial macro forms present in these areas are thought to have formed during this stage.

During flow stage III (Fig. 2.7), which is thought to reflect ice flow during the Early Weichselian, the ice-flow direction was from NW to SE, with the exception of north Lapland where the direction was towards the NNE. During this stage the rare NW-SE-trending drumlins and larger drumlinoids are believed to have developed (Hirvas, 1991). Between Till beds II and III sorted sediments have been found at a number of sites. Deposits containing organic material between Till beds II and III are rare.

The till stratigraphy in south Finland is less well developed than in the northern part of the country. Outside the Salpausselkä end moraines the uppermost till is the 'younger' till, which occurs inside the moraines covered by the 'youngest' till. In central and south Finland, Rainio and Lahermo (1976), have studied a dark grey till which occurs in bedrock depressions. This till has been interpreted as having been formed during the advance phase of the glaciation following the Peräpohjola by mixing of organic deposits with glacial till.

In summary; five till units have been identified in north Finland on the basis of till fabric correlation. Till I and II are believed to have formed during the Middle and Late Weichselian. Till III has been correlated with the Early Weichselian. One of the major problems of the above method is that there is no single section where the complete stratigraphy is present. The regional correlation of the different till units and the stratigraphic interpretation largely depend on till-fabric measurements.

In section 6.6 different palaeo-ice-flow indicators (till fabrics and striae data) (Nordkalott Project, 1986a-d) will be compared with the lineation patterns found in this study. The idea, on which the correlation in north Finland is based, that the different till units formed during prolonged stages when the ice flow pattern remained unchanged for thousands of years, will be disputed in section 6.6. Till II, believed to have formed during the Middle and Late Weichselian and to represent a single flow stage (Hirvas, 1991) is shown in the

present study to correspond to flow systems migrating over Lapland during deglaciation.

### 2.2.2 Norway

Several sites in Norway have been described where deposits containing organic material are intercalated with glacial material. At Fjøsanger, Mangerud *et al.* (1981) have described a section where glacio-marine silts conformably overlie Interglacial (Eemian) deposits. This is seen as evidence that during the Herring Stadial (see Table 2.1), isotope stage 5d according to Mangerud (1991), the glaciers at this site had almost the same extent as during the Younger Dryas. Above the glacio-marine silts a gravel deposit occurs which formed during a warm interstadial stage. Miller *et al.* (1983) correlated this stage on the basis of amino analyses with the Brørup Interstadial. Mangerud *et al.* (1981) argue that the Bønes Till must be correlated with the Rederstall Stadial (isotope stage 5b)

From Karmøy, interstadial sand (Torvastad Sand) has been reported which overlies Eemian deposits. Amino-acid analyses suggest a date of 78 ka BP for this interstadial deposit (Sejrup, 1987) which would correlate with isotope stage 5a. On top of the Torvastad Sands are two tills separated by the interstadial Bø Sand. C<sup>14</sup> dating indicates a date around 40 ka BP, while amino-acid analyses on molluscs and foraminifera gave 40 and 60 ka BP respectively (Miller *et al.*, 1983). Although the age cannot be determined with any precision, this site is thought to indicate a Middle Weichselian ice-free period between the post-Odderade Stadial (isotope stage 4) and the Late Weichselian Maximum, Table 2.1 (Mangerud, 1991).

In Nordland, Lauritzen (1984) investigated karst caves. Speleothemes can only precipitate when a cave is not frozen. Uranium series datings of speleothemes from over 100 caves west of the watershed in Nordland show major peaks around isotope stages 1 (Holocene) and 5e (Eemian) and a lack of dates at stage 2.

Three dates suggest extensive deglaciation around 30ka BP (Ålesund Interstadial). The dates reinforce, or are at least compatible with, conclusions drawn from other stratigraphical evidence. There is one main conflict, from easterly caves two speleothemes indicate continuous growth from 135-95 ka BP. That is till the end of stage 5c (Brørup), indicating ice-free conditions of the coasts and valleys of Nordland until the beginning of the Rederstall Stadial. This contradicts the extensive glaciation further south at Fjøsanger that was postulated by Mangerud (1991).

In wave-cut caves at Skjonghelleren, Sunnmøre, C<sup>14</sup> dates on bones and uranium series also suggest an ice-free period around 30ka BP, indicating warm marine conditions that suggest that the North Atlantic current must have entered the North Sea (Mangerud, 1991).

#### *Conclusions: Norway*

Mangerud (1991) argues that before the Ålesund Interstadial around 30 ka BP, Weichselian Scandinavia had seen at least two more periods of extensive deglaciation. The first at stage 5c (Brørup), the second at stage 5a (Odderade). A possible third period of deglaciation (Bø- stage, see Table 2.1) is tentatively dated between 60 and 40 ka BP.

#### 2.2.3 Sweden

Many sites are known where sediments have been found underlying till. Almost all deposits are composed of minerogenic sediments. In Brumunddal (Helle *et al.*, 1981) and Pilgrimstad (Lundqvist, 1967) sub-till organic deposits are present. In Brumunddal, the lithostratigraphy and pollen stratigraphy suggest a full stadial/interstadial cycle. A till deposit is overlain by peat which shows evidence of a change from tundra vegetation to birch forest (*Larix*, *Picea* and *Betula*) and back to tundra vegetation. The peat is overlain by a till. The climatic conditions during the forested period are thought to have been colder than Interglacial conditions. In Pilgrimstad, a similar cycle has been described (Lundqvist, 1967), lacking *Larix* during the forested period. These Interstadial deposits (Jämtland) have been correlated by Lundqvist with the Brørup.

In northeast Sweden, Lagerbäck (Lagerbäck, 1988; Lagerbäck and Robertsson, 1988) have presented a new interpretation of the glacial stratigraphy. One area here is dominated by an older system of NW-SE-trending drumlins, formed by ice from the NW. Almost parallel to these drumlins large, sharp-crested eskers continue for tens of kilometres. In parts of the area younger drumlinoids occur, often superimposed on the older NW-SE drumlins. These younger drumlinoids have been formed by ice coming from the S/SSW. Finally, a system of westerly drumlins exists, its age relation with the other systems is unknown.

In kettle holes related to the NW-SE-trending eskers an identical stratigraphy has been found at four locations. Lagerbäck & Robertsson (1988), Lagerbäck (1988) and Robertsson & Rohde (1988) have described sites where two Early Weichselian interstadials are separated by tills. On the basis of till fabric and pollen analyses Lagerbäck (1988) and Lagerbäck & Robertsson (1988) correlate the lower interstadial with the Peräpohjola and the upper interstadial (Tärendö) tentatively with the Odderade. Lagerbäck (1988) argues that the Veiki moraines (extensive hummocky moraines in northeast Sweden, and generally thought to date from the deglaciation of the Late Weichselian Ice Sheet (Lundqvist, 1981) were formed during the deglaciation phase directly preceding the Peräpohjola Interstadial. Thus, in his interpretation, the Veiki moraines have been overrun twice: first during the glaciation following the Peräpohjola Interstadial; and second during the Middle/Late Weichselian glaciation. These later glaciations have modified the Veiki deposits only to a very limited extent.

There has been much debate about the interpretation of organic finds in glacial deposits. Punkari (1991) and Livrand (1991, 1992) argue that organic material can be transported and redeposited into younger glacial deposits. Punkari and Forsström (1995) have studied organic remains in the flanks of eskers in west Finland, comparable to the situation described above. Their conclusion was that the organic remains most likely belonged to the end of the Eemian Interglacial and were mixed in to the esker sediments as a result of erosion.

#### *Conclusions: Scandinavia*

In south Norway, Mangerud postulates three, possibly four, ice-free periods during the Weichselian, the last one as recent as 30 ka BP. In north Sweden, Lagerbäck (1988) found indications for two extensive ice-free periods during the

Early Weichselian. In north Finland and central and south Sweden, only one ice-free period has been recognised. Ice is thought to have covered these areas continuously during the Middle and Late Weichselian. These different stratigraphic concepts are shown in the glaciation curve of Fig. 2.9. However, controversy remains about the correct interpretation of organic remains in glacial sediments.

#### 2.2.4 Problems associated with stratigraphic correlation and interpretation

The Scandinavian Weichselian stratigraphy still presents a number of major problems. The ages of the older ice-free periods on the basis of radio-carbon dating are now regarded as unreliable if the sample is more than 22-35 ka old. Dates obtained using the TL method should be used very carefully because of large discrepancies in the results (Clark *et al.*, 1993). According to Mott and DiLabio (1990) the last cooling phase of an interglacial is often better preserved in the organic remains than earlier, warmer phases. This may lead to false correlations with interstadials. Examples from Estonia and Finland of dislocation of peat fragments by ice-sheet or meltwater activity show that the assumption that organic remains are in situ is not always correct (Punkari and Forsström, 1995; Litvrand, 1991).

In addition to these methodological problems there are important correlation problems between different areas of Fennoscandia. For example, between Finland and central and south Sweden, where only one interstadial has been recognised and northeast Sweden where two Early Weichselian interstadials have been found. Because a comprehensive, uncontroversial stratigraphic scheme that correlates the stratigraphy of Fennoscandia does not exist as yet, it was decided not to try and tie the evolution of the Scandinavian Ice Sheet as deduced from the lineation data to a particular stratigraphic scheme. Instead, the glacio-dynamic evolution will be presented here independently. Hopefully, the two approaches can be combined one day. But for the time being, this method may shed more light on the evolution of the Scandinavian Ice Sheet when it is used independently.

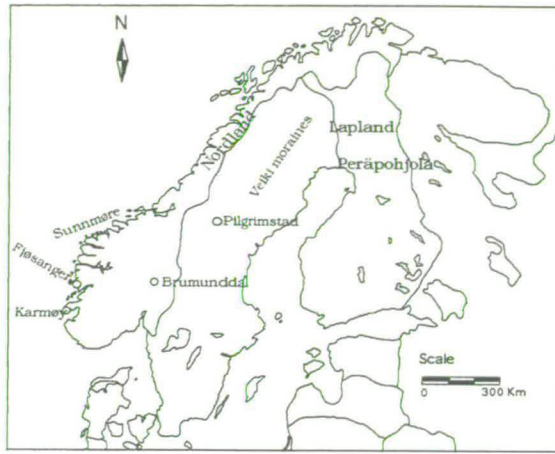


Fig. 2.8 Location map of stratigraphic sites.

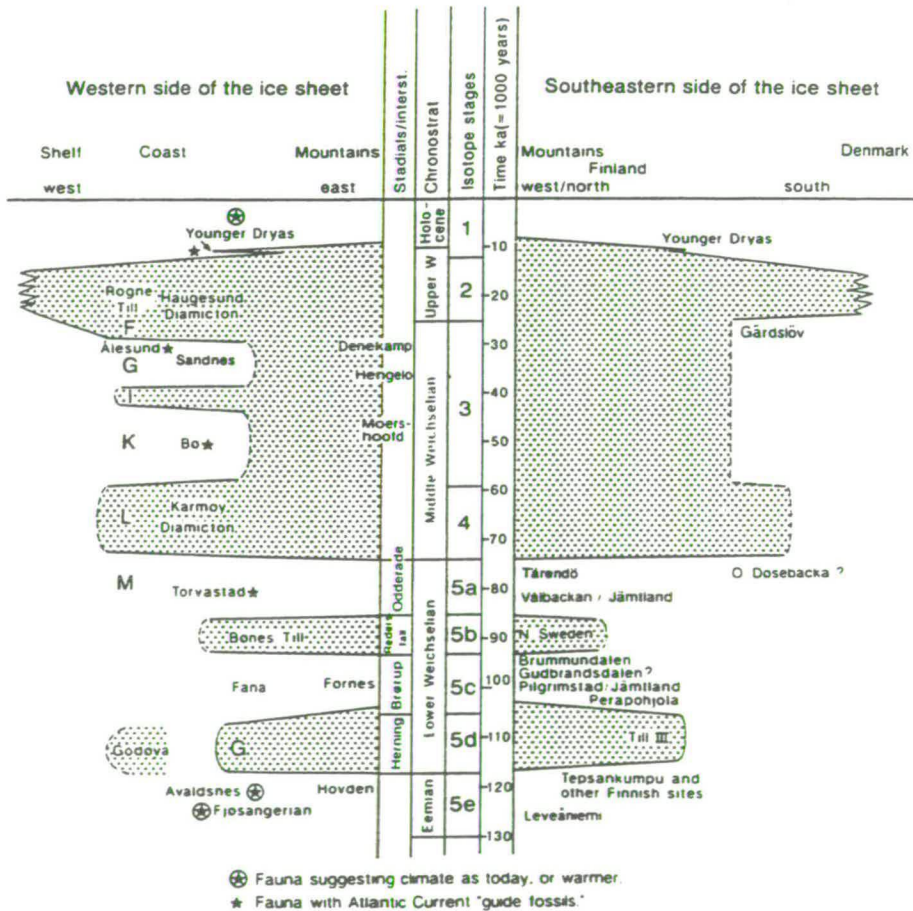


Fig. 2.9 Proposed glaciation curve for the last glacial (Weichselian) in Fennoscandia by Mangerud (1991). The curve at the left is for the west side of the Scandinavian mountains, the curve at the right is for the east side of the mountains in northern Sweden and Finland and towards Denmark in the distal parts.

## 2.3 Deglaciation and palaeo-geographic reconstructions

### 2.3.1 Introduction

Figure 2.10 shows the ice-recession lines in Scandinavia resulting from the IGCP 24 work (Lundqvist, 1986). Along the southern edge of the ice sheet, there was a continued recession since 13 ka BP. During the climatic deterioration of the Younger Dryas (11-10 ka BP), the rate of retreat decreased. Well-defined frontal moraines in Sweden (Middle Swedish end moraines) and Finland (Salpausselkä moraines) mark the almost stationary position of the ice sheet during this period. Further north, clear frontal positions are lacking, recession lines are based on  $C^{14}$ -dated bogs and give an approximate idea of the recession (Ignatius *et al.*, 1980). After 10 ka BP the rate of recession increased again and continued uninterrupted until Fennoscandia was ice free. The dates of the recession lines in north Sweden and along the Baltic coast are based on varve chronology.

The interaction between the retreat of the ice margin, isostatic recovery and the rising eustatic sea level resulted in a constantly changing environment along the ice margin during deglaciation. The southern margin of the ice sheet was, for most of its length, bordered by seas or lakes which varied in depth and extent depending on the balance between these processes. The presence of these water bodies influenced ice dynamics in parts of the ice sheet and played a role in the rapid deglaciation after 10 ka BP.

Relative sea-level (RSL) change is the change of the sea level measured relative to a point on land. Both the eustatic sea level and the land may undergo vertical movements: relative sea level therefore measures differences in vertical displacement between the local sea surface and the local land surface. RSL data can therefore be used for the reconstruction of conditions at the margin of the ice sheet. With the aid of over 50 relative sea-level curves the land uplift has been reconstructed for different periods. Geographic reconstructions showing the land/water distribution and the extent and depth of the water bodies along the margin of the ice sheet are also presented.

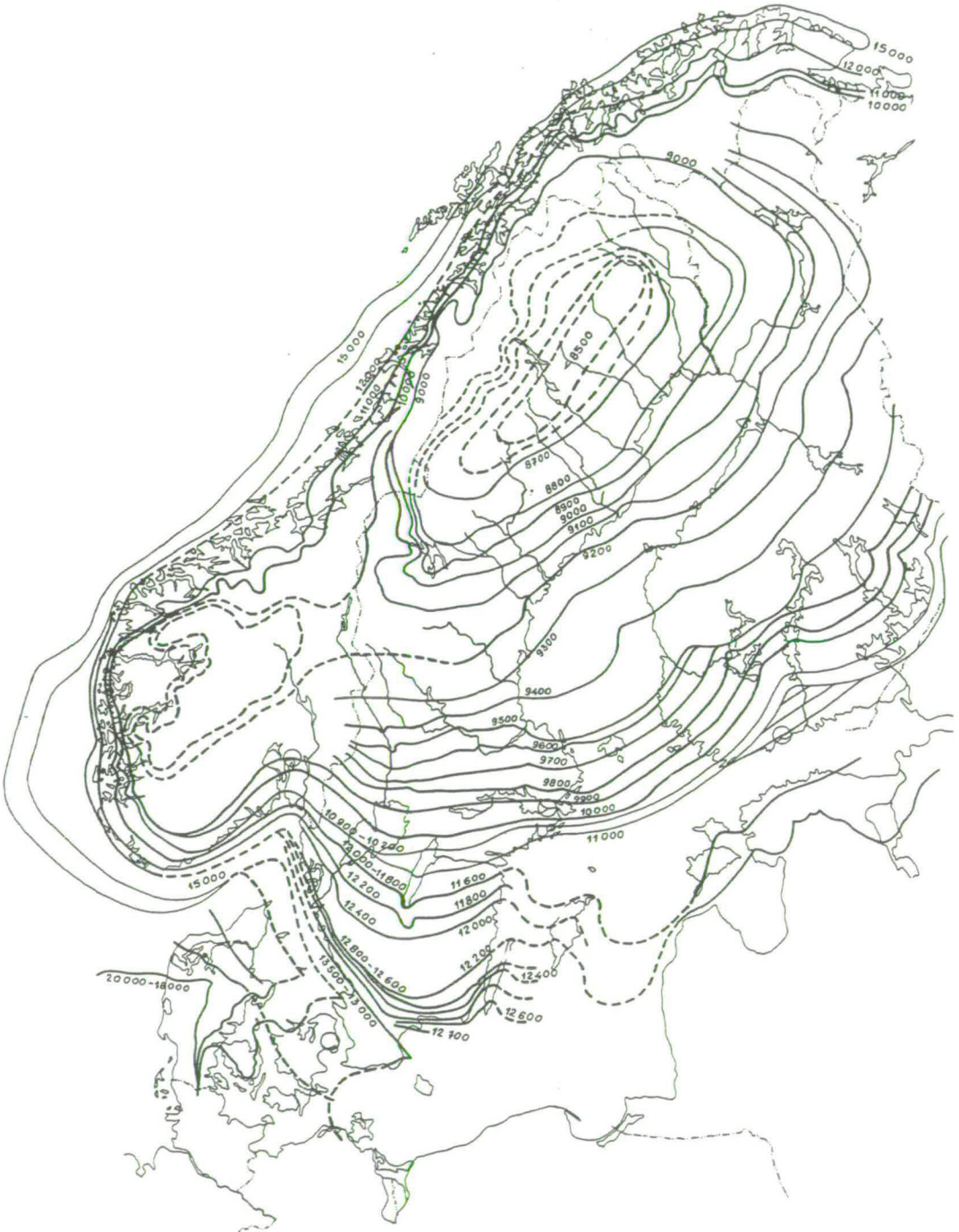


Fig. 2.10 Ice-recession lines in Fennoscandia. (From Lundqvist, 1986).

In Appendix A the collection of RSL data and the uncertainties and errors involved in data collection and interpretation are discussed. This is followed by a discussion of the different components of isostasy and the effects of crustal loading on RSL around the globe. The RSL curves used in this study are included in this Appendix.

### 2.3.2 Relative sea-level data

Figure 2.11 shows the locations of the RSL curves that were used in this study, just over 50 in total. The spatial distribution of the curves is far from even. For the Kola Peninsula and the White Sea coast, no reliable material has been published. The entire eastern flank of the ice sheet is poorly represented. This is unfortunate, because RSL curves might have provided information on the extent of the ice sheet to the east. Moreover our knowledge of the extent and timing of the confluence and break up of Scandinavian and Barents Sea ice might have benefited from more eastern RSL data. The RSL curves shown allow the reconstruction of the land uplift in Fennoscandia from ca. 12 ka BP on.

Figure 2.12 shows examples of RSL curves from areas that have been covered by a substantial thickness of ice. Land uplift in these areas has been consistently higher than the eustatic sea level rise, resulting in a continuous regression since deglaciation. In south Norway, the area around Oslo (Hafsten, 1956) has risen 220m relative to the sea level since deglaciation, the curve shows an exponential decrease in uplift through time. Västernorrland (Miller & Robertsson, 1979) in central Sweden, close to the centre of the ice sheet during its maximum extent, recorded an uplift of approximately 260 m. Taking the eustatic sea level rise into account, the Västernorrland region has risen approximately 290 m since deglaciation.

A series of four curves from the west coast of Norway is shown in Fig. 2.13 (see Fig. 2.11 for locations). In the Stette area (Svendsen & Mangerud, 1987) relative sea level fell since deglaciation of the area until just after 9 ka BP. For the next 1000 years the eustatic sea level rise prevailed over the isostatic uplift and the area was subjected to a marine transgression. The marine

## Locations of relative sea-level curves

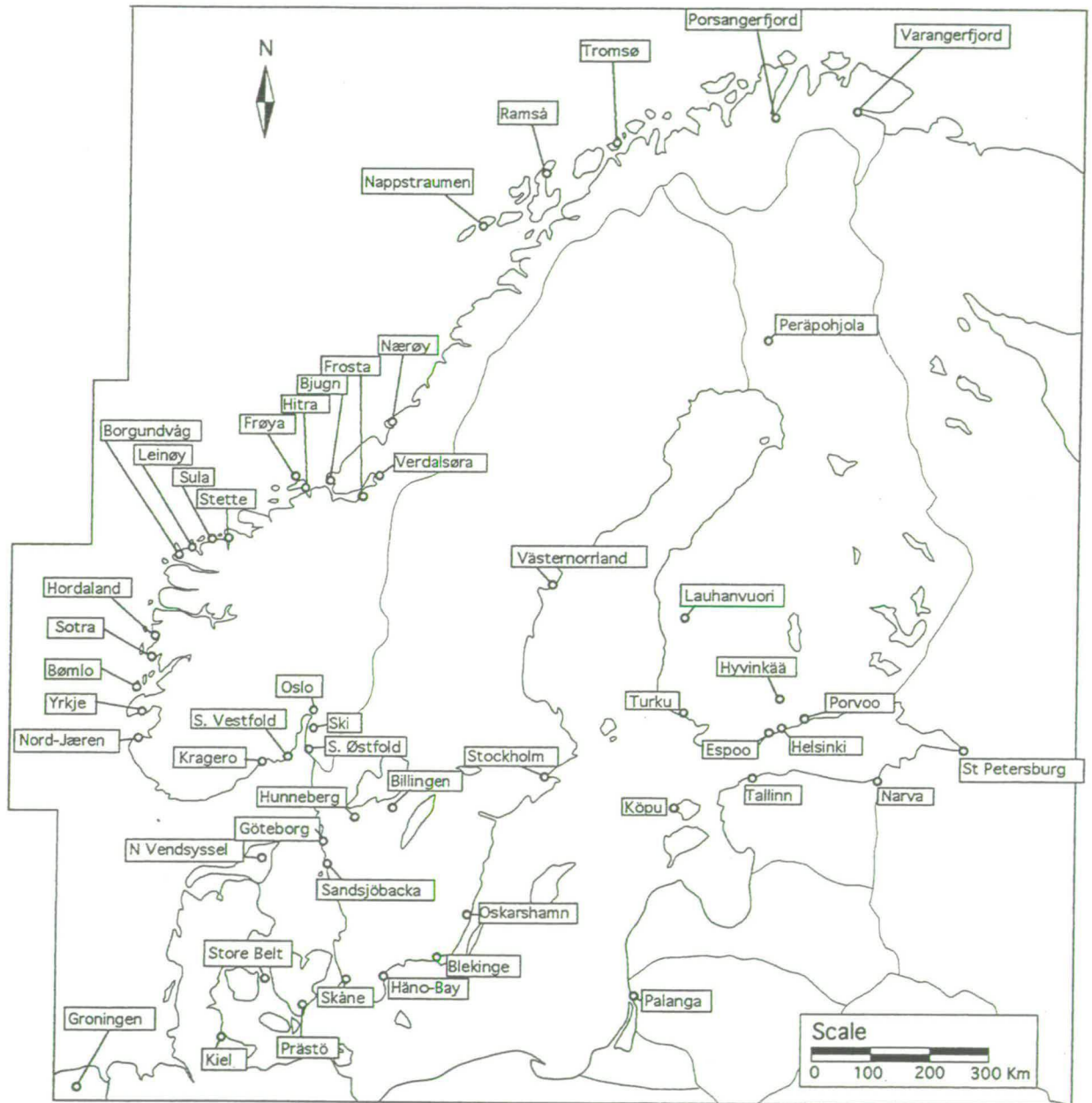


Fig. 2.11 Location map of relative sea-level curves

Porsangerfjord (Donner et al., 1977), Varangerfjord (Donner et al., 1977), Tromsø (Hald & Vorren, 1983), Ramså (Møller, 1986), Nappstraumen (Møller, 1984), Nærøy (Ramfjord, 1982), Verdalsøra (Sveian & Olsen, 1984), Frosta (Kjemperud, 1981), Bjugn (Kjemperud, 1986), Frøya (Kjemperud, 1986), Hitra (Kjemperud, 1986), Stette (Svendsen & Mangerud, 1987), Sula (Lie et al., 1983), Leinøy (Svendsen, 1985), Borgundvåg (Longva et al., 1983), Hordaland (Kaland, 1984), Sotra (Krzywinski & Stabell, 1978), Bømlo (Fægri, 1944), Yrkje (Ånundsen, 1980), Nord-Jæren (Thomsen, 1981), Kragero (Stabell, 1980), S. Vestfold (Henningsmoen, 1979), Oslo (Hafsten, 1956), Ski (Sørensen, 1979), S. Østfold (Danielsen, 1970), Billingen (Björck & Digerfeldt, 1986), Hunneberg (Björck & Digerfeldt, 1982), Göteborg (Bergsten & Dennegård, 1988), Sandsjöbacka (Påsse, 1987), Skåne (Digerfeldt, 1975), Håno-Bay (Björck & Dennegård, 1988), Blekinge (Björck, 1979), Oskarshamn (Svensson, 1985), Stockholm (Åse & Bergström, 1982), Västernorrland (Miller & Robertsson, 1979), Peräpohjola (Saarnisto, 1981), Lauhanvuori (Salomaa, 1982), Turku (Glückert, 1976), Espoo (Hyvarinen, 1980), Helsinki (Hyvarinen, 1980), Porvoo (Eronen, 1983), Hyvinkää (Synge, 1982), St Petersburg (Dolukhanov, 1979), Köpu (Kessel & Raukas, 1979), Tallinn (Kessel & Raukas, 1979), Narva (Kessel & Raukas, 1979), Palanga (Gudelis, 1979), N Vendsyssel (Petersen, 1984), Store Belt (Krog, 1960), Prästö (Mikkelsen, 1949), Kiel (Winn et al., 1986), Grøningen (Jelgersma, 1980).

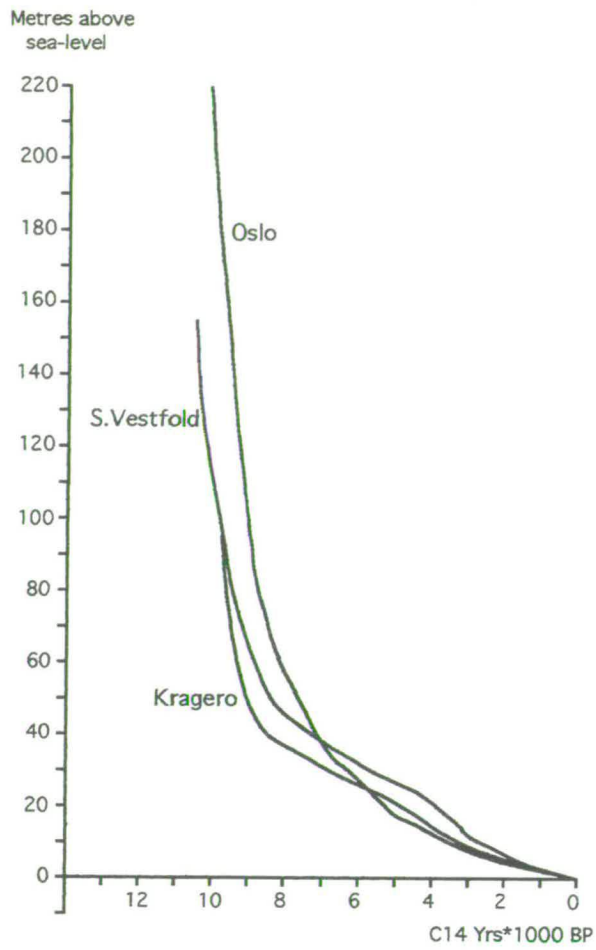


Fig. 2.12 RSL curves of Oslo (Hafsten, 1956), South Vestfold (Henningsmoen, 1979) and Kragero (Stabell, 1980).

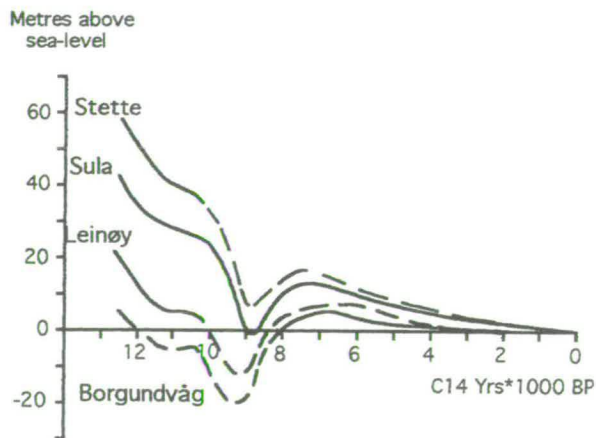


Fig. 2.13 RSL curves of Stette (Svendsen & Mangerud, 1987), Sula (Lie et al., 1983), Leinøy (Svendsen, 1985) and Borgundvåg (Longva et al., 1983).

transgression started earlier and lasted longer in Borgundvåg which has experienced a smaller uplift. Around ca. 7 ka BP when melting of the large Weichselian Ice Sheets was complete, a new regressive phase started. All four curves show a marked slowdown in the uplift rate during the Younger Dryas, when the retreat of the ice sheet was halted as a result of climatic deterioration.

Figure 2.14 shows two examples of RSL curves from areas that experienced a continued rise of relative sea level throughout the Holocene. Kiel (Germany) was only briefly covered by ice during the last glaciation. Isostatic depression was limited and the average trend of the curve resembles the eustatic curves (Fig. A.1). Groningen (The Netherlands) is situated well outside the area covered by the last glaciation. Relative sea level at 10 ka BP was -60m, well below the estimated eustatic sea level at that time (approximately -38 m). It is possible that this strong subsidence is related to the collapse of the forebulge (see Appendix A).

### 2.3.3 Palaeo-geographic reconstructions

The situation in the Baltic Basin is complicated by the fact that from time to time, freshwater lakes formed in this region, with lake levels above contemporary oceanic levels. Local ice-dammed lakes were present at the southern and eastern margins of the retreating ice sheet before the formation of the Baltic Ice Lake (BIL) at ca. 12 ka BP. From ca. 15 ka BP local ice-dammed lakes have been reported in the Leningrad area (Dolukhanov, 1979). Around 12 ka BP, these local lakes coalesced to form one continuous lake south and east of the ice sheet. This Baltic Ice Lake drained through the Danish Straits, but as eustatic sea level had fallen below the threshold of the Danish Straits, there was no direct connection between the BIL and the oceans. The area occupied by the ice lake increased as the ice sheet retreated to the north. During the Younger Dryas, 11-10 ka BP, the retreat slowed down as a result of the impact of climatic deterioration on the ice sheet. In south Finland the Salpausselkä moraines formed during this period. These ridges are composed primarily of glacio-fluvial sands and gravels. These sands and gravels form extensive deltas and sandur deltas whose upper surfaces correspond to the

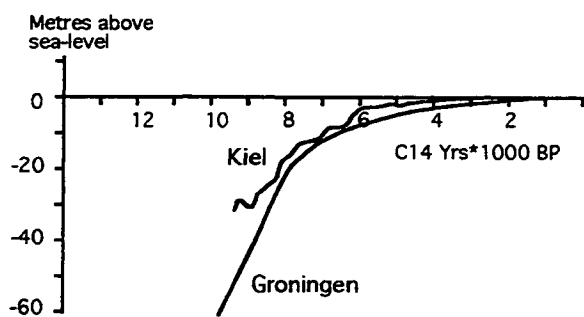


Fig. 2.14 RSL curves of Kiel (Winn et al., 1986) and Groningen (Jelgersma, 1980).

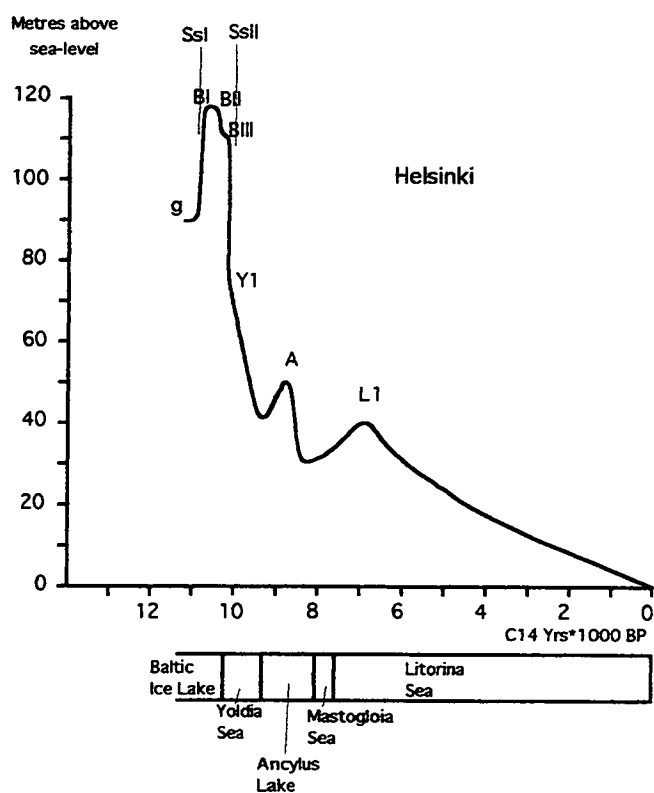


Fig. 2.15 RSL curve of Helsinki area (Alhonen, 1979). SsI = Salpausselkä I, SsII = Salpausselkä II, BI, BII and BIII are different lake levels during the Baltic Ice Lake.

water levels that prevailed during their formation. The delta surfaces, which can be found at various levels in the Salpausselkä zone, have been used to study the fluctuations of the lake levels during the BIL stage (Sauramo, 1958; Donner *et al.*, 1979; Synge, 1980, 1982; Saarnisto, 1982).

Reconstruction of the lake levels from these delta surfaces is far from straightforward. As a result of differential land uplift contemporary shorelines are at present at different altitudes and different schemes have been proposed (Donner, 1969; Synge, 1982). The exact causes of the fluctuating lake levels remain unclear. It is not known what extent the fluctuations are caused by land uplift and to what extent they are a result of changes in meltwater influx and changes in the outflow threshold (Eronen, 1983).

Isobases are lines connecting points that have experienced the same amount of uplift or subsidence during a specified amount of time. Figures 2.16 and 2.17 show the land uplift in Fennoscandia and reconstructions of the extent of the BIL during 12 ka BP and 10.5 ka BP.

The BIL stage ended around 10.2 ka BP, when the retreat of the ice was resumed and the ice sheet withdrew north of the hill of Billingen in central Sweden (Agrell, 1979). There is extensive evidence for a strong and sudden drop in lake level at ca. 10.2 ka BP. Deglaciation of central Sweden north of Billingen opened a direct connection between the Baltic Basin and the oceans. In the sediments the influx of salt water into the Baltic is reflected in the occurrence of diatoms indicative of brackish conditions (Eronen and Haila, 1982). This marks the beginning of the Yoldia Stage (Figs 2.18 and 2.19).

After ca. 9.5 ka BP, a transgressive phase started in the Baltic Basin that culminated at ca. 9 ka BP, the Ancylus transgression (Gluckert & Ristaniemi, 1982), see Fig. 2.20. This transgression was accompanied by the gradual disappearance of brackish diatoms from the sediments. The reasons for the Ancylus transgression remain unclear. It is not known whether the Ancylus Lake overflow continued to be through central Sweden or through the Öresund (Eronen, 1976). It is possible that the central Swedish outflow channel stopped functioning as a result of continued land uplift and that, after the lake level had risen sufficiently, the Öresund acted as the outflow channel.



Fig. 2.16 Geographic reconstruction and uplift pattern of Northwest Europe at 12,000 yr BP. Land/water distribution based on Eronen (1983).



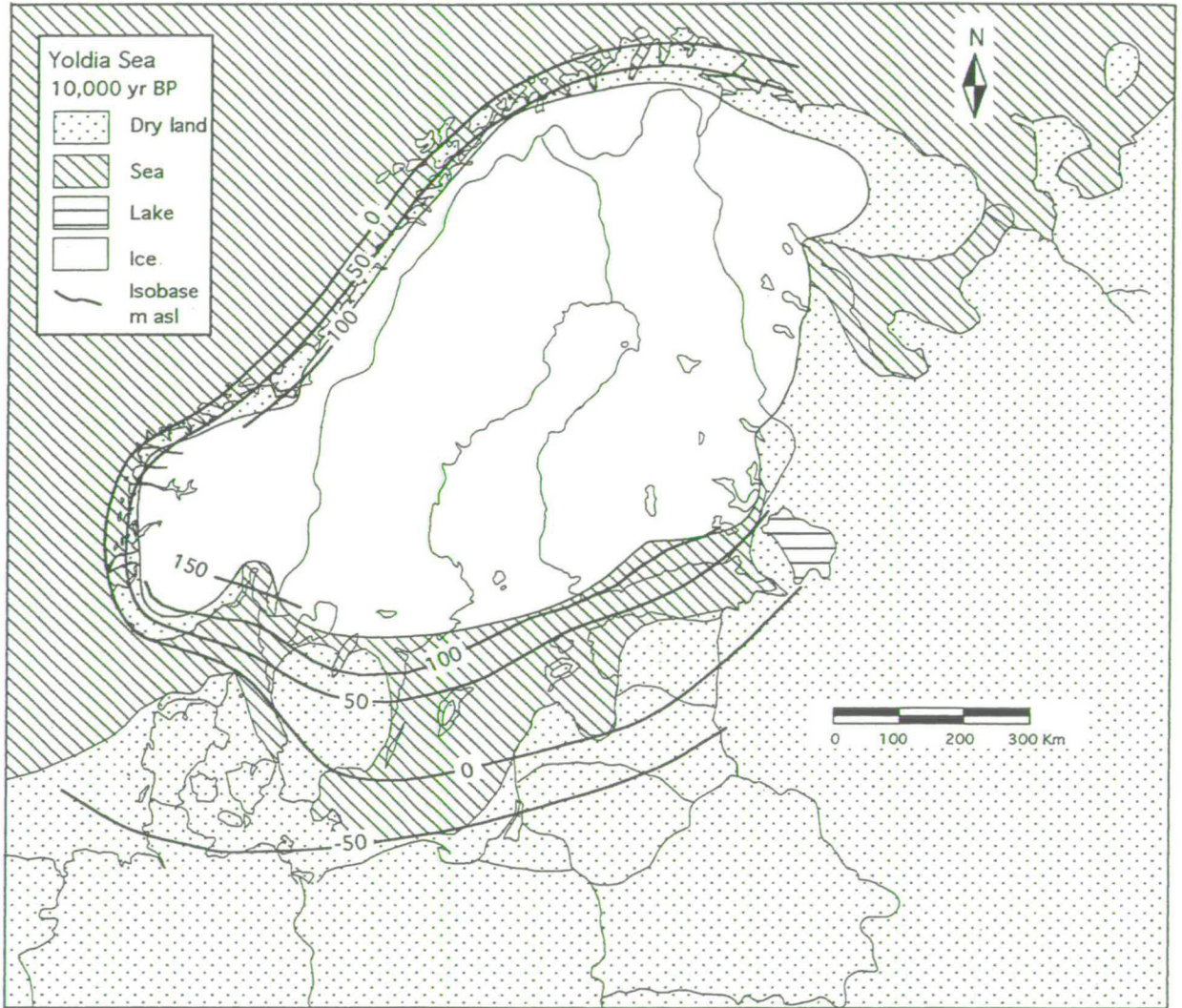


Fig. 2.18 Geographic reconstruction and uplift pattern of Northwest Europe at 10,000 yr BP. Land/water distribution based on Eronen (1983).

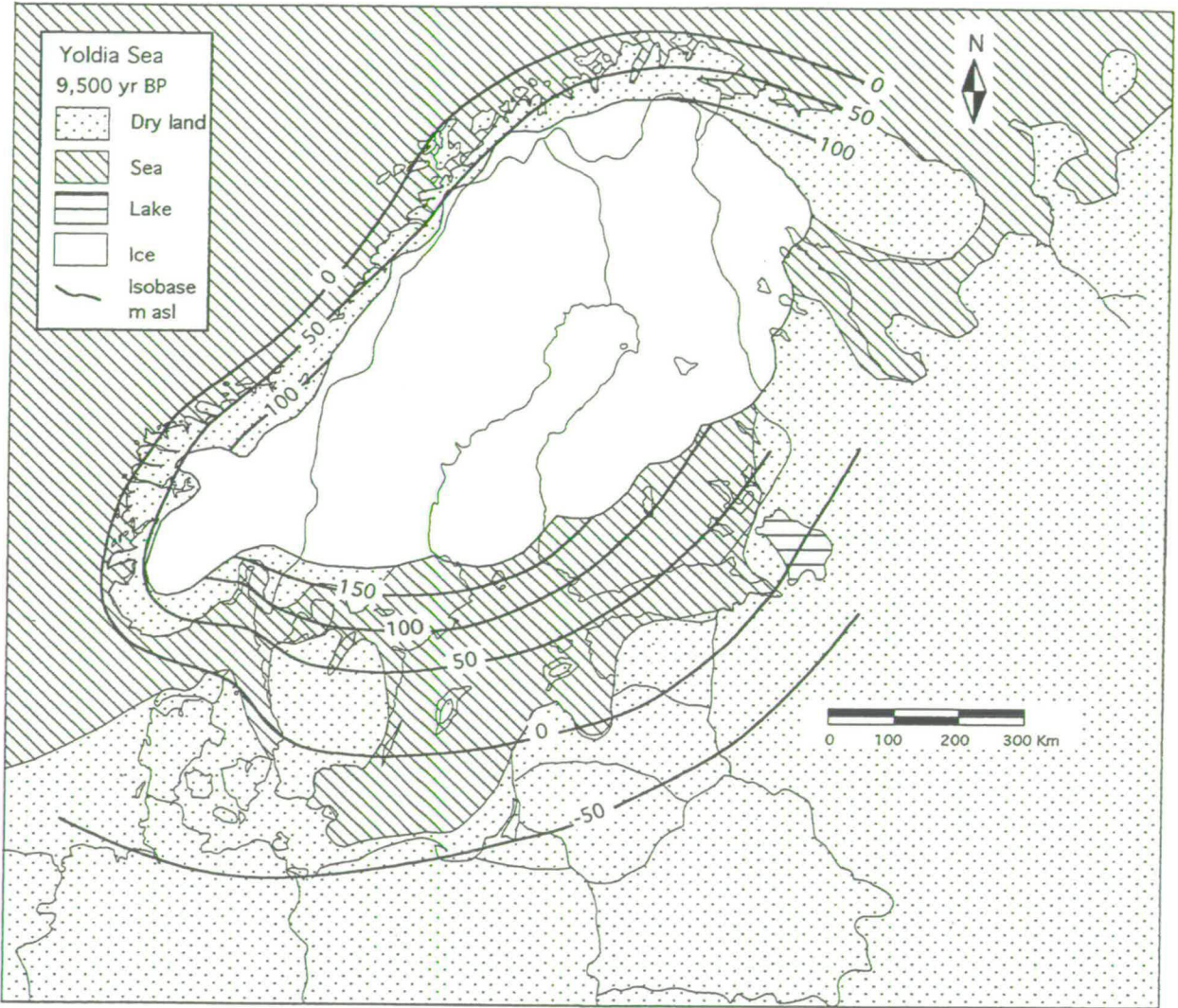


Fig. 2.19 Geographic reconstruction and uplift pattern of Northwest Europe at 9,500 yr BP. Land/water distribution based on Eronen (1983).

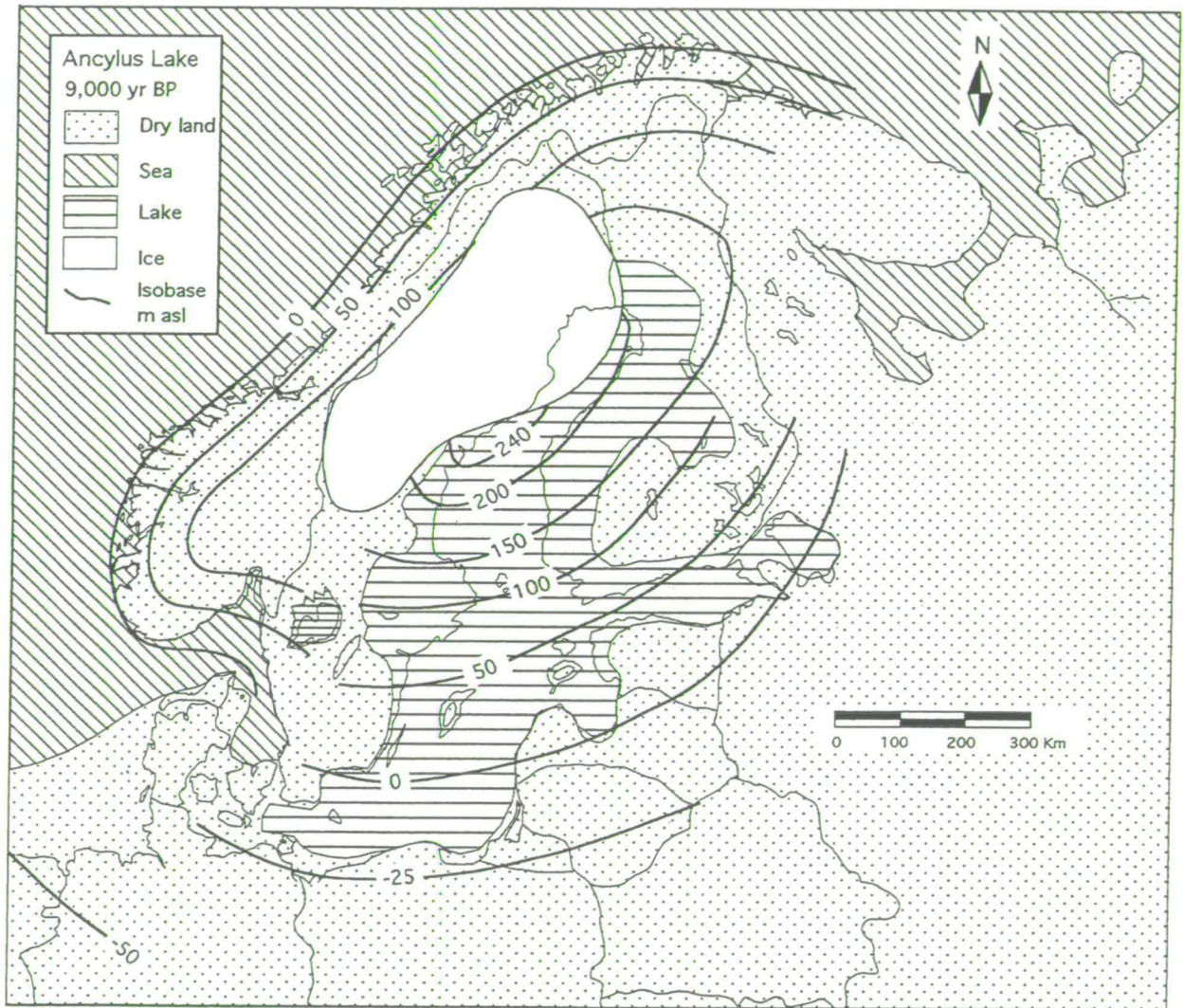


Fig. 2.20 Geographic reconstruction and uplift pattern of Northwest Europe at 9,000 yr BP. Land/water distribution based on Eronen (1983).

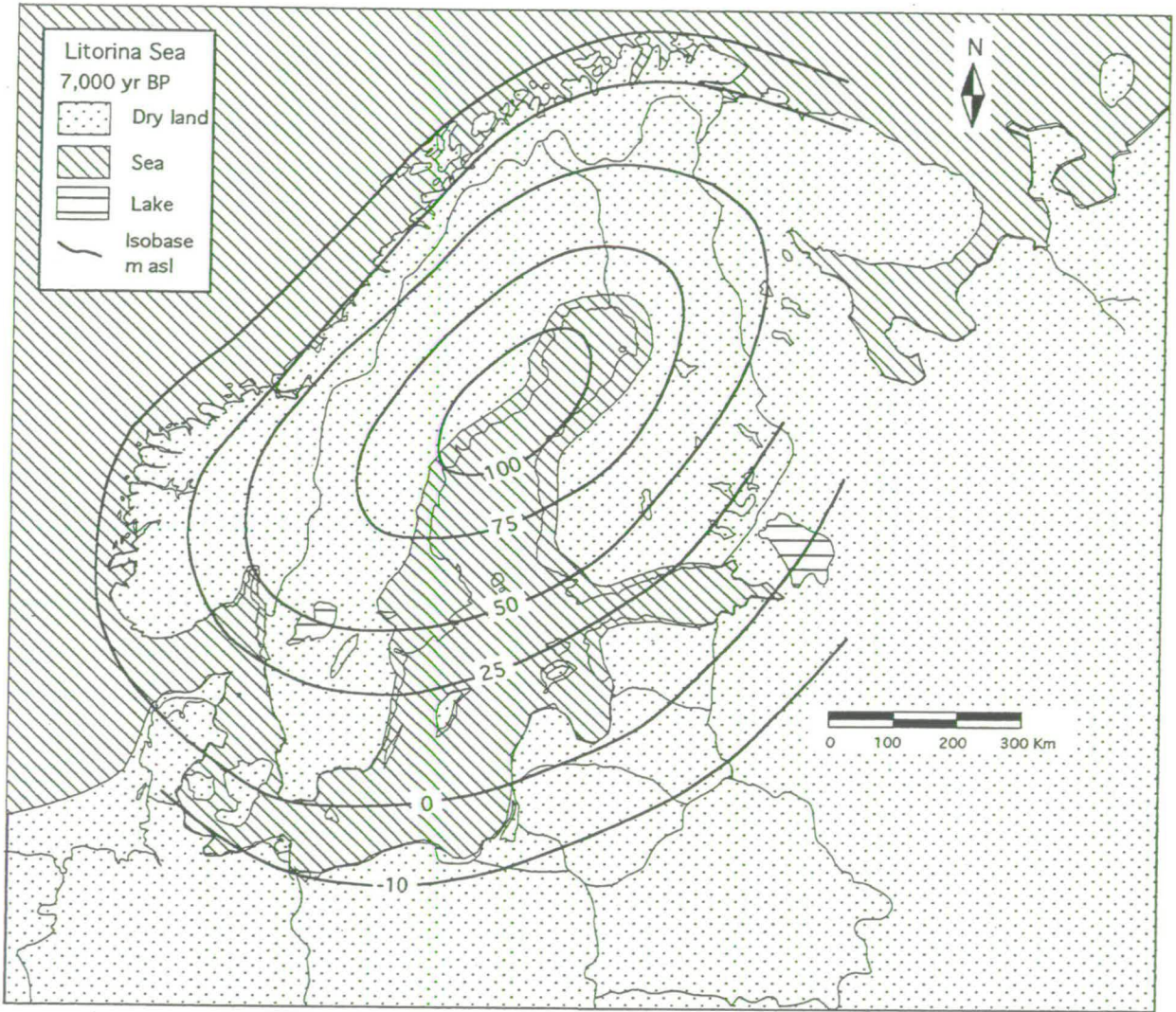


Fig. 2.21 Geographic reconstruction and uplift pattern of Northwest Europe at 7,000 yr BP. Land/water distribution based on Eronen (1983).

The Ancylus transgression was followed between ca. 9 ka and 8.5 ka BP by a sharp regression. Between 8.5 and 8 ka BP the regression slowed down, probably as a result of a lower rate of land uplift. Sometime during this period the direct connection between the Baltic Basin and the oceans was restored. This was caused by the ocean level rising above the threshold of the Danish Straits. Salt water again entered the Baltic Basin and brackish diatoms reappeared in the sediments. This marks the beginning of the Litorina Sea. The early Litorina Sea was dominated by a transgressive phase which influenced the entire southern Baltic Basin (Fig. 2.21). According to Hyvärinen (1982), the 34 m isobase is the limit below which the Litorina Sea was transgressive. The transgression was caused by the gradual slowdown in land uplift and rise in eustatic sea level.

After 6.5- 6.0 ka BP, a regressive trend started because the eustatic sea-level rise virtually stopped and land uplift prevailed once more. In the southern Baltic and south Sweden there is evidence for short-lived transgressive periods of a limited extent (Miller, 1982; Agrell, 1979). On the whole, the regressive trend remained dominant in the Baltic Basin and continues up to the present-day, albeit at a decreasing rate.

The palaeo-geographic maps of Fennoscandia (Figs 2.16 to 2.21) summarise the spatial pattern of land uplift for a number of periods. They also provide insight into some of the conditions that prevailed during different stages of deglaciation. The land/water distribution is partly based on earlier work from Eronen (1983). The isobases are drawn on the basis of the collected RSL curves (Appendix A).

Although the topography shown is only schematic, these maps give a good overall view of the land/water distribution for during these periods. They also enable us to estimate the depth of the water standing at the ice-sheet margins. Figure 2.15 shows the RSL curve for the Helsinki area (Alhonen, 1979). According to Donner (1969), the BI level only occurs in the Salpausselkä I ridge, while level BIII is restricted to Salpausselkä II. The drainage route that opened up through central Sweden at the end of the Baltic Ice Lake phase (10.2 ka BP, BIII-level) was accompanied by a sudden drop in water level of about

28m (Donner, 1983). The eustatic sea level during that period was approximately -35m. This implies that the lake level during the latest stage of the Baltic Ice Lake was ca. -7m. asl.

Because RSL curves reflect the local changes in relative sea level, it is straight forward to estimate the local water depth during deglaciation around the Baltic Basin. The local water depth during a particular period can be obtained by subtracting the total relative uplift from the present-day altitude. During the BIL phase (Fig. 2.16) at 12 ka BP, the 125 m isobase runs close and approximately parallel to the present-day Finnish coast. This implies that the ice sheet terminated in approximately 125 m of water. To the south this increased to about 150m in the Finnish Gulf and then rapidly decreased towards Estonia. To the west, the water depth reached approximately 225-250 m in the deepest parts of the Baltic Basin. Here too, the water depth decreased rapidly towards the south. South Sweden was dry and bordered by 225-250 m deep water to the east and over 500 m deep water to the west (the Skagerrak). The isobases in the Atlantic and in the Baltic could not be connected because the lake levels were too high compared with the ocean levels.

Figure 2.17 shows the palaeo-geography and uplift pattern around 10.5 ka BP. The ice had retreated considerably over Sweden but no connection with the ocean had been established as yet. The continued uplift of the Danish Straits, which functioned as an outlet, caused lake levels to rise from 11 ka BP onwards (Alhonen, 1979) (see Fig. 2.15). The water depth around Lake Ladoga was approximately 65 m. In Finland the water depths in front of the ice sheet were around 115m in the southeast and around 150m in the south, assuming that the ice-sheet margin was grounded at or near the present-day 50 m contour. In the Baltic Sea water depth was 225-250 m. In the northeast a lake is present in the White Sea (Eronen, 1983).

Around 10.2 ka BP the BIL phase ended when the Baltic and the Atlantic became connected via central Sweden (Agrell, 1979). The water level in the Baltic fell sharply, approximately 28m according to Donner (1983). Figure 2.18 shows the situation at ca. 10 ka BP. The connection with the ocean resulted in a reduction of water depths around the ice sheet. In south Finland to around 50 m and in the Baltic to approximately 200 m. To the east, the land has risen

above sea level. The uplift pattern along the Atlantic Coast is much the same as during the BIL stage, however, in the Baltic area the pattern is quite different. The 0 isobase migrated north and maximum uplift was reduced to 100 m. Along the southern Baltic Coast, a subsidence belt was present. In the northeast, the White Sea became reconnected to the Barents Sea.

Following the rapid post Younger Dryas retreat, uplift rates increased, which is shown in Fig. 2.19. During the Yoldia Stage, water in the Baltic became brackish as a result of marine influence (Eronen and Haila, 1982). The Danish Straits were still closed and the marine influence entered through Sweden. Despite higher uplift, water depths in Finland fell as the ice sheet retreated over higher ground. In the Bothnian Gulf, the water depth was approximately 250/275 m. In Sweden ice retreated mostly over dry land. Along the Atlantic Coasts the isobases are further apart than during the previous stages as the rapid uplift which followed deglaciation gradually slowed down.

Figure 2.20 shows the culmination of the Ancylus transgression, the brackish influence had disappeared and it is not clear whether the lake overflowed through Sweden or the Danish Straits (Glückert and Ristaniemi, 1982). Figure 2.15 suggests that the lake level was no more than 10-15 m above the contemporaneous ocean level. Only a small part of the ice sheet remained, clinging to the eastern flank of the mountains. The very rapid retreat resulted in extremely high uplift rates. The centre of uplift is situated over the Swedish Bothnian Gulf coast. Here the total ice thickness was largest as a result of its topographic position in the centre of the Baltic Shield depression. Water depth in the Bothnian Gulf was well over 300 m. All low-lying areas around the Bothnian Gulf were submerged. The uplift to the west of the mountains was relatively modest, implying that the ice sheet was not particularly thick over the Scandinavian mountains.

The isobase patterns during the different periods clearly show the differences in retreat pattern of the southern margin compared to the western margin. In Figs 2.16 and 2.17 the picture is distorted by the higher BIL lake level. However, the spacing of the isobases is much wider to the south than it is to the west. In the west, deglaciation had just started and uplift rates were very high. In the south, deglaciation had started thousands of years earlier and the initial rapid

uplift phase had long since passed. Only in central Sweden and south Finland, close to the retreating margin, the spacing became closer. This effect is most conspicuous in Figs 2.18 and 2.19. The closely spaced isobases along the Atlantic coast spread out over the Skagerrak and the Baltic Basin.

### *Summary*

The reconstruction of the palaeo-geographic setting of the retreating Scandinavian Ice Sheet shows that substantial water bodies existed to the south and east of the ice sheet. Over Sweden and most parts of Russian Karelia, ice retreated mostly over dry land or through shallow water. But in south Finland and especially the Baltic Sea and Bothnian Gulf, water depths were considerable. The deep water must have affected the behaviour of the Baltic Ice Stream and the rapid retreat may be partly a result of increased calving at the terminus. The very rapid disintegration of the ice sheet after 9500 years BP is undoubtedly partly the result of the buoyancy effects of the water mass on the rapidly thinning ice sheet.

It is interesting that the Norwegian southwest coast also shows this rapid uplift and that the zero isobase is close to the coast. If the Scandinavian ice sheet had crossed the Norwegian Channel into the North Sea, one would expect the isobases in this region to be considerably wider apart. The isobase patterns suggest that if the ice sheet crossed the Norwegian Channel, the ice stopped being grounded at a very early stage in the deglaciation. In the Skagerrak area (-500 m asl), the isobase pattern suggests that the ice did cross to north Denmark but that deglaciation was more rapid here than along the west coast of mainland Norway.

Another interesting feature is the isobase pattern in the Lake Ladoga area. In Fig. 2.17 this pattern coincides with the deglaciation isochron pattern (Fig. 6.1) in that the easterly ice-sheet margin bends sharply to the northeast in this region. In the Finnmark area and along the north coast of Kola, the isobases indicate that ice occupied at least a part of the Barents Sea shelf area. The lack of data in this region preclude the deduction from the uplift pattern alone that the Fennoscandian and Barents Sea Ice Sheets coalesced.

## Chapter 3

### Remote sensing and geomorphology

#### 3.1 Introduction

The objective of this study was to map glacial linear bedforms over entire Fennoscandia in order to reconstruct the ice-flow patterns and glaciodynamics of the Scandinavian Ice Sheet. The only method to carry out such a comprehensive mapping programme over such a large area is by using remote-sensing techniques. In this chapter the advantages and disadvantages of the most commonly used and widely available remote sensing-systems are described briefly, and an overview is given of the systems that were used in this study.

#### 3.2 Spectral sensitivity of different remote-sensing systems

Figure 3.1 shows the spectral sensitivity of several remote-sensing systems. For Landsat MSS, the sensitivity is confined to the visible light and near infra-red wavelengths. The Landsat TM system includes bands in the middle infra-red and the thermal infra-red. Figure 3.2 shows the reflectance of some earth-surface materials in the visible and near to middle infra-red range. The reflectance is the percentage of incoming light that is reflected back. An object that has a high reflectance will show up clearer on the image than an object that has a low reflectance. In the near infra-red, the reflectance of vegetation is at an optimum, dropping strongly for both higher and lower wavelengths. The reflectance of soils is higher for wavelengths in the middle infra-red range (Swain & Davis, 1978).

Linear features will show up on an image because of their different reflectance characteristics compared to the immediate surroundings. These differences in reflectance are caused by differences in vegetation, moisture content and material characteristics. By far the best results for our purpose were obtained using the bands in the near infra-red range.

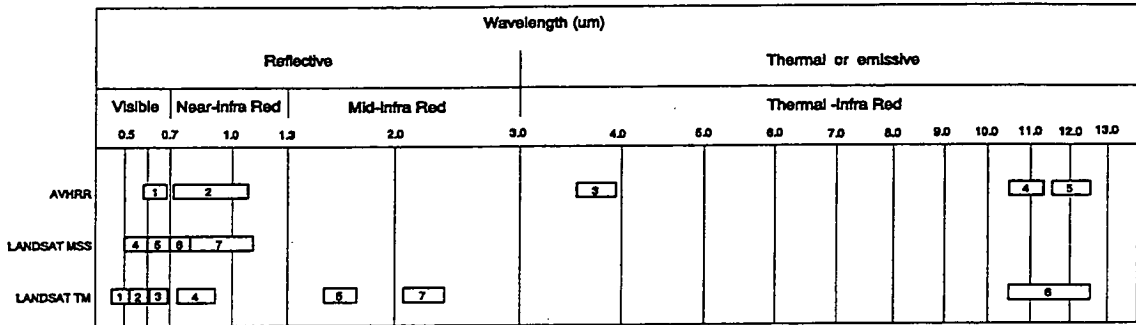


Fig. 3.1 Spectral sensitivity of AVHRR, Landsat MSS and Landsat TM. (After Lillesand and Kiefer, 1987).

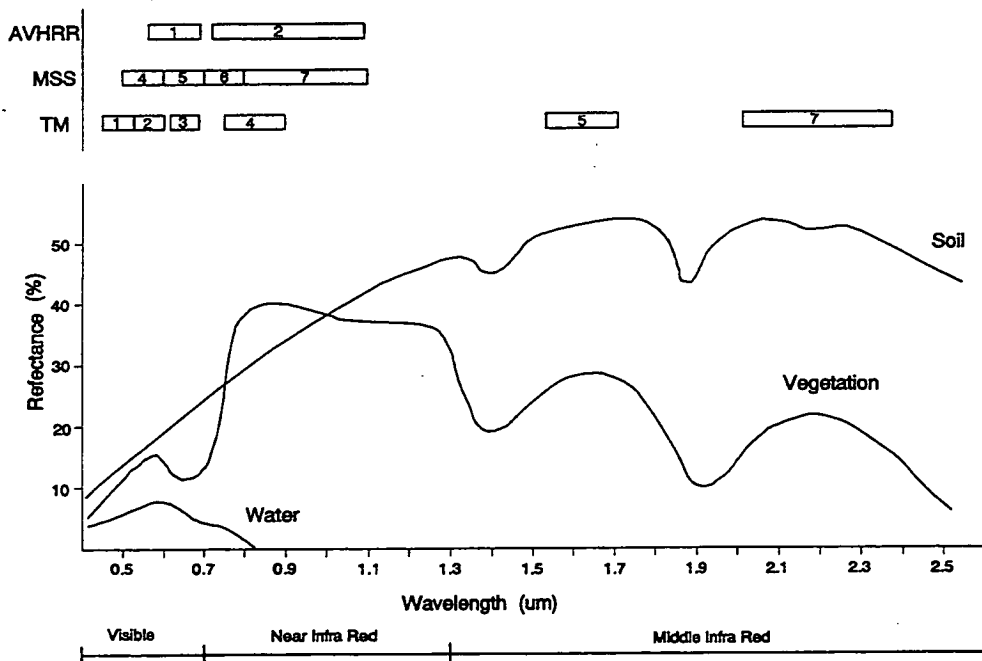


Fig. 3.2 Spectral reflectance characteristics of common earth-surface materials in the visible and near-to-middle infra-red range. The positions of the spectral bands of AVHRR, Landsat MSS and Landsat TM are shown at the top. (After Swain and Davis, 1978).

### 3.3 Resolution versus Instantaneous Working Area

Table 3.1 shows the resolution and instantaneous working area (IWA) of different remote-sensing systems. Aerial photographs have the advantage of a very high resolution: 5 m for aerial photographs on a 1:150,000 scale, compared to 30 m for Landsat TM and 80 m for Landsat MSS. The higher resolution of aerial photographs makes it possible to perform a more detailed mapping of glacial linear features. Table 3.2 shows some dimensions of glacial linear features. Figure 3.3 shows the size of the features that can be observed using different remote-sensing systems. The size of the smallest observable features is determined by the resolution of the system, while the IWA limits the size of the largest features that can be observed. The lower half of the figure shows the length and width scales of the glacial linear features. Using 1:150,000 aerial photographs, it is possible to pick out linear features the size of small flutes. Using Landsat MSS this is impossible, the smallest observable features are the size of small drumlins.

A major disadvantage of aerial photography for this type of study is its small IWA. The 30 by 30 km IWA for a 1:150,000 aerial photographs compares to the 185 by 185 km IWA for Landsat imagery. The obvious problem is that to map the same area covered by one satellite image, at least 36 aerial photographs might have to be studied (in the ideal case of zero overlap) which is both expensive and time-consuming.

The limited IWA of aerial photographs has other drawbacks as well. The small IWA limits the size of the linear features that can be recognised. Although in theory it is possible to see large megadrumlins on 1:150,000 aerial photographs (Fig. 3.3), in reality it is very often impossible to see features that are of the same order of magnitude as the IWA (Lillesand & Kiefer, 1987).

So, although aerial photographs have the advantage of providing more detail, they tend to be of limited use for mapping large linear features. Moreover, on the ice-sheet-wide scale this study is interested in, not just mapping of individual features is important, but even more so the possibility to recognise the spatial patterns in which they occur. It is far easier to understand the spatial relations of large quantities of lineations on a large IWA than on a small

Table 3.1 Areal coverage and resolution of several remote-sensing systems.

Type	Resolution (m)	Instantaneous Working Area (IWA) (km)
Airphotos	5	30 * 30
Landsat TM	30	185 * 185
Landsat MSS	80	185 * 185
Landsat MSS Mosaics	80	500 * 500
AVHRR	1100	3000 * 3000

Table 3.2 Dimensions of glacially streamlined landforms (After Rose, 1987).

Type	Length (m)	Height (m)	elongation ratio (l/w)
Flute	< 100	< 3	> 4
Megaflute	> 100	< 5	> 4
Drumlin	> 200	> 5	< 4
Megadrumlin	> 1000	> 10	< 4
Streamlined Hill	> 1500	> 50	< 4

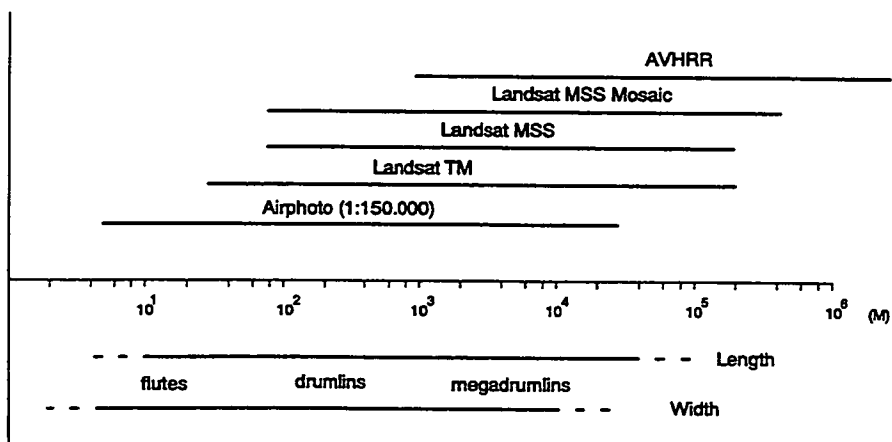


Fig. 3.3 Comparison of the resolution and areal coverage of remote-sensing systems with the dimensions of glacially streamlined landforms. (After Clark, 1990).

one. On the Landsat images drumlin swarms show up clearly and it is far easier to see their spatial coherence. The spatial coherence and continuity of a large-scale diverging flow within a marginal lobe that is 200 km wide, will not be readily recognised on individual aerial photographs that cover only 30 by 30 km areas. So, although detail is lost, the use of Landsat images has a number of distinct advantages.

### 3.4 Imagery used

Figure 3.4 shows the coverage of the Landsat mosaics, the Landsat TM and MSS satellite pictures and the black & white aerial photographs used in this study. For Finland, Karelia and the Kola peninsula, complete coverage by Landsat MSS images was available (Fig. 3.5). Each image covers an area of 185 by 185 km. The resolution of Landsat MSS images is approximately 80 m. Four Landsat TM images were available for north Finland and north Karelia, covering the area just north of the Bothnian Gulf and all the way towards the White Sea. Their better resolution (30 m) enabled more detailed mapping in this area.

For the basic interpretation of the glacial linear bedforms black and white photocopies of the Landsat MSS images on a 1:400,000 scale were used. For Sweden and Norway, individual Landsat MSS or TM images were not available, instead photographic mosaics of the Landsat MSS images were used. These mosaics are on a 1:1,000,000 scale. The resulting reduced resolution of these mosaics sometimes precluded working out the relative age relations between different lineation directions. Therefore, it was decided to order 1:150,000 black and white aerial photographs for several selected areas (Fig. 3.4), for which knowledge of the relative age relations was crucial.

In addition, the interpretations of the aerial photographs were compared with those of the Landsat mosaics to check whether the diminished resolution had affected the result. The result was encouraging in that all main lineation directions mapped from the aerial photographs were also recognised on the Landsat mosaics.

**Fig. 3.4**  
**Remote-sensing imagery**  
**used in this study.**

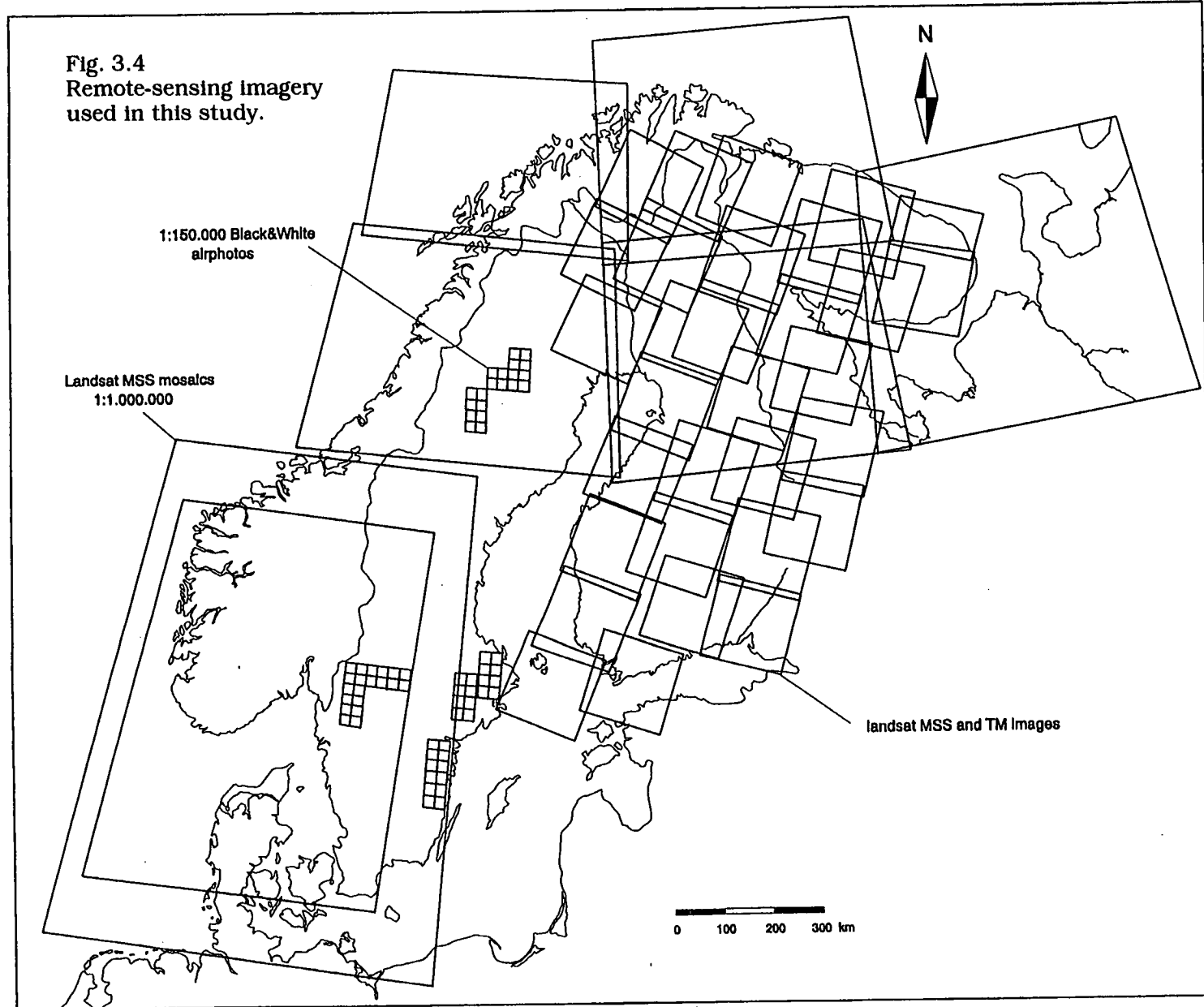
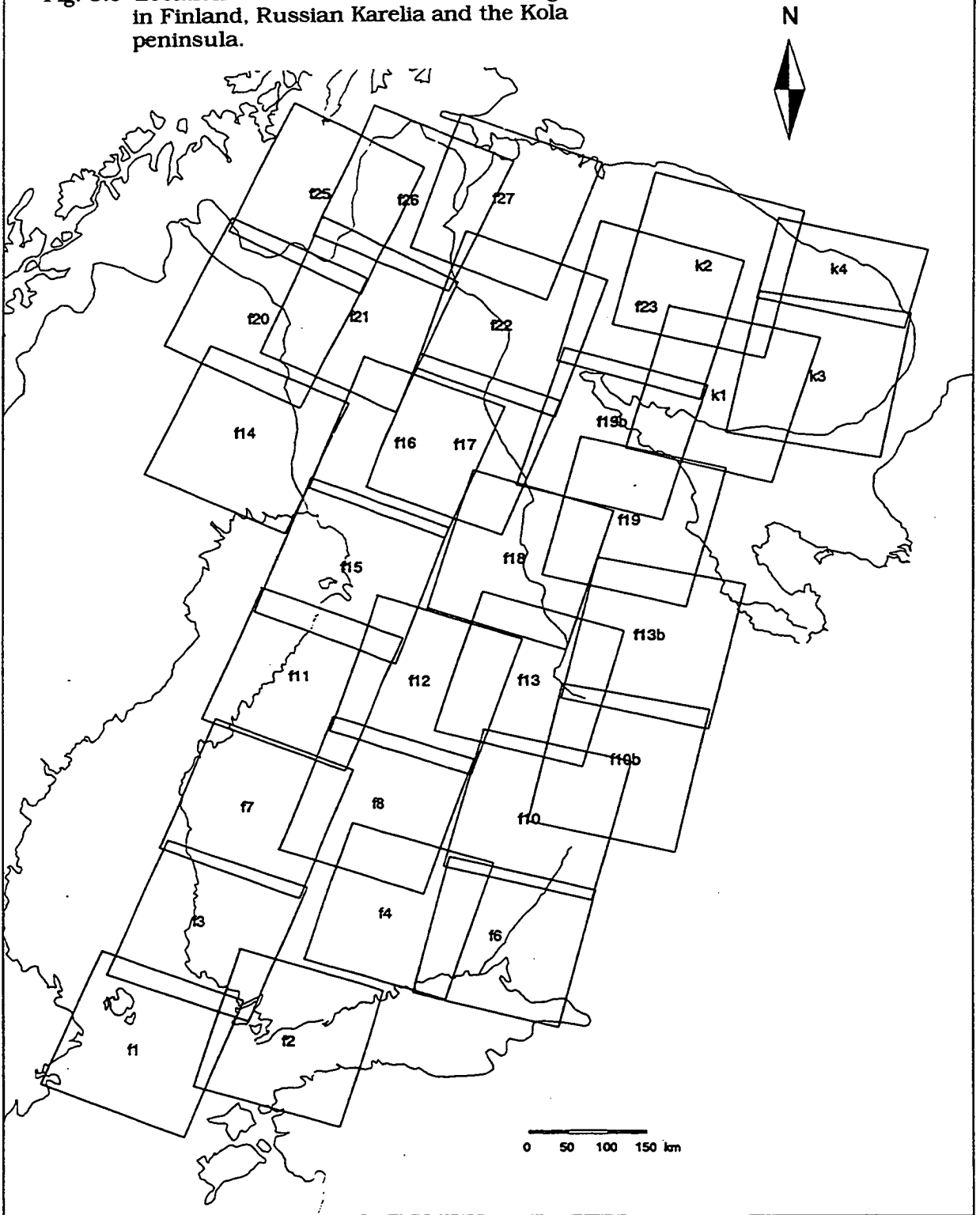


Fig. 3.5 Locations of Landsat MSS and TM images in Finland, Russian Karelia and the Kola peninsula.



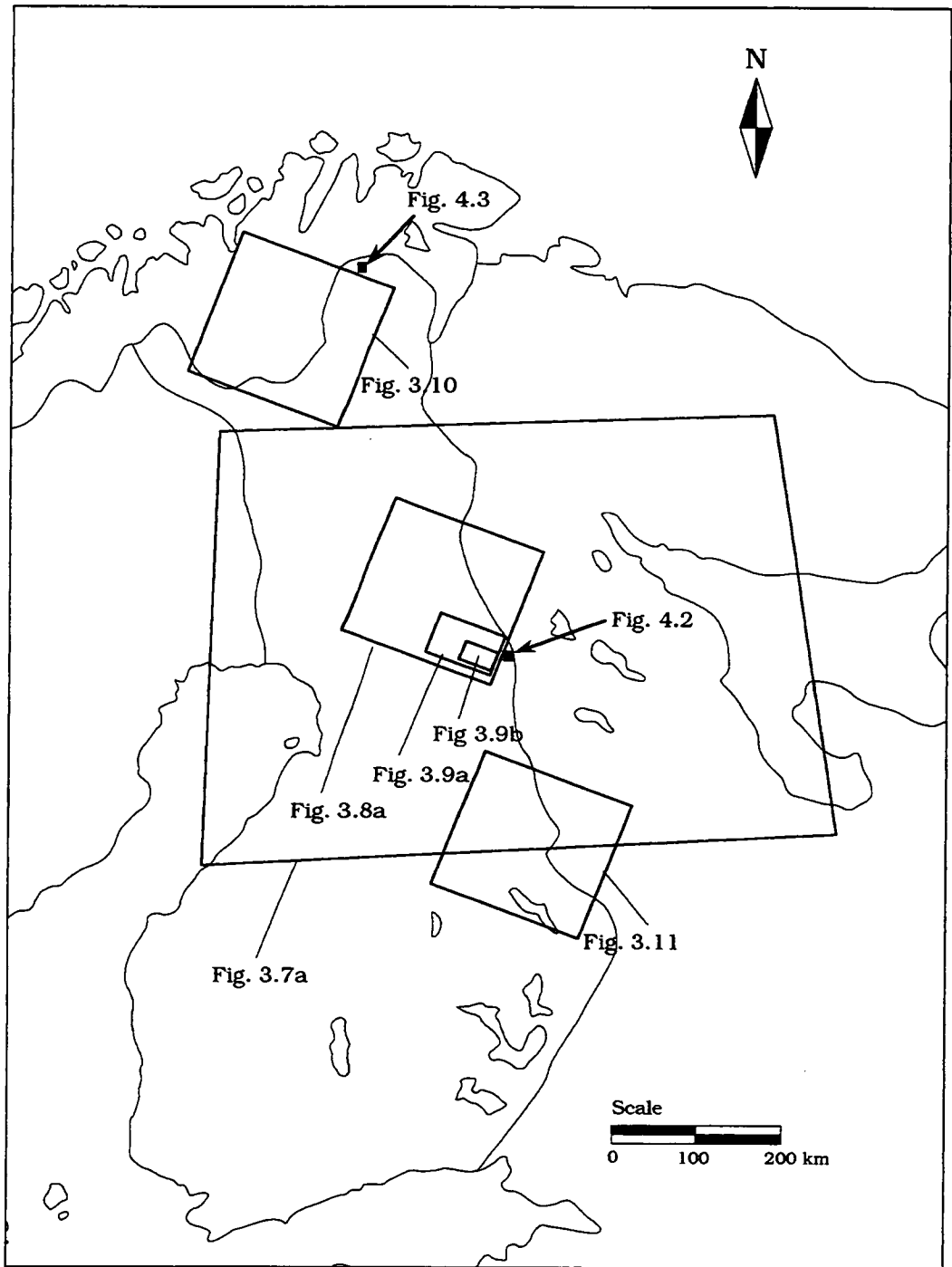


Fig. 3.6 Locations of images shown in Figs 3.7-3.11, 4.2 and 4.3.



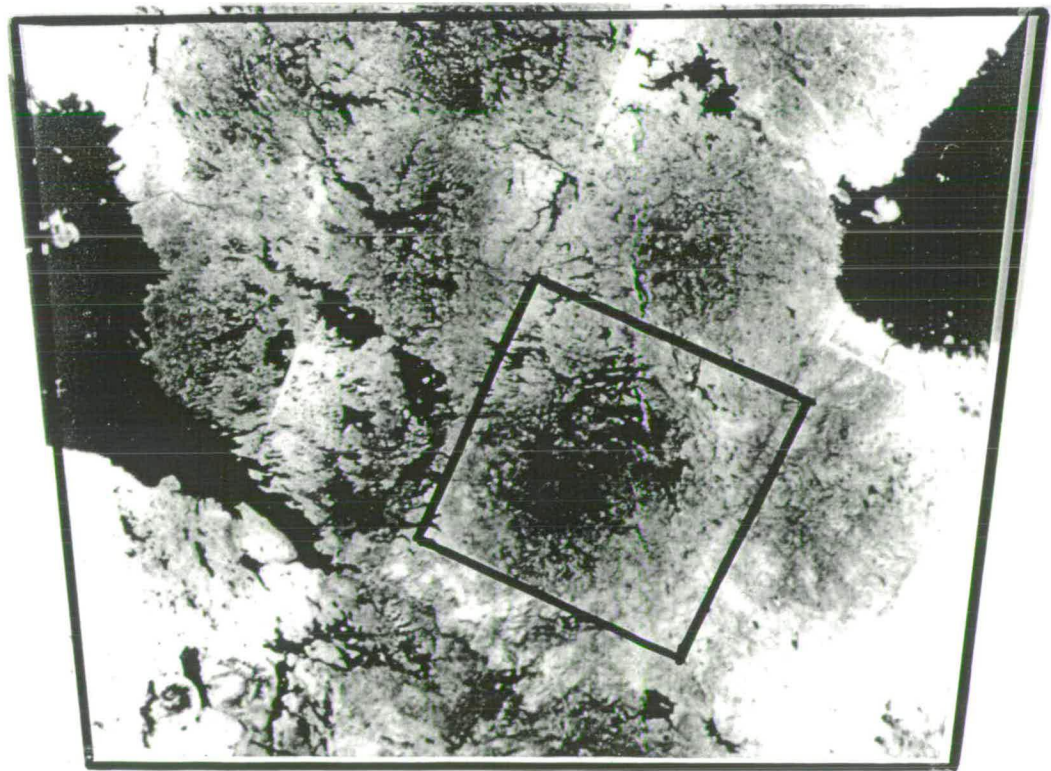
For this study features and patterns greatly varying in sizes have been mapped. From lineations of tens of metres, via 200 km wide fan systems, to ice-sheet-wide flow patterns. In Figs 3.7 to 3.9 some examples are shown of the different scales of imagery used. The locations of these examples are shown in Fig. 3.6.

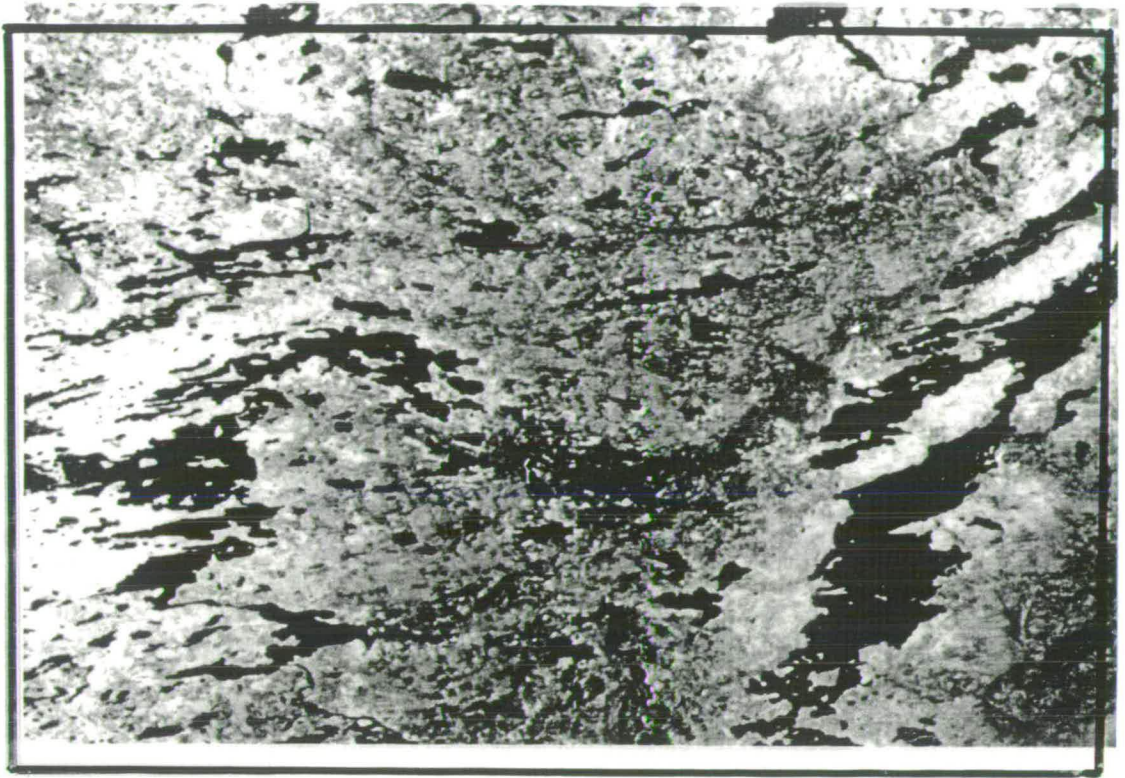
Figures 3.7 to 3.9 show a number of consecutive enlargements, the scale of which increases in three steps from 1:4,800,000 (Fig. 3.7a) to 1:250,000 (Fig. 3.9b). Unfortunately, the reproduction quality of some of the photographs is poor, so much of the detail is lost. However, they still provide an indication of the different scales this study deals with.

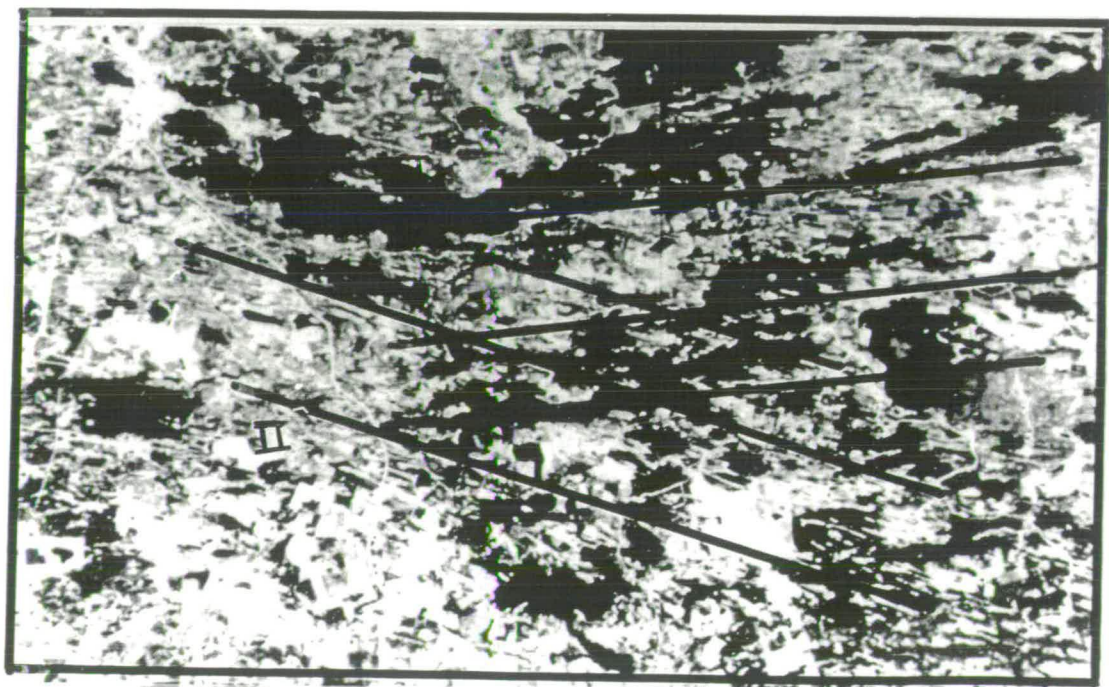
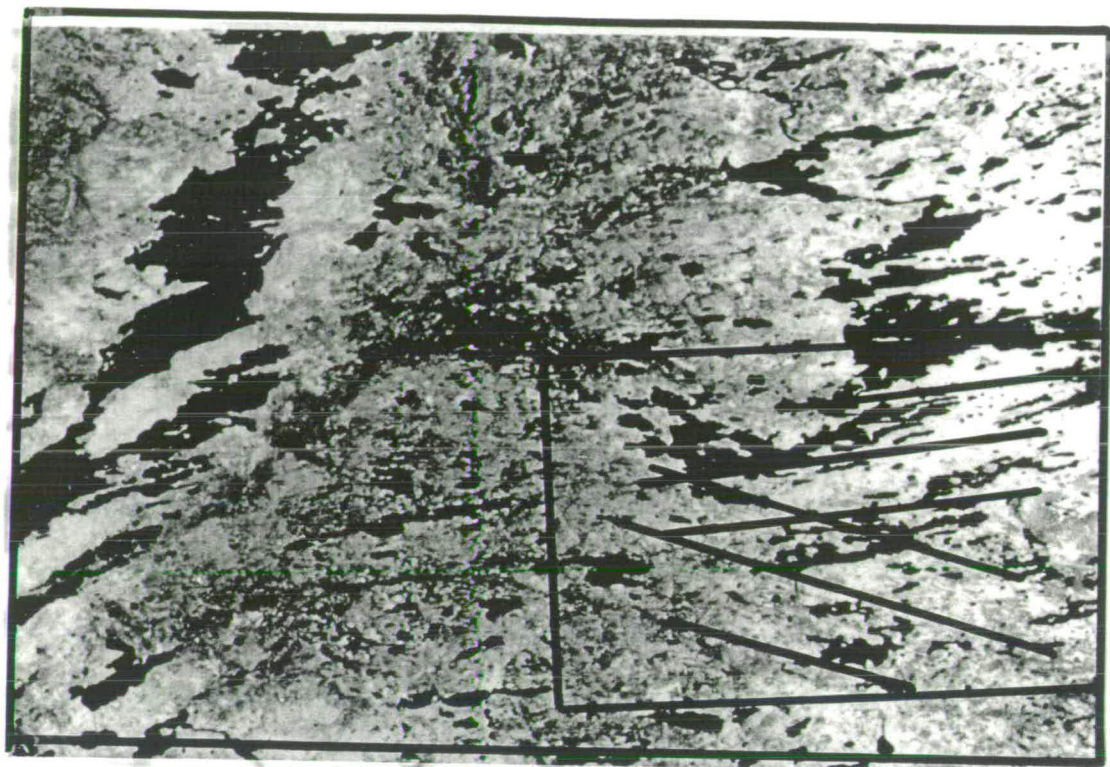
Figure 3.7a shows a Landsat MSS mosaic covering an area of 480 by 600 km in north Finland and north Karelia. In the lower left corner the Bothnian Gulf can be seen and in the upper right the western half of the Kola peninsula, see Fig. 3.6 for location. Figure 3.7b is an enlargement of part of Fig. 3.7a. This is the full IWA of a Landsat image, 185 by 185 km. The same image is shown in Fig. 3.8a. Figure 3.8b is an enlargement of the Landsat image 3.8a. It covers an area of approx. 53 by 75 km. The same image is shown again in Fig. 3.9a. Finally, in Fig. 3.9b the maximum resolution of the Landsat TM image is reached. This picture covers an area of 24 by 37 km.

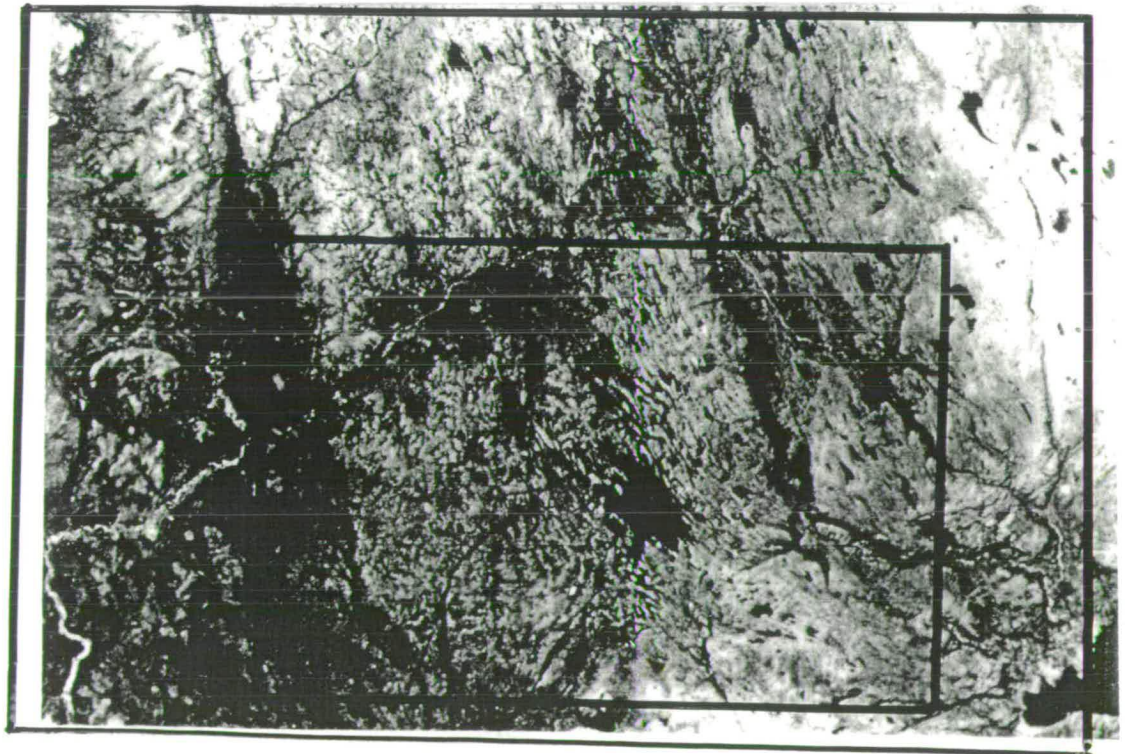
In Fig 3.9a, sets of linear features which have different orientations can be observed. One set is oriented W-E (Flow I) and another set is oriented WNW-ESE (Flow II). The ice-flow directions were from the W and WNW. In Fig 3.9a and b it can be seen that the scale of the individual features that make up the two sets differs strongly. Flow I is made up of large, relatively narrow features that continue for several kilometres. The lineations are sometimes discontinuous but can be seen to line up in a W-E direction. Flow II on the other hand is composed of features of 100 of m's in length that are sometimes superimposed on the Flow I lineations. Flow I lineations are in places reshaped by the younger WNW-ESE flow.

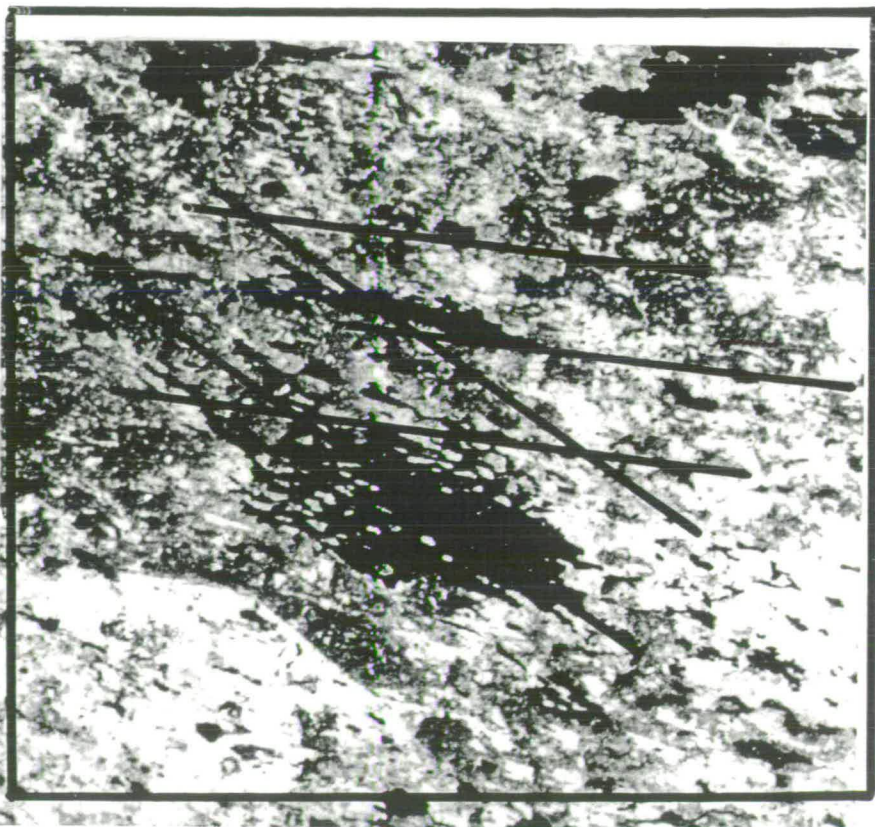
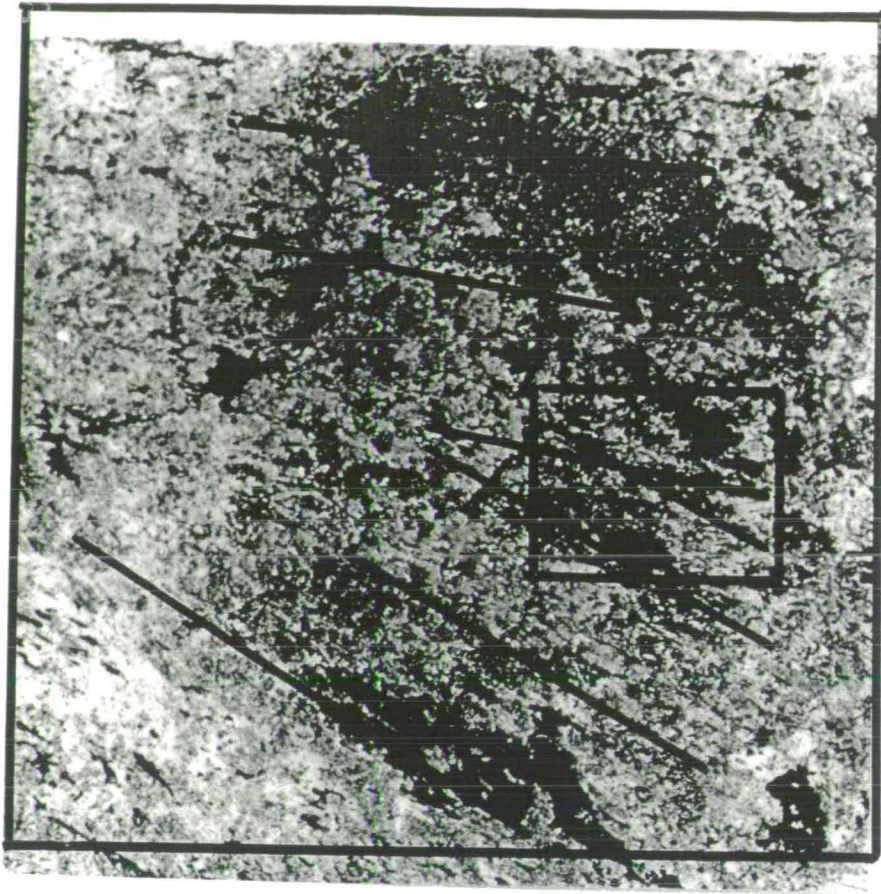
- 
- Fig. 3.7 a,b (p. 53) Landsat mosaic of north Scandinavia and enlarged area,  
see Fig. 3.6 for location and scale.  
Fig. 3.8 a,b (p. 54) Landsat TM image and enlarged area,  
see Fig. 3.6 for location and scale.  
Fig. 3.9 a,b (p. 55) Detail of landsat TM image and enlarged area,  
see Fig. 3.6 for location and scale.











## Chapter 4

### Subglacial streamlined bedforms

#### 4.1 Introduction

In this chapter the morphology and formation of glacial landforms is discussed. In section 4.1 different landform types are described. The streamlined landforms are the most interesting as these are accurate and widespread indicators of the ice-flow direction. The conditions required for the formation of subglacial lineations are reviewed in section 4.2. These pre-conditions are important as they enable us to reach conclusions concerning the thermal and glacio-dynamic conditions of the ice sheet during the formation of lineations. In section 4.3 superimposition of younger lineations on older ones is discussed, this enables the determination of relative age relations between different generations of lineations.

Landforms associated with glacial processes display a wide variety of shapes, sizes and sedimentary assemblages. Because of this variety there are numerous ways to classify sedimentary glacial landforms. The classification used here is based on Prest (1968) and has been modified by Sugden and John (1976). This classification describes landforms in terms of their genesis within the glacial system (see Table. 4.1). The classification distinguishes linear and non-linear features. Both types can be deposited subglacially or at the ice margin. Within the group of linear features a distinction is made between those landforms that are parallel to the ice flow and those that are transverse to it.

#### *Subglacial, longitudinal features*

Subglacial, ice-parallel, linear features range in size from small flutes (several metres in length, decimetres in height) to megadrumlins the length of which can be of the order of tens of kilometres and which can be tens of metres high. The sedimentary composition of these bedforms is highly variable. They may consist solely of till or of stratified sediments. In general, however, they contain varying amounts of both till and stratified sediments. In many areas linear bedforms contain a core of bedrock, often at the upstream side. Lineations

Linear features		Non-linear features
Parallel to ice flow (controlled deposition)	Transverse to ice flow (controlled deposition)	Lacking consistent orientation (controlled or uncontrolled deposition)
Subglacial forms with streamlining: (a) Fluted and drumlinized ground-moraine (b) Drumlins and drumlinoid ridges (c) Crag and tail ridges	Subglacial forms: (a) Rogen or ribbed moraine (b) De Geer or washboard moraine (c) Kalixpinnmo hills (d) Subglacial thrust moraines (e) Sublacustrine moraines	Subglacial forms: (a) Low-relief ground moraine (b) Hummocky ground moraine
Ice-pressed forms: longitudinal squeezed ridges	Ice-pressed forms: minor transverse squeezed ridges and corrugated moraine	Ice-pressed forms: random or rectilinear squeezed ridges
Ice marginal forms: lateral and medial moraines, some interlobate and kame moraines	Ice front forms: (a) End moraines (b) Push moraines (c) Ice thrust/shear moraines (d) Some kame and delta moraines	Ice surface forms: (a) Disintegration moraine (controlled) (b) Disintegration moraine (uncontrolled)

Table 4.1 Classification of morainic landforms. (From Sugden and John, 1976).

display a wide variety of shapes (Fig. 4.1) but they all have in common that they are elongated in the direction of ice flow. The direction of lineations tends to be perpendicular to the position of the ice margin.

Linear streamlined bedforms are often the result of accumulation, but erosion and scouring of older till surfaces or other unlithified sediments produces similar forms (Lundqvist, 1990). Fluted ground moraine is an example of this type of landscape. Here the ridge crests are at the same level as the adjacent ground-moraine surface and the origin of these fluted ground moraines is most likely erosional. In an drumlinized ground-moraine landscape the ridge crests are higher than the surrounding moraine surface and accumulation is thought to have played a major role (Prest, 1968).

Areas of linear streamlined bedforms show up in a very distinct manner on aerial photographs and satellite images. The morphology is very smooth and regular and is often dominated by an dense pattern of elongated forms. In most cases it is evident that the entire area was shaped and remoulded by moving ice.

#### *Subglacial, transverse features*

Rogen or ribbed moraines are subglacial, transverse linear features dominated by large-scale lineaments (several kilometres wide) that are perpendicular to the ice-flow direction. The lineaments give a ribbed, irregular appearance to these landscapes. The ridges are made up of a complex of crescentic parts, the convex side of each of which is pointed upstream (Lundqvist, 1990). These moraines are often found in close association with ice-parallel bedforms such as flutes and drumlinized till. Both types of bedforms seem to merge into one another. They are often found in depressions of till sheets or in broad bedrock valleys.

De Geer moraines often occur as a succession of discrete, narrow ridges, ranging from short and straight to long and undulating. De Geer moraines are often more delicate than Rogen moraines and may be spaced regularly, up to 300m apart. According to Prest (1968), De Geer moraines form some distance behind a calving ice-sheet margin. They tend to be roughly parallel to the ice-sheet margin. De Geer moraines are numerous in north Sweden and south

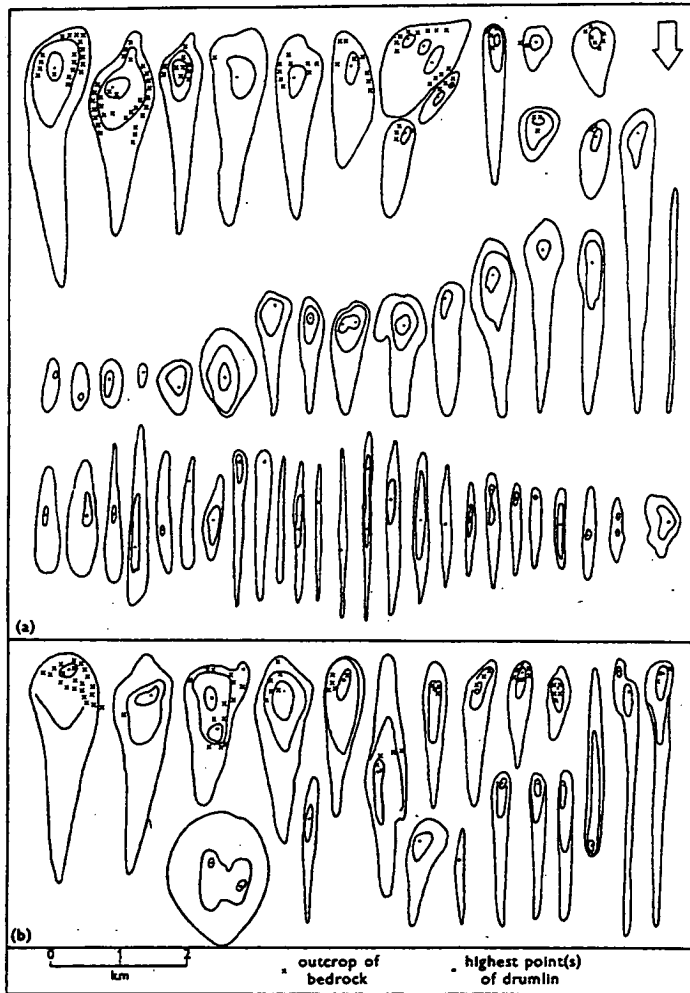


Fig. 4.1 Different types of drumlins. (From Glückert, 1973).

Finland, both areas where calving margins were active during deglaciation (see section 2.3). The De Geer moraines in these areas are developed as discrete, regularly spaced ridges. They are the youngest features present and are roughly parallel to the retreating ice margin.

#### *Ice-marginal, transverse features*

End moraines are very variable in size, shape and mode of formation. Till may be the dominant material, but in other settings fluvio-glacial deposits make up the bulk of these features (*e.g.* the Salpausselkä moraines). Push moraines are a special category of ice-marginal, transverse features.

This study focused on mapping the streamlined bedforms for a number of reasons. These bedforms accurately reflect the ice-flow direction. They can be identified readily on aerial photographs and satellite images and are easily distinguished from transverse linear features by their smooth and regular, ice-moulded appearance. They dominate large areas and thus enable spatially continuous mapping of flow directions.

A distinction was made between large glacio-fluvial complexes and (deltaic) end moraines on the one hand and small, discrete transverse ridges on the other. End moraines are useful as evidence of the position of the ice margin. Especially the Salpausselkä moraines were identified easily from satellite imagery. Transverse, subglacial linear features were mapped as well, but have not been used for ice-flow reconstruction as the directions of their long axes may differ considerably from that of the ice margin. In general, it is easy to distinguish streamlined and transverse glacial features, but it is sometimes impossible to distinguish between ice-marginal and subglacially deposited transverse ridges. Therefore, no distinction was made in the interpretations between ice-marginal and subglacially deposited transverse ridges.

## 4.2 Subglacial processes

The exact mechanisms that produce streamlined bedforms are as yet unknown and are the subject of heated debate. Small-scale fluting is generally thought to be produced by water-soaked till that has been squeezed into cavities on

the lee side of (lodged) boulders (Hoppe and Schytt, 1953). But there is far less consensus on the formation of larger scale bedforms. Menzies (1989) distinguishes three groups of hypotheses that have been proposed to explain the formation of large-scale streamlined bedforms.

#### *Deformable sediment*

The first hypothesis centres on the fact that, given the right conditions (high pore-water pressures reducing the effective subglacial pressure), unconsolidated sediment can be deformed by the shear stress exerted on it by moving ice. The deforming sediment is transported along with the ice and is moulded into streamlined bedforms as a result of stress variations underneath the moving ice (Boulton, 1987).

#### *Deformable sediment and anisotropy*

The second hypothesis builds on the above notion of deformable sediment and tries to include more variables. The idea is that drumlin formation is caused by anisotropic conditions within the subglacial sediment. These anisotropic conditions, resulting from differences in dilatancy, pore-water dissipation or localised freezing, are thought to play a vital role in determining where reduced effective pressure will lead to mobilisation of the subglacial sediment (Boulton and Jones, 1979; Aario, 1987; Menzies and Rose, 1987).

Later the idea was expanded and it was proposed that the anisotropy in the ability of subglacial sediments to dissipate high pore-water pressure may result in a continuum of subglacial streamlined bedforms (Boulton, 1987; Menzies, 1989). According to this hypothesis, whether flutes, drumlins, megadrumlins or streamlined hills will develop, depends on other variables that affect subglacial conditions. The critical factors that determine the conditions at the bed of a warm-based ice sheet are related to the capacity of the ice/sediment system to discharge subglacial meltwater and dissipate high pore-water pressure. Boulton and Hindmarsh (1987) distinguished three types of warm-based subglacial bed conditions: the rigid bed; the deforming bed; and the quasi-rigid/quasi-soft bed.

In the first case, ice is underlain by impermeable bedrock or sediments that have such a low permeability that infiltration of meltwater from the ice/bed

interface into the sediment itself is virtually impossible. Thus, in the rigid-bed case, all meltwater has to be drained along the ice/sediment or ice/rock interface. This may lead to high sliding velocities as a result of decoupling of the ice from the bed. The most effective way to discharge meltwater in this case is through tunnels (Rothlisberger, 1972; Shoemaker, 1986; Boulton and Hindmarsh, 1987). A special case of rigid-bed conditions might occur when a basal sediment layer of high permeability overlies an aquifer. This configuration might result in subglacial meltwater to be drained as ground water combining a low pore-water pressure with a high effective pressure.

In the second case, deforming or soft-sediment beds occur where the discharge of meltwater is ineffective and pressurised subglacial meltwater can infiltrate the sediment. This leads to high pore-water pressures and sediment deformation under shear.

The third case, quasi-rigid/quasi-soft beds, encompasses all those situations where both rigid- and soft-bed conditions may occur depending on the other variables that determine the subglacial conditions which vary in time and space. These variables can be local, such as changes in sediment rheology upon deformation (Boulton and Hindmarsh, 1987) or the result of changes on a larger scale. Fluctuations in the stress field, meltwater discharge, ice velocity or ice temperature all play a role in determining whether or not the sediment will deform. This type of bed represents the intermediate case between the rigid and the soft bed and may account for the majority of subglacial settings.

#### *Meltwater action*

The third hypothesis on streamlined bedforms highlights the role of active basal meltwater in drumlin formation. It is argued that streamlined features are, in fact, either the infill of subglacial cavities that formed at the sole of the ice sheet by catastrophic subglacial floods or the result of subglacial meltwater erosion of in-situ sediments (Shaw, 1983; Sharpe, 1987). These ideas are based on the fact that in some areas drumlins consist predominantly of stratified sediments, and that these stratified sediments (diamictons as well as fluvio-glacial material) show no signs of having been deformed by overriding ice.

### *Summary*

In this study a number of assumptions has been made concerning the formation of lineations. They are believed to have formed parallel to the ice-flow direction and perpendicular to the ice margin. To produce lineations, conditions at the base of the ice must be warm and wet for sliding and soft-sediment deformation to occur. The size and density of streamlined bedforms depend on a number of inter-related variables (effective pressure, basal shear stress, sliding velocity, sediment supply and time). The ability or inability of the ice sheet to produce lineations and remould pre-existing sediments will be designated as "basal activity". A high basal activity thus implies that conditions were favourable for lineation formation: low effective pressures, high sliding velocities and the basal shear stress exceeding the soft-sediment shear strength. Thus basal activity is a qualitative description of the ability of the ice sheet to rework its subsurface, by erosion or deposition.

### 4.3 Superimposed linear bedforms

Streamlined subglacial landforms dominate extensive formerly glaciated areas. A recurring zonation has been noticed in the lay-out of glacial landscapes (Aario, 1987; Sugden and John, 1976; Prest, 1968). Prest (1968) described a landscape zonation from the Northwest Territories in Canada where a gradual transition is found from a landscape dominated by drumlins at the outer margin, into a landscape of highly elongated drumlinoid forms; into a drumlinized ground moraine; into a fluted ground moraine; and finally into an inner zone where the till cover is discontinuous and scouring features are dominant. This highly generalised picture of landscape transition has led to the formulation of a depositional model which relates the specific landscape types to specific zones within the ice sheet. In this model, a particular stage during the glaciation (usually the maximum extent) is considered to have produced the majority of landforms (Sugden, 1977)

However, in many areas different types of lineations are found in close association within the same area. Many authors have drawn attention to the fact that smaller lineations can occur superimposed on larger, partly remoulded, older lineations (Rose, 1987, 1989; Heikkinen and Tikkanen, 1989;

Lagerbäck and Robertsson, 1988; Boulton and Clark, 1990; Stea and Brown, 1989).

Heikkinen and Tikkanen (1989) describe the Kuusamo drumlin field in north Finland (Fig. 4.2) where older lineations can be recognised underneath younger drumlins and flutes. The direction of the former deviate in many cases from the latter. In general, smaller flutes show more directional variability than drumlins. The authors attributed this to the fact that the smaller bedforms are formed closer to the ice margin and reflect the lobate character of the margin more closely. The area shown in Fig. 4.2 is close to the one shown in Fig. 3.9b. Although on a different scale, the same two ice-flow directions can be recognised here.

Figure 4.3 shows a fluted ground-moraine surface and drumlins at Utsjoki (see Fig. 3.6) in north Finnish Lapland. The ice-flow direction shifted about  $25^\circ$  to the east after deposition of the drumlins. However, this new flow did not substantially erode the previously deposited landforms. Instead, small grooves and drumlins were formed superimposed on the older landscape.

Stea and Brown (1989) described lobate or reoriented drumlins from Nova Scotia where they could identify two principle axes which were parallel to two different directions of ice movement. Lagerbäck and Robertsson (1988) reported several generations of superimposed lineations from north Sweden. Rose (1987) described examples from Scotland where streamlined bedforms of up to 4 km in length are overprinted by drumlins of up to 300m in length. Rose (1987) related the differences in size of the associated lineations to the thickness of the ice during formation. He suggested that lineations form a continuum in which the largest forms are created underneath the thickest ice and subsequent smaller forms reflect thinning of the ice sheet as the margin approaches.

It seems unlikely that ice thickness in itself is responsible for the formation of different sizes of landforms. The pore-water pressure inside the sediment and the magnitude of basal shear are the vital parameters that determine basal sliding and sediment deformation and they are not solely dependent on ice thickness. The size to which lineations can grow depends on a number of

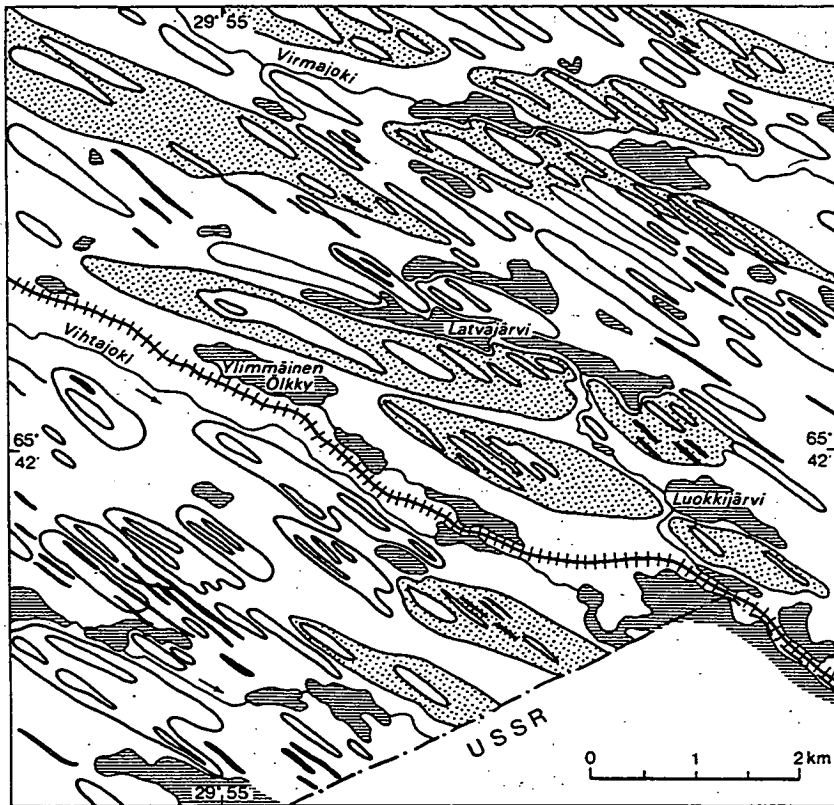


Fig. 4.2 The Kuusamo drumlin field (see Fig. 3.6 for location) where younger flutes and drumlins are superimposed on larger, older drumlins that differ slightly in orientation. 1= old drumlin, 2=young drumlins and flutings, 3=esker, 4= lakes and rivers, 5=border, the North is up. (From Heikkinen and Tikkanen, 1989).

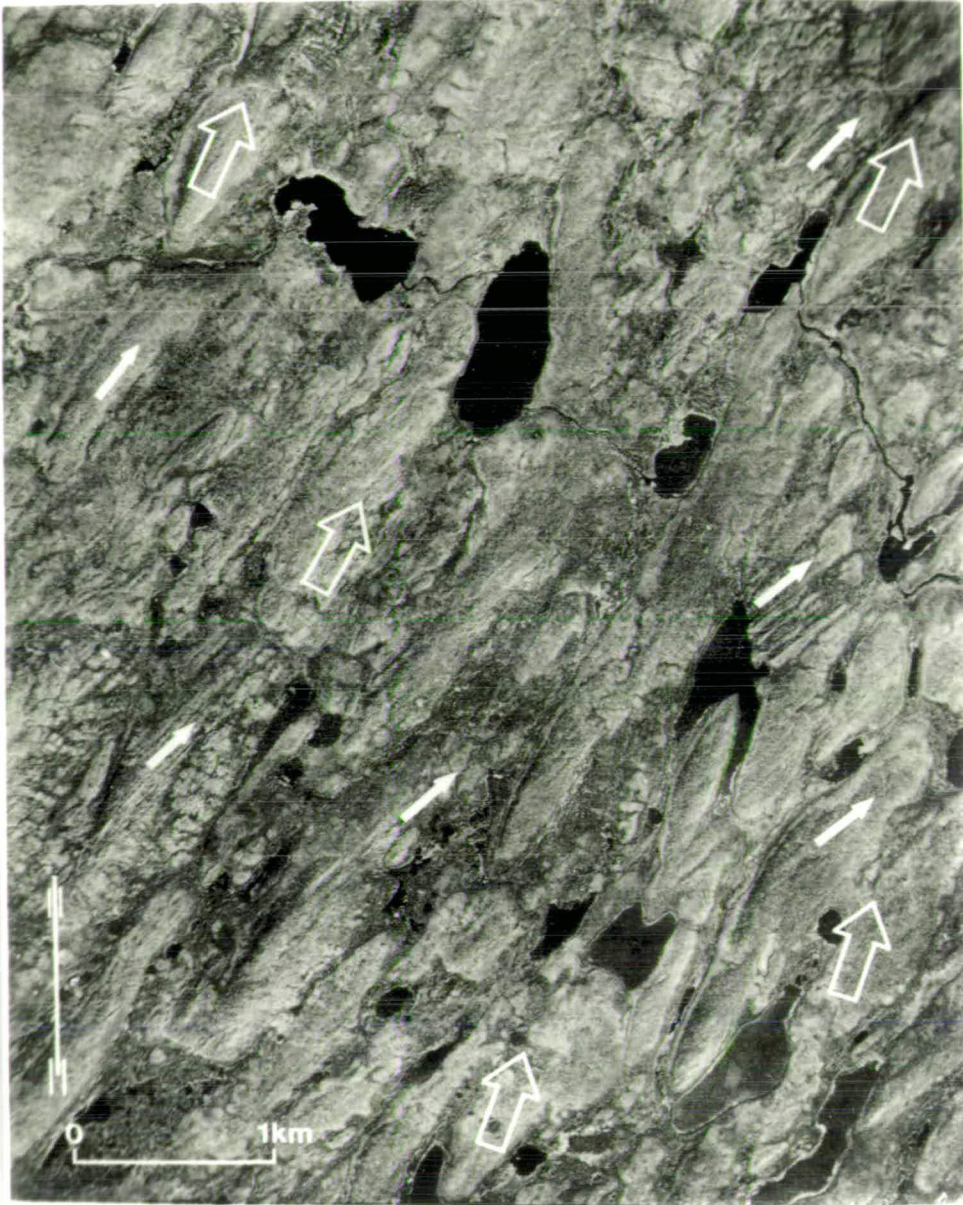


Fig. 4.3 Aerial photograph of fluted moraine surfaces and drumlins at Utsjoki, northern Finland, the North is up (see Fig. 3.6 for location). Ice flow shifted about  $25^\circ$  after deposition of the SSE-NNW trending drumlins. The younger, weaker flow formed superimposed SE-NW trending drumlins, flutes and grooves. (From Kujansuu, 1990).

variables, *e.g.* effective pressure, basal velocity (sliding velocity), sediment supply and time. The first three variables vary within ice sheets but conditions favourable to lineation formation do not follow a simple concentric pattern. Ice velocities can vary laterally as a result of ice streaming. Subglacial water-pressure depends amongst other things on subglacial meltwater production, supra-glacial water reaching the bed and on the permeability of the subsurface. The potential sediment supply is linked to the underlying geology. To attribute the size of lineations to a specific position within an ice sheet seems therefore too simplistic.

Most descriptions of superimposition come from deglaciation areas where the shifts in ice flow can be attributed to changes in ice geometry resulting from the approaching margin. The small, youngest lineations do not necessarily reflect an equilibrium between the above mentioned variables and may be partly the result of a limited period of formation.

### *Summary*

The superimposition of different generations of landforms shows that a shift in ice-flow direction modifies but not necessarily eradicates all previous bedforms. Thus, lineations reflecting older ice-flow directions are sometimes preserved underneath younger generations. Streamlined subglacial landscapes potentially contain records of ice-flow directions that go much further back than the deglaciation phase. The possibility to establish the relative ages of generations of lineations by superimposition was used extensively in this study.

The hypothesis that different types of lineations are formed under certain conditions or are related to specific processes is potentially very important. However, it was decided that basal conditions and processes are still poorly known and that linking lineation types to specific processes or conditions would be too speculative.

## Chapter 5

### Methodology and case studies

#### 5.1 Introduction

This study uses a number of assumptions concerning the formation of lineations. Lineations may be formed parallel to the ice flow, and under temperate basal conditions, by sliding or sediment deformation. Superimposition of lineations can be used to establish relative age relations between different sets of lineations. Coherent lineation patterns are related to dated positions of the ice margin. This provides an estimate of the absolute age of certain flow patterns and enables correlation of ice flows on an ice-sheet-wide scale.

To advance from first-order lineation interpretations to a reconstruction of ice-sheet-wide flow, a number of interpretative steps have been taken. In the following section these steps will be discussed. In the final section a number of case studies are discussed to show how the method works in practice.

#### 5.2 Methodology

In Figs 5.1-5.3 cartoon images summarise the steps required to interpret ice-flow patterns from lineation data. Figure 5.1a gives an example of first-order lineation data. Two directionally continuous, coherent, sets of lineations can be distinguished, one trending NW-SE (flow 1) and one WNW-ESE (flow 2). Flow 1 is also spatially continuous, in that there are no gaps between the related lineations. Flow 2 is only present in part of the area. Ice-flow directions can be reconstructed from the shape of individual lineations (see Fig. 4.1). In Fig. 5.1b the two sets have been interpreted as being related to two ice-flow directions, the relative ages of the two lineation sets are unknown.

Figure 5.1c shows an enlargement of the inset in Fig. 5.1a. The large lineations of flow 2 are overprinted by smaller lineations from flow 1. This relative age

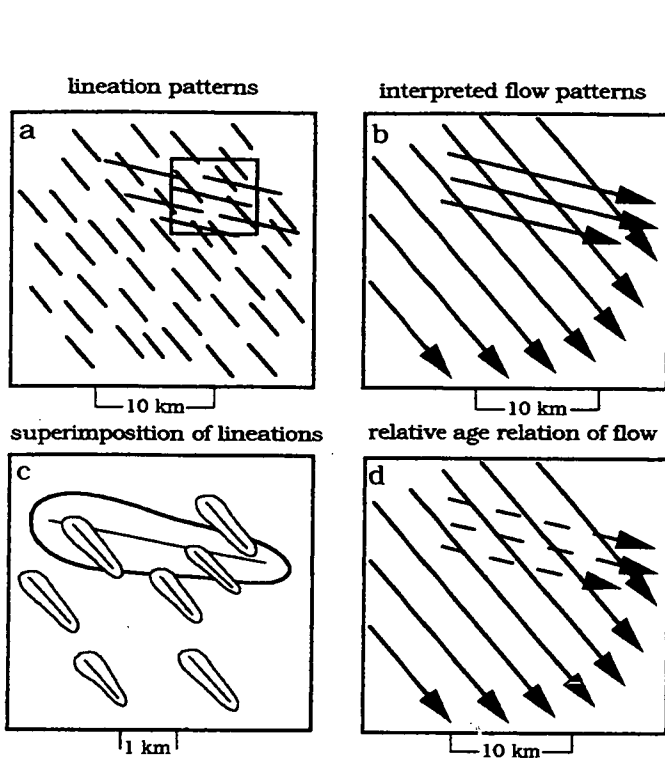


Fig. 5.1  
Cartoon of the interpretation of flow patterns (second-order) from lination data (first-order).

a:  
First-order interpretation of lination data, two coherent, spatially continuous sets of lineations can be distinguished.

b:  
These two sets are translated into two flow systems.

c:  
Shows inset from Fig. 5.1a. Younger, lineations are superimposed on older lination. This enables relative dating of the two lination sets.

d:  
This results in an older flow pattern (dashed lines) overprinted by a younger flow (solid lines).

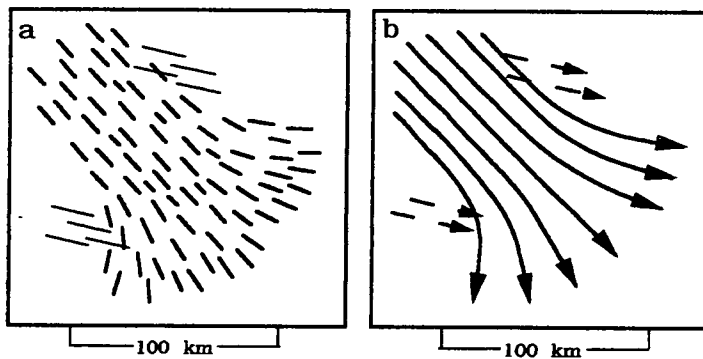


Fig. 5.2  
Cartoon of large-scale organisation of flow systems.

a: First-order interpretation of lination data

b: Interpreted younger flow (fan) and older flow.

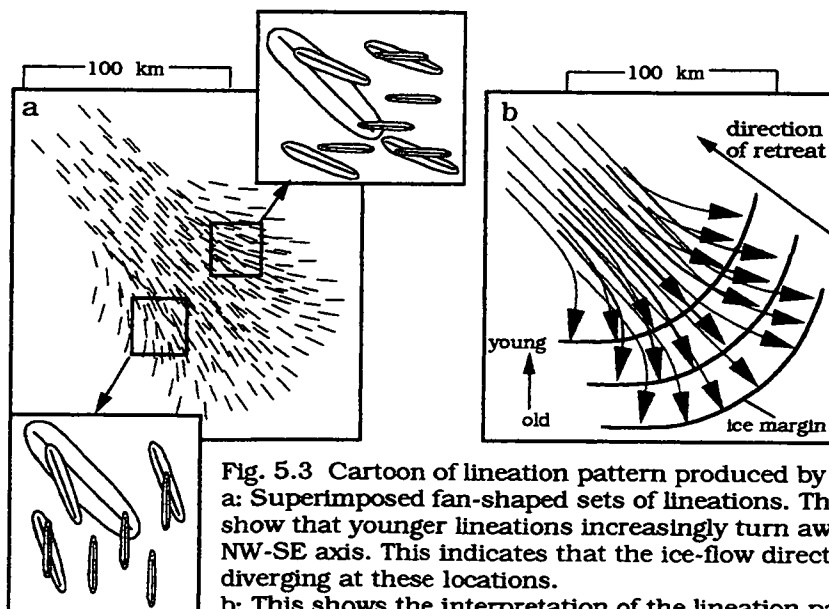


Fig. 5.3 Cartoon of lination pattern produced by a retreating fan.

a: Superimposed fan-shaped sets of lineations. The two insets show that younger lineations increasingly turn away from the central NW-SE axis. This indicates that the ice-flow direction becomes more diverging at these locations.

b: This shows the interpretation of the lination patterns. A retreating, active fan produces superimposed, diachronous, fan-shaped sets of lination.

relation results in the interpretation in Fig. 5.1d: flow 1 is younger than flow 2. The time relation between the lineations within each set is still unclear. They can be the result of contemporaneous or diachronous ice flow, all we know is that lineations from flow 2 are older than flow 1.

On a larger scale a set of lineations such as shown in Fig. 5.1a is often part of a larger fan shape (Fig. 5.2a). Thus, the directions of lineations do not have to be identical to be grouped together in one set. However, the change in trend must be gradual to be judged directionally continuous. Ideally, a set of lineations is spatially continuous, this tends to be the case with the deglaciation lineations, older lineations often appear in small clusters separated from each other by younger lineations (see Fig. 5.2a). Assuming the same situation as in Fig. 5.1c, again different stages of flow can be distinguished (Fig. 5.2b). In this case, two isolated WNW-ESE lineation sets are present. From this situation alone it is not clear how to relate these two sets.

In Fig. 5.3a a more realistic picture of how lineation data looks is shown. A dense and sometimes confusing picture of cross-cutting lineations emerges. The two insets show examples of systematic shifts in the direction of the younger lineations. The oldest (largest) lineations in both insets are trending NW-SE, parallel to the main axis of the fan. In the upper (northeast) part of the fan, the younger (smaller) lineations change from NW-SE to W-E. In the lower (southwest) part of the fan, they change to a N-S direction. Thus, parallel flow is giving way to increasingly diverging flow. This is interpreted to be the result of the migration of a fan from SE to NW as is shown in Fig. 5.3b. Thus an active, retreating fan produces diachronous, fan-shaped sets of lineations. If the retreat pattern of the ice margin is known, contemporaneous sets of lineations and thus contemporaneous flow patterns can be reconstructed. In areas of diverging retreating flow (the marginal areas), contemporaneous flow lines can be drawn with confidence. However, the parallel flow in the apex of a retreating fan (the upstream part) becomes increasingly difficult to separate as cross cutting becomes rarer.

The dated positions of the ice margin are used to correlate spatially separated flow patterns and to reconstruct a number of "snap shots" of the glaciodynamics of the ice sheet.

## 5.3 Case Studies

### 5.3.1 Introduction

In this section examples of Landsat MSS images and interpretations are shown. The first-order interpretations of these images of the presence of glacial linear features, and the second-order interpretations concerning ice-flow directions and their relative ages are described. The examples are from Finland, the sheet numbers correspond to the map shown in Fig. 3.5. Each image covers an area of 185 by 185 Km.

Figure 5.4 shows the legend belonging to the first- and second-order interpretations of the satellite images. In the first-order interpretations, ice-parallel linear features are represented by single lines showing the trends of their long axes. The thick lines represent ice transverse features, no distinction has been made between a subglacial, or an ice-marginal, depositional origin. Only the trend of the long axes is shown. The more extensive fluvio-glacial and ice-marginal deposits, such as the Salpausselkä end moraines or interlobate fluvio-glacial complexes are shown by their areal extent (dotted areas).

In the second-order interpretations, the different ice-flow patterns are represented by lines and arrows. The arrows point in the direction of ice movement. The different line styles represent the relative ages of ice-flow directions on each individual sheet. Ice-flow directions drawn in identical line styles on different sheets are therefore not necessarily related. The thick continuous lines correspond to the dominant lineation pattern formed during deglaciation on that particular sheet.

It is important to stress here that the individual linear features that form a coherent lineation pattern are not necessarily of the same age. In Fig. 5.6b for example, the thick continuous lines imply that, during deglaciation of this area, the dominant ice flow in this sheet continued to be from N-NNW to S-SSE. However, it is very likely that the ice sheet was still actively reworking the northern area while the southern area had already been deglaciated. The

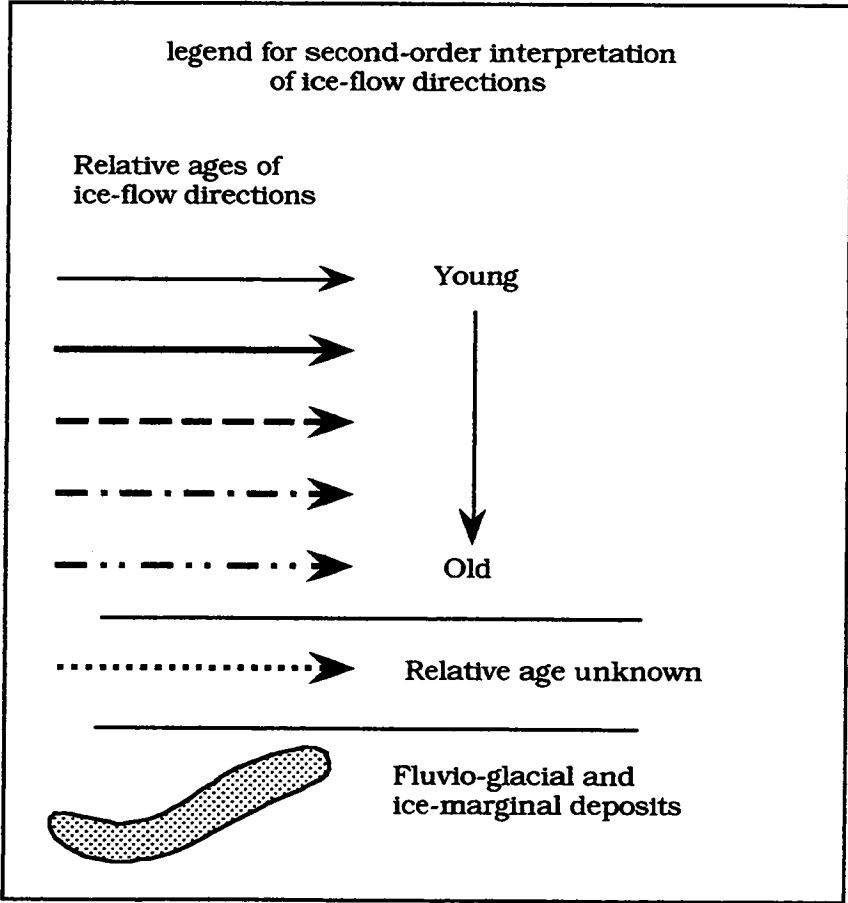
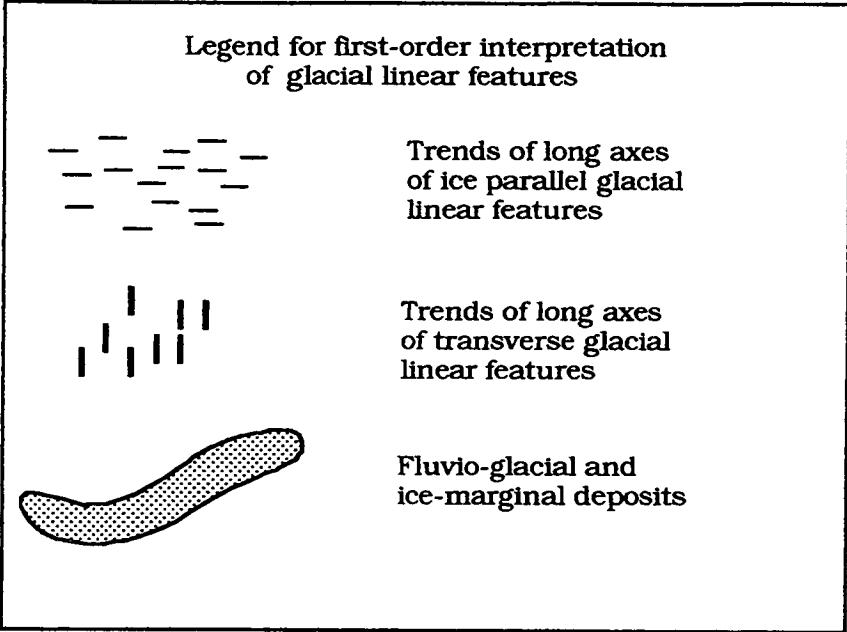


Fig. 5.4 Legend used for interpretation of satellite images.

different ice-flow directions shown in the second-order interpretation maps therefore reflect periods of different duration during which linear features formed with a high degree of spatial and directional consistency. These coherent lineation patterns are likely to have formed diachronously. The different ice-flow directions in the case studies shown have been given individual numbers as well as a different line styles. Number 1 is the youngest ice-flow direction on a particular sheet, number 5 the oldest.

### 5.3.2 Sheet F4

#### *Identification of lineation sets*


Figure 5.5a shows a satellite image from southeast Finland, in the lower right hand corner a small part of the Gulf of Finland can be seen. Figure 5.5b is the first-order interpretation of the satellite image showing linear glacial features. In the satellite picture (Fig. 5.5a), the wide arcs of the ice-marginal deltaic deposits of the Salpausselkä I & II moraines can be seen. To the north and south of the Salpausselkä moraines, bedrock exposure is significant. The till cover is thin and discontinuous over the entire area but its thickness increases towards the north and west of the area (see also Chapter 2). The variation in till cover is also reflected in the change in lineation density over the area.

Immediately to the north of the inner Salpausselkä arc there is a 40 km wide belt of exposed bedrock where lineations are rare. In the southwest corner of the sheet, the retreat of the ice sheet is marked by the presence of numerous De Geer moraines (thick lines).

To obtain second-order interpretation (Fig. 5.6b) from the first-order interpretation (Figs. 5.5b, 5.6a) a number of steps are required as described in section 5.2. Thus coherent sets of lineations have been identified on the basis of their corresponding trends and spatial continuity. Superimposed lineations are then used to establish the relative ages of the different sets.

To group together linear features on the basis of spatial coherence, it is not necessary for them to have the same orientation. In Figs 5.6a and 5.6b, for

Figs 5.5 a & b Satellite image (sheet F4) and first-order interpretation.

Scale (Km)  0 40

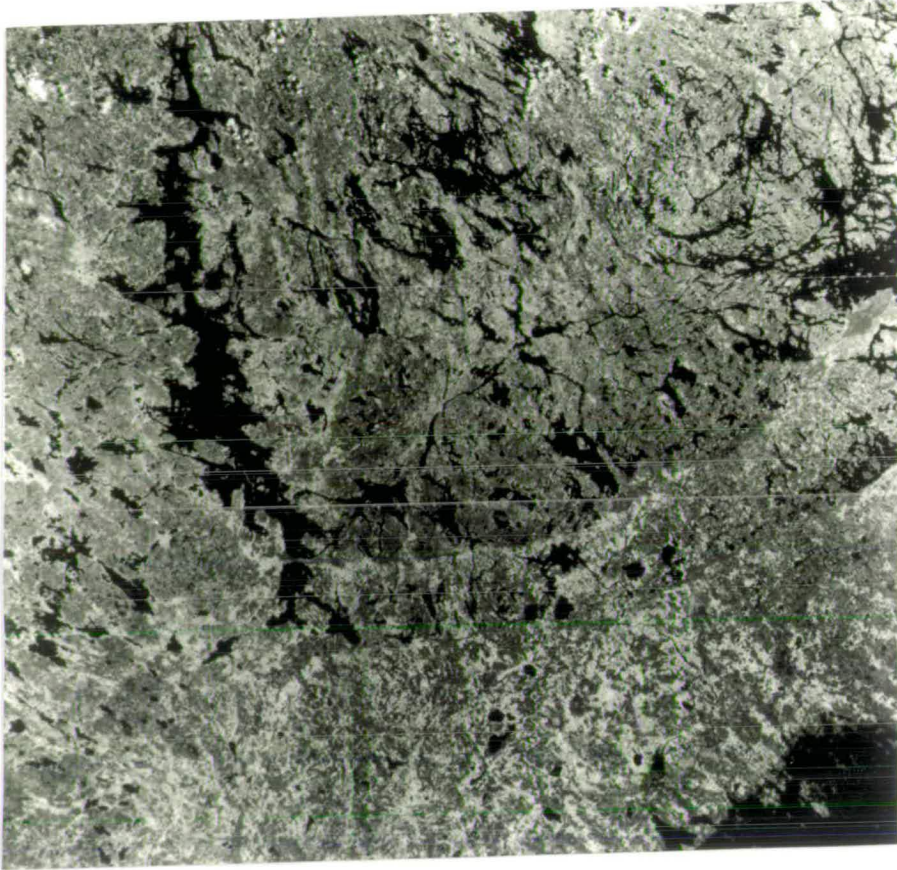
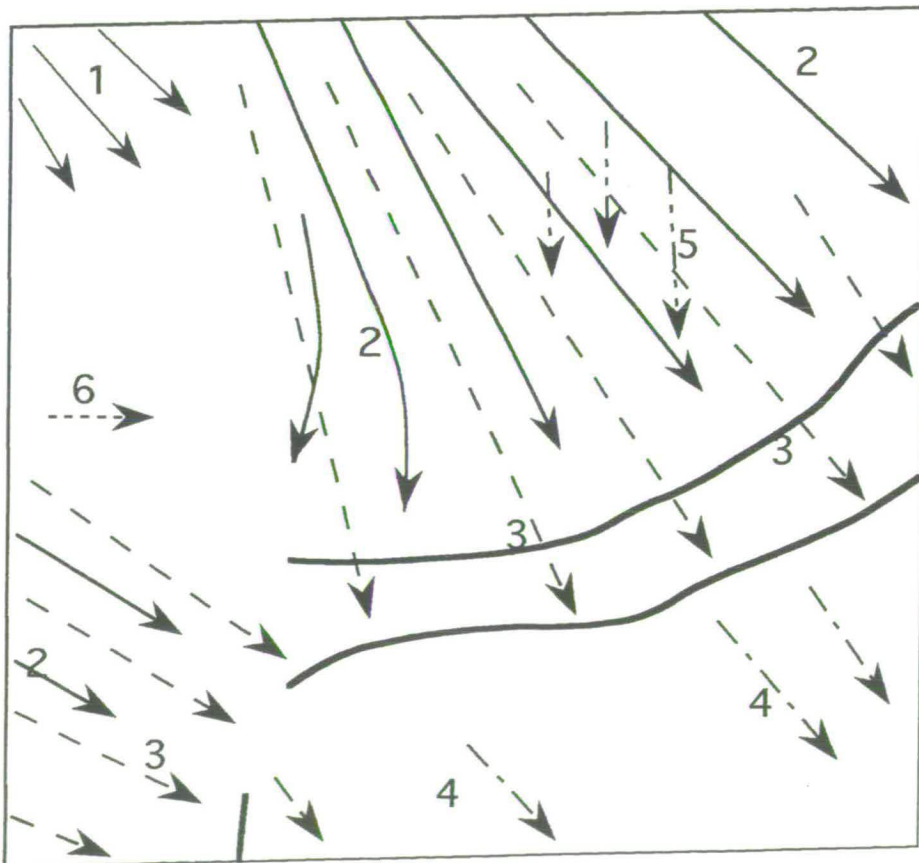


Fig. 5.6 a & b Interpretation of glacial linear features and iceflow directions (Landsat image F4)

Scale (Km) 0 40



example, the orientations of the linear features correlated to the Salpausselkä phase II (flow no 2) shift from N-S in the middle part of the area to NNW-SSE in the eastern part. Despite this shift in orientation, it is obvious that these lineations are part of one, coherent, lobe pattern. The lineations in the southwest corner of the sheet, which are running NW-SE, are clearly not part of the same lobe pattern, although they were formed during the same period (flow no 2).

This example shows the importance of the scale at which one is looking at the linear features. On the scale of an aerial photograph, the diverging trend of the lineations will be very difficult to recognise. However, the relative ages of cross cutting lineations will be easier to see. On the scale of satellite images diverging and converging flow patterns can be identified readily while Landsat mosaics are very useful to recognise ice-sheet-wide flow geometry, .

By using the known deglaciation history of an area it is possible to establish which flow patterns were contemporaneous (see Chapter 6). This also provides an additional check on the sequence of events as established by interpretation of satellite images and aerial photographs..

#### *Flow patterns*

In Fig. 5.6b, six different flow directions have been recognised. The oldest flow direction (flow 5) is approximately NNE-SSW and is only represented by a few lineations. The linear features related to this direction are older than any other flow directions and have also been mapped on other sheets. The relative ages of flow 6, which has a W-E direction, is unknown. There were no clear cross-cutting relations, nor was it possible to establish relative age using the flow sequence from the deglaciation. As this flow event could not be linked to any of the flow directions on other sheets it was further ignored.

Outside the Salpausselkä moraines, lineations that have a NNW-SSE directions have been mapped. These belong to flow 4, which pre-dates the Younger Dryas and the formation of the Salpausselkäs. The direction of these lineations is comparable to those of flow 1, the youngest flow stage in this sheet. But the relative age relations between flow 1 and flow 2 and 3 showed that this was a separate flow event. Flow 3 is dominated by two divergent, lobe-shaped,

patterns. This divergent flow pattern is associated with the Salpausselkä I moraines. Flow stage 2 is to a large extent identical to flow stage 3, only at the edges of the central lobe an increased divergence of flow is noticeable. In other words, at the end of the Younger Dryas, the lobe-shaped pattern was enhanced as the ice flow on the sides increasingly diverges from the central flow lines. The youngest flow (flow 1) is in the northwestern part of the area and also shows a vague tendency towards divergent flow.

The large majority of the lineations observed in this sheet is related to deglaciation. During deglaciation there was a striking transition in flow dynamics in this region. The oldest flow that can be connected to deglaciation is flow 4 (flow 5 has been interpreted to pre-date the deglaciation, see Chapter 7). The linear features related to this period are parallel, implying that the ice-flow direction over this region was uniform. No traces of lineations related to flow 4 have been found within the Salpausselkä arcs, this implies either that they never were there, or that they have been completely removed by younger ice flow.

During the Younger Dryas the flow dynamics were completely different. Two large lobes, which can also be seen on neighbouring sheet, developed. One coming from a northern direction and one from the northwest. At the western end of the inner Salpausselkä arc there are indications that the two lobes coalesced, but further to the north there is an area where no traces of lineations related to either of the lobes can be found. The only linear forms present here are De Geer moraines and W-E lineations from flow 6. In the northwest corner lineations are found that belong to the youngest flow stage, related to the fourth Salpausselkä moraine. On the satellite pictures (full scale) it can be seen that the inter-lobate area is covered by fluvio-glacial deposits. There are other examples of areas in-between two ice lobes where the deglaciation left hardly any subglacial bedforms.

### 5.3.3 Sheet F6

Figure 5.7a shows satellite image F6, located immediately to the east of sheet F4 (see Fig. 3.5). This sheet covers the border area between Russian Karelia and south Finland. In the south the Gulf of Finland can be seen, while Lake Ladoga is in the northeast. Again, the morainic arcs of the Salpausselkä stand out clearly. Inside the morainic belt the surface is dominated by exposed bedrock which has only a thin, discontinuous till cover. Towards the southeast corner of the sheet, the till cover becomes more continuous and thicker as the Baltic Shield gives way to the sedimentary lowlands of the East European Platform. Figure 5.8b shows the interpretation of ice-flow directions in this area. Flow directions 1 to 3 are all related to deglaciation. There is a general shift in flow direction from a WNW-ESE flow in the earlier stages of deglaciation (flow 3) to a NNW-SSE direction during the Salpausselkä phases. Unlike sheet F4 (Fig. 5.6b) there is no dramatic change from uniform to divergent ice flow. During deglaciation the ice flow was already slightly diverging before the Salpausselkä phase (flow 3).

The lineations classified as flow 4 show a high degree of directional variability compared to the controlled lineation pattern associated with flow 1-3. These lineations are mostly lobe-shaped, the ice flow coming from the N-NNE. It was very difficult to establish the relative ages of these lineations with absolute certainty as the photo tone was very unclear and marine and lacustrine deposits form a drape over the lineations in this area. But it is most likely that the northern lobe predates flow 3.

It is not clear, however, how flows 4 and 5 are related. Flow 5 is part of a northern ice-flow direction that can be traced on many satellite images of middle and south Finland. Flow 4 shows a far higher degree of variability and the diverging flow pattern is unlike anything seen in flow 5. Flow 4 might reflect the development of an ice lobe/ice stream at the southern margin of the ice sheet. It is not clear whether this happened during the advance or during the retreat of the ice sheet. As no pictures from further south were available, it could not be determined how far to the south flow 4 reached.

Figs 5.7 a & b Satellite image (sheet F6) and first-order interpretation.

Scale (Km) 0 40

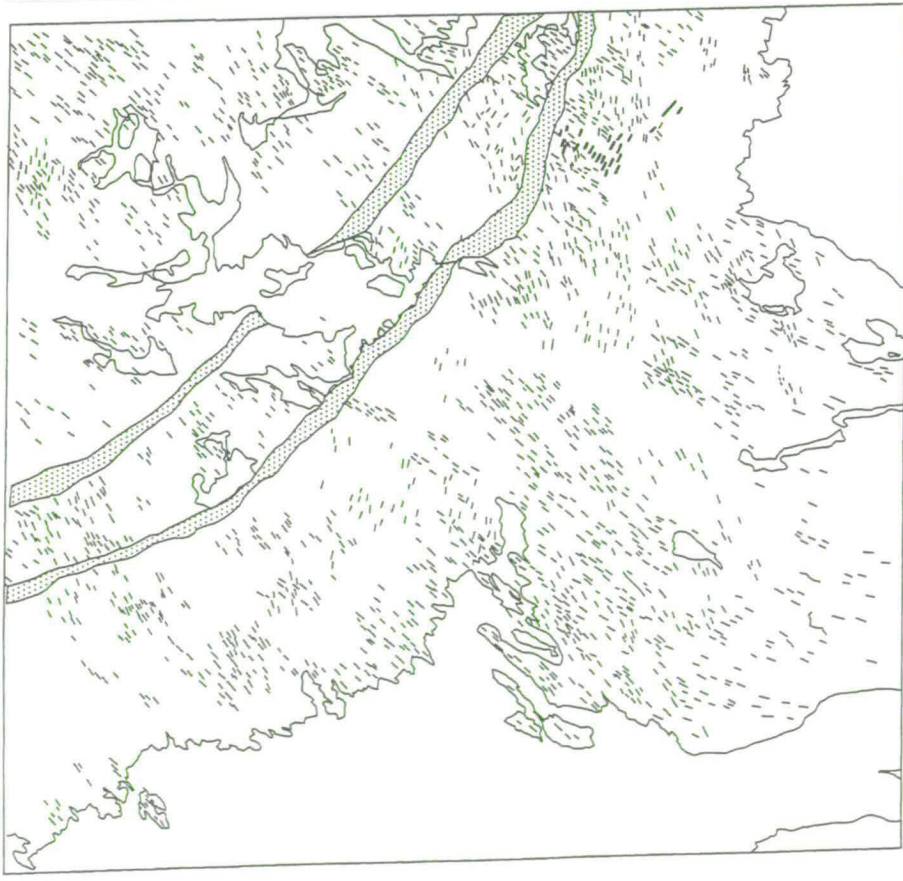
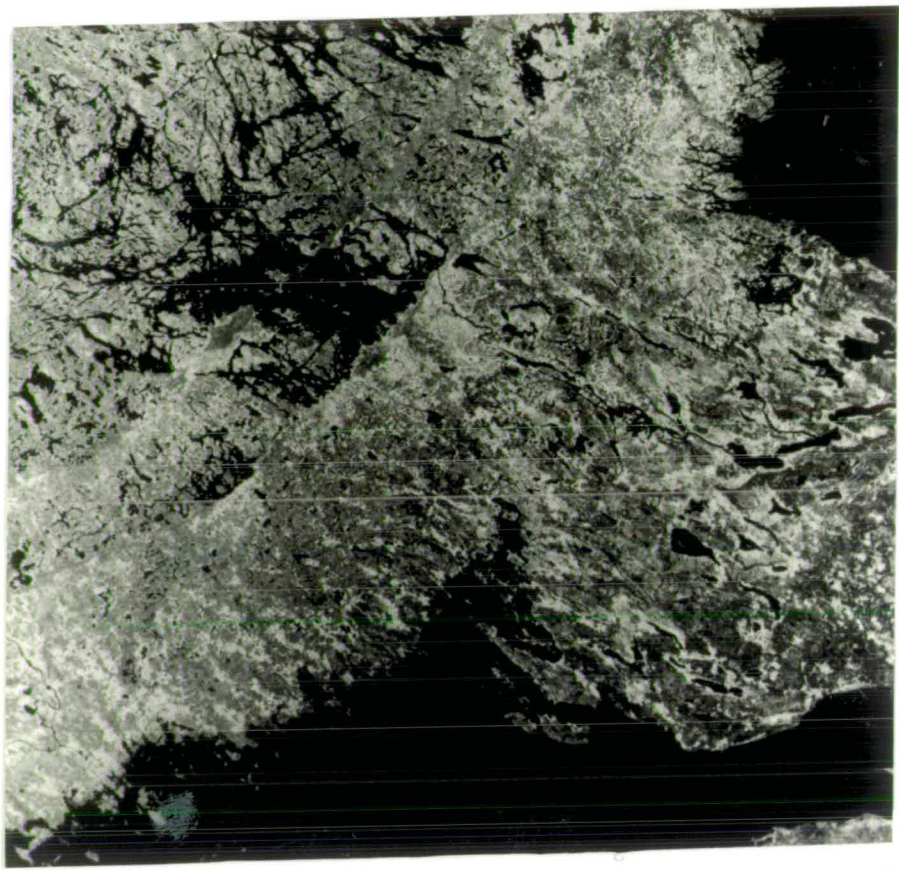
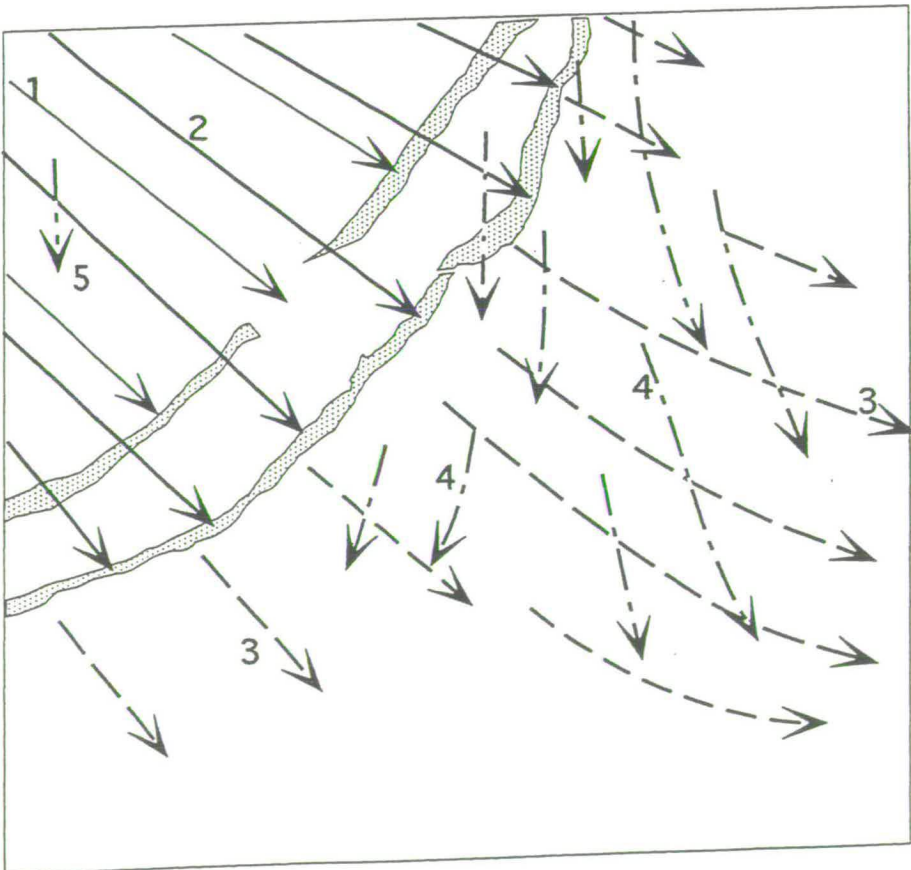


Fig. 5.8 a & b Interpretation of glacial linear features and iceflow directions (Landsat image F6)

Scale (Km) 0 40



#### 5.3.4 Sheet F13b

Sheet F13b is located to the southwest of the White Sea (see Fig. 3.5). There is a continuous till cover in this area. In Fig. 5.9a sheet several flow directions can be recognised even on the scale of this photo. The older flow directions stand out from the lake shapes in the western and middle parts of the picture. Four major ice-flow phases have been recognised in this sheet (Fig. 5.10b). In this picture a 90° shift in ice flow from flow 4 ( N-S) to flow 1 (radial flow, approximately W-E) can be observed. No continuous transition from flow 4 to flow 3 exists. This shift takes place two discrete steps,

The oldest flow direction (flow 4) shows uniform flow from N to S. In the central part of the satellite picture there is evidence of large-scale glacio-tectonic activity, where flow 3 has remoulded the older lineations without completely destroying them. Associated with flow 3 are extensive fluvio-glacial deposits. As the ice margin retreated over this area, here as well a change in the ice-flow dynamics occurred from parallel flow to diverging flow (flow 1 and 2). This change occurred during the Younger Dryas event as well (see also section 5.3.2).

Figs 5.9 a & b Satellite image (sheet F13b) and first-order interpretation.

Scale (Km) 0 40

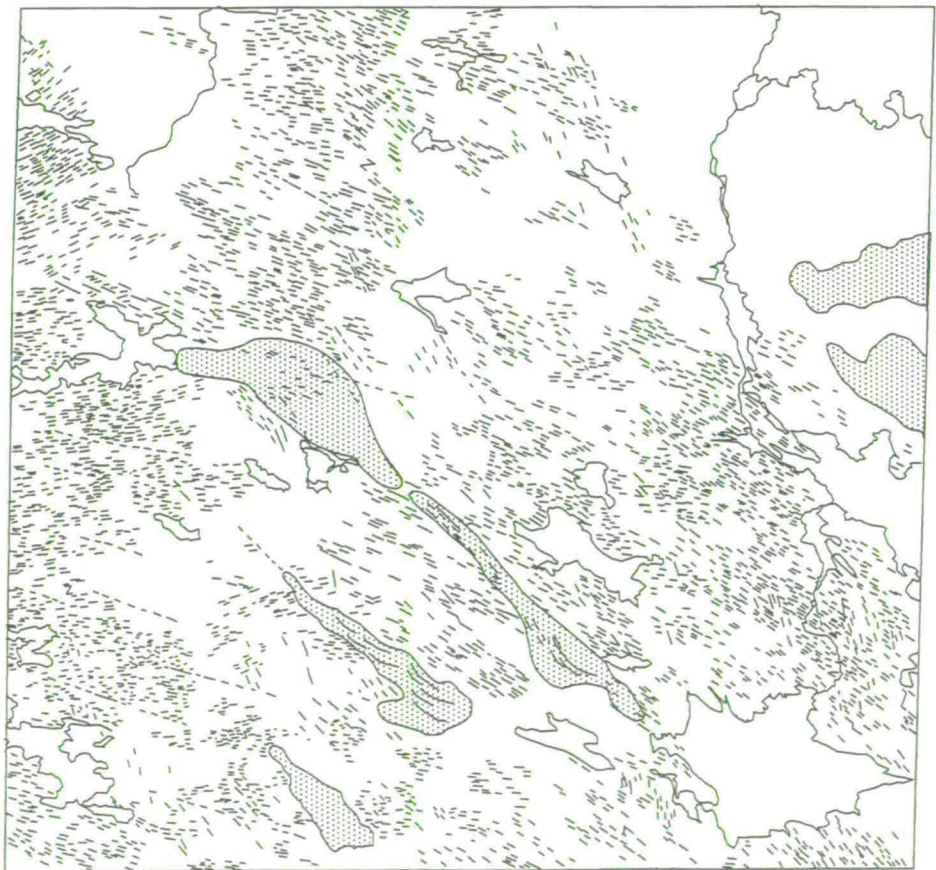
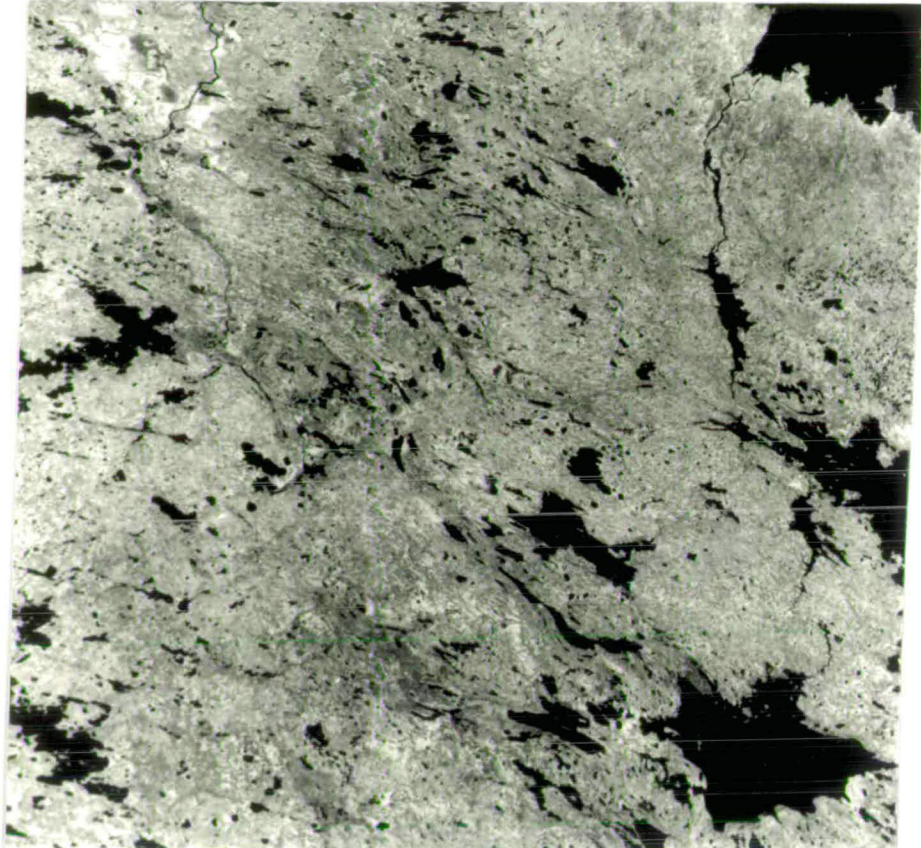
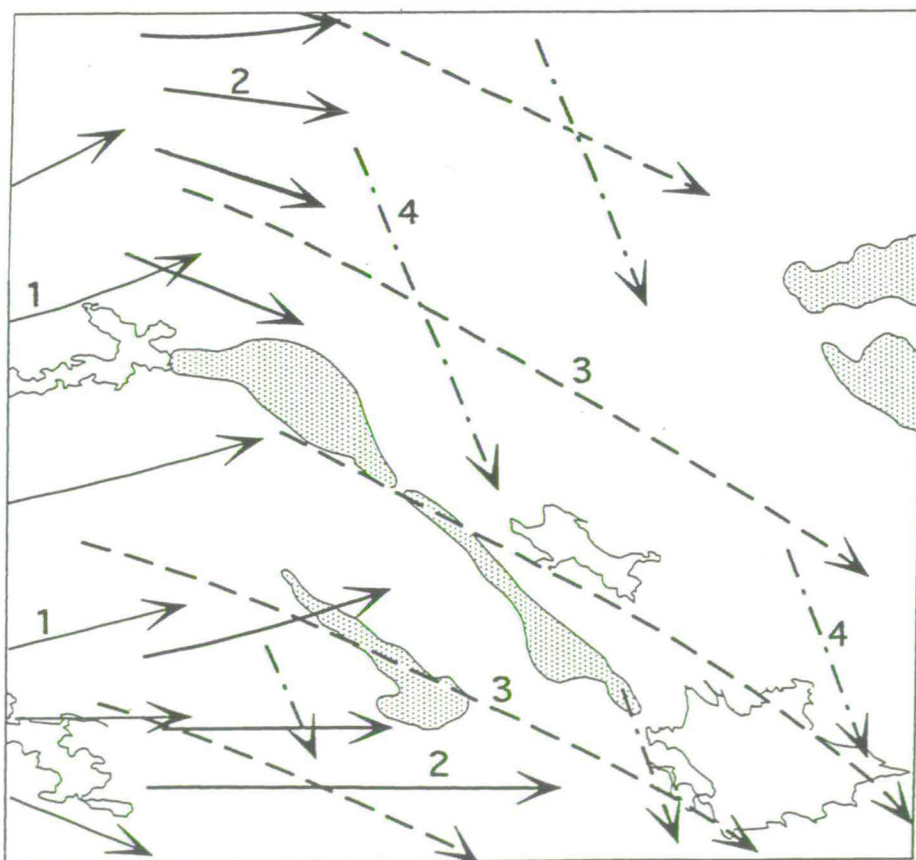
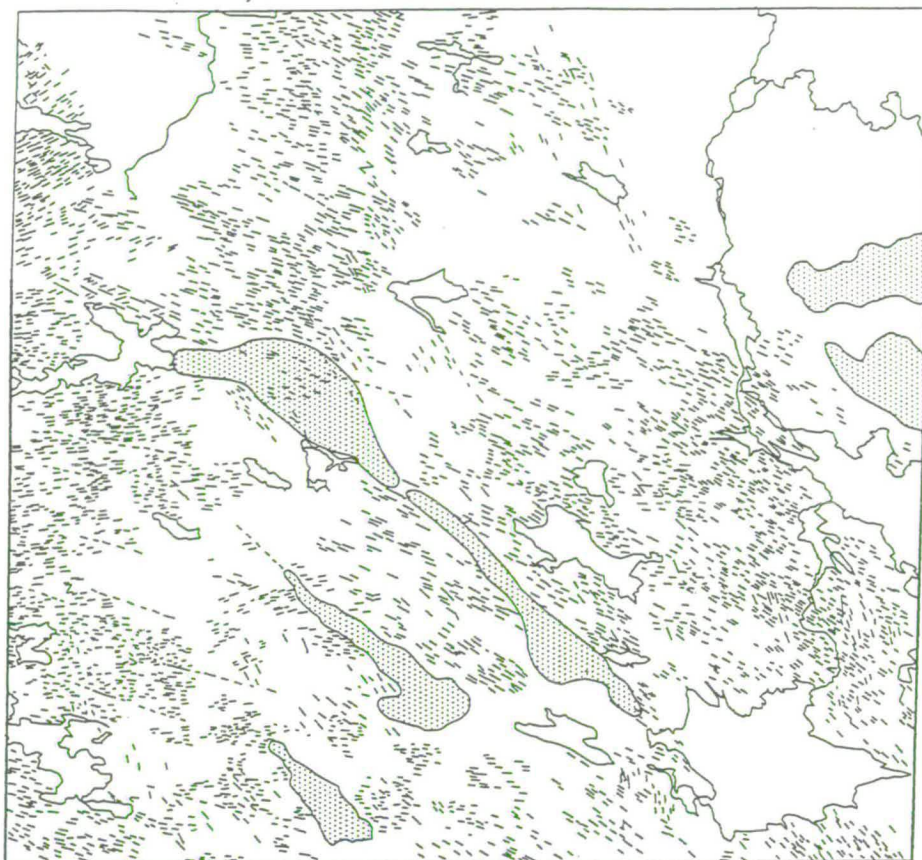


Fig. 5.10 a & b Interpretation of glacial linear features and iceflow directions (Landsat image F13b)

Scale (Km) 0 40



Figs 5.11 a & b Satellite image (sheet F15) and first-order interpretation.

Scale (Km) 0 40

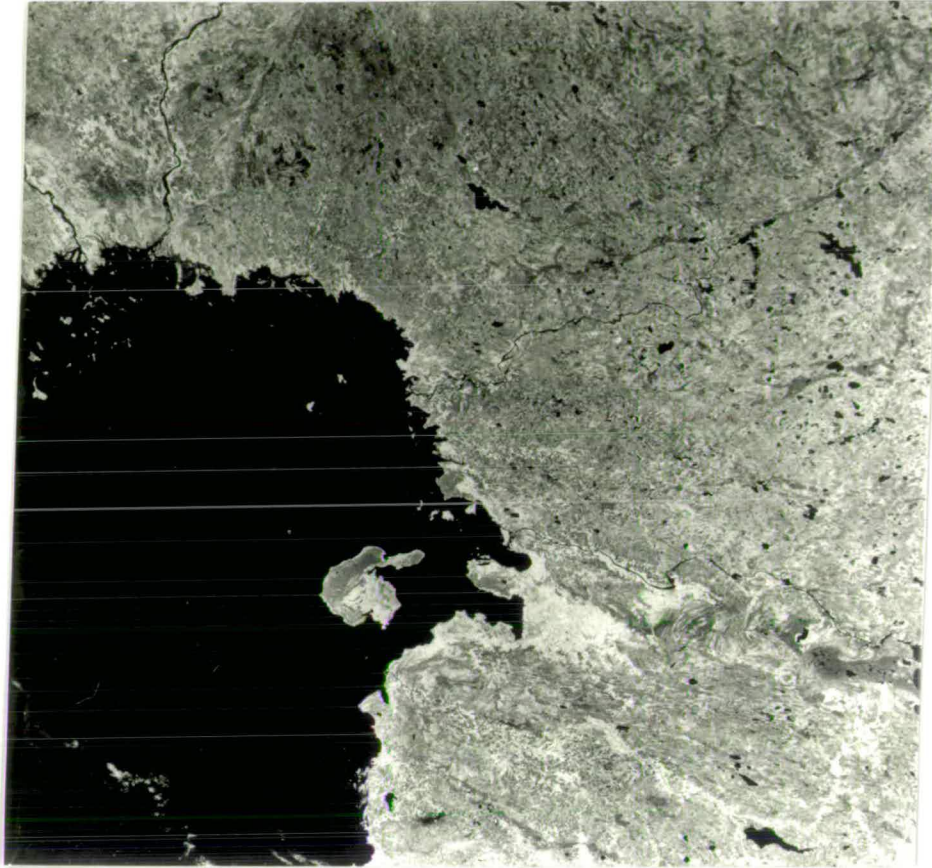
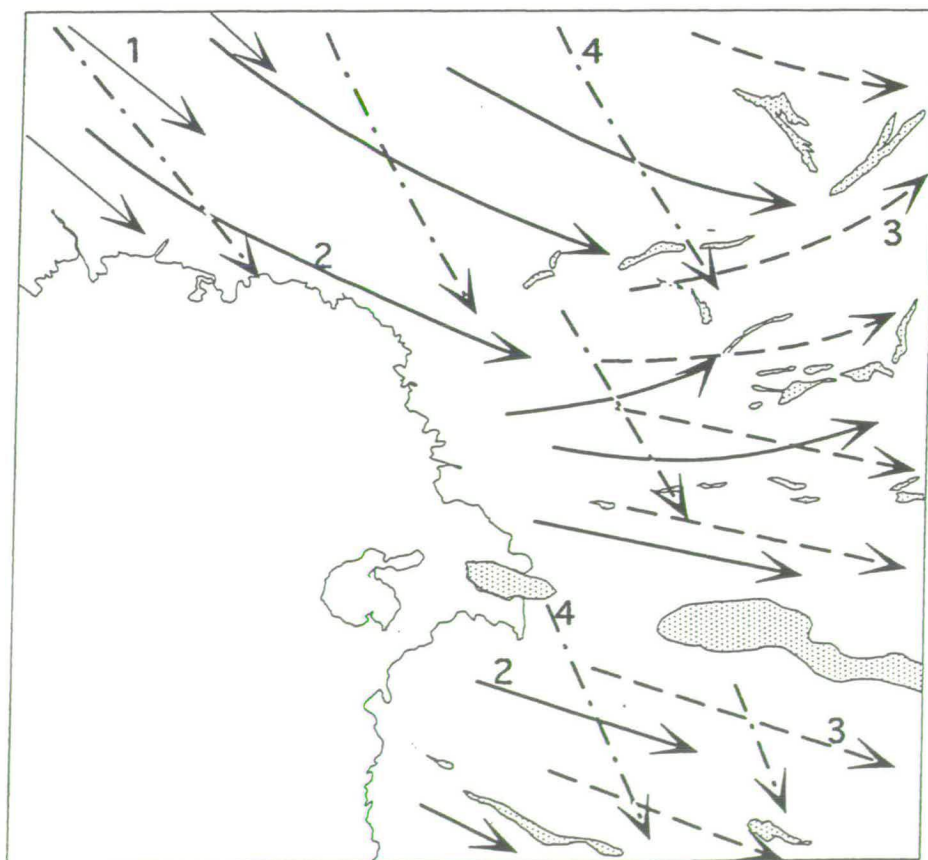


Fig. 5.12 a & b Interpretation of glacial linear features and iceflow directions (Landsat image F 1 5)

Scale (Km) 0 40



### 5.3.6 Sheet F19

This sheet is located north of sheet F13b. In the northeast corner the White Sea can be seen. The area has little relief and slopes gently towards the White Sea. The vast majority of the lineations in this sheet is related to a W-E-flowing ice lobe, draining the ice sheet towards the White Sea (Fig. 5.14a and 5.14b). In the southeast corner of this sheet, there is evidence of a shift in ice flow from N-S (flow 4) to almost W-E (flow 2). This flow shift was observed in sheet F13b as well (Fig. 5.10b).

Flows 4 and 5 show slightly different orientations (NNW-SSE and NW-SE). These are the northerly extensions of the pre-Younger Dryas flow also seen in sheet F13b. Here, the change in flow direction from pre-Younger Dryas (flow 4 and 5) to the Younger Dryas flow configuration is even more abrupt than in sheet 13b: from N-S to W-E without any clear traces of intervening flow configurations. Evidently, the change in flow configuration must have been very rapid.

In the southwest corner, there are lineations related to an ice lobe that developed during the rapid deglaciation following the Younger Dryas. The flow directions marked by dotted lines could not be relatively dated. The W-E flow could be a slight divergence upon deglaciation, but the SSW-NNE flow pattern does not fit in with any of the observed flow systems.

Figs 5.13 a & b Satellite image (sheet F19) and first-order interpretation.

Scale (Km) 0 40

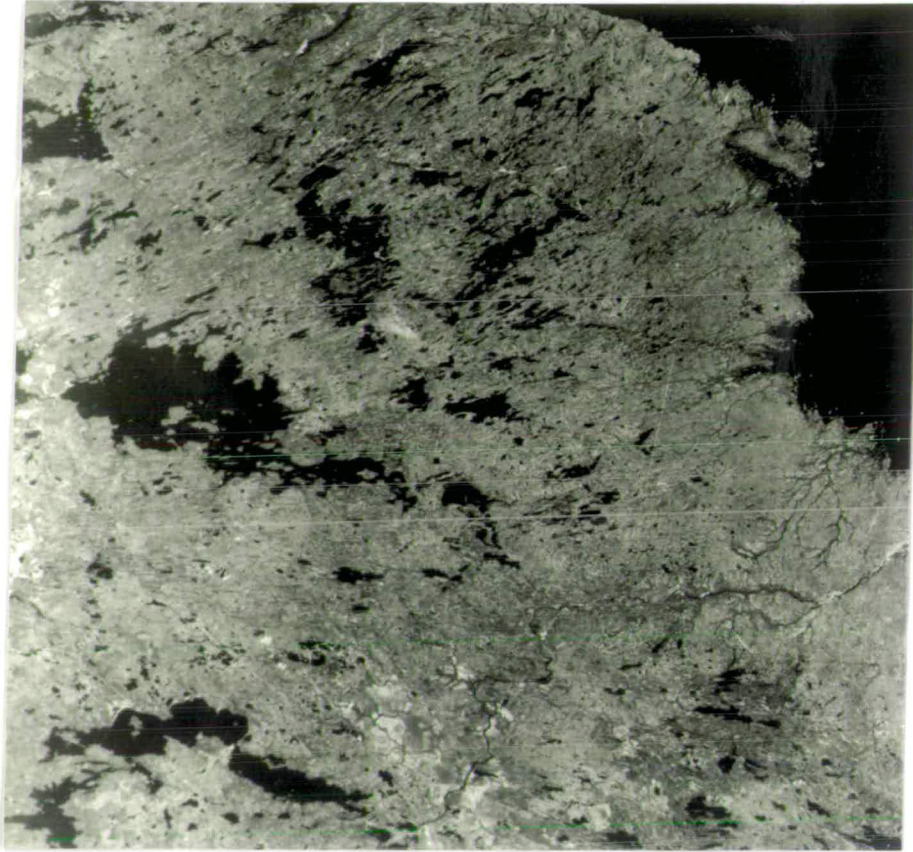
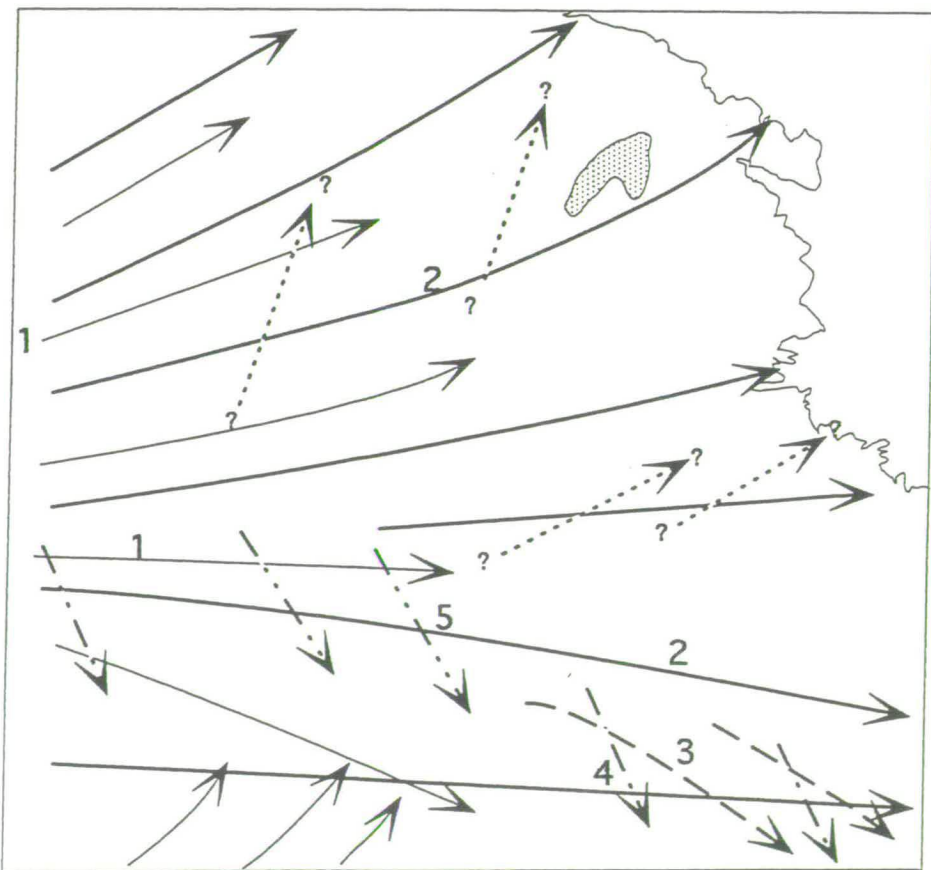


Fig. 5.14 a & b Interpretation of glacial linear features and iceflow directions (Landsat image F 1 9)

Scale (Km) 0 40



## Chapter 6

### **Reconstruction of ice-flow patterns in Fennoscandia using remotely sensed lineation data**

#### 6.1 Introduction

In this chapter the evolution of ice-flow dynamics during the Late Weichselian Glaciation in Fennoscandia is discussed. The reconstruction of the flow patterns and their evolution through time, is based on subglacial lineation data derived from satellite imagery. Crucial for the reconstruction of time-transgressive flow systems is the pattern of ice-marginal retreat (see chapter 3). Figure 6.1 shows the positions of the ice margin that have been used in this reconstruction, they are based on Boulton *et al.* (1985), Lundqvist (1986) and Kleman (1990) and have been calibrated using radio-carbon C<sup>14</sup> and varve chronology (Cato, 1985).

Figure 6.2 shows a lineation map of Fennoscandia. This map gives a summary of the lineations that have been traced using different remote-sensing systems. To cope with the large amount of data, the discussion of the evolution of the flow systems in Fennoscandia has been divided into four parts.

This chapter starts with a short overview of the deglaciation and flow directions south of the Baltic Sea. No satellite imagery has been interpreted for this area, but events in this region are important to understand the ice-sheet behaviour on the larger scale. Development of ice flow over the Baltic Shield area is discussed in three different sections: central and south Sweden (section 6.3); central and south Finland (section 6.4); and north Scandinavia (section 6.5). This chapter ends with a comparison between palaeo-ice-flow data from the Nordkalott Project (1986a-d) and the lineation data presented in this chapter. The emphasis is on the deglaciation phase, the timing of which is constrained by the known positions of the ice margin. Pre-deglaciation lineation patterns in each region are considered, but the advance phase as a whole will be discussed in Chapter 7.

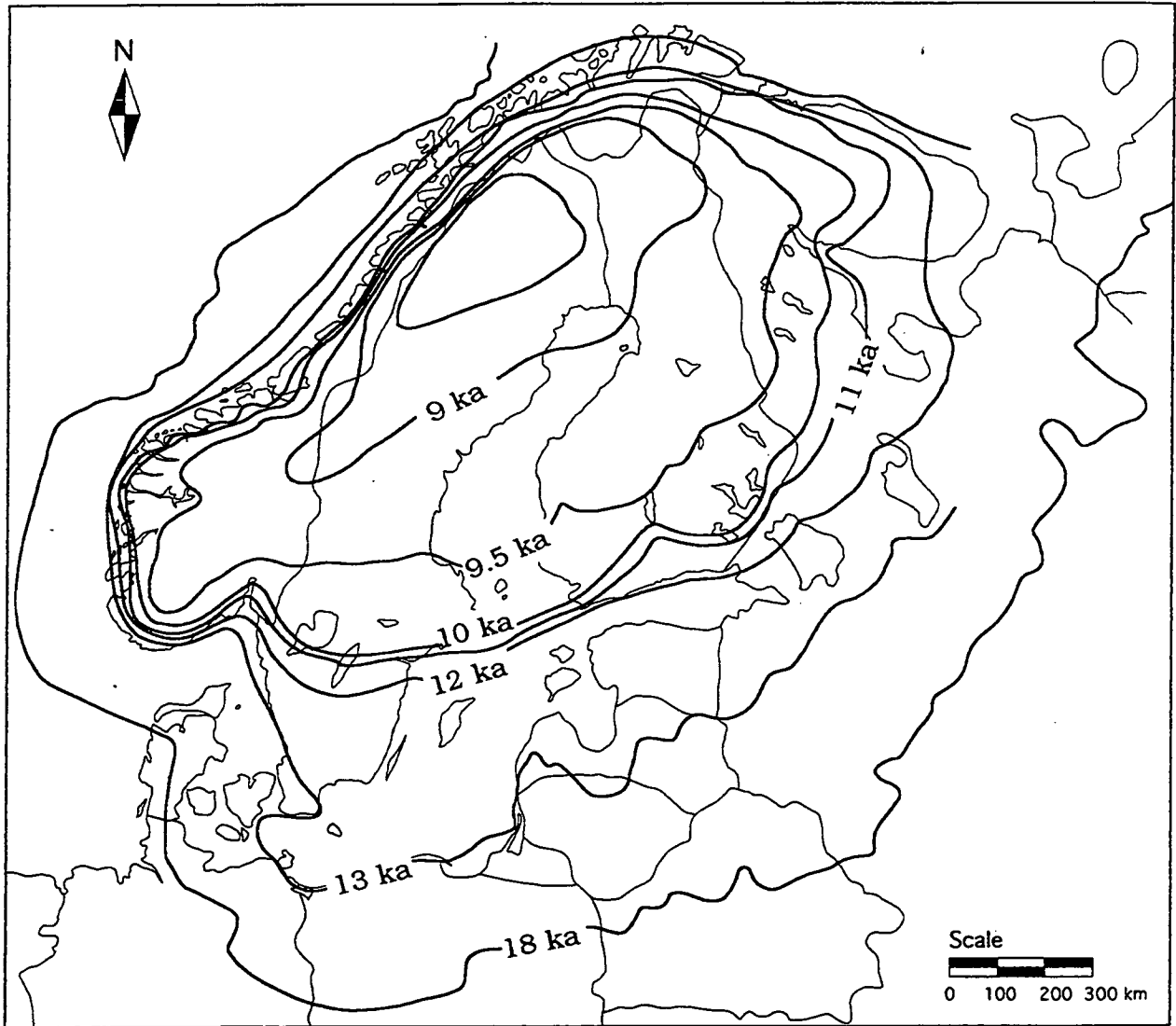


Fig. 6.1 Isochrons on ice margin retreat during deglaciation of the Fennoscandian Ice Sheet. Reconstruction based on Boulton et al. (1985), Lundqvist (1986) and Kleman (1990). Isochrons have been calibrated by C14 and varve chronology (Cato, 1985).

Fig. 6.2  
Simplified lineation map  
of Scandinavia, interpreted  
from Landsat mosaics, Landsat  
MSS and TM images and  
aerial photographs.



## 6.2 Southern Baltic Lowlands

### *Introduction*

Although the satellite images used did not cover Denmark and the area south of the Baltic Sea, this area is important to understand the reconstruction of the last glaciation. Glacigenic sedimentary sequences of sometimes considerable thickness have been deposited during the Pleistocene glaciations. Stratigraphic studies have yielded important information on the timing and geometry of the Late Weichselian advance and retreat phases. In particular the activity of the Baltic Ice Stream is known to have had profound effects on the glacio-dynamic behaviour of the entire southwest area of the Fennoscandian Ice Sheet. Stratigraphic studies in south Sweden (Ringberg, 1988; Lagerlund, 1987), Denmark (Sjørring, 1983; Houmark-Nielsen, 1983, 1987) and Germany (Ehlers, 1990, 1992; Böse, 1990) have demonstrated Late Weichselian ice advances, and shifts in ice-flow directions that are closely linked to the fluctuating activity of the Baltic Ice Stream. To the east, in the Baltic States, correlative shifts in ice-flow directions during the Late Weichselian Maximum and the Pomeranian Stage could be reconstructed (Raukas, 1977; Basalykas and Gudelis, 1977; Raukas and Gaigalas, 1993; Mojski, 1982).

From the early stages of the Weichselian, two ice advances are known in Denmark (Sjørring, 1983; Houmark-Nielsen, 1987). The Old Baltic Advance (Fig. 6.3a), when ice from the Baltic Sea moved to the west and reached the southeast margin of Denmark. The Norwegian Advance (Fig. 6.3b) crossed the Skagerrak from south Norway and reached the northern margins of Denmark. Houmark-Nielsen (1987) and Ringberg (1988) concluded, contrary to what was thought before (Sjørring, 1983), that the Old Baltic Advance was older than the Norwegian Advance and probably of Early Weichselian age. The Norwegian Advance was considered by Houmark-Nielsen (1987) to be of Late Weichselian age, preceding the maximum advance.

At the time of the Main Ice Advance (Fig. 6.3c), which coincided with the Late Weichselian Maximum (Houmark-Nielsen, 1987), the Norwegian ice had already withdrawn from Denmark. During this period, ice flow was radial and coming from south Sweden. After the Main Ice Advance, the ice sheet retreated partially from Denmark, followed by a new advance, the East Jylland Advance

Fig. 6.3 Weichselian flow stages in Denmark and south Sweden,  
(modified from Houmark-Nielsen (1987) and Ringberg (1988).

Fig. 6.3a Old Baltic Advance  
(Early Weichselian)



Fig. 6.3b Norwegian Advance  
(Early Late Weichselian)



Fig. 6.3c Main Danish Advance  
(Late Weichselian Maximum)



Fig. 6.3d East Jylland Advance  
(Pomeranian Stage)



Fig. 6.3e Baelthav Advance  
(ca 13,200 y BP)



(Fig.6.3d). Flow directions during this phase were from NE/ENE, pointing to renewed activity of the Baltic Ice Stream (Houmark-Nielsen, 1987). A last advance phase has been recorded in southeast Denmark, the Baelthav Advance (Fig. 6.3e). Ice flow was E-W coming directly from the Baltic. Ringberg (1988) estimated that this advance lasted only from 13,200-13,000 years BP. After the ice had withdrawn from Denmark and south Sweden following the Baelthav Advance, there was no further influence of Baltic ice during the deglaciation..

On the basis of till-fabric measurements and glacio-tectonic studies, Ehlers (1990, 1992) reconstructed the flow dynamics of the Late Weichselian glaciation in Northwest Germany (Figs 6.4a and 6.4b). He found that ice flow during the maximum extent of the Late Weichselian glaciation was radial, and that a clockwise shift in flow direction occurred later. For Schleswig-Holstein, this implied a shift in ice-flow direction from NE-SW to the E-W. Böse (1989, 1990) found a similar shift in Meckelenburg and the area around Berlin, here flow directions changed from N/NE-S/SW, during the Weichselian maximum, and to E/NE-W/SW, during the Pomeranian stage (contemporaneous with the East-Jylland Advance in Denmark). Ehlers (1990) concluded that the radial flow during the maximum extent indicates that no ice stream was active in the Baltic Basin, whereas the clockwise flow shifts in Denmark, Schleswig Holstein and Meckelenburg are seen as indications that ice streaming was active during the Pomeranian flow stage.

Raukas and Gaigalas (1993) argue that flow directions derived from till fabrics and streamlined glacial features in the Baltic States, reflect cyclic changes in climate. During the advance phase the flow direction was NW-SE because the centre of the ice sheet was close to the Scandinavian mountains. During the maximum extent, when the ice divide had moved further to the east, the flow direction over the Baltic States was N-S. The same direction can be seen deduced the distribution of erratics. During deglaciation, flow directions once more shifted back to a NW-SE direction.

### *Summary*

In Denmark, there are indications of an incursion of Norwegian ice into Denmark prior to the maximum extent (Houmark-Nielsen, 1987). In Denmark and Germany ice flow during the maximum extent of the ice sheet was radial

§. 6.4 Late Weichselian flow stages to the south of the Baltic Sea.

Fig. 6.4a Main Late Weichselian stage (see also fig. 6.3c).

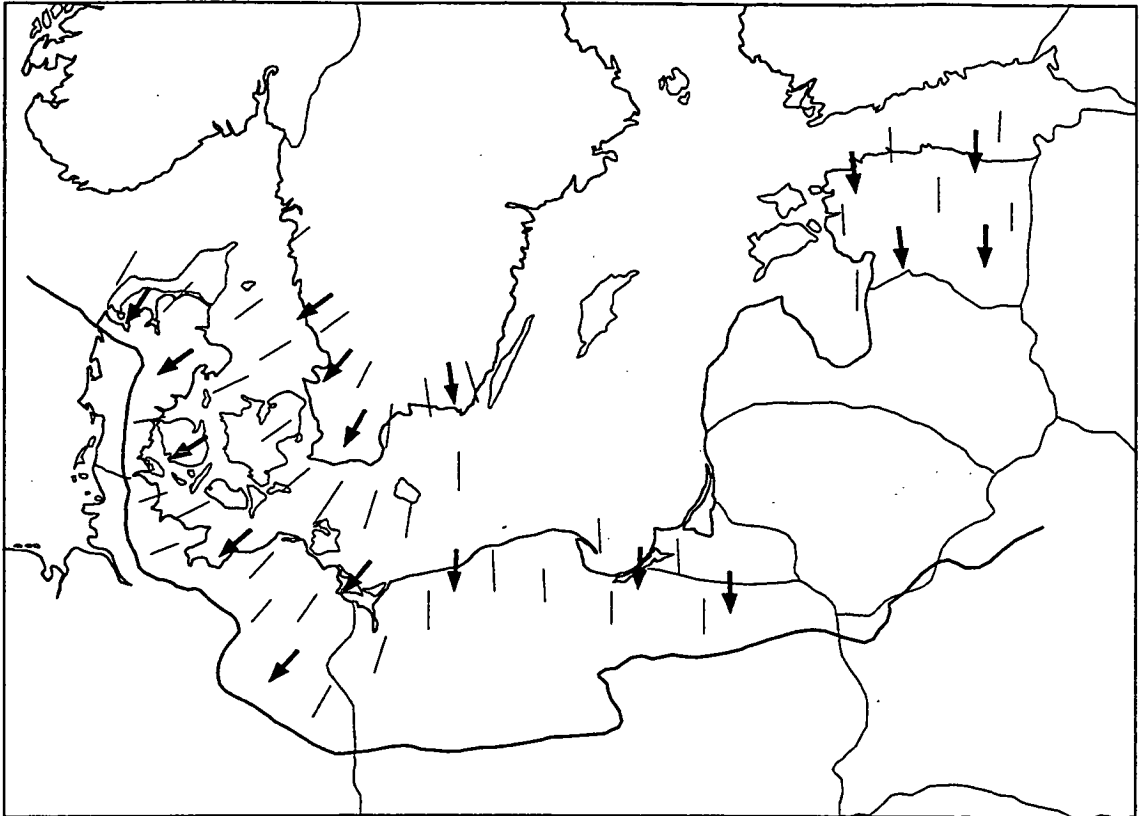
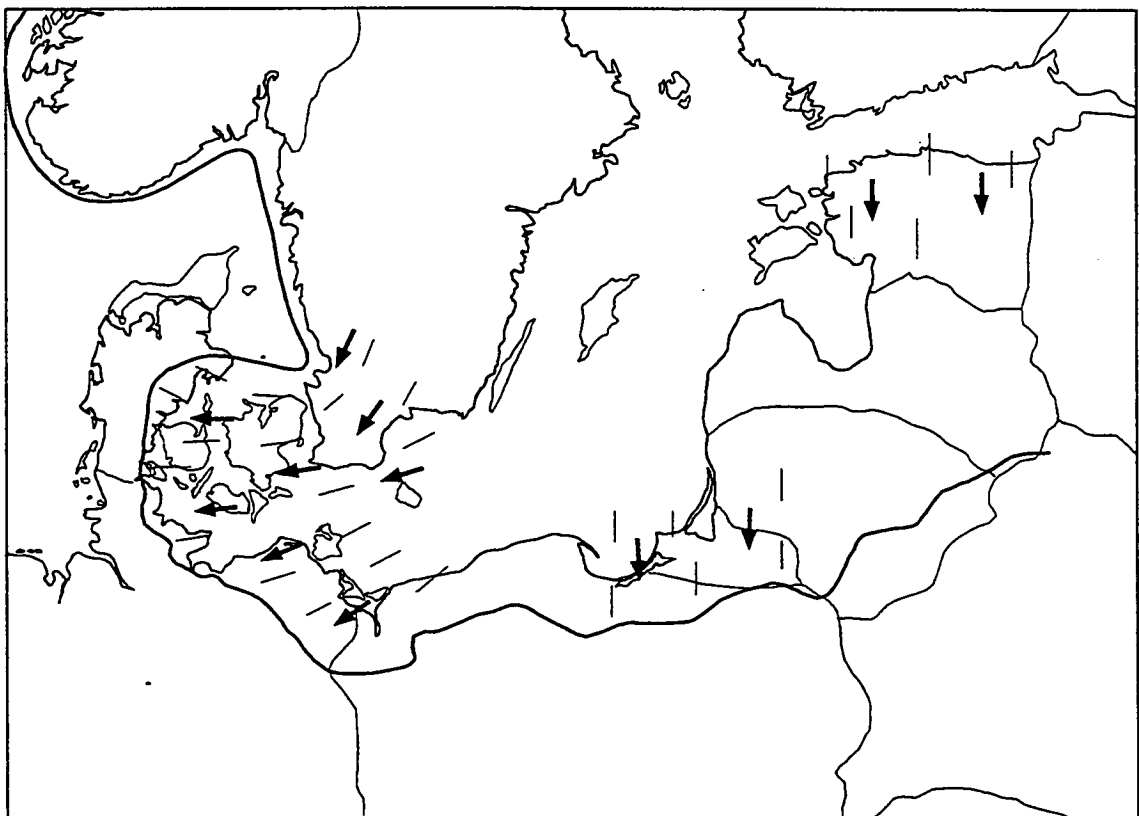


Fig. 6.4b Pomeranian stage (see also fig. 6.3d).



(Fig. 6.4a). Later a pronounced clockwise shift in flow direction took place that affected the entire southwest part of the ice sheet. This shift is probably related to renewed activity of the Baltic Ice Stream.

### 6.3 Central and south Sweden

#### 6.3.1 Introduction

Figure 6.5 shows the lineation map of south Sweden and parts of central Sweden. This map is made using Landsat mosaics (1:1,000,000). The area to the northwest of Lake Vänern, the east coast of Småland and the Stockholm area which was not covered by the satellite images, have been studied in detail using 1:150,000 black and white aerial photographs (see Fig. 3.4 for locations). The lineations are evenly distributed over the area. The gaps in Fig. 6.5 are related to poor image quality. In the northwest the presence of mountains made lineation mapping impossible.

Figures 6.6a to 6.6h show a series of flow stages that are derived from the analysis of the mapped lineations. This analysis includes establishing the relative age relations of superimposed lineations, recognising coherent lineation patterns, and where possible, combining these patterns with dated positions of the ice margin. The eight flow stages shown, represent time slices of a continuous process of ice sheet growth and decay. These particular stages were chosen because they are thought to reflect the changing flow geometry of the ice sheet.

#### 6.3.2 Deglaciation flow patterns of central and south Sweden

Figures 6.6d to 6.6h show a number of flow phases for which it was possible to relate the lineation patterns to positions of the ice-sheet margin. Figure 6.6d shows position of the ice margin at ca. 13 ka BP (see Fig. 6.1). Sweden was still entirely covered by ice, with the exception of Skåne in the south. There is evidence from Skåne (Ringberg, 1988) and Denmark (Houmark-Nielsen, 1983, 1987) that during this time, ice from the Baltic Sea was advancing into

Fig. 6.5  
Lination map of central and south  
Sweden, interpreted from Landsat  
mosaics.



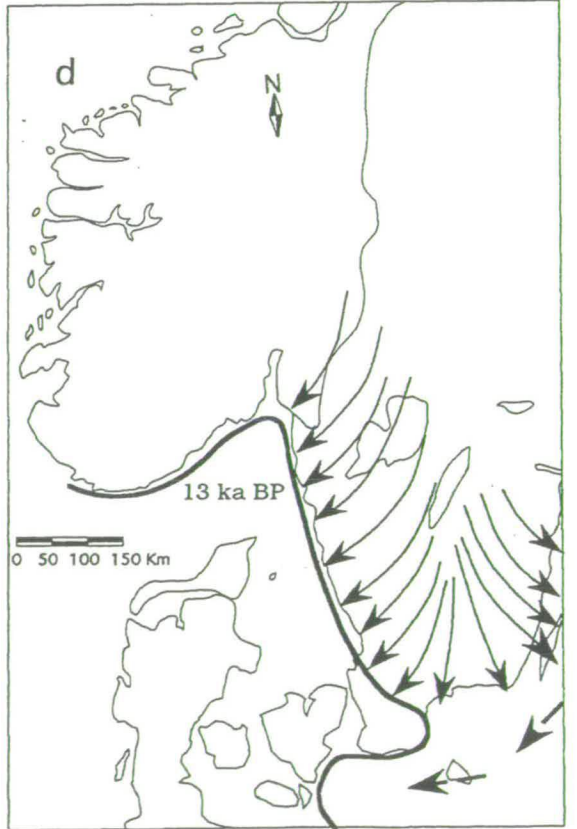
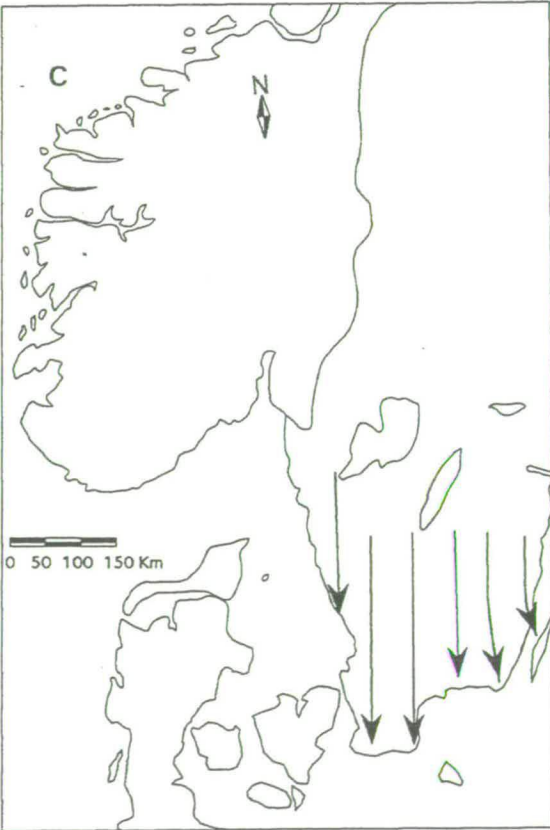
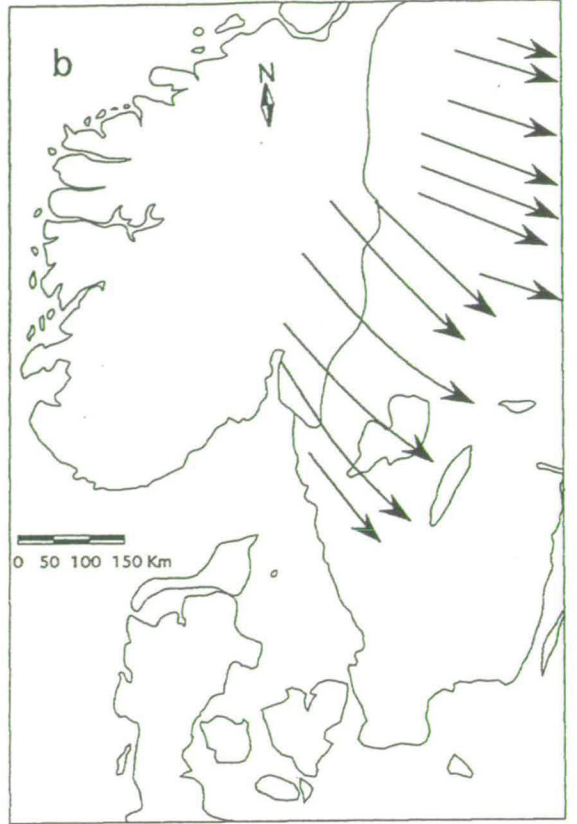
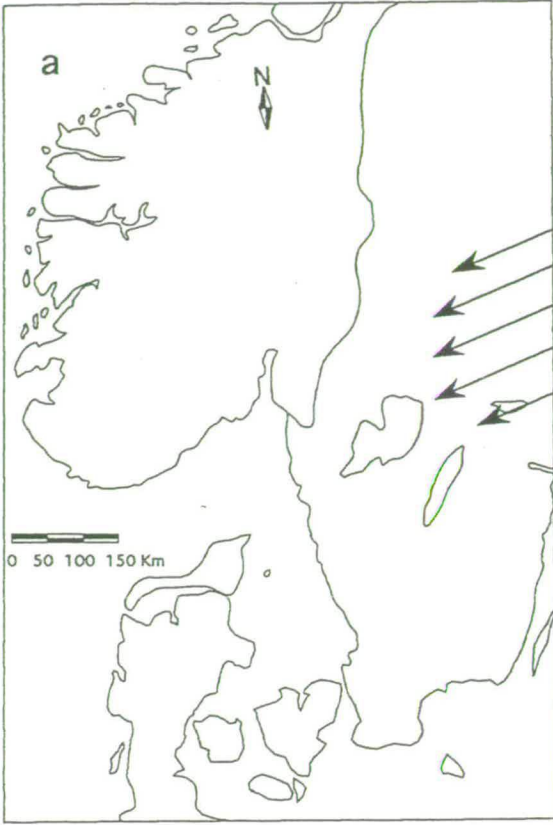


Fig. 6.6 Interpreted flow stages in central and south Sweden, based on lineation data.

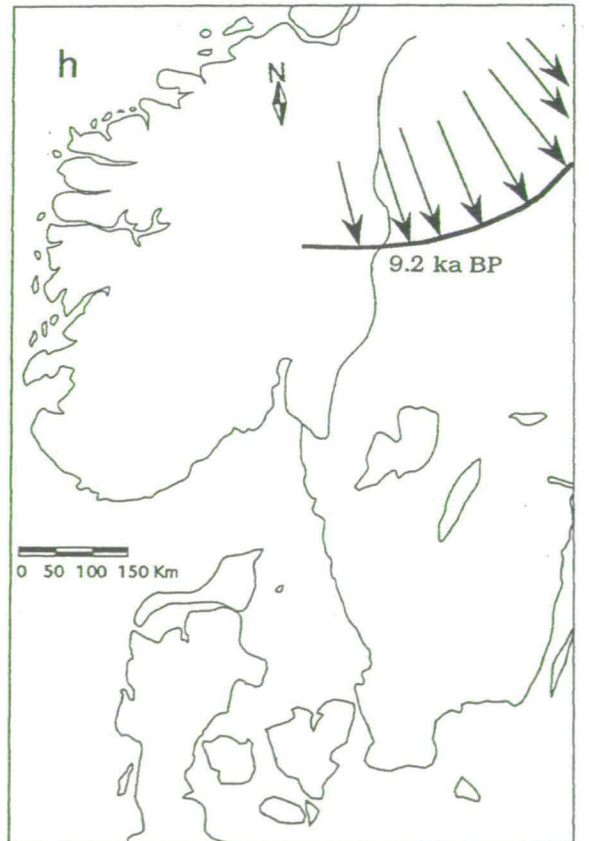
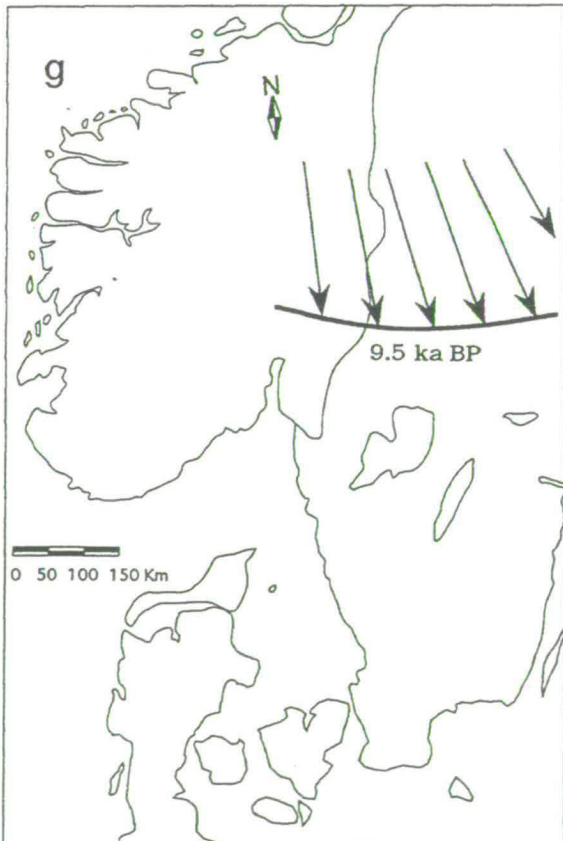
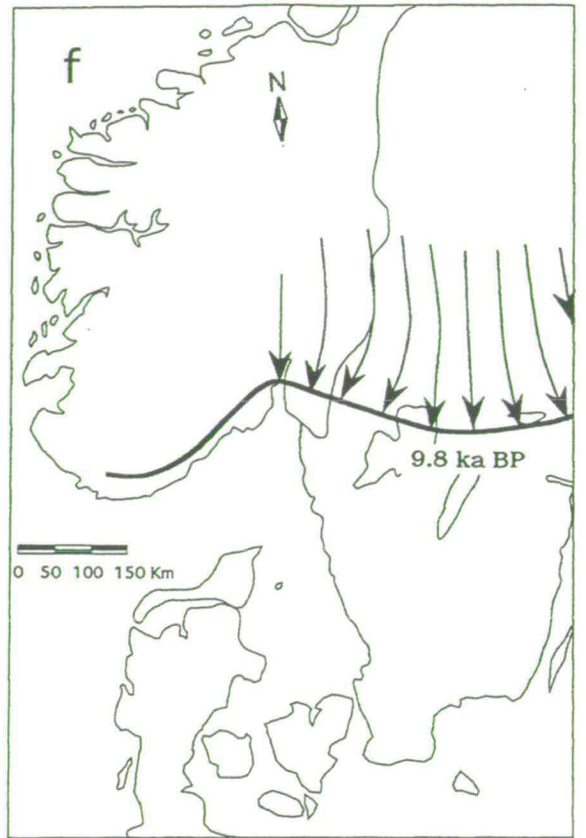
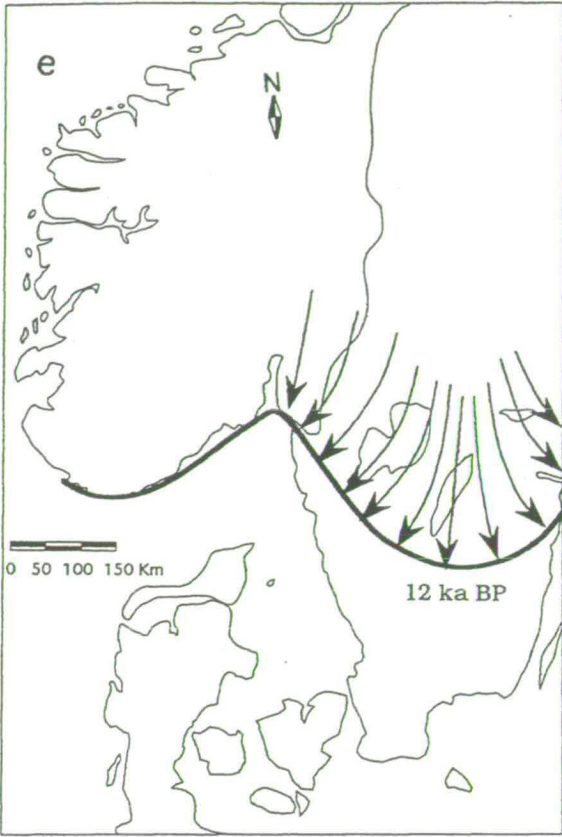


Fig. 6.6 (continued) Interpreted flow stages in central and south Sweden, based on lination data.

Denmark: the Baelthav Advance (Fig. 6.3e). A radial flow pattern can be observed over central and south Sweden (Fig. 6.6d). To the west, ice flowed into the already deglaciated Kattegat and Skagerrak areas.

In Fig. 6.1 it can be seen that the ice sheet still occupied what is now the Baltic Sea and that an ice lobe occupied parts of the Danish Islands. The fact that over the eastern half of Sweden, ice flowed towards the Baltic Sea has obvious implications for the ice-sheet topography and ice fluxes in this area. It implies that the Baltic Ice Stream was responsible for the influx of ice in Denmark which resulted in a lowering of the ice-sheet surface in the Baltic Basin at least as far north as the island of Gotland. Mass transfer of the ice sheet in the Baltic Basin was thus substantially higher than that over Sweden. The Baltic Ice Stream drained a substantial part of the southwestern and central areas of the ice sheet during this period. This has also been suggested for this period by others (Boulton *et al.*, 1985; Ehlers, 1992).

Figure 6.6e shows the ice flow pattern around ca. 12 ka BP. After 13 ka BP, the ice in the Baltic Basin retreated very rapidly compared to the ice over central Sweden (Fig. 6.1). The ice front in central Sweden was lobe shaped. But unlike the flow configuration over central and south Finland, which will be discussed later, there are no indications that an ice stream was active over south Sweden. The lobe shape is the result of ice calving into the Kattegat/Skagerrak area in the west and the deglaciated, isostatically depressed Baltic Basin in the east, while over Sweden itself ice was retreating over dry land (see Figs 2.17 and 2.18).

Figures 6.6f, g and h show the gradual shift in flow pattern during the later stages of deglaciation. The ice margin shifted slowly around (Fig. 6.6f), from E-W at ca. 9,700 years BP (the end of the Younger Dryas period), to a SW-NE position at ca. 9,000 years BP (Fig. 6.6h) as the ice sheet retreated towards the mountains. This shift is the result of the rapid deglaciation over Finland and the Bothnian Gulf during this period (Fig. 6.1). The areas to the west received ice from the Scandinavian mountains and therefore retreated more slowly.

### 6.3.3 Ice-flow patterns prior to 13 ka BP.

Figures 6.6a to 6.6c show three ice flow patterns that pre-date the deglaciation phases. The NE-SW lineations (Fig. 6.6a), which imply ice moving from the Bothnian Gulf over central and north Sweden and perhaps further towards the Skagerrak are of an unknown relative age. These lineations extend as far south as Lake Vättern. It is not clear whether this flow configuration records ice from the Bothnian Gulf draining towards the Skagerrak through the central Swedish lowlands or simply a limited encroachment of Bothnian Gulf ice into central Sweden.

The idea of Bothnian Gulf ice draining towards the Skagerrak is interesting. Central Sweden is a lowland area, containing Lake Vänern and Lake Vättern, which connects the Bothnian Gulf with the west coast of Sweden (Fig. 2.4). It is possible that ice-stream-like flow configurations could have developed at the west coast of Sweden where huge quantities of ice were funnelled into the Skagerrak deep. Such a stream could expand upstream to connect to the Bothnian area. If such flow configurations developed, the linear bedforms that might be expected at the west coast, would be similar in orientation to the deglaciation features. A disadvantage of the method used in the present study, is that two or more ice-flow phases in the same area which have identical flow patterns are difficult to separate. One would expect to identify only the dominant one. However, further to the east, the flow directions of the ENE-WSW Bothnian Gulf ice and the ice sheet during deglaciation should become increasingly different and therefore easier to separate. Unfortunately, it is not clear what the age of the NE-SW flow is relative to the other flow phases.

Figure 6.6c shows a N-S flow pattern in south Sweden that pre-dates the 13 ka BP flow configuration from Fig. 6.6d. It is not clear when exactly this pattern formed. Either the advance phase, or the maximum extent or the early deglaciation phase could have induced ice-sheet geometries compatible with the pattern shown. It is likely that this pattern is the result of prolonged N-S flow in this area and that it cannot simply be attributed to one single stage.

Figure 6.6b shows ice flowing out of the Scandinavian mountains. It pre-dates the deglaciation phases shown in Figs 6.6d to 6.6h. In the south,

deglacial lineations dominate and older lineations related to the pattern shown in 6.6b are rare. Further to the north, however, this changes as the number of older lineations increases relative to the deglacial ones. The flow pattern thus becomes increasingly well-defined towards the north.

The flow pattern of Fig. 6.6b is not compatible with flow during the maximum extent of the Fennoscandian ice sheet (Fig. 6.4a). Flow outwards from the south Norwegian mountains seems consistent with formation during an advance phase. It indicates that ice coming from the Jotunheimen area advanced over central Sweden past Lake Vänern. This configuration is possibly related to the Norwegian Advance (section 6.2).

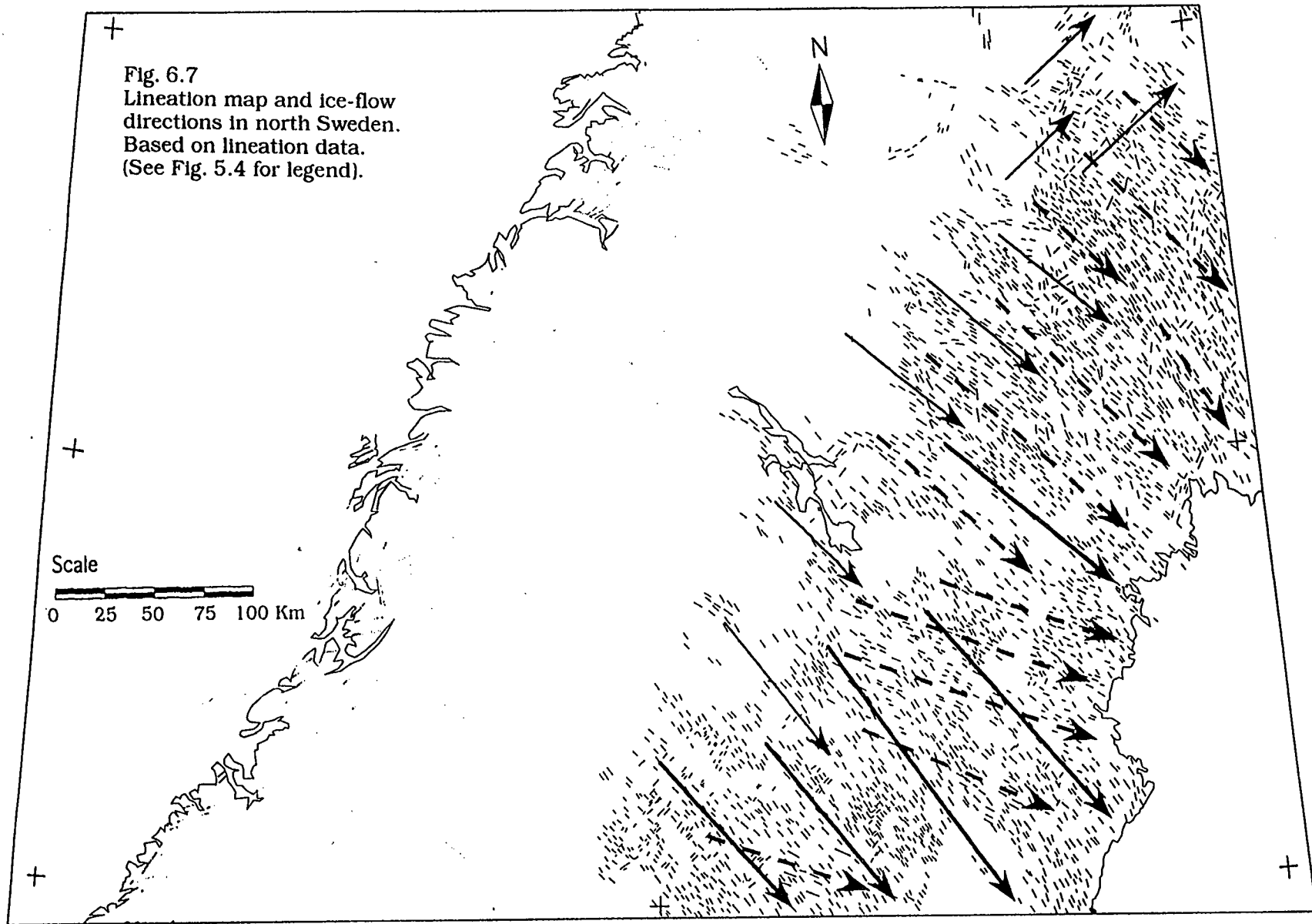
There is no indication of deflection towards the Skagerrak or Kattegat in this early phase. This lack of deflection is important because it indicates that ice from south Norway was able to cross the Skagerrak at an early stage of the glaciation without being diverted to the west through the Norwegian Channel, and could reach northern Denmark. However, during the maximum ice extent and the deglaciation, flow patterns indicate that the Skagerrak was an important channel draining ice towards the west. This earlier advance pattern in Fig. 6.6b suggests that this process was not active during the glacial advance.

A likely reason why westward drainage only became important later on in the glaciation, is the gradual isostatic depression of the area upon glaciation. This subject will be discussed further in Chapter 8.

#### 6.3.4 Deglaciation of central and north Sweden

Figure 6.7 shows the lineations and interpreted flow patterns for north Sweden mapped from Landsat mosaics (1:1,000,000). The deglaciation flow direction was almost uniformly NW-SE in the southern half of the area. This is the same pattern that as over south and central Sweden (Figs 6.6g and 6.6h). There is a pronounced pre-deglaciation flow pattern to the ESE in the south that shifts to SE in the north, where it has virtually the same direction as the deglaciation flow. From south to north the older flow system becomes more dominant, a

Fig. 6.7  
Lineation map and ice-flow  
directions in north Sweden.  
Based on lineation data.  
(See Fig. 5.4 for legend).



pattern that was also observed in the south (section 6.3.3). The pre-deglaciation flow direction is parallel to the general trend of the Swedish valleys that all run towards the Bothnian Gulf. In the northernmost part of the area there is also a SW-NE flow, the result of Ice Stream I activity (see section 6.5).

The most exceptional information from this area is the way the pre-deglaciation flow system shown in Figs 6.6b and 6.7 can be traced all the way to north Sweden. The number of lineations related to the pre-deglaciation system increases gradually from central to north Sweden.

#### *Ice-sheet activity*

The above pattern has been interpreted to reflect both a gradual decrease in basal activity of the ice sheet and acceleration of the deglaciation after the Younger Dryas (Fig. 6.1). The decrease in basal activity may be related to a number of processes. The combination of a rapid improvement in climate and deepening proglacial water bodies may have caused pronounced thinning of the ice sheet. As a result the ice flux and flow velocities would have fallen, causing lineation formation to slow down. The rapid retreat in itself implied that less time was available for lineation formation. Thus a weakening of the erosive and sedimentary processes during deglaciation, resulted in the pre-deglaciation landscape surviving destruction.

#### 6.3.5 Summary

The oldest lineations in Sweden point outwards from the Scandinavian mountains and follow the existing topography. The pattern becomes more pronounced towards the north, where older lineations become more abundant relative to deglacial ones. The lineation pattern is consistent with a small ice sheet covering the Scandinavian mountains which advanced later into the surrounding lowland areas.

A N-S lineation pattern over south Sweden may reflect ice flow during a considerable time when the ice margin was further to the south. The time of formation is not clear, but sometime during the maximum extent of the ice sheet is most likely.

The deglaciation flow in south Sweden since 13 ka BP consists of consecutive, superimposed, lobate sets. These have been interpreted as having formed continuously underneath a retreating, lobe-shaped, warm-based ice margin. This warm based area is estimated to have extended 100-150 km upglacier. The lineation distribution provides no indications of strong spatial variability which might reflect ice streaming (see section 6.4). The deglaciation lineations of central Sweden reflect the changing geometry of the ice sheet during the rapid retreat after the Younger Dryas.

## 6.4 Central and south Finland and Russian Karelia

### 6.4.1 Introduction

Figure 6.8 shows a map of glacial lineations in east Fennoscandia. This map has been compiled from the Landsat MSS and TM images that have been interpreted and represents a summary of the total number of lineations that were traced. The interpretations of the individual satellite pictures are included in appendix B.

The lineation distribution produced during deglaciation of the Weichselian Fennoscandian Ice Sheet is dominated by the effects of ice streaming. This is most conspicuous in central and south Finland and adjacent Russian Karelia. In Fig. 6.9 a number of interpreted flow patterns are shown that reflect the changing flow geometry during deglaciation. The ice-flow patterns within the 11 ka BP ice margin are dominated by large lobate features. The areas occupied by these lobes are dominated by streamlined bedforms. Their distribution is not uniform. The central areas of the lobes tend to have the highest density of streamlined bedforms, oriented parallel to the axes of the lobes. Streamlined bedform densities diminish away from the axes while orientations shift away from that of the axes (see also Figs 6.8 and 6.10a).

A longitudinal zonation in the landforms produced by the ice lobes exists as well. Upstream, towards the apex of the lobe, erosional streamlined bedforms are widespread. Eroded valleys and large roches moutonnées become more

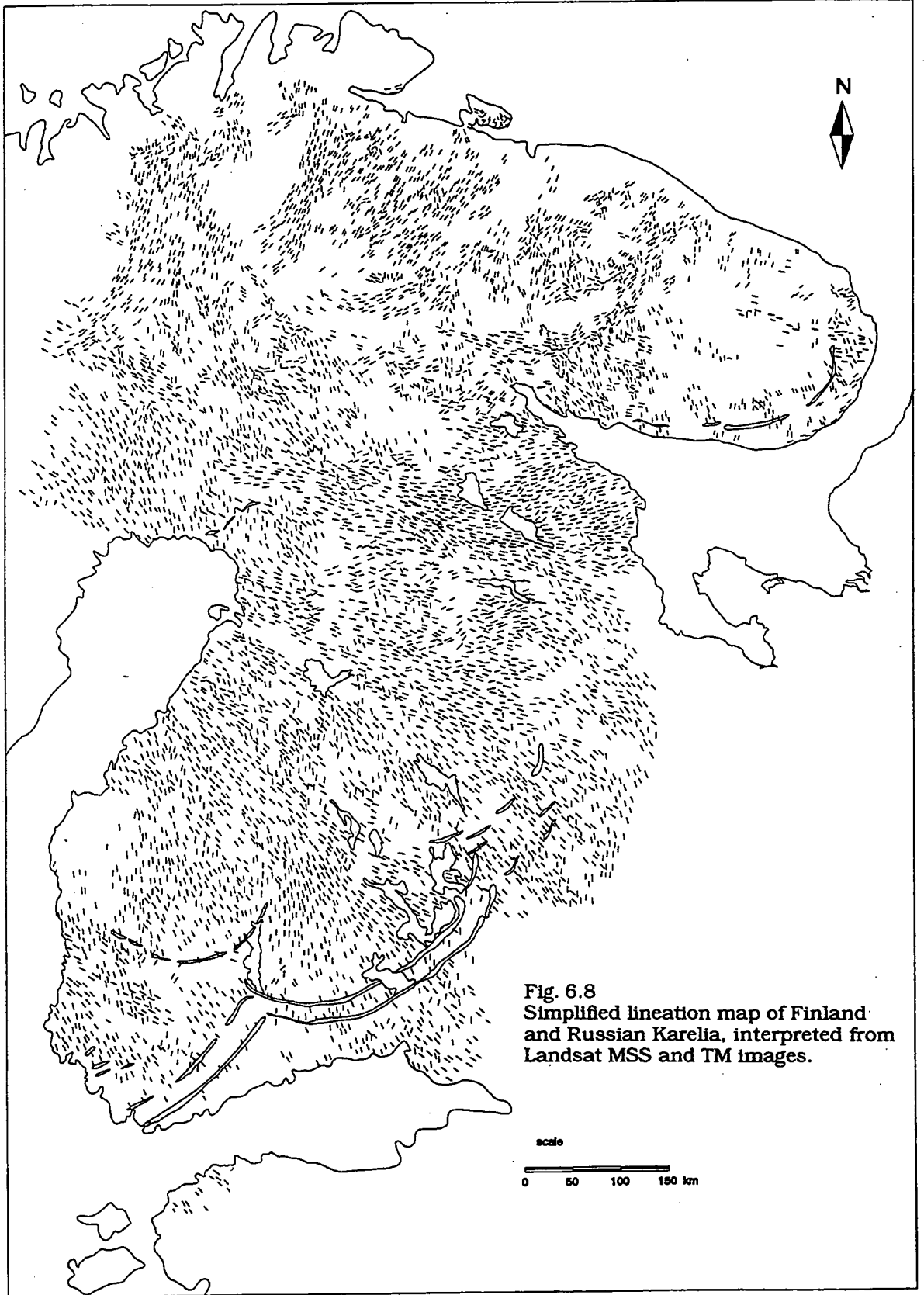
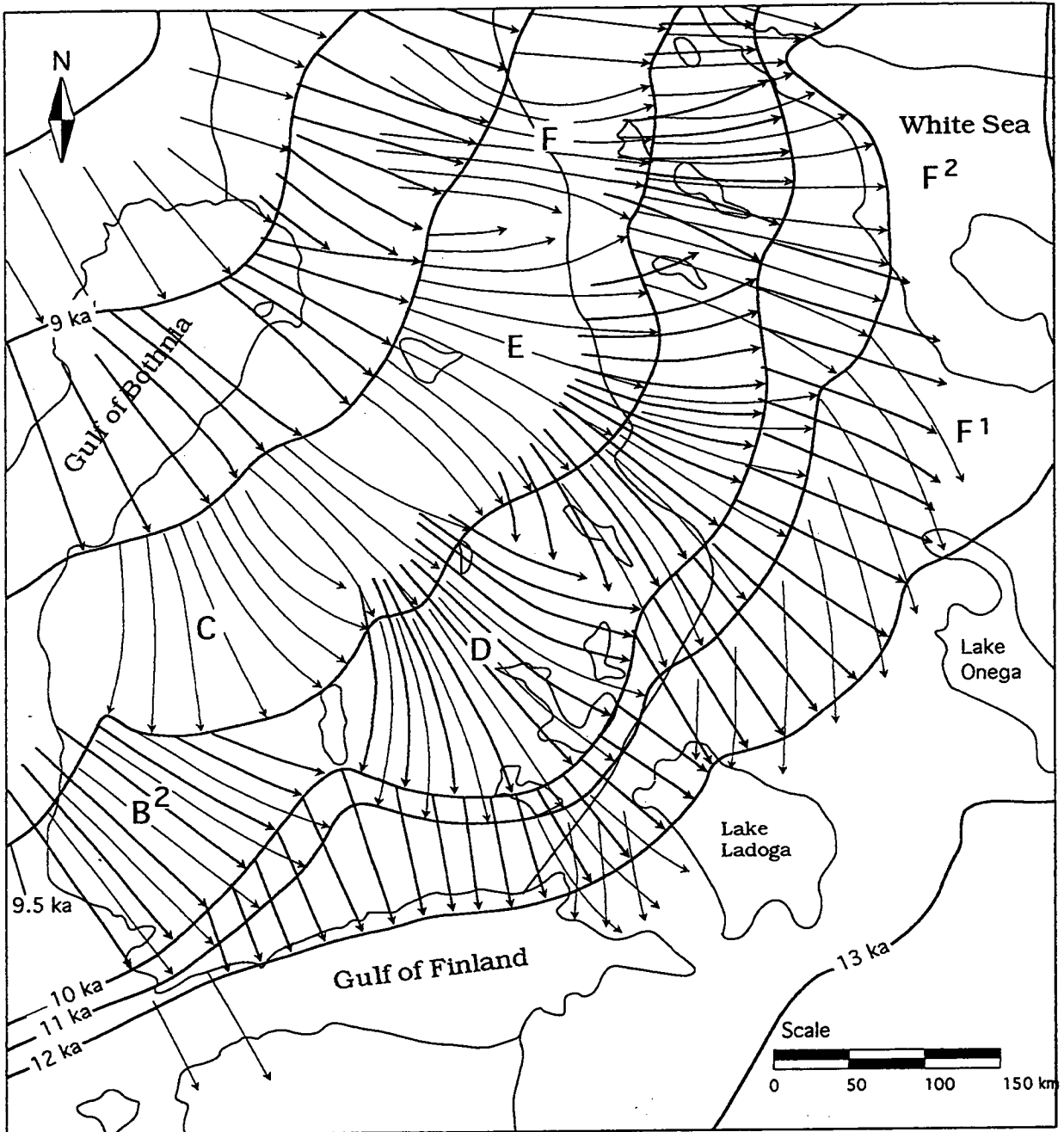


Fig 6.8  
Simplified lineation map of Finland  
and Russian Karelia, interpreted from  
Landsat MSS and TM images.

Fig. 6.9  
Deglaciation and associated ice-flow  
patterns in Finland and Russian Karelia.



numerous upstream of the large Younger Dryas fans. Downstream, in the zone of radial spreading, deposition occurred, here drumlins and flutes are dominant. During the retreat phase, this zonal pattern of upstream erosion and marginal deposition migrated upstream as well. During deglaciation the same areas were occupied by these different zones successively. This has produced diachronous sequences of superimposed streamlined bedforms.

Outside the 11 ka BP margin two flow systems occur superimposed. An older northerly flow and a younger, slightly diverging, flow coming from the WNW/NW. The latter can be related to the 12 ka BP ice marginal position. In section 6.4.3, a quantitative analysis of the spatial distribution of lineations is presented.

#### 6.4.2 Deglaciation flow systems

##### *Deglaciation 12-13 ka BP*

Figure 6.9 shows interpreted ice flow patterns during deglaciation of central and south Finland and Russian Karelia. The oldest flow system that belongs to the deglaciation is the northerly flow outside the Salpausselkä morainic arcs where ice flowed towards Lake Ladoga and Lake Onega. This flow system lies within the 12 ka BP ice margin but is older than the WNW/NW flow that can be related to this marginal position. Therefore, the northerly system must have been formed prior to 12 ka BP. The retreat pattern of the ice margin from 13 to 12 ka BP is poorly known, it is therefore not possible to relate the northerly flow to a particular configuration of the ice margin. It is likely that the northerly flow system operated for a considerable period and does not reflect a particular flow stage but formed diachronously.

Between 13 and 12 ka BP the ice margin was retreating to the north and west in this region. The retreat to the north was more rapid than that to the west, as a consequence the orientation of the ice margin changed from SW-NE to SSW-NNE. Near Lake Onega, the flow direction was from the NW, northeast of Lake Ladoga it was from the NNE. This flow system may have extended to the east. To the northeast of the Gulf of Finland a northerly flow can be traced. The rapid northerly retreat of the eastern margin resulted in a conspicuous shift in

flow direction along the entire eastern margin of the ice sheet between 12 and 13 ka BP. The shift amounted to about 30° just north of the Finnish Gulf but increased towards the north to more than 90° near the White Sea (Fig. 6.9). In the north, where deglaciation was more rapid, the shift is recorded by numerous superimposed bedforms (Fig. 6.8). Gradually, Ice Stream F1 retreated along its central flow line to the NNW. At the same time, to the south, the ice was no longer forced southward and, invaded the area occupied by Ice Stream F1.

In probably less than 1000 years, the flow geometry on the eastern flank of the ice sheet had changed completely. Flow prior to 12 ka BP was mainly N-S. Ice from the White Sea area and central Finland discharged in a southerly direction. It is likely that some form of ice streaming was active at that time as well. Ice Streams D, E and F1 probably flowed close together (section 6.4.3). This configuration was helped by the presence of mountainous terrain to the east (see Fig. 2.4). Although not particularly high, the relief is well above 100 m with an area of about 300 m high north of Lake Onega. To the relatively thin ice of the margin this may have proved an obstacle for expansion to the east.

Recent work in the Barents Sea has improved our understanding of the timing of growth and decay of the Barents Sea Ice Sheet (Elverhøi *et al.*, 1992; Solheim *et al.*, 1990). On the basis of glacial geomorphological features, such as till ridges and glacial flutes, and the presence of till, Elverhøi *et al.* (1990) concluded that grounded ice covered large parts of the Barents Sea during the Late Weichselian. An influx of light oxygen isotopes in the North Atlantic was dated by Duplessey *et al.* (1981) as lasting from 13.5 to 15.3 ka BP. Jones and Keigwin (1988) dated an influx of light oxygen isotopes in Fram Strait at 13-15 ka BP. Both events have been related to significant decay of the Barents Sea Ice Sheet. Well-defined glacio-marine accumulation in the central and northern Barents Sea at 300 m below sea level indicates a halt in deglaciation. Elverhøi *et al.* (1992) concluded that before 13 ka BP significant parts of the Barents Sea were deglaciated. Their reconstruction shows that the central parts of the Barents Sea were free of ice by 13 ka BP. There was still an area of contact between the Novaya Zemlyan ice and Fennoscandian ice over the Kola peninsula and the White Sea area. The Barents Sea north of Kola was virtually ice free by then.

It seems plausible to relate the shift in ice flow direction along the eastern margin between 12 and 13 ka BP (Fig. 6.9), to the deglaciation of extensive parts of the Barents Sea prior to 13 ka BP. Thinning of the Barents Sea Ice Sheet would have enabled ice from North Karelia and Finnish Lapland to flow through the White Sea and discharge into the Barents Sea (Fig. 6.9). This route is considerably shorter and more effective than flow to the south. It is difficult to say how long it would take for the development of such a new drainage route to affect the southern margin. Firstly, because a White Sea Ice Stream draining North Karelia may have developed early during the deglaciation phase of the Barents Sea Ice Sheet. And secondly because this deglaciation phase may have affected the drainage of the area north of the Maanselkä mountains in northernmost Finland. However, it seems reasonable to suggest that the rapid decay of the Barents Sea Ice Sheet affected the deglaciation flow pattern of the entire eastern flank of the Fennoscandian Ice Sheet and ultimately caused the observed westerly shift.

#### *Deglaciation since 12 ka BP*

The flow patterns of the deglaciation since 12 ka BP are dominated by ice streams and lobes identified as B to F in Fig. 6.9. The ice streams evolved and shifted through time. In the south, Ice Streams B and D formed along the Salpausselkä moraines during the Younger Dryas, but gave way to single Ice Stream C by 9.5 ka BP. In the north, Ice Streams E and F persisted along the same axes from 12 to 9 ka BP. The width of the lobes, perpendicular to the ice-flow direction can be up to 250 km. From the snout to the apex of the lobe its longitudinal distance can be up to 200/250 km. The ice lobes are separated by interstream areas in which deglaciation lineations are less frequent than in the lobate areas.

From ca. 12 ka BP, until the formation of the Salpausselkä moraines during the Younger Dryas (11-10 ka BP), the above mentioned shift in flow direction continued, albeit less rapidly. The White Sea area was almost completely deglaciated by 11 ka BP (Elverhøi *et al.*, 1992) and thus Ice Stream F1 had virtually disappeared. In response to this the ice streams in the south shifted to the north. The ice flow north the Gulf of Finland showed hardly any radial flow between 11 to 12 ka BP. This changed, however, during the Early Younger

Dryas, when radial flow of Ice Streams B and D became more pronounced with time.

To the north, Ice Stream E became more pronounced from 11 to 10 ka BP, at the expense of Ice Stream F2. The decline of the latter may to some extent have been topographically controlled. At around 10 ka BP the apex of the ice lobe was positioned over the highest part of the northern Maanselkä mountains, which are up to 500 m in elevation. This would have hindered ice flow from Finnish Lapland to the east as the ice sheet became considerably thinner over this area. To the north, the Maanselkä mountain chain bends to the west, cutting off Ice Stream F2 from its drainage area in the north.

In contrast, Ice Streams B to E are not related to topography, suggesting that glaciological mechanisms, within the ice sheet, are responsible for its functioning and evolution (see Chapter 8). Such internal mechanisms could perhaps explain the strong reduction of Ice Streams B and D at around 9.5 ka BP (Fig. 6.9). By then the ice from the Baltic Sea that fed lobe B had virtually gone and the lobate flow of Ice Stream D had almost disappeared as well. In between these two ice streams a new one had developed around 9.5 ka BP, Ice Stream C. The deglaciation chronology of this area (Glückert, 1977, Ignatius *et al.*, 1980) shows that while the adjacent ice margins continued to retreat, the position of ice margin Ice Stream C remained stationary for approximately 200 years along the Näsijärvi-Jyväskylä end moraine, sometimes called the 4th Salpausselkä.

Not only the activity of Ice Streams B and D declined. The activity of Ice Streams E and F also diminished during the retreat of the ice sheet. This can be seen in Figs 6.10a and 6.10b; the densities of deglaciation lineations decrease, while preservation of the pre-deglaciation lineations improves from east to west.

#### 6.4.3 Quantitative analysis of lineations

To quantify the variations in lineations distribution, the region was covered by a 20x 20 km grid. In Fig. 6.10a the number of lineations related to

Fig. 6.10a Spatial distribution of deglaciation lineations in central and south Finland.

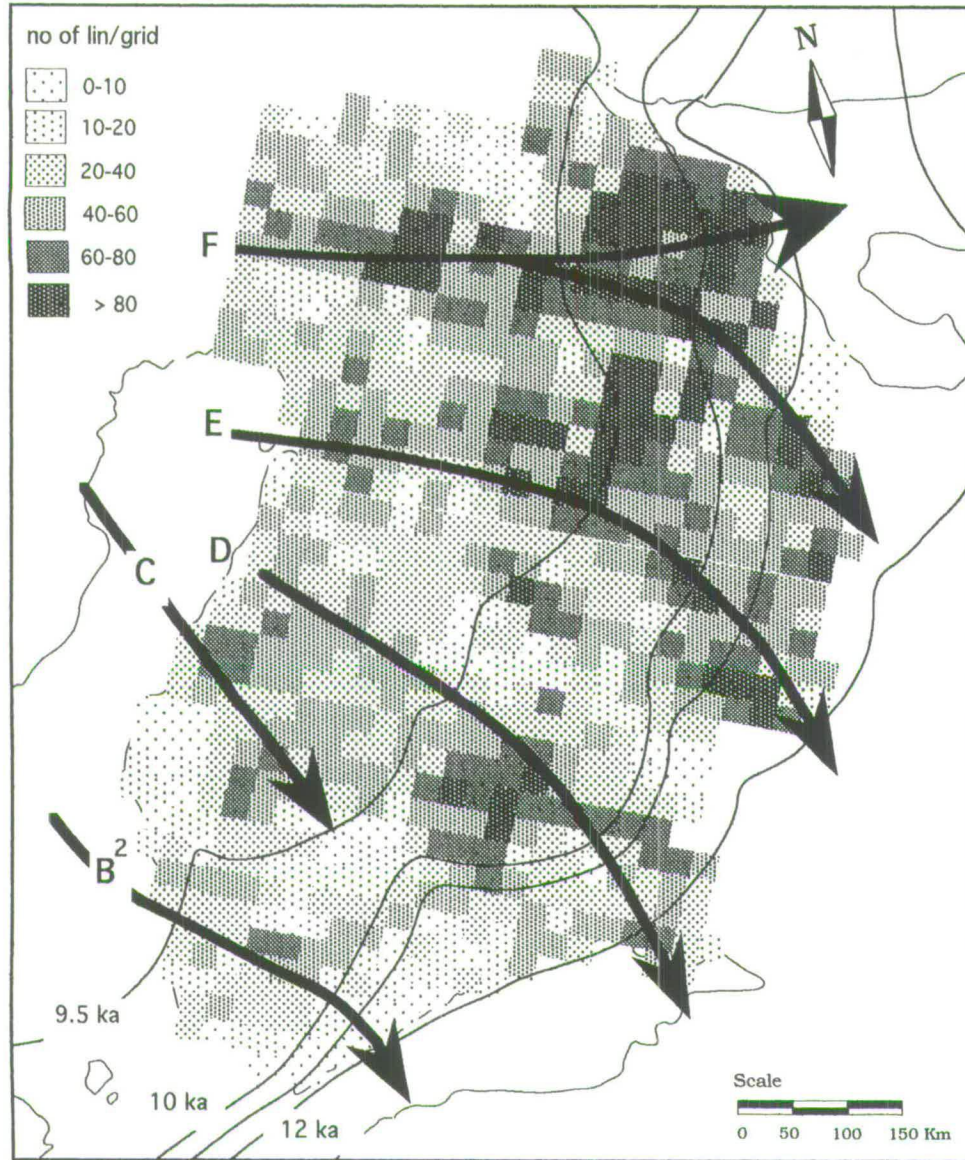
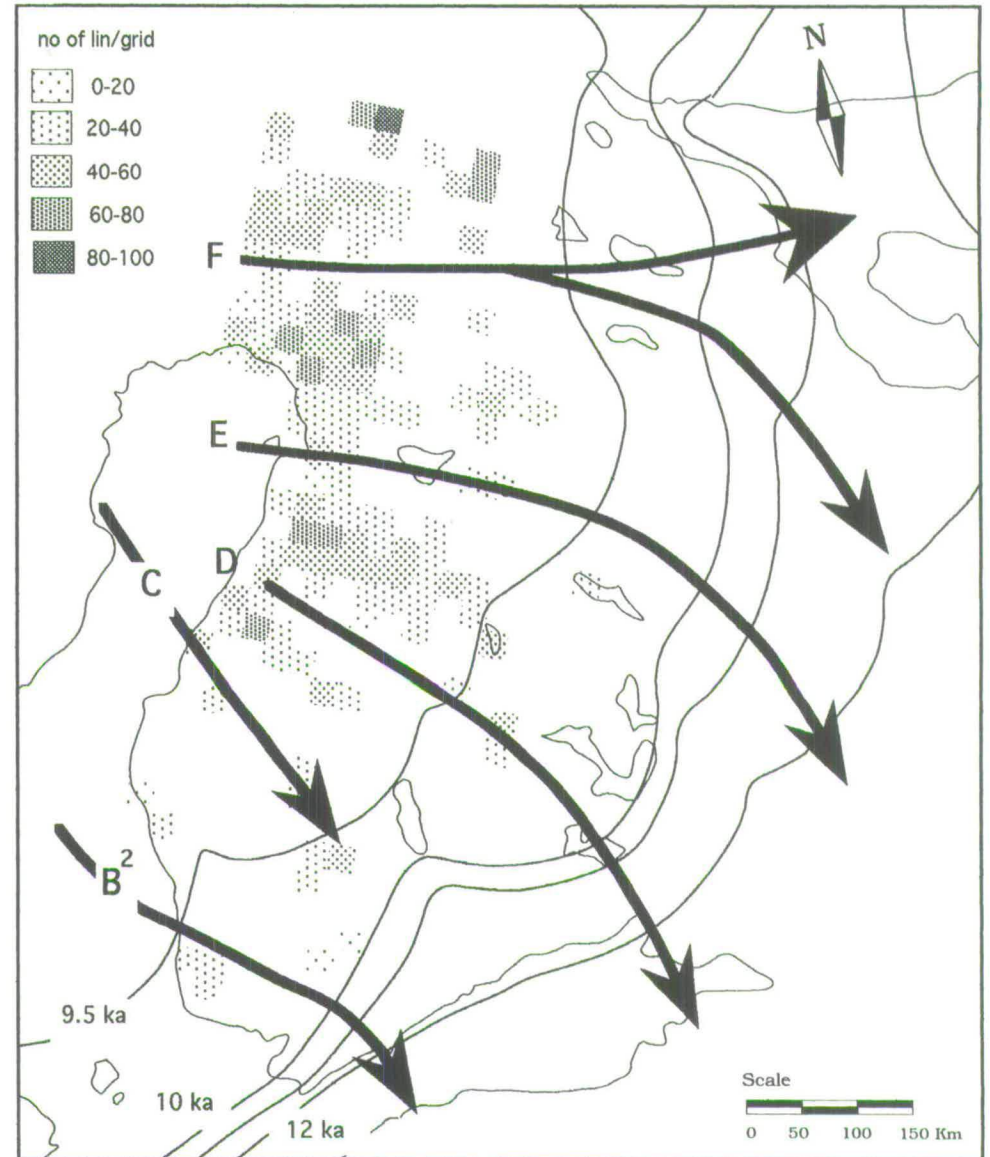


Fig. 6.10b Percentage of pre-deglaciation lineations of total number of lineations in central and south Finland.



deglaciation are shown per grid cell. Also shown are the diachronous centre lines of the ice streams (thick arrows), and the positions of the ice margin for 9.5, 10, 11 and 12 ka BP. Approximately 95% of total number of lineations in the area shown are related to deglaciation, leaving approximately 5% of a pre-deglaciation age. To the north and west of the area shown, the percentage of pre-deglaciation lineations is considerably higher.

Two superimposed patterns are apparent in the lineation distribution. The first is a zonation that runs perpendicular to the consecutive ice margins, the second runs parallel to the consecutive ice margins. The pattern perpendicular to the margins is formed by an alternation of zones of higher and lower lineation densities. The central axes of these zones remain approximately normal to the ice margins. The high-density zones coincide with of the axes of the ice streams. Although within each zone anomalies are present, a good fit between the density patterns and the directional patterns can be observed (Figs 6.8 and 6.10a). The anomalies are partly a result of topography and lake distribution, as is the case with the low lineation densities on the southern part of Ice Stream E and the northern part of Ice Stream D inside the Salpausselkäs.

East of the 11 ka BP ice marginal position the trend of Ice Streams F and E changes abruptly which also shows up in the density pattern. The high-density zones are separated by zones of lower lineation densities. These density variations could reflect the alternation of zones with different flow velocities. This suggests that ice streaming was also active prior to 11 ka BP.

The second, margin-parallel, pattern is formed by a very high density of lineations directly inside the Salpausselkäs (to the north also outside them), which diminishes to the west. During the Younger Dryas, which lasted for approximately 1000 years (Lundqvist, 1986), the ice margin in the area retreated by only 30 to 60 km. This almost stationary position of the ice sheet resulted in a well-developed lineation pattern reflecting this ice-sheet geometry. Very high densities within the Salpausselkäs suggest that the marginal zones of the ice streams had a warm base for 200-250 km inside the margin. The active zones have a roughly triangular shape, becoming narrower towards the apex of the lobes. The estimate of the size of the warm-based zone is a

minimum, upstream of the apex the ice stream may also have been warm based. However the diachronous nature of the lineations makes it difficult to determine the exact dimensions of the ice streams at any particular moment.

To the west, lineation densities decrease. The axes of Ice Streams E and F still stand out but the number of lineations decreases. In contrast, the low-density interstream areas have the tendency to become wider towards the west.

The lineation density distributions of Ice Streams C and D reflect the way in which their relative importance changed after the Younger Dryas. The activity of Ice Stream D diminished rapidly after 10 ka BP. Within the 9.5 ka BP ice margin, lineation densities along the ice stream axis are low compared to those just inside the Salpausselkä moraines. In the case of Ice Stream C the reverse applies. Outside the 9.5 ka BP ice margin, lineation densities are comparable to interstream areas, suggesting only limited basal activity. Within the 9.5 ka BP margin however, densities are substantially higher, reflecting the development of a warm-based ice lobe.

Figure 6.10b shows the percentage of lineations of pre-deglaciation age in each grid cell. Pre-deglaciation lineations are more abundant in the interstream areas and decrease in number towards the axes of the ice streams. In the east they are virtually absent, towards the west they increase in number. The decrease in deglaciation lineations (Fig. 6.10a) and the increase in lineations formed prior to deglaciation (Fig. 6.10b), is consistent with lower flow velocities in the interstream areas, and with the increase in ice-margin retreat rates towards the west. The overall activity of ice streams may have decreased during deglaciation as the mass transfer from accumulation to ablation area continuously decreased as a result of the shrinking drainage areas.

#### 6.4.4 Summary

The lineations produced by the oldest deglaciation flow form a N-S pattern outside the Salpausselkä. The high density of these lineations indicates that ice streaming was already active but no lobate configuration developed, perhaps as a result of topographic obstruction to the east.

Between 13 and 11 ka BP ice-flow direction along the eastern margin underwent a conspicuous anti-clockwise shift that was probably related to deglaciation of the Barents Sea.

Around 12 ka BP a number of lobes developed in the eastern marginal zone, this pattern was enhanced during the Younger Dryas. The almost stationary position of the ice margin for almost 1000 years, resulted in a strong geological imprint of this configuration (Fig. 6.10a). The lateral zonation of lineation densities reflects the internal organisation of the ice sheet in a number of ice stream/ice lobe systems.

The rapid deglaciation after the Younger Dryas has resulted in a decrease in the lineation densities towards the west. However, the number of pre-deglaciation lineations increases in this direction. Ice streams B and D rapidly diminished in areal extent and around 9.5 ka BP a new Ice Stream (C) had developed in-between these two.

## 6.5 North Scandinavia

### 6.5.1 Introduction

Figure 6.11 shows the lineations mapped over north Scandinavia using Landsat mosaics (1:1,000,000). Figure 6.12 shows the interpreted evolution of the flow patterns during deglaciation of the area. Quaternary deposits cover most of the low-lying areas in north Scandinavia (Hirvas, 1991). Ice-sheet dynamics during the deglaciation of north Scandinavia were dominated by a number of large ice streams (section 6.5.2). Ice Streams H and I drained ice from the areas to the east of the Scandinavian mountains to the North Atlantic (Fig. 6.12). Further to the east, Ice Stream G developed over the Kola peninsula, possibly in response to the disintegration of the Barents Sea Ice Sheet after 15 ka BP (Duplessey *et al.*, 1981; Elverhøi *et al.*, 1992). The dotted area in Fig. 6.12 reflects the presence of strongly weathered pre-glacial bedrock at or near the surface, this phenomenon will be discussed in section 6.5.3.

Fig. 6.11  
Lineation map of  
north Scandinavia,  
interpreted from  
Landsat mosaics.

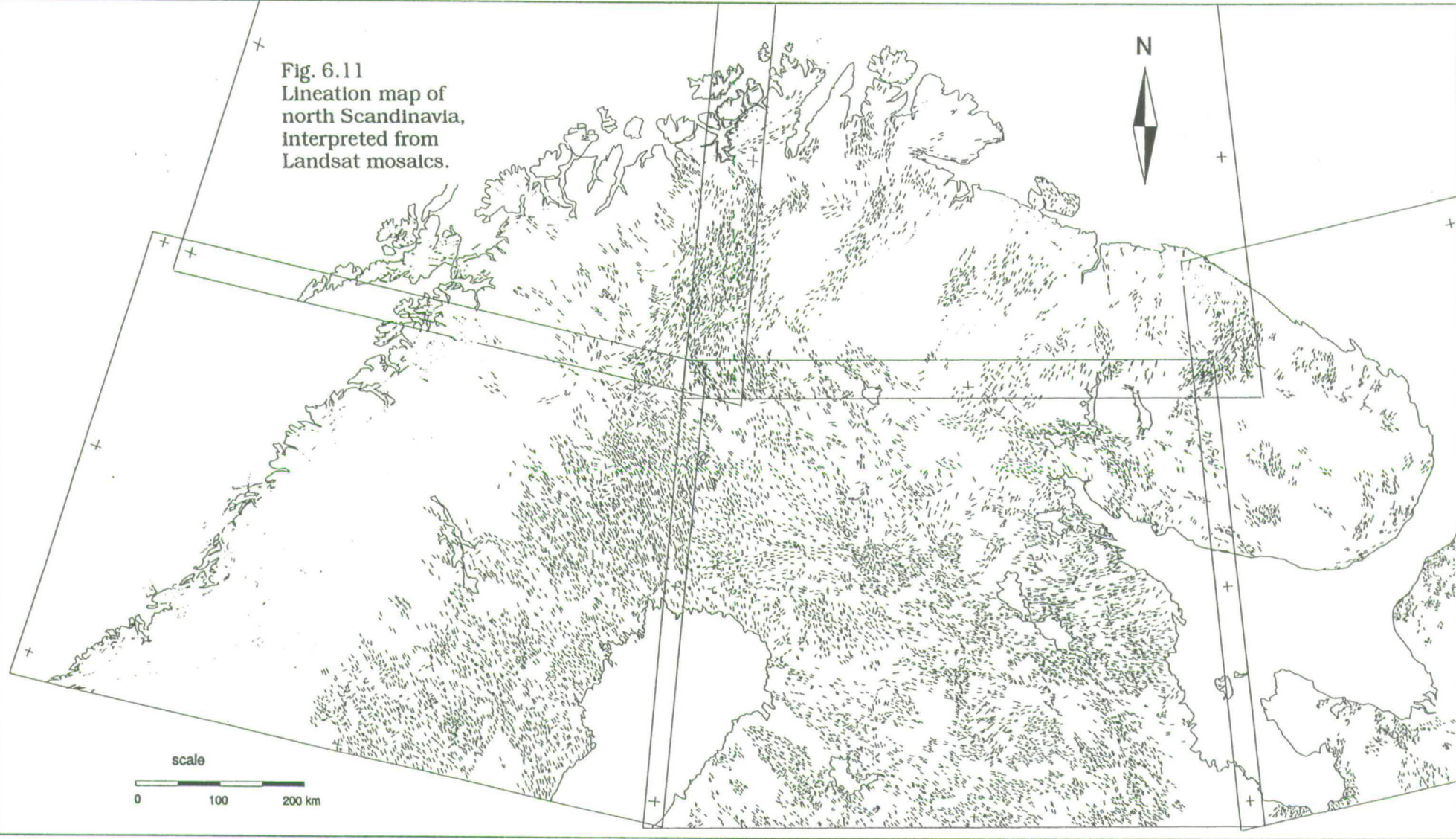
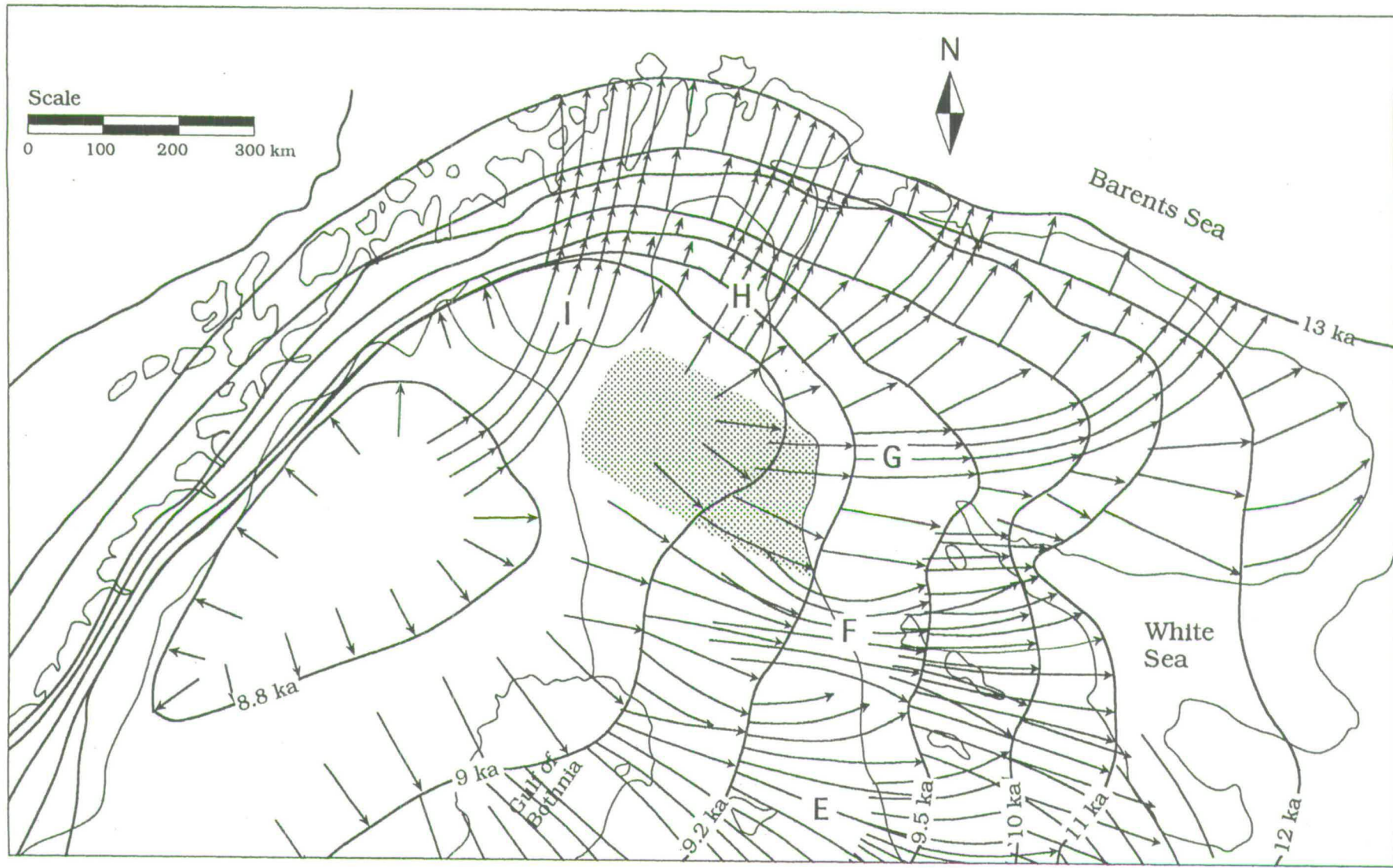


Fig. 6.12 Deglaciation and associated ice-flow patterns of north Scandinavia. Dotted area shows where Tertiary weathered bedrock is at or close to the surface.



### 6.5.2 Deglaciation flow systems

The lineation patterns produced by the northern ice streams differ from those described earlier from central and south Finland. The linear bedforms of the northern ice streams lack the divergent pattern common to the ice stream/lobe systems in central and south Finland. The flow lines of the northern ice streams remained parallel throughout most of the early and late deglaciation. There are two reasons why the behaviour of the northern ice streams was different from the Finnish ice streams. The first is that before ca. 12 ka BP (see Fig. 6.1) Ice Streams H and I terminated in the full marine condition of the North Atlantic. Figure 6.13 shows the bathymetry of the Barents Sea area. Ice Streams H and I could discharge icebergs into the Bear Island Trough which is 300-500 m below sea level. The area offshore Ice Stream G is more shallow (100-200 below sea level) but is connected to the Bear Island Trough. Although eustatic sea level was lower during deglaciation, this was easily offset by the isostatic depression of the marginal area.

The above implies that ice calving into the Bear Island Trough played an important role at the northern margin of the Scandinavian Ice Sheet. The deep water offshore, the tidal effects and the proximity of the shelf break ensured that calving was a very effective way of draining the ice streams, which would have resulted in a considerable drawdown of the ice sheet.

Along the eastern and most of the southern margins of the ice sheet, calving was a less important mechanism because the marginal lakes or seas were considerably less deep and of more limited extent (see Figs 2.16 and 2.17) and tidal effects were negligible. In these areas, therefore, ablation played a more important role and drawdown effects were small. The situation in the Baltic Basin between Finland and south Sweden was different. In this area deep standing water may have influenced the flow dynamics of the ice sheet during deglaciation (section 2.3)

The second reason for the parallel flow lines is the topographic control on the ice streams in north Scandinavia (Fig. 2.4). The ice streams occupied large valleys connected to the fjords and offshore troughs. Flanking mountain ranges prevented divergence of flow. Ice Stream I was flanked to the east by

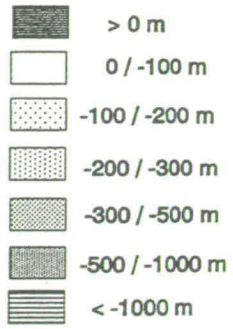
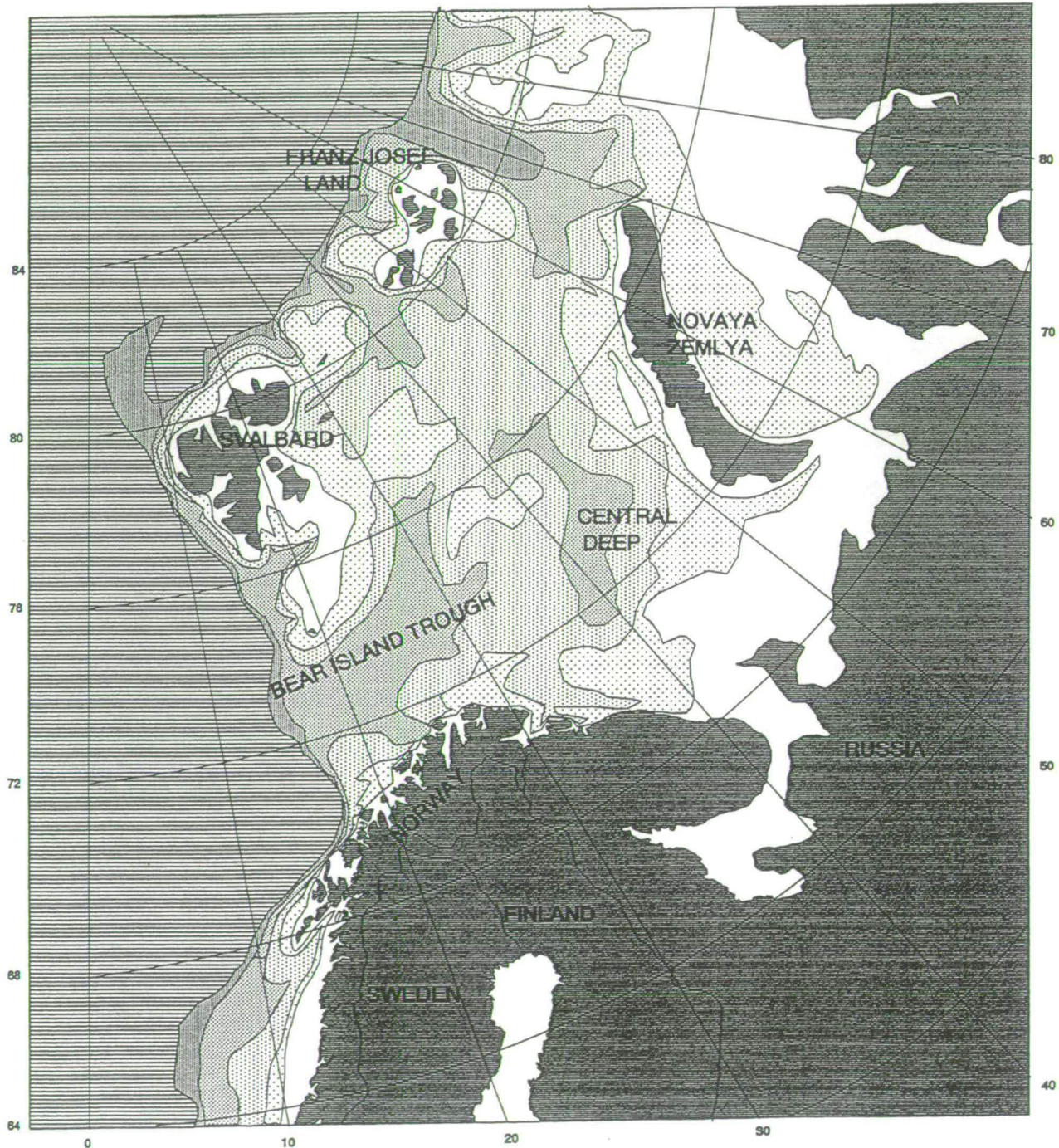


Fig. 6.13 Bathymetry of the Barents Sea.



the Pallastunturi Mountains and to the west by the Scandinavian Mountains. To the north the ice stream occupied a wide shallow trough through the Finnmark area connected to the Porsangerfjord and the Altafjord. Ice Stream H crossed the Maanselkä mountain range just to the northwest of the Saariselkä Mountains, where it is relatively low. Further to the northeast, the ice stream followed the wide, flat valley now occupied by Lake Inari and drained into Varanger Fjord. When, after 12 ka BP, the ice-sheet margin in the north retreated on to the shield area, the topography still favoured fast flow through the deep valleys and prevented diverging flow. This effect was strongest in the Finnmark area.

The position of Ice Stream G is controlled by the Chibiny mountains on the Kola Peninsula and the W-E running valley to the west of these mountains. In the low-lying coastal area between Ice Streams G and H, there is ubiquitous evidence of active ice flow to the northeast with a clear concentration in the Moermansk area. It is possible that for some time an ice stream of limited size was active here.

As the margin of the ice sheet retreated towards the Scandinavian mountains, ice-stream activity diminished, probably because the drainage areas were shrinking. Only Ice Stream I remained active almost to the last stages of deglaciation. With the gradual dying of the ice streams, the geomorphological impact on the landscape of the later deglaciation stages becomes weaker. This is especially clear in north Sweden where the W-E flow system belonging to Ice Stream F weakens rapidly near the Swedish/Finnish border (Figs 6.11 and 6.12).

#### *Pre-deglaciation lineations*

The pronounced NW-SE lineations to the north and west of the Bothnian Gulf (Fig. 6.12) have been interpreted as belonging mostly to flow systems preceding deglaciation. Apart from Ice Stream I, which produced a well-developed SW-NE flow system, most of the lineations belonging to the last stages of deglaciation are weakly developed and are superimposed on the older and larger NW-SE lineations. The pre-deglaciation lineations will be discussed in Chapter 7.

### 6.5.3 Pre-glacial weathered bedrock

In Finnish Lapland in-situ weathered bedrock has been reported from many localities (Hirvas, 1991). This area is shown by dots in Fig. 6.12. The abundance of clay minerals in the weathered material indicates that weathering took place in a warmer climate than the present (Saarnisto and Tamminen, 1987). Tynni (1982) dates the weathering as Late Tertiary on the basis of Early Tertiary marine diatoms found in secondary positions. The weathered rocks are to a varying degree mixed with the overlying tills. The thickness of the weathered bedrock varies considerably, from only a few metres in most places to over 50 m (Hirvas, 1991). Outside the area shown in Fig. 6.12, weathered material have been reported only rarely. The abundance of this often very loose material, close to and sometimes at the surface, is a clear indication that Pleistocene glacial erosion was limited in this area .

Hirvas (1991) interpreted the presence of the weathered bedrock as indicative for the limited impact the Late Weichselian glaciation had on most of the north Scandinavian landscape. He argued that during the Late Glacial Maximum, when the ice divide was located over Finnish Lapland (Lundqvist, 1986), the ice sheet in north Scandinavia was frozen to its bed. He also assumed that the Late Weichselian deglaciation had only a limited effect in most of north Scandinavia (see also section 6.6) .

In Fig. 6.12 it can be seen that the weathered bedrock is situated in an area where ice-stream activity was limited. By the time the ice margin reached this area, Ice Streams F and G had stopped functioning altogether and Ice Stream H was rapidly diminishing in importance. It is likely that ice-sheet erosion underneath the ice divide was limited because it was probably frozen to its bed. However, the reason that the weathered bedrock in this area survived so close to the surface while other areas were reworked during this stage of the deglaciation, is probably related to the organisation of the deglaciation ice flow.

Erosional and depositional processes are not uniformly distributed over the ice stream areas but are highly localised. Overall ice stream activity diminishes during deglaciation and after ca 9.5 ka BP sheet flow seems to have been the dominant flow mechanism in the shrinking ice sheet. The combination of rapid

retreat and sheet flow was probably unable to substantially rework the subsurface, not only in the weathered bedrock area but also in large areas of north Sweden (with the exception of the area occupied by Ice Stream I).

If the Late Tertiary weathering age is correct (Tynni, 1982) the weathered bedrock has survived several glaciations. This might indicate that the flow organisation in this area was a recurrent feature in earlier deglaciations and resulted from the strong topographic control. Moreover, the survival of the weathered material points to a limited erosional capacity of the ice sheet in this region during the advance phases.

## 6.6 Comparison of different palaeo-ice-flow indicators

### 6.6.1 Introduction

A large amount of palaeo-ice-flow information from north Norway, north Sweden and north Finland has been published in the Nordkalott Project (1986a-d). The published maps show striae, till fabrics and subglacially streamlined bedforms. In this section, the striae and till fabric measurements from the Nordkalott Project are compared with the lineation data derived from the remote-sensing studies.

Striae, till fabrics and lineations all record ice-flow directions during formation. There are, however, important differences in the spatial and temporal resolution they provide. Striae provide accurate information on local ice-flow directions and their relative ages. In general, flow directions from striae measurements show a higher degree of directional variation than those derived from lineation data. This is partly because striae reflect ice flow on a very local scale, where flow divergence resulting from small topographic variations is of influence (Kleman, 1990). Moreover, striae form on a short time scale compared to lineations. Even local, short-lived shifts in flow direction can potentially produce new striae. This implies that striae potentially record shifts in flow direction very accurately but since they reflect local ice flow, spatial correlation can be a problem. The youngest striae typically record ice-flow

directions very close to the ice margin and thus reflect the final stages of the deglaciation (Kleman, 1990).

Till fabrics also provide point measurements, with the added advantage that they can be correlated with the local stratigraphy and can therefore potentially yield absolute dates (Hirvas, 1991). A disadvantage is that till fabrics can be remoulded by later ice-flow directions thus obscuring the relation between the stratigraphy and flow directions. In addition units may have been removed by erosion resulting in incomplete records. For this reason spatial correlation of fabric measurements over large areas can be hazardous.

The formation of lineations is still hotly debated, where exactly they formed and how long this process takes are, as yet, not well known and probably depend on glaciological and geological conditions which may vary strongly from one location to another (Rose, 1987). However, most authors agree that they are formed by subglacial erosional and deformational processes and that they accurately reflect flow directions during formation. The superimposition of several generations of lineations provides relative age information about successive flow directions (Lagerbäck and Robertsson, 1988; Rose, 1987). The longer periods necessary for their formation and the limited resolution of the satellite images limits the resolution one can achieve from lineations as compared to striae. A major advantage, however, is the fact that in many formerly glaciated areas lineations completely dominate the surface topography, enabling spatial correlation over very large areas (Sugden and John, 1977; Boulton and Clark, 1990).

However, the use of these data sets to reconstruct ice-sheet evolution is far from straightforward. This is shown by the difference in the conclusions concerning the glacio-dynamic behaviour of the last ice sheet of Hirvas (1991) and the ones in this study. Irrespective of these differences in interpretation, the basic data collected in the Nordkalott Project provide information on the behaviour of the last ice sheet and can therefore be used for comparison with the lineation data to check the consistency of the method.

### 6.6.2 Striae and till fabric data compared to lineation data

The Nordkalott maps provide about 3000 striae and 600 till-fabric measurements. Plotted at their approximate geographical positions they are distributed unevenly over the 600 by 350 km wide area. To deal with the large amount of data the area has been overlain by a grid with individual cells of 45 by 45 km. All measurements of both striae and till fabrics within each gridcell have been plotted in rose diagrams at the centre of the gridcell (Figs 6.14 and 6.15). Each rose diagram has been divided into 72 sectors of 5°. The size of the petals is proportional to the number of measurements within each sector. Relative ages are shown by different colours, the youngest directions in red, the oldest in yellow.

The rose diagrams, especially those showing the striae measurements (Fig. 6.14) still show a high degree of variability. To facilitate comparison with lineation data, the youngest measurements, which in the case of striae account for 90% of the total, have been plotted separately from the combined older measurements. In Figs 6.16, 6.17, 6.19 and 6.20 the rose diagrams have 10° sectors. For the youngest striae data (Fig. 6.16) sectors that contain only a single measurement have been ignored, reducing the amount of striae data by approximately 15%. The results are shown in Figs 6.16 and 6.19 for the striae data, and Figs 6.17 and 6.20 for the till fabric data. Figures 6.16 and 6.17 show only the youngest relative ages, while the older relative ages have been grouped together in Figs 6.19 and 6.20.

The lineations (this study) have been presented by arrows showing the major ice flow directions in each grid cell. There is no quantitative information on how many measurements each arrow represents. In Fig. 6.18 the main deglaciation flow directions are shown, Fig. 6.21 shows the flow directions prior to deglaciation.

#### *Striae versus lineations (young)*

When comparing Figs 6.16 and 6.18, the main deglaciation flow patterns defined from large-scale lineations turn out to be consistent with the youngest striae directions. The flow directions of Ice Streams (I), (H) and (F) (see Fig. 6.12) dominate in Finland and northernmost Norway. In the southern part of

Fig. 6.14 Striae measurements in North Scandinavia. (Data from Nordkalott, 1986b).

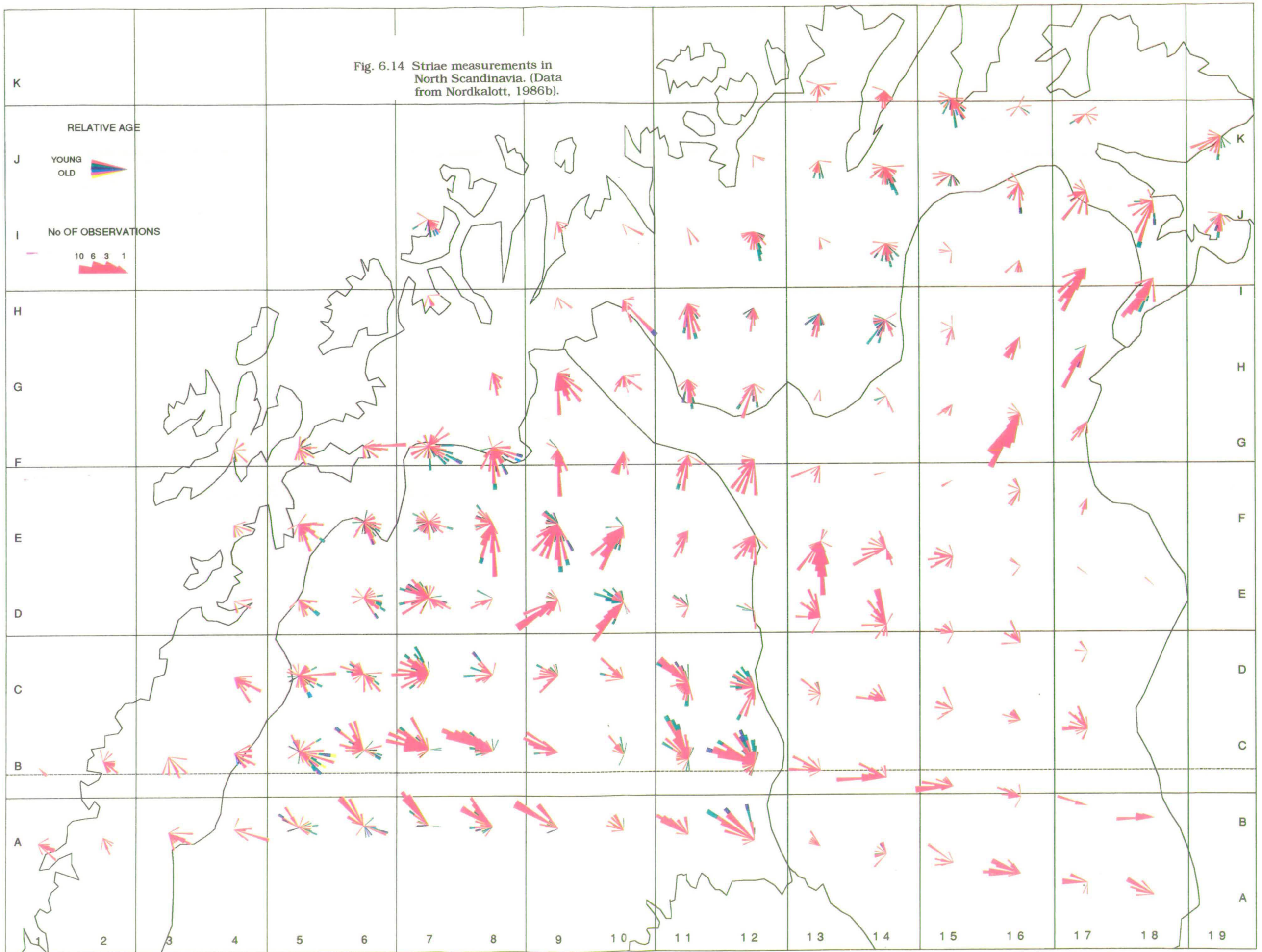
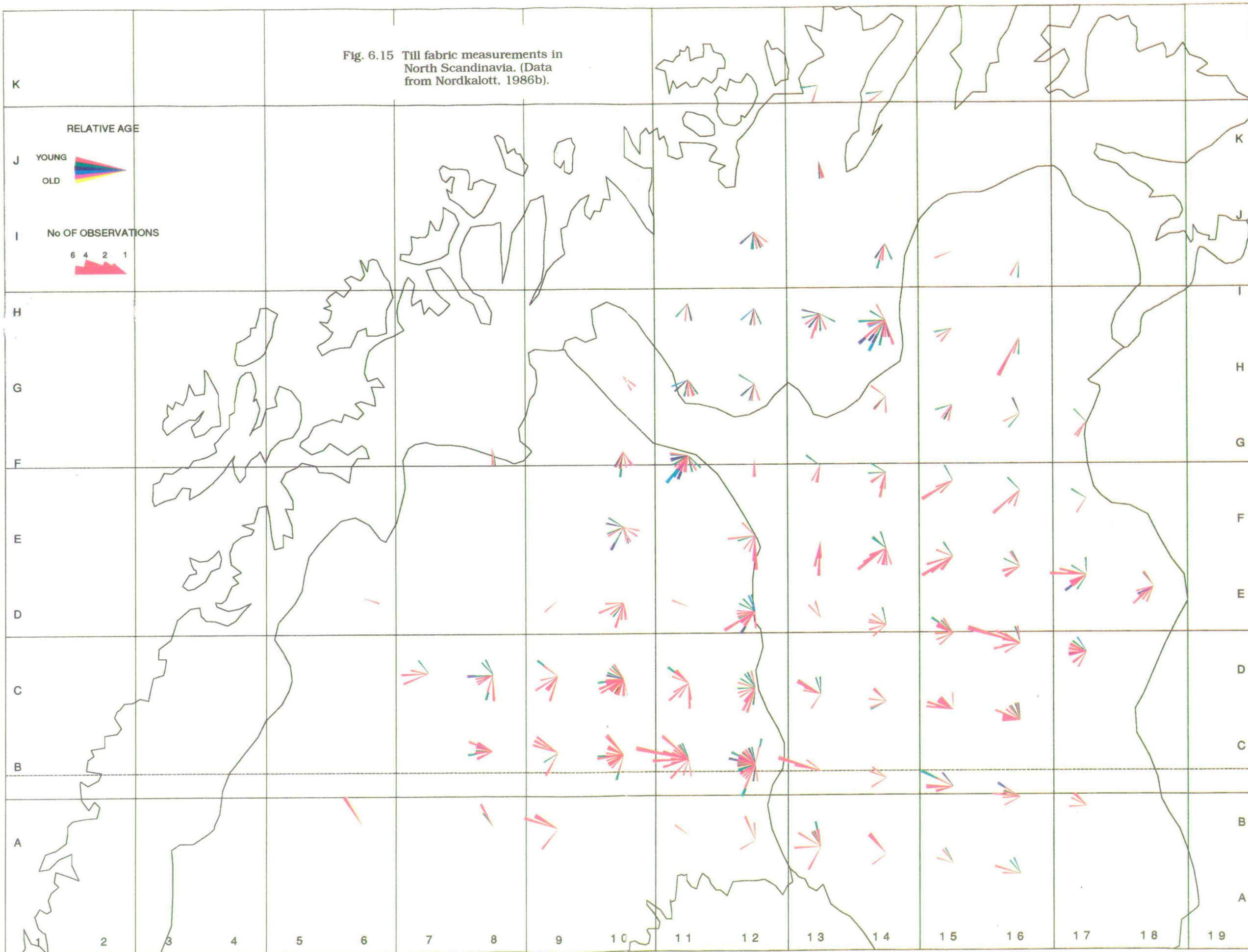


Fig. 6.15 Till fabric measurements in North Scandinavia. (Data from Nordkalott, 1986b).



the area the dominant W/SW-E/NE flow directions of the White Sea Ice Stream (F) are present in both data sets. In north Sweden the striae data give a more detailed picture of the eastward shift of the waning Finnmark Ice stream (I) than the lineation data. In general, the striae data show more directional variability than the lineation data as can be expected (see above). Correlation in the areas covered by Ice Streams I, H, G and F is good, but towards the southwest the increasing scatter of striae flow directions makes comparison more difficult.

#### *Striae versus Lineations (old)*

Comparison of Figs 6.19 and 6.21 is somewhat less straightforward. In Fig. 6.19 the older striae directions have been grouped together. Some of these older directions may belong to the deglaciation phase. This is probably the case with the N-S flow directions in grid cells C, D/11 and E/9,10. The former group corresponds to a local flow event during deglaciation. The latter directions correspond to Ice Stream I. In the eastern part of north Sweden two main directions can be seen, a younger one in the SE and an older one in a S/SSE direction (see also Fig. 6.14). The lineation data in Fig. 6.21 also shows this transition, although much stronger in grid cells C, D/13,14. In north Norway older flow directions have not been recognised from the lineation data. The older striae directions in this area show a good correlation with the youngest striae directions and the deglaciation lineations.

#### *Till fabric versus lineations (young)*

Comparison of the till-fabric data in Fig. 6.17 and Fig. 6.18 yields less agreement than comparison with the striae data. In the north and east of the Nordkalott area the two are comparable. Again there is more variability in the till data but dominant flow directions do agree with the lineation data. In the southern half of north Sweden the contrasts are greater. In grid cells C/7-12, B/8-12 and A/9 the till fabric measurements indicate S/SW-N/NE flow. The lineation data reflect a weak, SSW-NNE flow (grid cell B11), but this could only be seen locally. In the striae data this direction is absent.

In grid cells B/10 and A/6,8,12 and 14, a NW-SE flow direction is present that agrees with pre-deglaciation lineation and striae directions. The NW-SE directions in the till fabric are probably the result of measurements in areas

where the older NW-SE lineations are directly at the surface. The more pronounced N/NE flow in the southern area of north Sweden is more puzzling. In Fig. 6.11 this flow direction is present, but much weaker than in the till measurements. This discrepancy could be the result of a weak, late-stage flow of the waning ice streams which was not capable of forming large lineations but strong enough to rework the existing till layer or deposit a thin new layer.

#### *Till fabric versus lineations (old)*

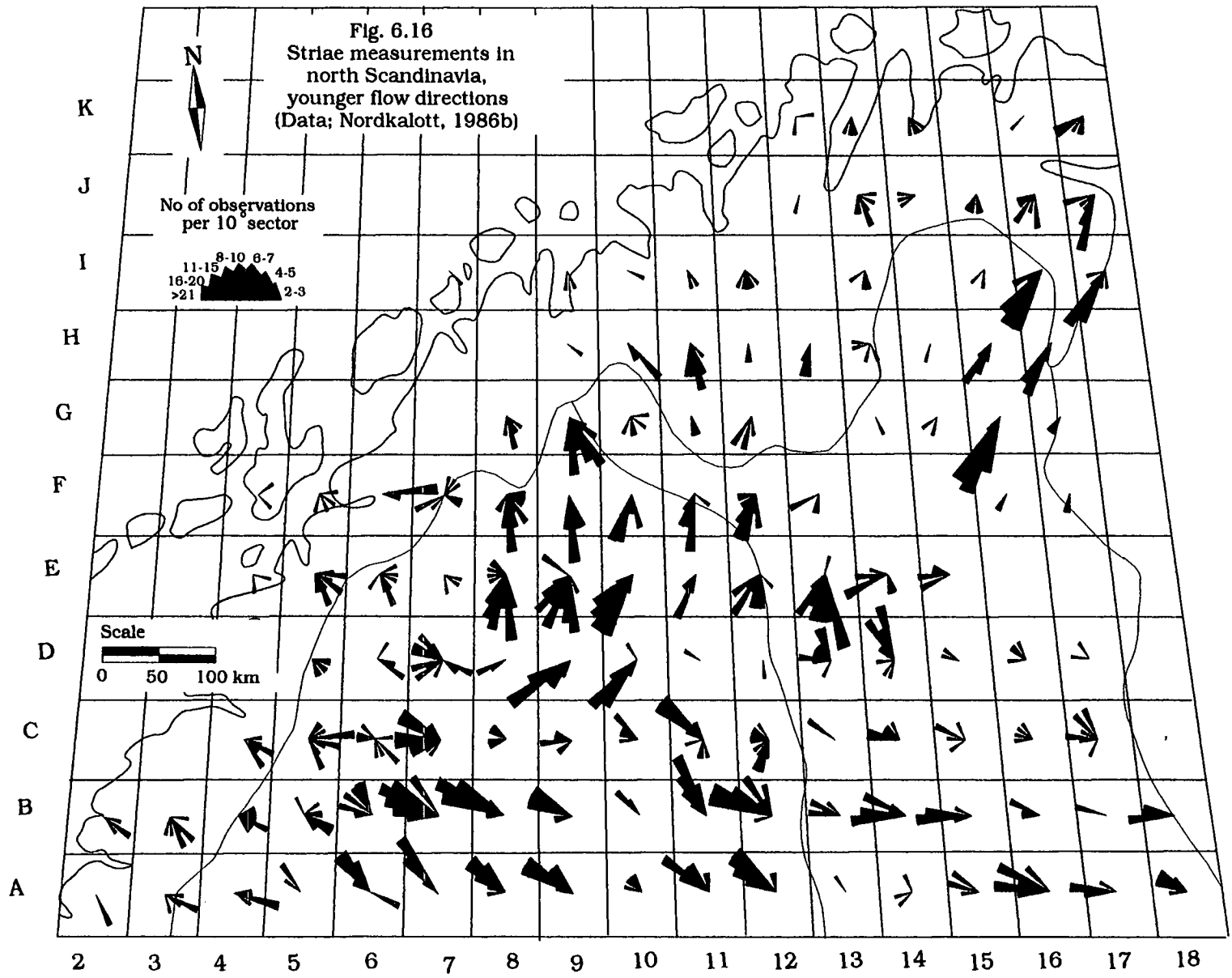
In Figs 6.20 and 6.21 the flow pattern is roughly comparable. In Finland, the older till fabrics clearly indicate a N/NW-S/SE- flow direction comparable to the pre-deglaciation lineations. In northernmost Norway, the till fabric shows a strong directional variability with directions ranging from NE to WNW. No older lineations could be traced in this area. In Sweden differences between the till fabric and the two other two data sets are once again large: a number of grid cells reflects a SSE/SE flow but there are indications of E and NE flow as well.

### 6.6.3 Interpretation

Comparing the three data sets and bearing in mind the differences in information they provide, a good correlation is found between the directional information derived from lineations and that from striae. Till fabrics, agree with the lineation data in most areas except in north Sweden, where the variability of till fabrics is large and the relative chronology of the events is more difficult to establish. All three data sets clearly reflect two major events separated in time. A young and an old flow system.

The three data sets differ strongly in the extent to which they allow correlation of the relative timing of different flow events over larger areas. As was described earlier (section 6.5), the deglaciation flow pattern in Figs 6.16, 6.17 and 6.18 (see also Figs 6.11 and 6.12) is time transgressive. It shows an integrated picture of lineations that have been formed or modified beneath the warm-based, active marginal areas during deglaciation of the Nordkalott area.

In the Nordkalott Project (1986a-d) this configuration was interpreted to reflect a Middle/Late Weichselian ice sheet. The time-transgressive flow pattern was



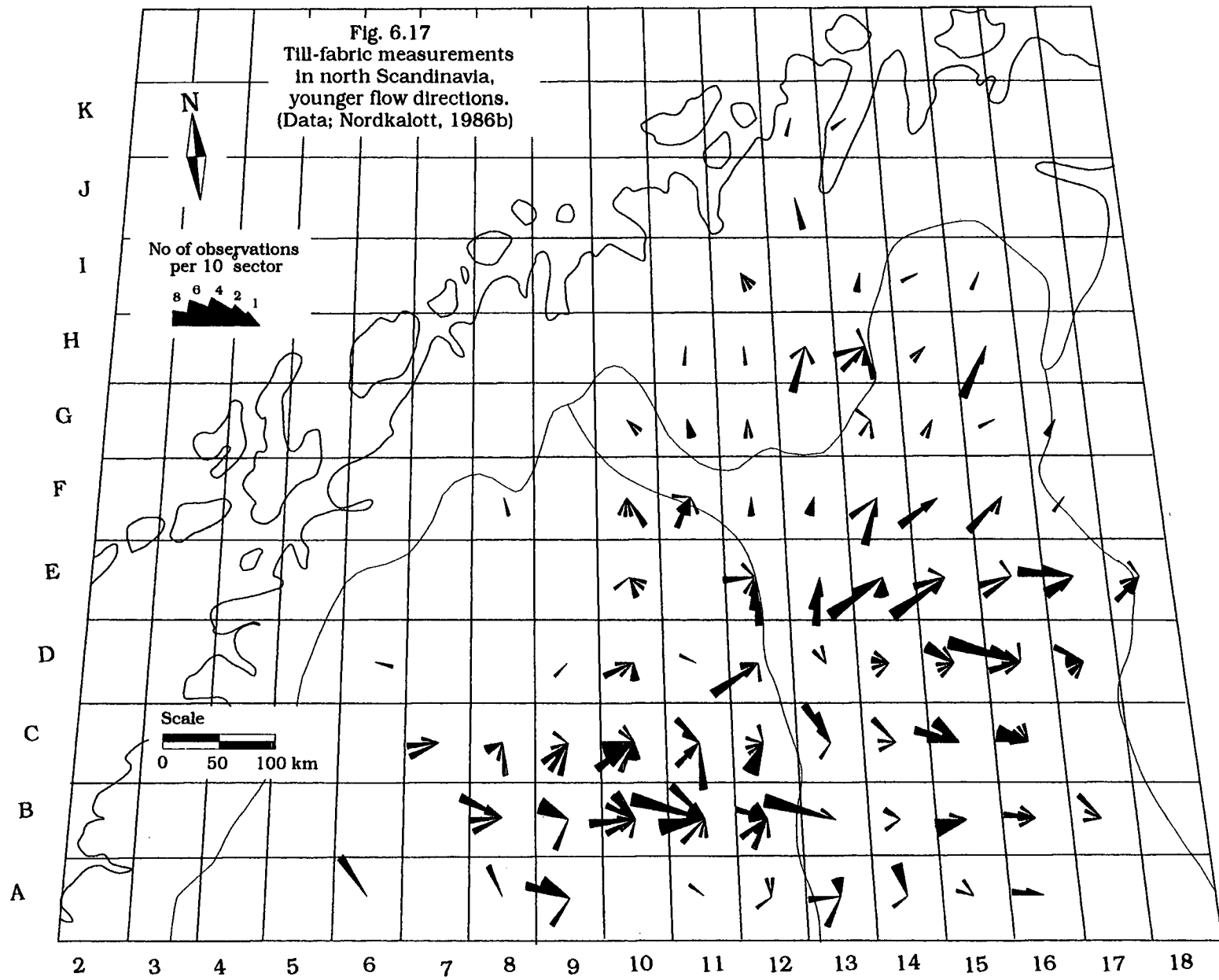
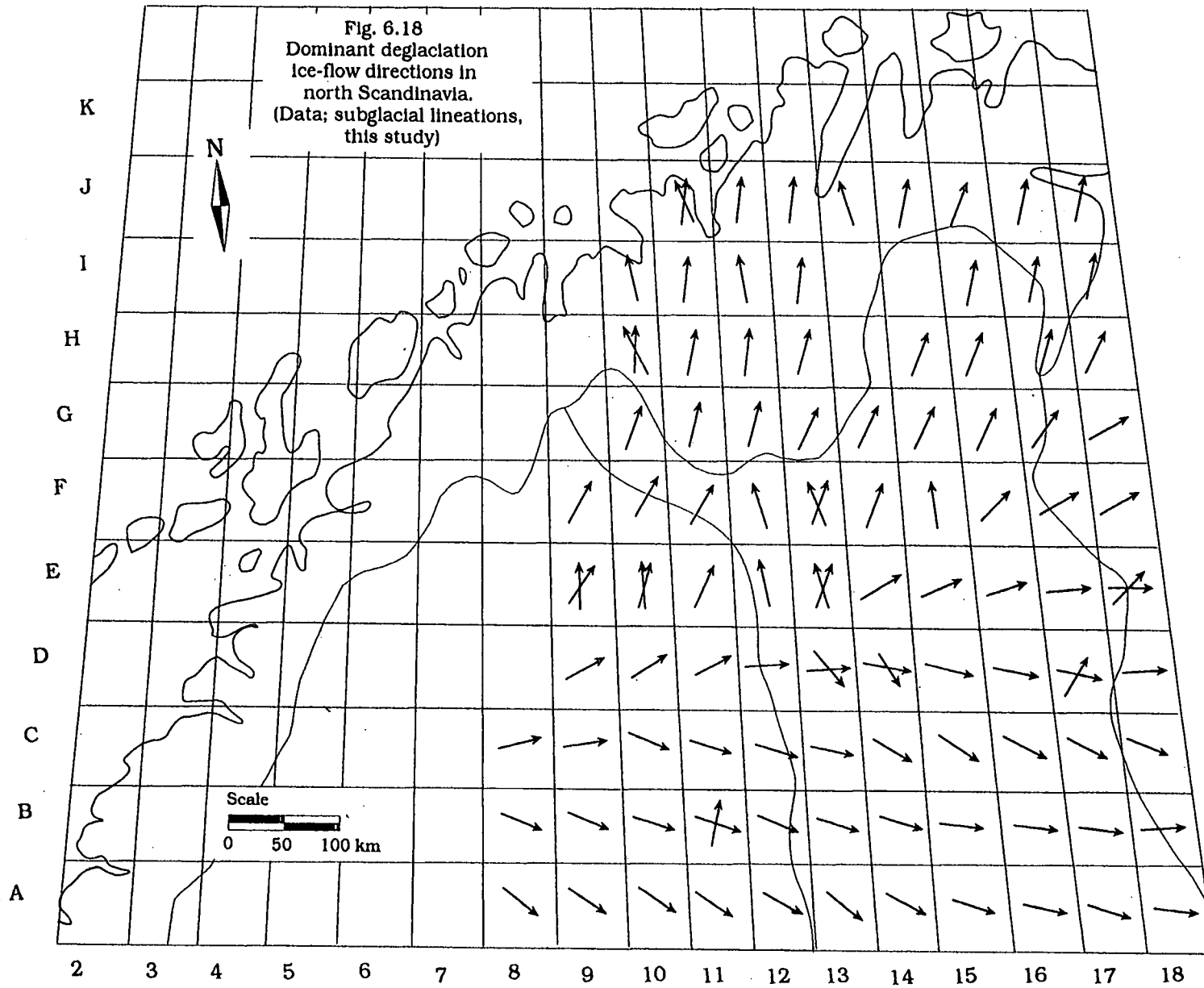
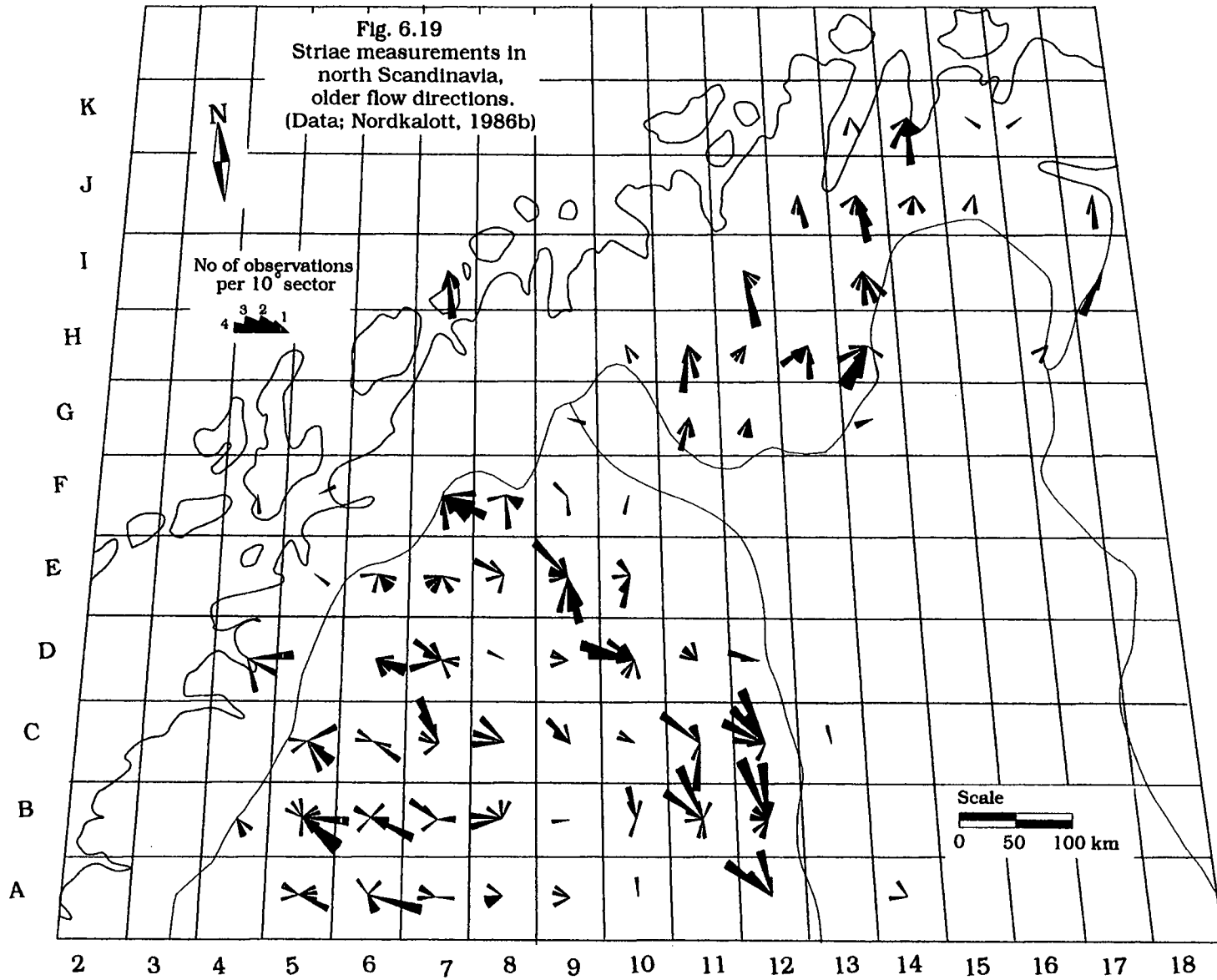


Fig. 6.18  
Dominant deglaciation  
ice-flow directions in  
north Scandinavia.  
(Data; subglacial lineations,  
this study)





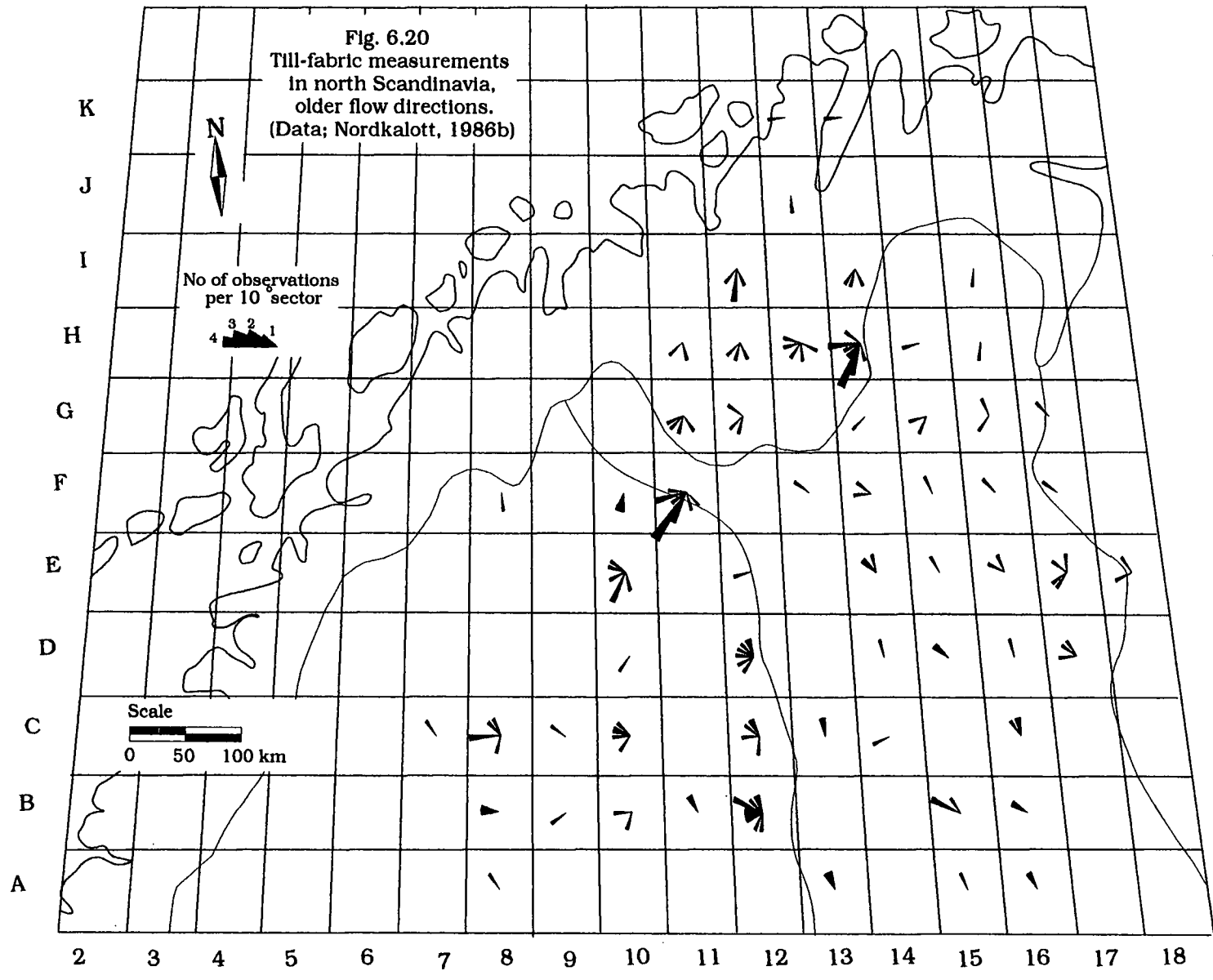
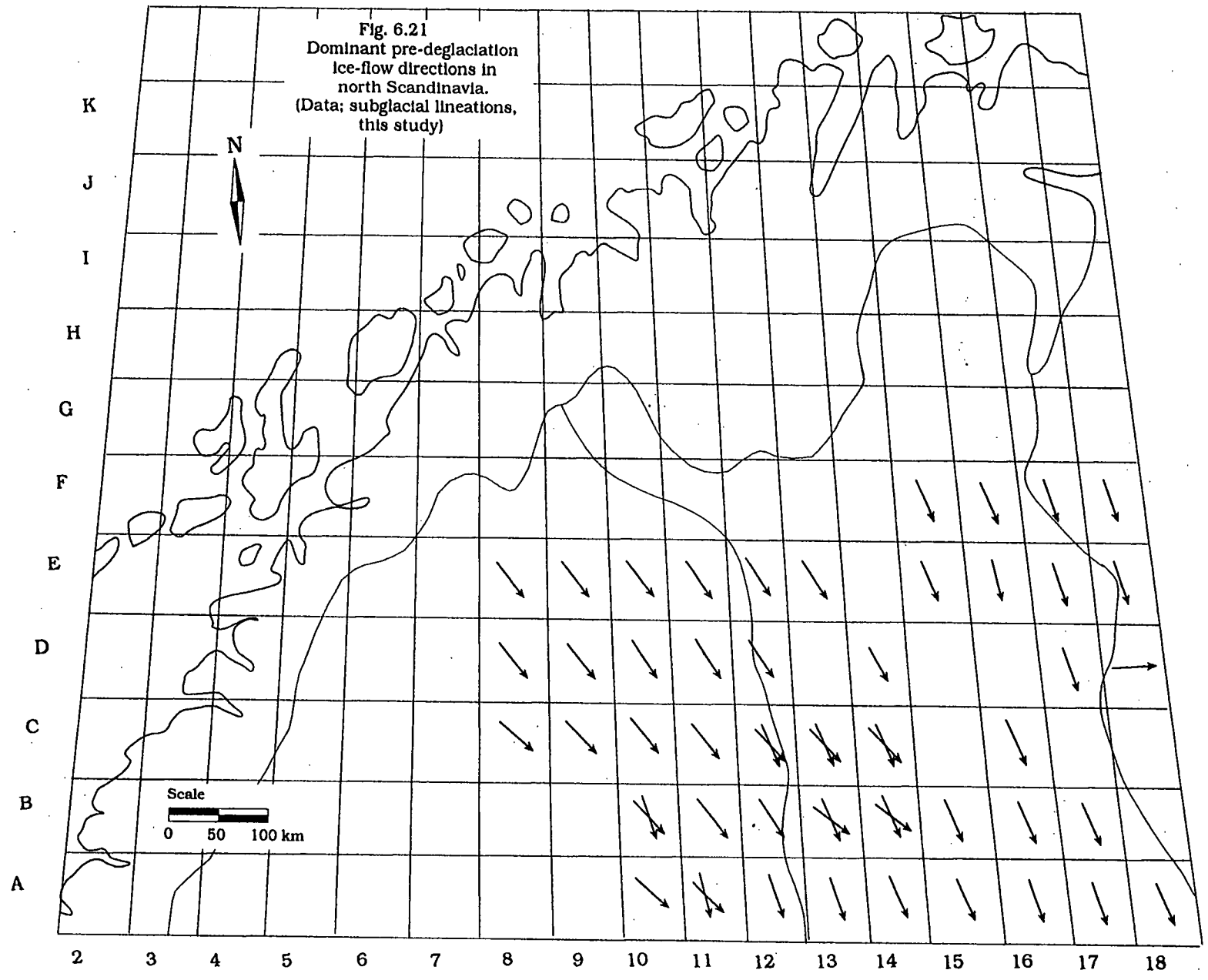


Fig. 6.21  
Dominant pre-deglaciation  
ice-flow directions in  
north Scandinavia.  
(Data; subglacial lineations,  
this study)



taken to reflect the result of mainly one ice-sheet configuration, during which Till II was deposited. The easterly flow over the southern half of north Finland (Ice Stream F) was interpreted previously by several authors (Hirvas *et al.* 1981; Hirvas and Nenonen, 1987; Hirvas, 1991) as reflecting a weak flow beneath the Middle/Late Weichselian ice-sheet divide. Upon deglaciation, Till I was deposited, basically showing the same flow directions as Till II. The older NW-SE flow pattern was interpreted as reflecting flow during the Early Weichselian (Hirvas and Nenonen, 1987).

#### 6.6.4 Summary

The three different sets of palaeo-ice-flow indicators show two related, area-wide, flow systems. With some exceptions, especially in the southwest corner of the area, a reasonable correlation in the flow patterns can be inferred from the three data sets. The explanation of the formation flow patterns in terms of ice-sheet dynamics, presented in the present study differs strongly from previous studies (Hirvas *et al.* 1981; Hirvas and Nenonen, 1987; Hirvas, 1991). In particular the role of time has been interpreted in a completely different way.

The interpretation presented in the Nordkalott Project, infers a static ice-sheet configuration responsible for the large majority of the features. This was inferred to be the case for both the younger and the older flow systems. In the present study, the continuous record of lineations enabled a detailed analysis of the time factor in the development of consecutive, superimposed generations of subglacial bedforms and the interactions of different ice streams. This has important consequences for the timing of the two integrated flow systems. The proposed Middle/Late Weichselian stage was found to reflect only deglaciation. The question now remains whether the older flow is the result of an Early Weichselian glaciation (Hirvas and Nenonen, 1987) or whether it reflects an integrated, diachronous flow system which developed during an ice-sheet advance. This problem will be discussed in Chapter 7.

## Chapter 7

### Advance phase flow

#### 7.1 Introduction

Using the methods described earlier, it was possible to reconstruct the ice-flow patterns during the successive stages of the Late Weichselian deglaciation. The large majority of the linear bedforms in south and central Finland, Russian Karelia, and south and central Sweden have been shown to belong to the deglaciation phase. However, some exceptions were found in these areas as well. In the inter-lobate areas in Finland and Russian Karelia lineations are present that are indicative of ice-flow patterns that cannot possibly belong to the deglaciation. In central and south Sweden lineations that precede deglaciation have also been found. The number of pre-deglaciation lineations is largest in the areas which were ice-covered longest. Near the northern end of the Bothnian Gulf pre-deglaciation lineations become more dominant than those that can be attributed to the ice flow during deglaciation (Fig. 6.7).

As discussed earlier, the importance of the ice streams over Finland decreased steadily after the Younger Dryas (Figs 6.9 and 6.12). Because the power of these ice streams decreased, the capacity of the ice sheet to remould its subsurface was diminished strongly as well. Ice Streams H and I remained active longest and can be traced inside the area that was still ice covered around 9 ka BP. Outside the areas occupied by these two ice streams, lineations belonging to the last flow stages become sparse and were often developed as small flutes superimposed on the older NW-SE drumlins belonging to an older phase (see also Lagerbäck, 1988).

In summary it can be said that the ability of the Scandinavian Ice Sheet to remould its subsurface diminished gradually as the ice sheet shrank. Lineations formed less frequently and their size diminished, whereas older lineations become more widespread and easier to recognise. However, within this large-scale pattern, important anomalies exist reflecting the spatial differentiation of ice-flow velocities that is the result of the coexistence of highly

active ice streams and inactive interstream areas. In this chapter, the spatial patterns of the older lineations are described and a hypothesis for the advance flow stages of the Scandinavian Ice Sheet is presented.

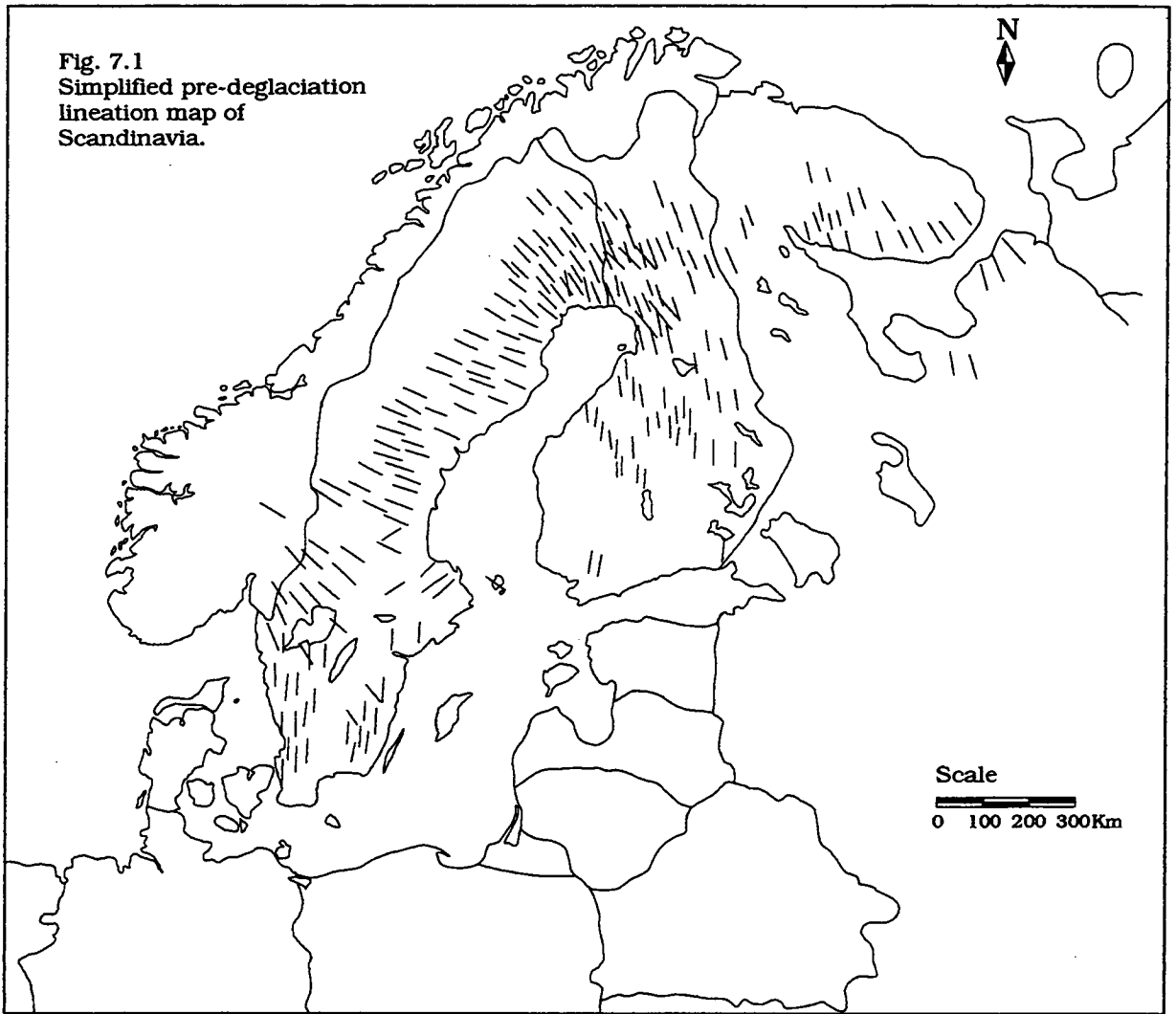
## 7.2 Pre-deglaciation flow patterns

Fig. 7.1 shows an overview of the lineations that were formed prior to deglaciation. There is a strong directional coherence in the lineation pattern. In south and central Sweden, the lineations show a radial pattern away from the Scandinavian mountains. In north Sweden and north Finland, the lineation directions change to a dominant NW-SE direction that gradually gives way to a N-S direction over central and south Finland. In south Sweden the NW-SE radial pattern also changes to a N-S pattern further south.

There are a number possible explanations for these features. They could reflect the geometry of a single flow stage of an ice sheet that was warm-based, and active throughout. Alternatively, they could reflect either the advance or retreat phase of a single glaciation. Finally, they could be the result of a number of glaciations. The lack of known positions of the ice margin during the advance phase and the absence of superimposition between the pre-deglaciation lineations, make it impossible to determine the temporal relationships of individual features from satellite interpretation solely. Therefore, a similar reconstruction as presented in Chapter 6 for deglaciation is not possible for the pre-deglaciation lineations.

The idea of a single flow stage of an ice sheet which was warm-based and active throughout, has been proposed by many authors. They assumed that the majority of subglacial linear features is produced by ice-sheet-wide flow during the maximum extent (Sugden, 1977). Boulton and Clark (1990) took the idea one step further. On the basis of a remote-sensing analysis of lineations they concluded that the Laurentide Ice Sheet had a warm base and was active throughout. Successive, discrete flow stages produced set after set of superimposed ice-sheet-wide patterns.

Fig. 7.1  
Simplified pre-deglaciation  
lineation map of  
Scandinavia.



As has been discussed earlier, the evidence from Scandinavia suggests a different ice sheet behaviour. During the entire deglaciation the only evidence for active remoulding was found in the marginal area. In Finland, the most powerful ice streams had active zones of 200/250 km wide (Punkari, 1982, 1984; this thesis). It is conceivable that the large, topographically controlled ice streams (such as the Norwegian Ice Stream (A) and the Finnmark Ice Stream (I)) had larger upstream zones of warm-based, active ice. But topographic constraints ensured that they could only influence an area of limited width. In the case of the Baltic Ice Stream (B) it is difficult to infer the size of the actively remoulding zone because any evidence there may have been is now covered by the Baltic Sea. However, the fact that this ice stream flowed over a considerable depth of deformable sediment makes it likely that its active area exceeded those of the Finnish Ice Streams.

Recently, studies have been performed of the growth and retreat of the Scandinavian Ice Sheet using a thermo-mechanically coupled ice-sheet model (Boulton and Payne, 1994). The results indicate the existence of a marginal zone of warm-based ice which was a few hundred kilometres wide and a cold-based interior, both during advance and retreat. On the basis of both the lineation studies and numerical modelling, the idea of contemporaneous, ice-sheet-wide lineation patterns must be rejected in favour of a time-transgressive submarginal mode of formation.

In the Nordkalott Project (Hirvas, 1991) the NW-SE lineations, Till III in their notation, were interpreted to be the result of an Early Weichselian glaciation (sections 5.1 and 6.6). Their Till I and II flow directions encompass all younger flow directions and are interpreted to result from a single Middle/Late Weichselian glaciation.

Tills I and II are ascribed to a Middle/Late Weichselian glaciation and Till III to an Early Weichselian glaciation on the basis of finds of organic material at a number of sites. However, there is no site where a complete stratigraphy has been found. Moreover there is considerable doubt whether the organic material is in situ (Punkari and Forström, 1995). In this study the flow directions related to Till I and II have been shown to belong to the deglaciation phase (see section 6.6).

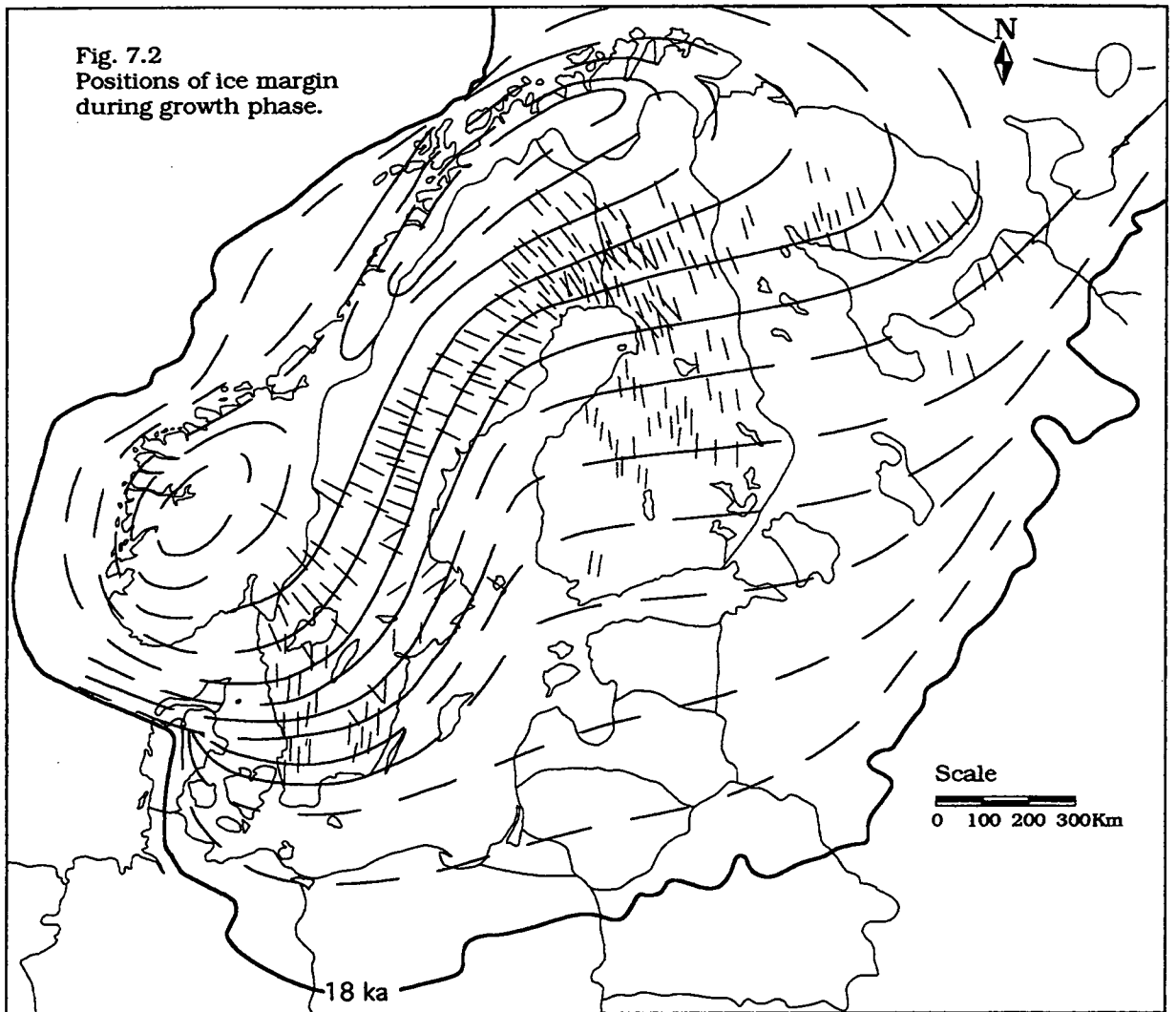
Because a firm basis for ascribing the pre-deglaciation lineations to an older glaciation is lacking, the most straightforward hypothesis is that these older lineations are related to the advance phase of the last glaciation. As mentioned before, it is not possible to prove that the pre-deglaciation lineations all belong to the same event. It may well be that, especially close to the Scandinavian mountain range where topographic control is strong, expanding ice sheets follow similar routes during consecutive glaciations. However, in spite of all these uncertainties, the strong coherence of the older flow pattern seems to justify the assumption that the large majority of lineations is actually related to the last advance phase.

### 7.3 Initiation and growth

Fig. 7.2 shows a hypothetical reconstruction of consecutive positions of the ice margin during the advance phase of the last glaciation. Ice margins have been assumed to run perpendicular to the lineations. A warm-based marginal zone of 100-150 km was assumed. The ice sheet was assumed to have grown outwards from the Scandinavian mountains to a maximum at the 18 ka BP ice margin. On the basis of these simple assumptions, a coherent picture of the hypothetical ice-sheet advance has been drawn.

#### 7.3.1 North Scandinavia

The advance in the north started from the Kebnekaise mountains and ice advanced from there in a southeastern direction (see Figs 2.1 and 2.4). The ice flow was in a NW-SE direction in both north Sweden and north Finland. The mountains farther to the east in Finnmark, north Finland and Kola also functioned as centres of ice-sheet growth soon after initiation of the ice sheet. Initially, flow directions were from the NW near the Scandinavian Mountains and changed to NNW over the Kola peninsula. The flow direction gradually changed from NW to NNW as ice reached the low-relief areas of north Sweden and Finland. As a consequence the ice-sheet margin in north Scandinavia



gradually changed from SW-NE close to the initiation areas, to WSW-ENE upon approach of the northern end of the Bothnian Gulf.

The shift in flow direction from NW to NNW in Finland and Sweden can be partially related to the N-S running Maanselkä mountains on the border of Finland and Russian Karelia. Although not very high, with peaks up to 500-600 m, these mountains could have influenced the flow pattern of relatively thin marginal ice. However, it is more likely that the shift in flow pattern is mainly related to the coalescence of ice from Scandinavia ice from Novaya Zemlya in the Kola and Kanin peninsula area. As flow towards the east was barred, ice diverged both to the north and south, changing the radial outflow pattern to a N-S flow pattern as observed. In central Finland, the older lineations maintain a N-S flow pattern. Locally, lineations show divergence, but this never exceeds 10°-15°. On the whole the lineations indicate parallel ice flow during the advance. There are no indications of large-scale diverging flow in marginal lobes, or of lateral zonation of lineation densities reflecting ice stream versus interstream areas.

### 7.3.2 South Scandinavia

From the growth centre over the Jotunheimen mountains, ice flowed radially outwards towards the Skagerrak and south Sweden. This radial outflow reached Lake Vänern in south Sweden and perhaps extended as far as Åland in the east and the southeast coast of Småland. To the northeast of the Jotunheimen mountains, the flow direction was almost perpendicular to the Scandinavian Mountains.

Gradually ice flow over southeast Sweden changed from NW-SE to N-S. The reason for this shift was probably that an increasing part of the ice which came from the Jotunheimen mountains discharged through the Norwegian Channel, thus allowing ice over south Sweden to shift to the west. The ice flux through this channel may have increased steadily from the beginning of the advance phase of radial outflow because subsequent isostatic depression of this region caused a rise in relative sea level. It is possible that, during the radial advance and the early stages of N-S flow, ice crossed the Skagerrak and

reached northern Denmark (see section 6.2). Another possible reason for the shift in flow direction is that ice coming from the north gradually coalesced with ice from the central and south Norwegian mountains.

In the area north of Stockholm, there are indications that ice from the Bothnian Gulf encroached upon the Swedish coast (Fig. 6.6a). It is not clear when this happened or how far this ice penetrated. It may well be that the shift in ice-flow direction over south Sweden continued, and that a NE-SW flow developed which fed ice from central Sweden into the Skagerrak. However, during deglaciation, a similar NE-SW pattern developed over southwest Sweden, preventing the detection of any older lineations even if they had not been obliterated by erosion.

The overall flow pattern during this stage in the advance was N-S in south Sweden as well as in central and south Finland. It is not clear how the flow pattern changed towards the eastern fringe of the ice sheet because the satellite images did not cover this area.

The southern Baltic Lowlands were not studied. However, from studies published about these areas (section 6.2), it can be shown that flow directions over the Baltic States during the Late Glacial Maximum were also N-S. In Germany and north Denmark, ice flowed radially out from south Sweden during the Late Glacial Maximum (see Fig. 6.4).

#### 7.4 Summary

The main centres of ice growth in the initial stage were the Kebnekaise area in the north and the Jotunheimen area in the south. Additional centres of early growth existed in the Finnmark area, the Maanselkä mountains and the mountains in the Kola peninsula. Drainage from central Scandinavia to the Atlantic Ocean in the west, was blocked by the Scandinavian Mountains. To the east, however, the Scandinavian mountains gave way to a region of low relief where only shallow basins existed. It was therefore in this direction that the ice sheet could expand over the Scandinavian Shield towards the sedimentary lowlands of Russia, the Baltic States, Poland and Germany.

Once the ice sheet expanded beyond the Scandinavian Mountains its overall growth pattern was influenced strongly by discharge of ice both towards the north (to the Barents Sea) and the south (through the Skagerrak and the Norwegian Channel). To the northeast, the advance was barred by coalescence with ice from Novaya Zemlya over Kola and the Kanin Peninsula. The development of the draining towards the north and south resulted in a counter clockwise shift in the ice flow lines in the north and a clockwise shift over south Sweden and Finland. On the southern and eastern sides the maximum extent of the ice sheet coincides with a change from flat sedimentary lowlands to higher, hilly terrain.

As was discussed above, no diverging flow patterns comparable to those over Finland formed during the advance phase. Moreover, there are no indications of spatial variations in lineation density that would be expected if ice streams/interstream systems developed during this phase. It could therefore be argued that ice streaming did not develop during the advance phase and is in fact a deglaciation phenomenon.

However, the lineation data of the advance phase show important hiatuses and do not provide a continuous, integrated record. Any spatial variations in lineation density would therefore be hard to detect. In section 6.3 it was argued that the high density of lineations pre-dating 12 ka BP might indicate ice streaming. Topographic forcing of the mountainous area to the east may have prevented individual lobes to develop. The separation into individual lobes at the eastern margin only developed after 12 ka BP, when a semi-circular configuration of the ice margin developed on a relatively flat surface. The lobate pattern was greatly enhanced during the Younger Dryas stationary period (section 6.3). It could be argued, therefore, that ice streams do not necessarily develop marginal lobes, but that this may depend on the overall setting in the ablation area. Bearing this in mind, it is concluded that whether ice streaming or sheet flow was dominant during the advance phase cannot be answered conclusively.

## Chapter 8

### Ice-sheet dynamics

#### 8.1 Introduction

Many studies have attempted to reconstruct the extent, timing and glaciodynamics of the Late Weichselian, mid-latitude ice sheets. In North America numerous studies have presented reconstructions of the Laurentide Ice Sheet (Shilts, 1980; Denton and Hughes, 1981; Boulton *et al.*, 1985; Dyke and Prest, 1987; Boulton and Clark, 1990). A major discussion issue is whether the Laurentide Ice Sheet had, at its maximum extent, one dome (Denton and Hughes, 1981) or two (Shilts, 1980; Boulton *et al.*, 1985).

In Scandinavia, the glaciation model presented by Ljunger (1949) is still generally accepted, although some modifications have been made (Lundqvist, 1986). In this glaciation model the Late Weichselian Ice Sheet initiated in the Scandinavian mountains. During the growth of the ice sheet, towards the east and south, the ice divide gradually moved eastward to a position east of the Bothnian Gulf. Upon deglaciation the ice divide migrated back to the mountains eventually breaking up into several domes. Later, instantaneous glaciation of the interior of Scandinavia was proposed by a number of authors (Lundqvist, 1981; Mangerud *et al.*, 1981).

Work in south Sweden (Lagerlund, 1987; Ringberg, 1988), Denmark (Houmark-Nielsen, 1987) and Finland (Punkari, 1984, 1985) shows that the glacio-dynamics of ice sheets were more complex than previously thought. To explain the complicated ice-stream fluctuations in the southern Baltic, Lagerlund (1987) proposed the existence of marginal domes, which formed on surged ice masses and were fed by southwardly diverted storm tracks of the Atlantic Ocean.

The fluctuating activity of the Baltic Ice Stream and the existence of several fast-flowing ice lobes in Finland and Russian Karelia (Punkari, 1980, 1985), showed that ice streaming played an important role in the Fennoscandian

glaciation. The idea that sheet flow was dominant could no longer be maintained.

## 8.2 Glaciological theory and ice-sheet reconstruction

An important contribution to the reconstruction of former ice sheets was the use of glaciological theory to model the temperature evolution of ice sheets. Budd *et al.* (1970) developed a vertical-column model that took horizontal advection into account. Using this model, studies of the two-dimensional temperature distribution in Antarctica, assuming a steady state, were performed. In his 1977 paper Sugden presented a model of the basal thermal regime of the Laurentide Ice Sheet which was based on the numerical model developed by Budd *et al.* (1970). For the calculation of the basal temperature field it was assumed that the ice sheet was in a steady state at its maximum extent. This would imply a stationary configuration of the ice sheet for 50 to 100 ka. The modelling results showed a concentric pattern of cold and warm basal zones. From the centre to the periphery, an alternation of warm, cold and finally warm basal ice existed. The pattern was more complicated in areas that had substantial relief, such as the Hudson Bay outlet. Sugden discussed the important role that freezing on of meltwater may have played in the entrainment of debris. He suggested that if a steady state was never reached the most likely effect would have been an increase in the size of the zone at which ice was at pressure melting point.

Reconstructions of the northern hemisphere ice sheets by Denton and Hughes (1981) were based predominantly on stratigraphy and deposits formed at the ice margin. These reconstructions enabled calculation of the surface contours of the maximum extent of the ice sheets on the basis of the assumption that ice behaves in a perfectly plastic manner. They presented two different reconstructions for the Late Weichselian northern hemisphere ice sheets. The two reconstructions reflect the different opinions among Quaternary scientists of the actual maximum extent. The differences focus mainly on the extent and timing of the marine ice sheets, such as the Barents Sea Ice Sheet and the Kara Ice Sheet.

Using these two reconstructions of the ice margins, they presented a minimum and a maximum reconstruction of the ice sheet elevation on the basis of a two-dimensional numerical ice-sheet model. The pattern of the basal thermal zones is comparable to the one presented by Sugden (1977). A wide zone in which the ice is at pressure melting point occurred in the centres of the Eurasian and North American ice sheets. This zone was surrounded by a zone where ice was frozen to the ground. In many areas the cold zone extended all the way to the ice margin. In a few areas, notably the southern margin of the Laurentide Ice Sheet, frozen conditions gave way to a melting peripheral zone.

During the 1980s, advances were made in the formulation of thermo-mechanically coupled ice-sheet models. Dahl-Jensen (1989) developed a vertically integrated model that also took the dependence of ice deformation on the temperature field into account. This approach led to the development of a three-dimensional fully coupled thermo-mechanical model for Antarctica (Huybrechts, 1990a, 1990b) and Scandinavia (Boulton and Payne, 1994). In these models only internal shear deformation is formulated properly, sliding and soft-sediment deformation are ignored or treated in a simplified fashion.

Boulton and Payne (1994) presented a three dimensional thermo-mechanically coupled ice-sheet model for the growth and maximum extent of the Scandinavian Ice Sheet. Topography was used as input data and only internal ice deformation was considered. The basal ice temperatures show a concentric pattern, with a cold based centre, and a broad, warm-based outer zone. During the growth phase the warm-based outer zone moved with the advancing margin and gradually expanded. During the maximum extent the outer, warm-based zone is approximately 200-300 km wide. In Norway and north Scandinavia the concentric basal temperature pattern was disrupted by the effect of topography on the ice flow. Deformation rates were very high in the valleys and fjords, and ice streaming developed in these locations. However, the ice streaming in the Baltic Basin and over central and south Finland is not represented in the model.

Topographically controlled ice streaming is reasonably well-represented in these numerical models as a result of two positive feedbacks. Higher shear stresses produced by thick ice in the valleys result in a non-linear velocity

increase as a result of the non-linearity of the flow law. Moreover, the thicker, faster flowing ice is warmer and will therefore deform more easily according to the temperature dependence of the flow-law parameter (Paterson, 1994).

Sliding and soft-sediment deformation have attracted considerable attention in recent years, especially through work on the West Antarctic Ice Streams (Clarke, 1987; Alley *et al.*, 1987a, 1987b; Bentley, 1987; Shabtaie *et al.*, 1987). At present, however, there is no consensus on formulating sliding and soft-sediment deformation laws. This is due partly to the difficulty of modelling the roles of meltwater and subglacial pore-water pressures and partly to the effects of the geology on these processes (Walder, 1986; Kamb, 1987; Fowler, 1987a; Walder and Fowler, 1994).

### 8.3 Modern ice streams

In modern ice sheets a strong contrast exists between sheet flow and ice streaming (Clark, 1987). In sheet flow, internal deformation of the ice is responsible for relatively a slow ice flow. The flow velocity in the streaming mode is much higher and is the result of reduced friction at the base of the ice. Water-saturated sediments have a strongly reduced shear strength and will therefore deform rapidly, even under very low driving stresses (Clarke, 1987). Low effective pressures lead to the formation of cavities which lower the friction that is exerted on the ice by the bedrock (Walder, 1986). An example of an ice stream is Jakobshavn Glacier on the Greenland Ice Sheet, it discharges approximately 6% of the net annual accumulation of the ice sheet (Clarke, 1987). McIntyre (1985) noticed that many fast glaciers had short segments in which surface slopes were steep, coinciding with both a bedrock step and the sheet-to-stream-flow transition. Shabtaie *et al.* (1987) and Bentley (1987) however, concluded that the transition from sheet to stream flow is not necessarily controlled by bedrock topography.

There is an important difference in the setting and behaviour of the Siple Coast Ice Streams in West Antarctica with most other ice streams. The East Antarctic Ice Streams occupy deep subglacial valleys, their driving stresses increase from the upstream area towards the coast. They peak approximately 100 km

from the coast and subsequently diminish again. This contrasts with the Siple Coast Ice Streams which feed into the Ross Ice Shelf. Here, very low surface elevation slopes and ice thicknesses, combine to produce very low driving stresses. The driving stresses increase continuously inland towards the head of the ice streams (Bentley, 1987). The relationship which exists in the Siple Coast Ice Streams with the bedrock topography is complex (Shabtaie *et al.*, 1987). These ice streams tend to follow relatively shallow bedrock troughs (approximately 300 m deep) but do not often fully occupy these or are situated on the trough edges.

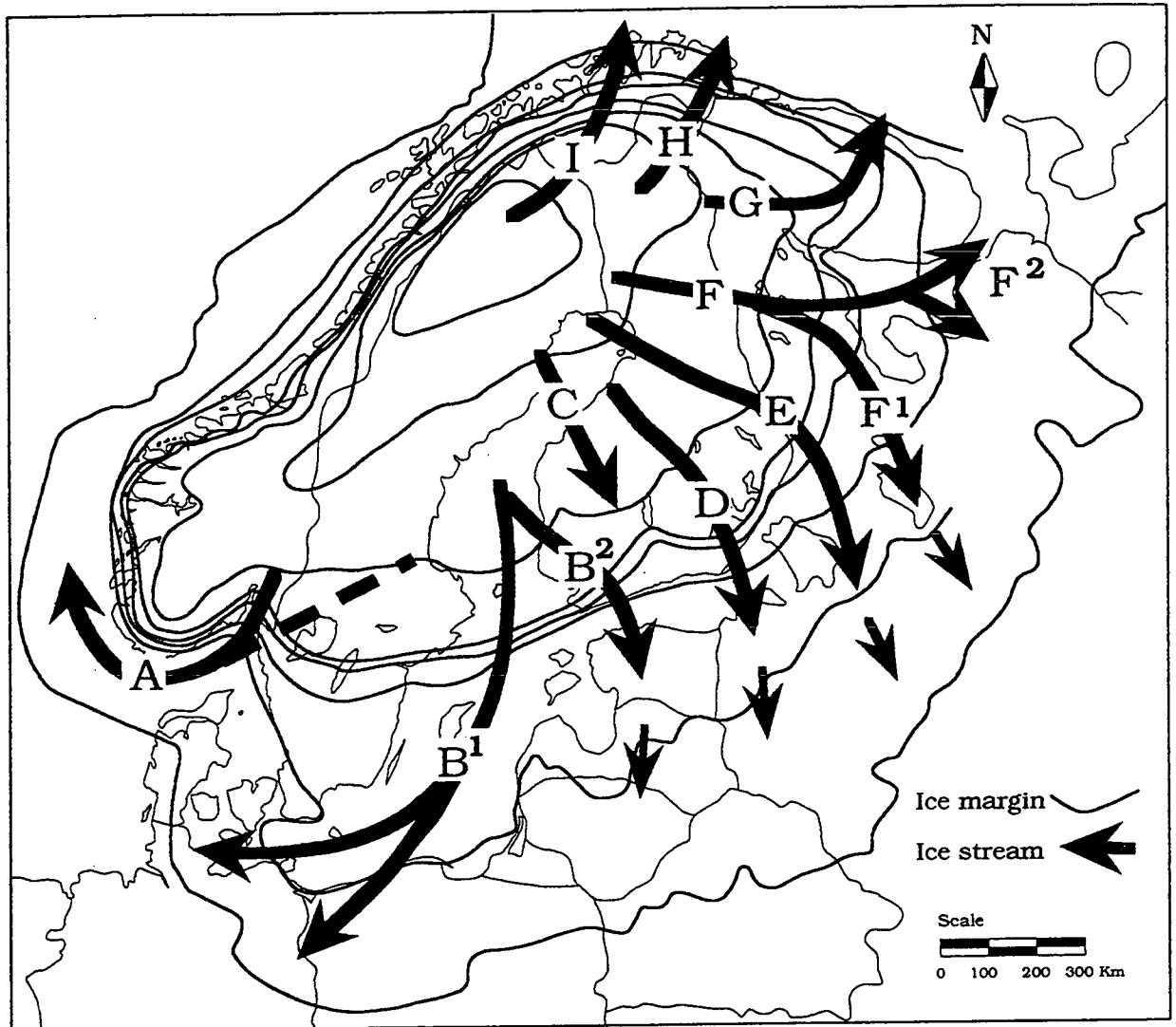
The surface topography of the active Ice Streams A and B is characterised by a longitudinal ridge-trough topography (Shabtaie *et al.*, 1987). The lateral boundaries of the ice streams exhibit strong crevassing and are zones of intense shearing. In many areas the ice streams are separated by smoother ridges which can be up to 300m higher than the ice-stream surfaces. The ice-flow velocities in these interstream areas are of the order of a few metres a year and flow direction almost perpendicular to the ice-stream (Whillans *et al.*, 1987). Rafts of ice from the heads of the ice streams have been incorporated into the ice streams and form topographic highs within the ice stream (Shabtaie *et al.* 1987, Whillans *et al.*, 1987). Whillans *et al.* (1987) conclude that the transition from sheet to stream flow occurs irregularly both in space and in time. This is also suggested by the very low flow velocities of Ice Stream C that appears to have switched off 250 years ago (Shabtaie and Bentley, 1987).

Ice Stream B appears to be underlain by a 6-8 m thick layer of water-saturated sediments that may be weak enough to deform (Alley *et al.*, 1987a). This may explain the combination of extremely low driving stresses and high ice velocities of Ice Stream B.

#### 8.4 Fennoscandian ice streams

Fig. 8.1 shows the position of the centre lines of the main ice streams that existed during deglaciation of the Fennoscandian Ice Sheet. Ice Streams A, B, I, H and G were topographically controlled and were probably comparable in

Fig. 8.1 Centre lines of ice streams during deglaciation of the Late Weichselian Fennoscandian Ice Sheet.  
(Modified from Punkari, 1993)



- A Norwegian Channel Ice Stream
- B<sup>1</sup> Baltic Ice Stream
- B<sup>2</sup> Finnish Gulf Ice Stream
- C Näsijärvi-Jyväskylä Ice Stream
- D Finnish Lake District Ice Stream
- E North Karelian Ice Stream
- F White Sea Ice Stream
- G Kola Ice Stream
- H Tuloma Ice Stream
- I Finnmark Ice Stream

setting and behaviour to the ice streams in east Antarctica and Greenland. The ice streams over central and south Finland occupied relatively flat areas where the soft-sediment cover of the basement rocks was thin and discontinuous. Their functioning was not controlled by specific topographic or geological conditions but was most likely the result of the internal dynamics of the ice sheet.

#### 8.4.1 Topographically controlled ice streams

In section 6.5 the activity of Ice Streams I, H and G during deglaciation was discussed. The main difference between these ice streams and those in Finland was the lack of marginal lobe formation, instead flow was mainly parallel. This was caused in part by calving ice margins but mainly by the location of the ice streams in bedrock valleys, which prevented radial spreading. Till is present at the valley bottom, but bedrock outcrops are numerous. Soft-sediment deformation undoubtedly played a role in the forward movement of the ice streams. However, the bedrock bumps provided sticky spots that may have supported a disproportional part of the basal shear stress (Alley, 1993), thus ice/bedrock sliding may have been the process governing the extent and velocity of the ice stream.

The ice streams to the south, the Norwegian Channel Ice Stream (A) and the Baltic Ice Stream (B) were also topographically controlled, but their setting is quite different from the northern Ice Streams. The Baltic Ice Stream occupied a wide (150 km) trough, cut into the sedimentary rocks of the East European Platform (Fig. 2.2). The deepest parts were around Gotland and may have been up to 200m deep. The parts to the southwest were less than 100m deep. The Norwegian Channel was cut at the contact between soft Mesozoic and Paleozoic sediments and the bedrock of the Baltic Shield. In the Skagerrak, this trough is 500m deep and approximately 50 km wide, to the north the Norwegian Channel becomes wider and shallower (Fig. 2.5).

Both Ice Streams A and B occupied troughs that were well below sea level during deglaciation. This was partly the result of isostatic depression in the preceding period. Water depth in front of the Baltic Ice Stream was 225-250m during the Younger Dryas (Figs 2.16, 2.17 and 2.18). As a result of rapid

deglaciation after 10 ka BP water depth increased to 250-275m around 9.5 ka BP (Fig. 2.19). In the Skagerrak the eustatic sea level fall was more than balanced by the isostatic depression of the area.

These two ice streams were underlain by sedimentary strata that offered far less resistance to glacial erosion than the Shield rocks. The repeated incursions of the Baltic Ice Stream into Denmark (section 6.1) indicate the fluctuating activity of Ice Stream B, which is possibly related to unstable, surging behaviour resulting from sediment deformation (Boulton *et al.*, 1985; Ehlers, 1992). The rapid deglaciation of the Baltic Ice Stream compared to the surrounding areas after 13 ka BP (Fig. 6.1) also indicates unstable conditions.

The trough formed by the Skagerrak and the Norwegian Channel formed a major barrier for expansion of the southern Norwegian ice to the south and west. Present-day water depths are over 500m in the Skagerrak and approximately 300m further to the north. In the Skagerrak, the eustatic sea level fall was offset by isostatic depression (section 2.3), although further north water depths may have fallen during the Late Weichselian. The deep standing water and the presence of deformable sediment make the Norwegian Channel a prime location for a topographically controlled ice stream of the type that is draining large parts of the Greenland and Antarctic Ice Sheets (Bentley, 1987).

In section 6.2 the invasion of Norwegian ice into Denmark and the subsequent clockwise rotation was discussed. It seems that ice had been able to cross the Skagerrak during the last glaciation. Later, Norwegian ice was deflected to the Atlantic Ocean by the Norwegian Channel Ice Stream, thus ending the expansion over Denmark. The lineation data provide evidence of Norwegian ice reaching Denmark during the advance period (Ch.7). The most likely reason for the improved transport capacity of the Norwegian Channel Ice Stream is an increased water depth resulting from isostatic depression. It may have been of the greatest importance for the final ice-sheet geometry whether the Norwegian Channel Ice Stream could cope with all the ice generated in the southern Norwegian mountains. If it could not ice must have crossed over to Denmark and the southern North Sea as it did during the Saalian, otherwise the western expansion would have been checked.

#### 8.4.2 Non-topographically controlled ice streams

Glacigenic landform distribution in Finland indicates that ice-stream activity played an important role in the internal organisation of the ice sheet. The setting of the Finnish Ice Streams differs from the ones discussed previously in that they do not occupy bedrock troughs. The Finnish Ice Streams drained partly into the marginal lakes but water depths were shallow compared to the Norwegian Channel and the Baltic area (Figs 2.16-2.21). In south Finland the maximum water depth in front of the ice sheet was 125m around 12 ka. During deglaciation, water depths fell as the ice sheet retreated over higher ground (Fig. 2.4). In central Finland the ice sheet retreated over dry land for most of the time. Only after 9.5 ka BP water depths became substantial when the ice sheet retreated over the Bothnian Gulf. Ice Stream F drained into the White Sea, however, lack of relative-sea-level data precludes an estimate of the local water depth.

##### *Setting*

Finland, with the exception of the northernmost part, is a low-lying, gently inclined peneplain. Strong fracturing during earlier geological history, and prolonged glacial erosion produced a surface topography of high-frequency, low-amplitude relief, with numerous small, isolated bedrock knobs. Sediment thickness increases from south to north, it is thickest in Lapland, where bedrock exposures are relatively rare (Nordkalott Project, 1986a) and constitute approximately 5% of the total area below 500m asl. Further to the south the overburden thickness decreases. In the southern half of Finland bare bedrock amounts to 40% of the area. The bedrock knobs are partly exposed, partly covered by thin deposits often of post-glacial subaqueous origin. Continuous sediment cover is found in lower areas in between.

##### *Landforms and ice streams*

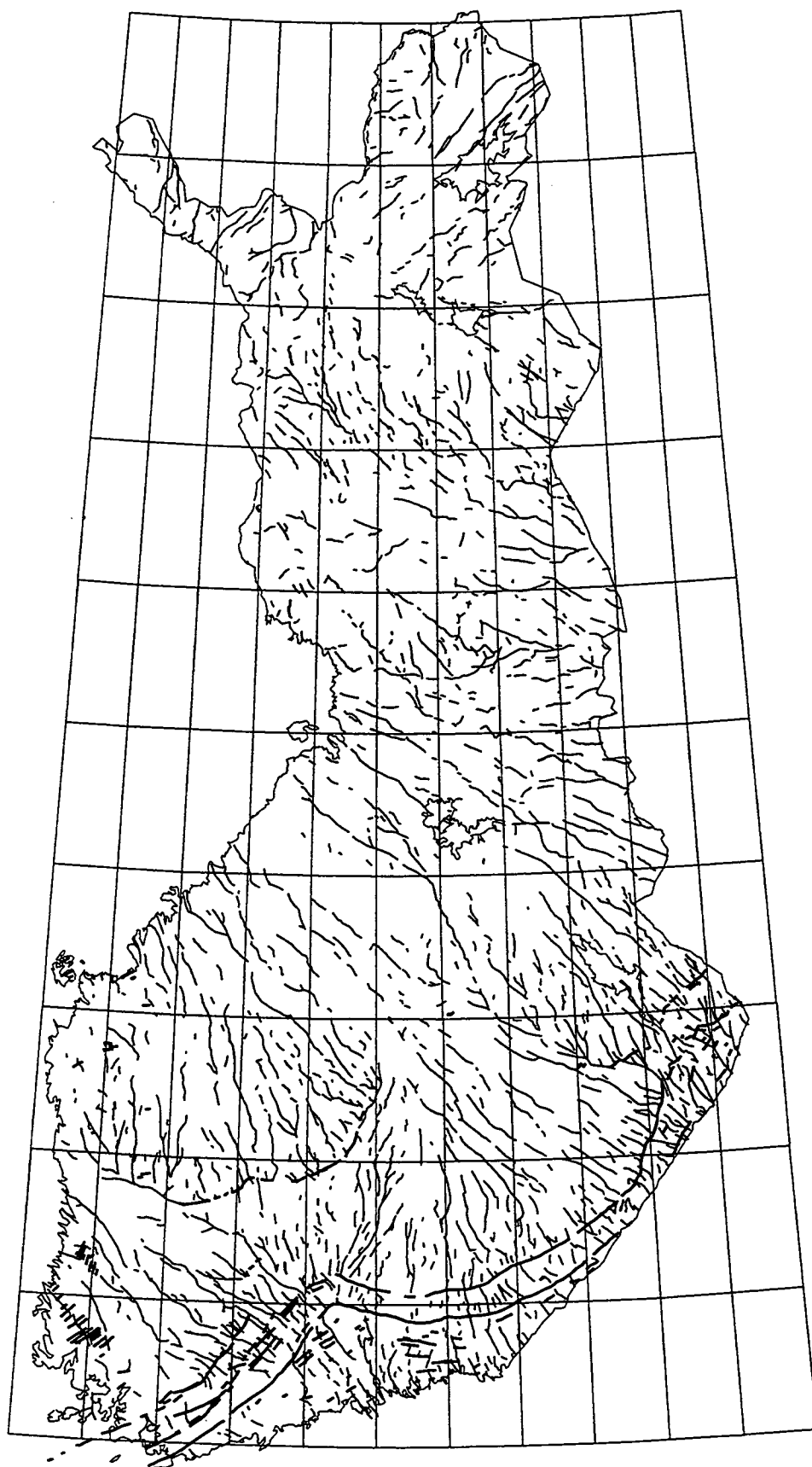
Section 6.4 showed that the lineation distribution over Finland displays a systematic zonation in lineation density. Highest lineation densities are found in lobate areas. Away from the centre lines of these lobes, lineation densities decrease towards the inter-lobate areas where they reach a minimum. The orientations of the lineations in the centres of the lobes are parallel to the trend of the central axes of the lobes, while away from the centre lines towards to

edges of the lobes, orientations shift increasingly away from the central axes. Thus the lineations reflect diverging flow in the lobate zones and converging flow in the inter-lobate zones. Superimposition of lineations indicates that the ice-flow directions in the inter-lobate areas become increasingly convergent with time.

This zonation is not limited to lineations, Punkari (1982) described that the occurrence of fluvio-glacial and hummocky deposits increased towards the inter-lobate areas. He argued that the converging, compressive flow in these areas enabled the ice to incorporate subglacial debris in englacial and perhaps supraglacial positions. The lack of lineations and other ice flow indicators and the absence of hummocky moraine to the south of Ice Stream C was interpreted by Punkari (1980) to reflect stagnating, perhaps cold-based, ice. The idea that the marginal parts of some interstream areas became stagnant altogether was also proposed by Haavisto-Hyvärinen *et al.* (1989).

Eskers are found in abundance in Finland, and indeed on the entire Baltic Shield. Figure 8.2 shows a map of the larger esker ridges in Finland. These esker ridges are generally thought to reflect time-transgressive tunnel sedimentation at or near the snout of a retreating ice sheet (Sugden and John, 1976). It is unknown how far subglacial tunnels extend underneath an ice sheet. Rothlisberger (1972) showed that tunnels can survive under hundreds of metres of ice because the overburden pressure of the ice is counterbalanced by high subglacial water pressures. The continuity of the esker ridges during deglaciation (Fig. 8.2) suggests that their positions within the ice sheet were relatively stable and that tunnels extended upstream in response to the retreat of the ice margin. Although subglacial meltwater can maintain the tunnels, it is thought that supraglacial meltwater reaching the bed plays an important role in the final transport and sedimentation of the sediments that make up the esker ridges (Banerjee and McDonald, 1975). Evidence from present-day glaciers shows that supraglacial meltwater does reach the subglacial drainage system. Unfortunately little is known about the exact mechanism that enables supraglacial meltwater to reach the bed. Moreover, the distance from the snout where this might occur is still strongly disputed (Iken and Bindschadler, 1986; Paterson, 1995).

Fig. 8.2 Eskers and fluvio-glacial deposits in Finland. Data from 1:1,000,000 map of Quaternary deposits of Finland (Kujansuu and Niemelä, 1984.).



Shreve (1972) showed that the subglacial flow direction is primarily determined by the slope of the overlying ice and only to a limited extent by the bed topography. The esker pattern therefore contains information about the surface topography of the ice sheet. The diverging flow in the lobate areas as was described in section 6.4 is also reflected in the esker pattern (see Fig. 8.2). The divergence of the eskers away from the centre lines of the lobes indicates that the ice surface was highest along these centre lines and becomes lower towards the inter-lobate areas. Supraglacial meltwater was also diverted towards the inter-lobate areas. The distance along which surface water could flow freely not only depended on the large-scale topography but also on the presence of crevasses and moulins that would capture the surface flow. However, it seems likely that the inter-lobate areas were zones of preferred supra-glacial meltwater collection. This is in agreement with the distribution of fluvio-glacial and hummocky deposits described earlier.

#### *Flow dynamics*

In Chapter 4 it was argued that conditions at the base of the ice sheet have to be warm and wet to produce lineations. The size and spacing of the produced streamlined bedforms depend on a number of inter-related variables, *e.g.* effective pressure, basal shear stress, sliding velocity, sediment supply and time. The duration of these basal processes at a given location is poorly known although the isochron pattern gives some indication how long a given flow geometry was active. The other variables vary through space and time and cannot be reconstructed separately. What the lineation record shows are the time-integrated accumulative effects of these basal processes. Densities and relative ages of lineations in combination with isochrons can be used as a measure of the local basal activity of the ice sheet during a certain period.

On the basis of the above assumptions it is argued that the Younger Dryas ice streams in Finland were warm/wet based in their downstream, diverging parts. The high lineation densities and lack of pre-deglaciation lineations point to very high glacial activity in the central parts of the ice streams. The warm/wet based zone extended upstream for at least 200/250 km.

The interstream areas, by contrast, reflect low glacial activity, deglaciation lineations are rare and the pre-deglaciation lineations survived. This indicates

cold-based conditions where the subsurface was protected from remoulding because the ice was frozen onto it. It is possible that basal conditions were (partly) temperate but that the circumstances were unfavourable for lineation formation (*e.g.* very low ice velocities). Between the two extremes of active ice streams and possibly frozen interstream areas a transition zone is situated which was influenced by the diverging ice streams to some extent but where some pre-deglaciation lineations survived nevertheless.

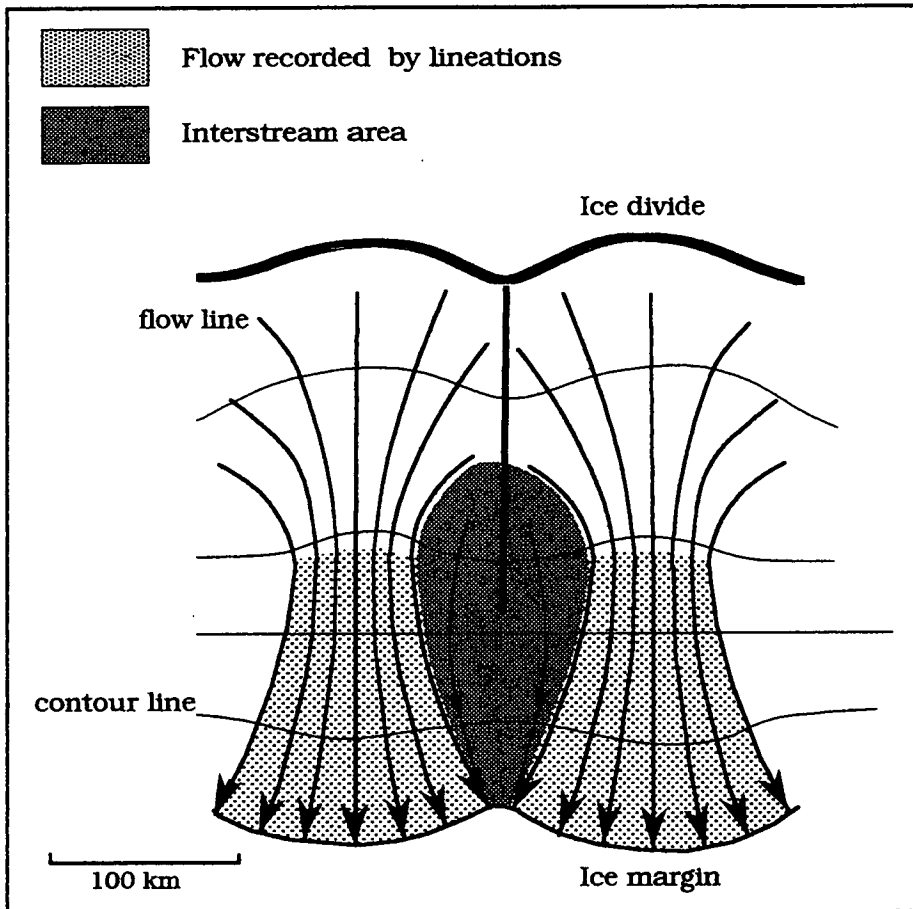
Fig. 8.3 shows a cartoon of the flow geometry in an ice stream/interstream system. The ice streams are 2 to 3 times wider at the margin than at the apex (Fig. 6.9). Ice fluxes through the apex must have been high in order to balance the ablation over the large downstream area. The fast-flowing ice stream draws in large amounts of ice in the accumulation zone. Flow converges towards the apex of the ice stream. To maintain this influx the surface elevation of the apex must be lower than that of the neighbouring interstream area. As ice is drawn into the ice streams, the interstream area is relatively starved of ice. Consequently flow velocities are low in the interstream area and ice may be cold-based. Downstream, the lower mass influx in the interstream area leads to a larger reduction in surface elevation for a given ablation. Thus, some distance downstream from the apex, the ice stream will become topographically higher than the interstream area. As a result of the starvation the interstream ice is replaced progressively by ice from the marginal lobes. Thus, the interstream area is progressively invaded by the ice stream.

The progressive expansion of the ice lobes explains why the lineation density diminishes away from the centre line of the ice streams. While during deglaciation the centre lines were remoulded continuously by active ice, the edges of the lobes were only invaded when the ice margin came closer. There was less time to rework these zones.

#### *Modern analogies*

When we try to find present-day analogies of the ice-flow organisation over Finland, the Siple Coast seems to offer an interesting comparison. In contrast to other ice streams the Siple Coast Ice Streams do not occupy well-defined bedrock troughs. The fast-flowing regions are separated from each other by

Fig. 8.3 Cartoon of flow geometry in ice-stream/interstream systems.



slow-flowing, topographically higher, interstream regions, and the contact zone between the fast- and slow-moving ice exhibits strong crevassing.

However, there are some important differences between the Siple Coast Ice Streams and the Finnish Ice Streams. Unlike the Finnish Ice Streams, the Siple Coast Ice Streams discharge their entire mass by calving, ablation is negligible. The bed of the ice stream is situated approximately 300m below sea level. In Finland, converging and extending flow in the accumulation area gave way downstream to diverging and compressive flow in the ablation area. There are good indications from the fluvio-glacial deposits that the topographic relation between ice streams and interstream areas in the accumulation area is reversed in the ablation area. So it seems that the Siple Coast Ice Streams have an organisation that may be comparable to the upstream areas of the Finnish ice streams. A down-stream lobate system such as the Finnish one can only develop fully in an ablation-dominated environment and has no equivalent in modern ice sheets.

#### *Conclusion*

In Finland a persistent system of ice streams/ice lobes developed that had a large impact on landform distribution. The Finnish Ice Streams developed over relatively flat, impermeable bedrock. The scale of the ice streams was an order of magnitude larger than that of the underlying topographic variations. As was described in section 6.4, the positions of the ice streams changed in response to changes in the overall drainage pattern of the ice sheet. This indicates that the ice streams were independent of local topographical and geological conditions.

During the early stages of these ice streams, local variations in geology or topography undoubtedly played a role by triggering positive feedback loops. Faster flow produces more frictional heat that will raise the temperature of the basal ice, warmer ice in turn deforms more easily. Once basal ice reaches the pressure melting point, meltwater can be produced and sliding or deformation can develop. With time, the ice streams expanded to become independent of local conditions.

The persistence of the ice streams, their relatively even spatial distribution and the fact that they could sustain their activity under changing conditions suggests that ice streaming is a reflection of internal glacio-dynamic processes. It suggests that given relatively uniform conditions, regularly spaced ice streams develop as a result of self organisation within an ice sheet.

Clark (1994) pointed out that rapid fluctuations of the large ice lobes at the southern fringe of the Laurentide Ice Sheet were limited to areas underlain by deformable sediments. The retreat of the ice sheet over areas with rigid beds did not show similar fluctuations and appears to have proceeded without any major readvances. There are indications that the Fennoscandian Ice Sheet behaved in a similar way. Whereas the Baltic Ice Stream expanded and retreated rapidly, the ice streams on the Baltic Shield showed a much more stable behaviour.

The behaviour of ice streams underlain by soft sediment casts some doubt on the notion of stable soft sediment deformation as proposed by Boulton and Hindmarsh (1987). Alley (1993) suggested that large bedrock bumps will support a disproportionate part of the basal shear stress. In south Finland some 40% of the bed may have been bare bedrock in direct contact with the base of the ice sheet. Sliding over bedrock was therefore the limiting factor. The Finnish Ice Streams indicate that ice streaming can be maintained by sliding over bedrock and that large-scale soft-sediment deformation is not a necessary precondition for ice streaming. The behaviour of ice sheets underlain by sediments even suggests that for stable ice streaming to develop, the presence of sticky spots may be necessary.

### 8.5 Reconstruction of deglaciation flow dynamics

Figures 8.4 to 8.6 show reconstructions of the ice-sheet dynamics for 11 ka, 10 ka and 9,5 ka BP. The continuous black lines depict flow lines, ice streams are shown by closely spaced flowlines. The flow lines of the Baltic Ice Stream are dashed as they have been inferred from the overall ice geometry and are not based on lineation observations. The darker, dotted zones represent interstream areas. Also shown is the inferred position of the ice divide (thick,

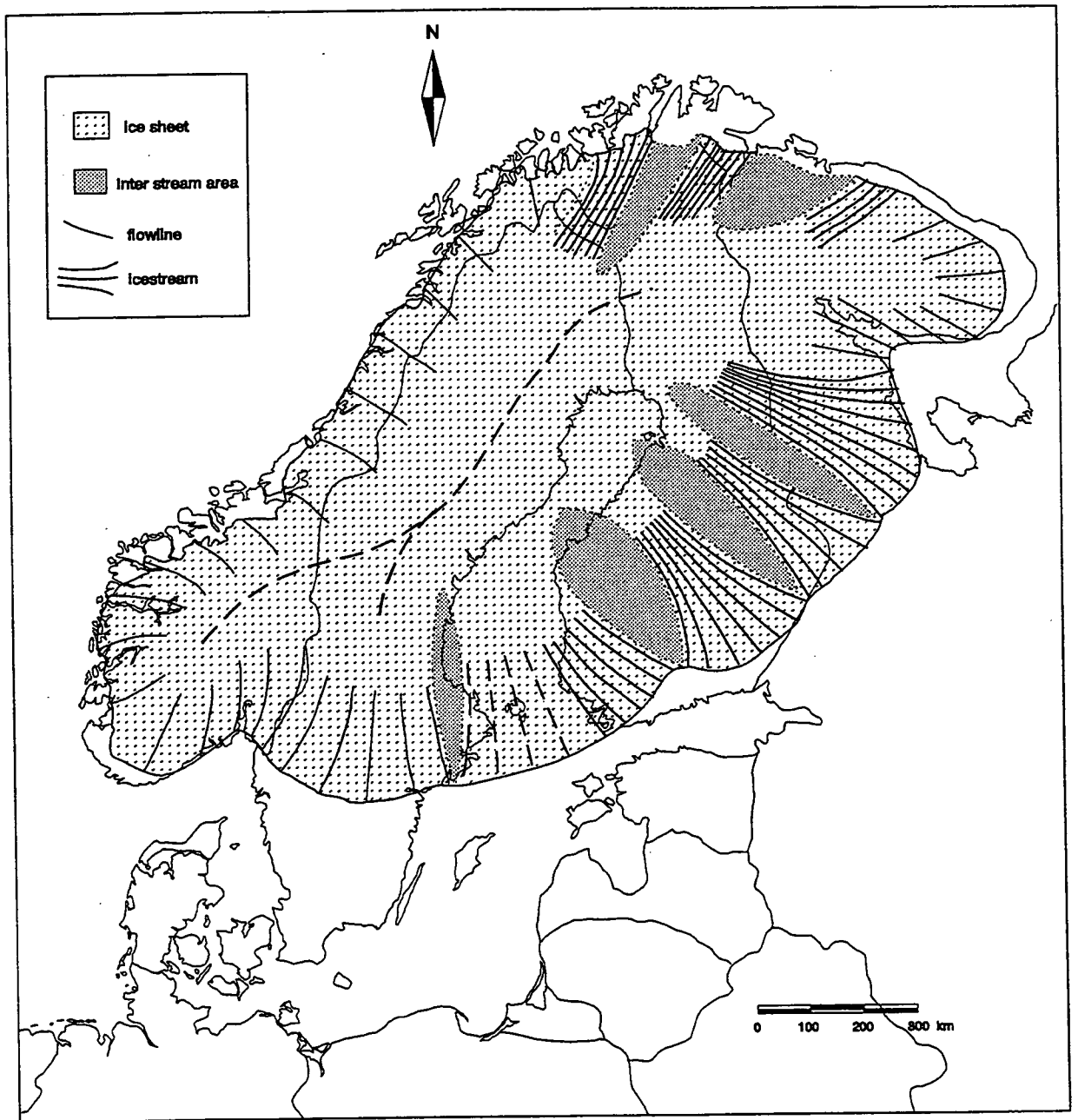


Fig. 8.4 Reconstruction of ice-flow dynamics at 11 ka BP. Ice sheet (dotted), interstream areas (shaded), flow lines (continuous lines), ice divide (dashed line).

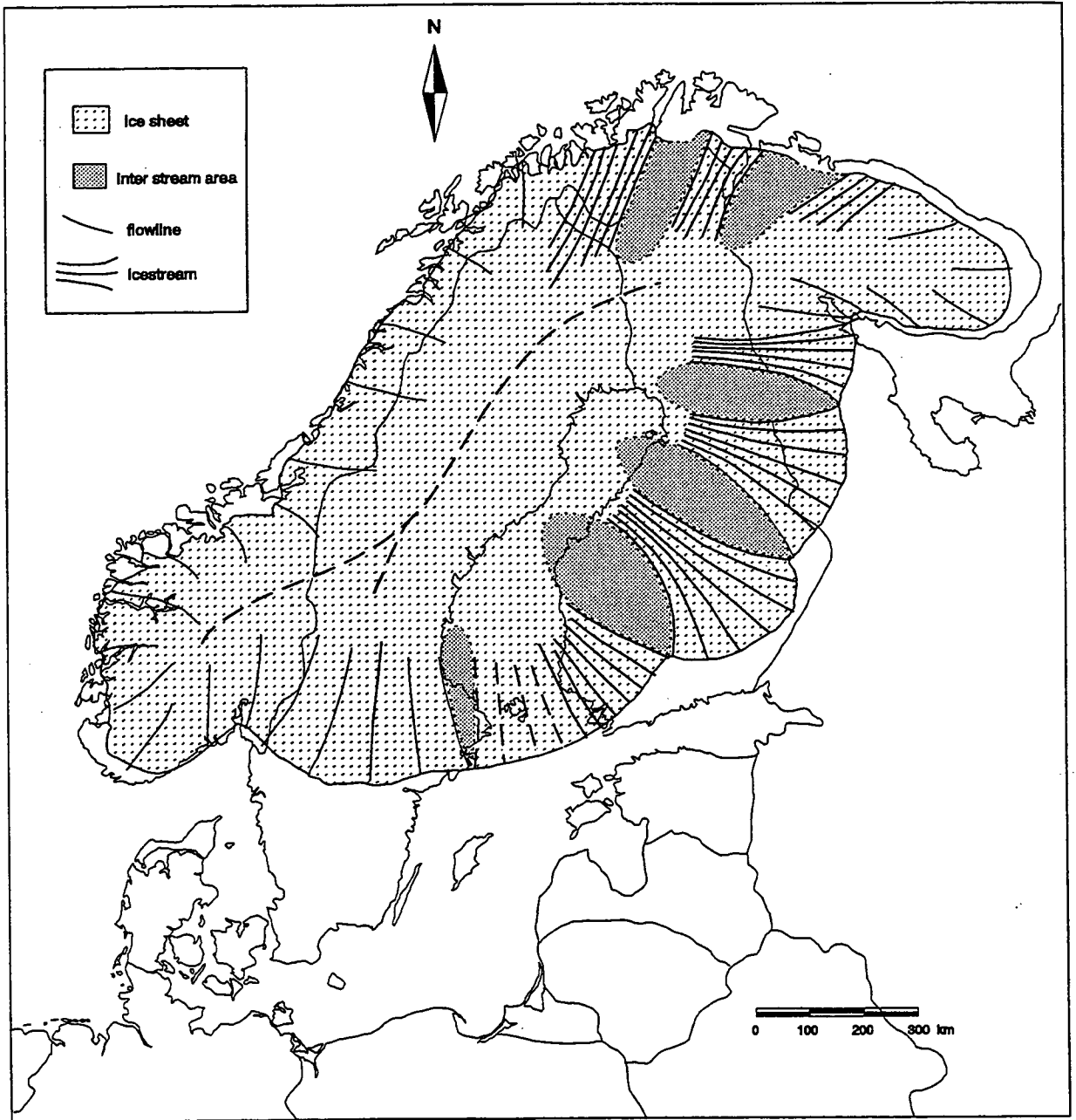
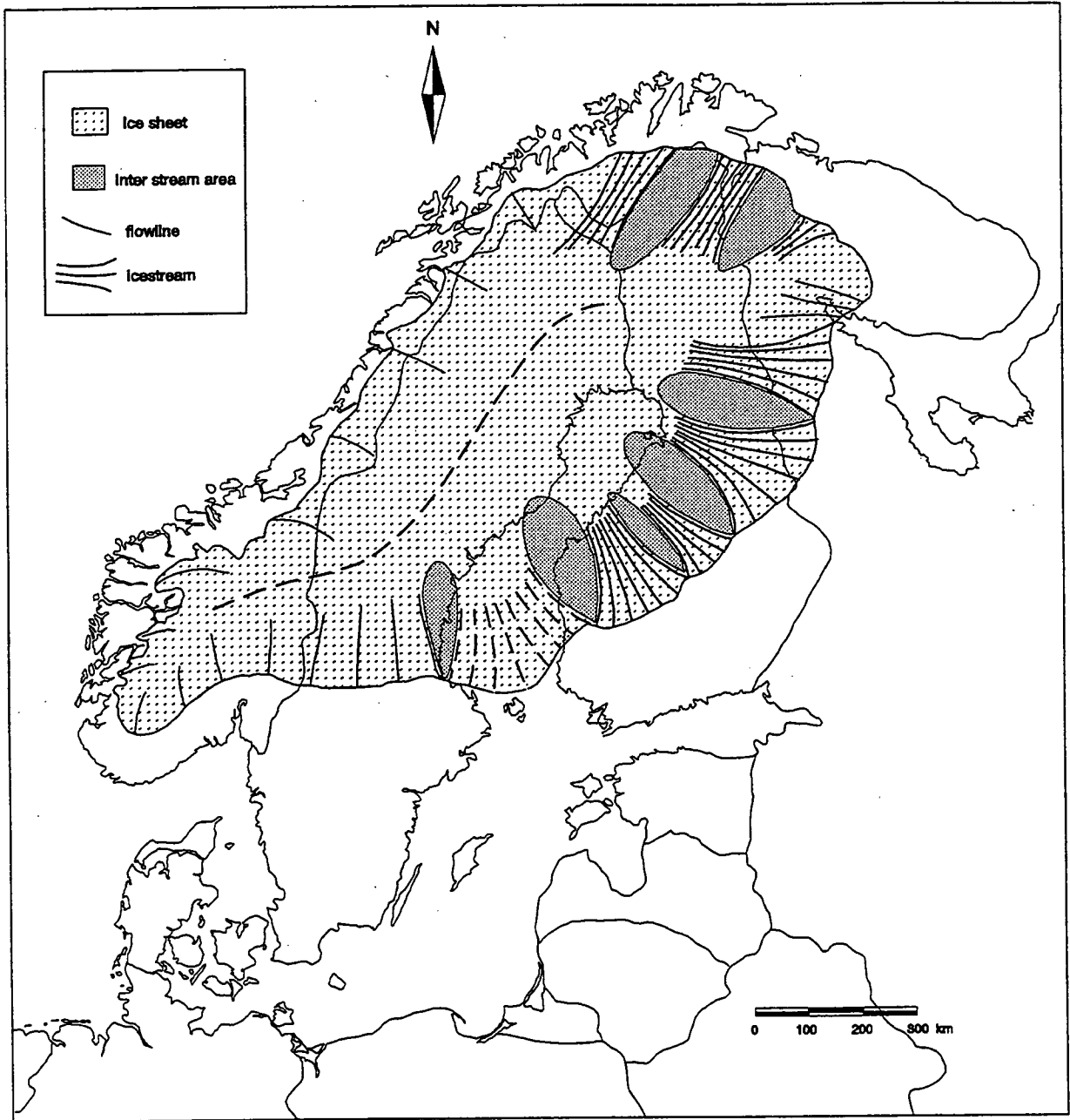


Fig. 8.5 Reconstruction of ice-flow dynamics at 10 ka BP.  
 Ice sheet (dotted), interstream areas (shaded),  
 flow lines (continuous lines), ice divide (dashed line).



**Fig. 8.6** Reconstruction of ice-flow dynamics at 9.5 ka BP. Ice sheet (dotted), interstream areas (shaded), flow lines (continuous lines), ice divide (dashed line).

dashed lines). These figures represent snapshots of the continuously changing ice-flow geometry during deglaciation.

The lineation pattern in Russian Karelia suggests that ice streaming was active prior to 12 ka BP (Fig. 6.9). The conspicuous separation of active ice-marginal lobes and inactive inter-lobate areas started to develop around 12 ka BP, following the deglaciation of the Barents Sea Ice Sheet. Around 11 ka BP (Fig. 8.4) the lobate pattern was well established over Finland. The relative starvation of the interstream areas led to a progressive expansion of ice lobes D, E and F into the intervening interstream areas. During the Younger Dryas the ice lobes coalesced in the marginal area and destroyed evidence of older flow within approximately 100 km of the ice margin (Fig. 6.10b). Between lobes B and D this didn't happen, here a triangular area remained where lineations are rare. Punkari (1980) suggested that this region became stagnant altogether.

The climatic amelioration following the Younger Dryas resulted in a strongly negative mass balance of the ice sheet which caused the ice margin to retreat rapidly (Fig. 6.1). The diminishing size of the ice sheet in combination with a rise of the equilibrium line altitude (ELA) led to a decreasing accumulation area and thus to a reduction in ice flux. As a result the ability of the ice streams to remould their subsurface diminished. The combination of decreased ice stream activity and rapid deglaciation resulted in a strong decrease in geological impact of the ice streams and an increased preservation of older lineations in the interstream areas (Fig. 6.10b).

Around 9.5 ka BP (Fig. 8.6) the ice-flow configuration had changed considerably from the 10 ka BP situation (Fig. 8.5). Ice Streams F and E had shrunk in size in response to their diminishing accumulation areas and the intervening areas where older lineations were preserved became wider (6.10b). In south Finland the changes were even more pronounced. Ice Streams B and D show a continuous reduction in extent and activity between 10 and 9.5 ka BP. Around 9.5 ka BP they became virtually inactive, in their place a single new ice stream had formed in between the previous two.

The gradual dying of the two ice streams, B and D, suggests that a minimum ice flux is needed to maintain the positive feedback loop of high velocities and

high frictional heat production. If the ice flux falls below this minimum requirement, ice stream activity starts to decrease and another positive feedback may develop. Decreasing influx leads to lower velocities and reduced heat production. Interestingly, the two ice streams were replaced by one single ice stream, positioned right in the middle of the two dying ice streams. This may point to a complicated set of events. Initially, falling fluxes caused a reduction in flow velocity and thus a fall in heat production. This would eventually have counterbalanced the discharge capacity of the two ice streams and the ice available for discharge. This however did not occur, the fall in activity of the two ice streams continued. So the discharge capacity of the ice streams became too low to drain the entire accumulation area. This must have resulted in a thickening of the ice mass in the accumulation area of the ice streams. One would expect this thickening to be greatest right in the middle of the two dying ice streams because the shrinking of the drainage areas on either side left this area undrained. The thickening of the ice, and the resultant steepening of the ice-sheet profile in this former interstream area, raised the ice velocities and the production of frictional heat. The development of the positive feedback loop described above eventually led to the formation Ice Stream C.

Another possible explanation for this change in ice-flow configuration is, that the activity of ice streams fluctuates as a result of internal mechanisms that are not necessarily related to the ice flux. Studies of the Siple Coast showed that Ice Stream C stopped functioning ca. 250 y. ago (Shabtaie and Bentley, 1987). The mechanisms that caused the ice stream to become inactive are as yet unknown, but different thermal and hydrological schemes have been proposed (Oerlemans and van der Veen, 1984; Fowler, 1987). In a numerical modelling study, Payne (1995) found that temporal transitions from sheet flow to stream flow occurred along a one-dimensional transect.

The situation over south Sweden is quite different. Here too, the ice flow was warm-based and diverging, but there are no indications of ice streaming developing. The ice retreated over dry land, and diverging flow resulted from the lowering of the ice-sheet surface to the east and west which was caused by the presence of deep basins. The warm-based marginal area is estimated to be approximately 100-150 km wide. Lineations related to the deglaciation of south

Sweden prevail but older lineations are still present, although not as frequently as in the interstream areas in Finland.

The exact position of the ice divide is not clear. The drawdown of the ice streams will have lowered the ice surface in the accumulation area, thus forming broad zones that sloped towards the ice streams. Secondary ice divides probably existed along the interstream areas up to the accumulation zone. Because of the dominance of the ice streams, the ice divide did not control the ice flow but formed a secondary feature, whose position was governed by the combined ice stream activity. Over central Sweden a ridge was present (Fig. 8.4), part of a (secondary) ice divide that continued to the north where it joined the main ice divide that ran from the Hardanger Vidda mountains over central and north Sweden towards Lapland.

From these reconstructions, it follows that the warm-based outer fringe of the ice sheet was discontinuous in most areas. In north Scandinavia 50 to 80 km wide bands of warm-based ice were present in the valleys, separated from each other by cold-based ice on the higher terrain. Over the flatter areas in Finland, triangular-shaped warm-based zones were bordered by cold-based interstream areas. These warm-based zones extended upstream for 200/250 km. Over south Sweden and possibly also the Kola Peninsula there was a continuous warm-based outer fringe of approximately 100/150 km wide.

Fig. 8.7 shows a simplified picture of the distribution of deglaciation and pre-deglaciation lineations. This distribution summarises the spatial and temporal variability of erosive and depositional processes during deglaciation of Fennoscandia. The areas which were covered by active ice stream are characterised by lineations related to deglaciation. In the diverging, lobate areas diachronous systems of superimposed lineation fans were produced during the retreat. The interstream areas where older lineations survived increase in extent towards the west as a result of a decrease in activity of the ice stream and an increase in retreat rate.

In the central part of northern Scandinavia and especially in north Sweden, pre-deglaciation lineations prevail. Field studies (Nordkalott, 1986, Lagerbäck, 1988), have shown that the glacial lineations which formed underneath the

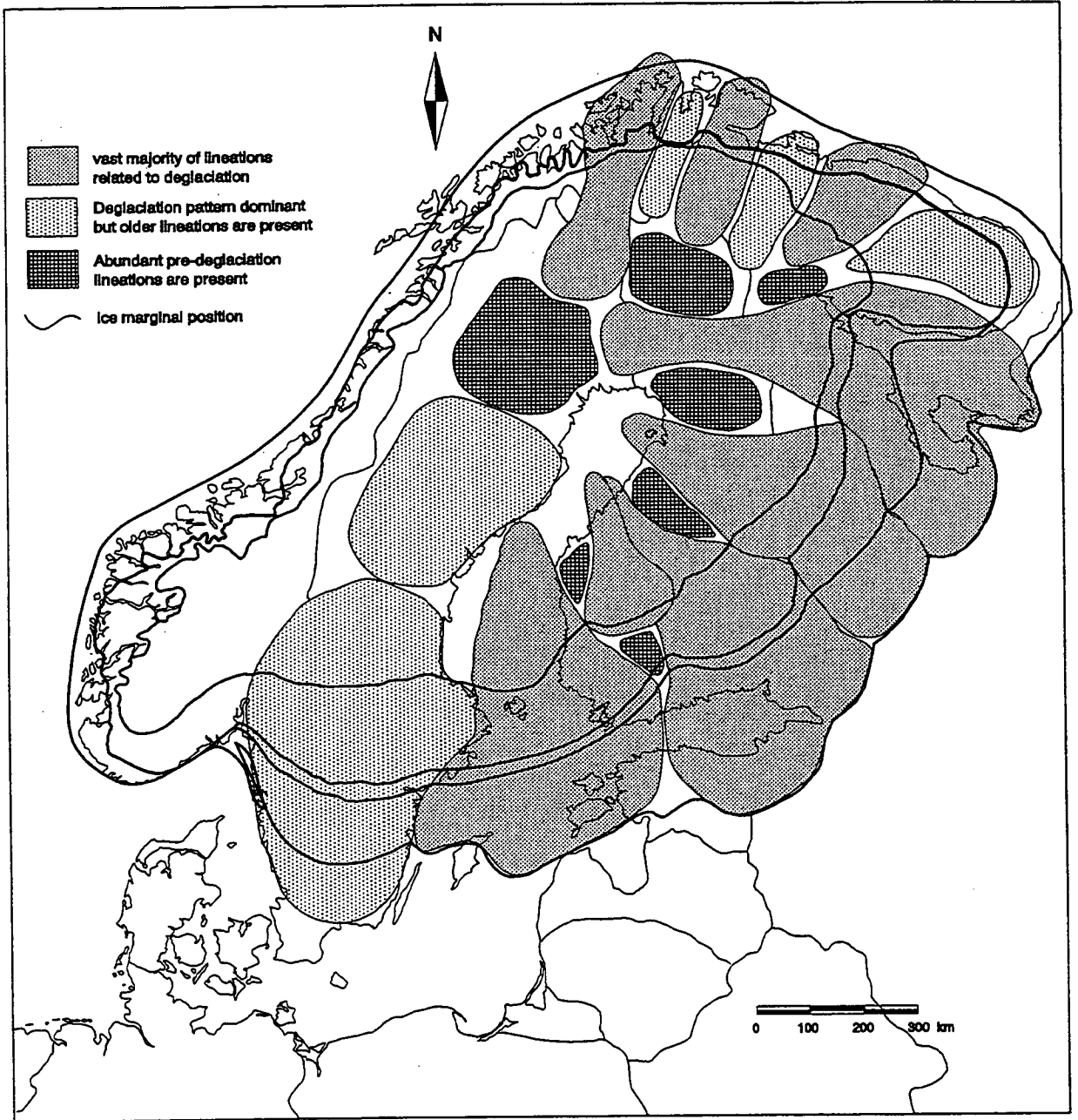


Fig. 8.7 Spatial pattern of deglaciation and pre-deglaciation lineations in Scandinavia.

last remnants of the ice sheet were considerably smaller than those formed earlier. The limited resolution of the satellite imagery, makes it difficult to pick out deglaciation patterns in these areas. It is most likely that the ice sheet remained active till the very last stages. Thinning of the ice sheet and reduction of the accumulation area must have decreased the ice flux and flow velocity. Disintegration of the ice-sheet margins into the Ancylus Lake (Fig. 2.20) must have further diminished the ability to rework its bed. As a result older lineations are more common in the areas where the ice sheet remained longest.

Summarising, on an ice-sheet-wide scale, a concentric pattern can be recognised with deglaciation lineations dominating the outer zone, gradually decreasing in number towards the centre of last refuge where older lineations prevail. This pattern is to a large extent overprinted by the lateral variation in ice-sheet activity reflecting in the presence of ice streams.

## Chapter 9

### Conclusions and future perspective

#### 9.1 Conclusions

The objective of this study was to analyse the dynamics of the last Fennoscandian Ice Sheet using the extensive terrestrial record of streamlined bedforms. A complete satellite coverage of the Baltic Shield area enabled ice-sheet-wide mapping of glacial lineations. The presence of superimposed sets of lineations made it possible to work out the relative ages for different coherent lineation patterns. In a number of cases, absolute dating was possible because lineation patterns could be connected with dated positions of the ice margin.

The shifting balance between isostatic recovery, eustatic sea-level rise and the retreat of the ice margin, resulted in considerably changing conditions at the ice-sheet margin. Water bodies, changing in extent and depth through time, fringed the southern and eastern margins. Published RSL curves were used to compile the land/water distribution and the uplift pattern for different periods.

#### *Ice streams*

The ice-sheet organisation in Scandinavia was dominated by the presence of a number of ice streams. In many areas these zones of fast flow were to a large extent controlled by the presence of valleys and troughs. In the case of central and south Finland and Russian Karelia, however, a persistent system of ice streams/ice lobes developed which was not topographically controlled. The areal scale of these ice streams was an order of magnitude larger than the scale of the underlying topographic variations. The ice streams changed position in response to changes in the overall drainage pattern of the ice sheet. This indicates that the ice streams were not dependent on local topographical or geological conditions to remain active. The regular distribution of these ice streams, their persistence and their independence of local topography and geology implies that they were the result of internal dynamic processes and reflect the ice flow organisation within the ice sheet.

In south and central Finland ice streaming developed over impermeable bedrock, covered by a thin, discontinuous till layer. Local topography must have ensured numerous ice/bedrock contacts. This implies that soft-sediment deformation, which was undoubtedly active considering the extensive drumlinization of the area, may not have been the only or even the dominant process responsible for the ice streaming. The numerous bedrock pinpoints indicate the importance of ice/bedrock sliding: it seems that, for fast flow to exist on this scale, soft-sediment deformation is not a necessity.

The interstream areas, which flanked the fast-flowing zones, were relatively starved of ice as a result of upstream funnelling of ice into the ice streams. Consequently ice velocities were much lower and ice may have been frozen to its bed for most of their length. Near the margin, the ice surface in the interstream areas was at a lower level than that of the ice lobes.

#### *Landform distribution*

Over central and south Finland, the ice streams displayed an identical flow pattern. At their narrowest, near the ELA, the ice streams were approximately 50 to 70 km wide, separated from each other by interstream areas of 100 to 150 km wide. Upstream, in the accumulation area, the ice flow was coalescing as ice velocities increased towards the ice stream. Downstream, in the ablation zone, ice flow was strongly divergent, producing large, coalescing, interacting, ice lobes near the margin.

The flow organisation in the ablation area is reflected in the landform distribution. Lineation densities are highest near the centre lines of the ice streams and decrease laterally towards the interstream areas. Towards the ice margin the diverging flow pattern became accentuated as the lobes increasingly occupied topographically lower interstream areas. The interstream areas are dominated by hummocky, fluvio-glacial deposits because surface meltwater accumulated in these areas. The deglaciation lineations in these areas reflect the coalescence of the flanking lobes. Because of the stagnation of ice and the short-lived ice lobe incursions, lineations that are older than the deglaciation have survived in the interstream areas.

The result of the flow organisation described above can be seen best directly inside the Salpausselkä moraines. The prolonged period of relative unchanged ice-sheet geometry during the Younger Dryas resulted in a well developed landforms distribution. Two trends are clear in the lineation distribution. The first is that lineation densities increase towards the ice margin in a 200 km wide-zone as flow becomes compressive in the ablation zone. Superimposed on this concentric distribution is the effect of the lateral variation in ice activity resulting from the development of ice streams. Consequently high lineation densities in the ice lobes are separated by low densities in the interstream areas.

The Baltic Ice Stream displayed a different behaviour than any of the other ice streams. From Denmark and south Sweden, two massive incursions of Baltic ice have been recorded in the till stratigraphy. These incursions influenced the ice-flow patterns as far east as the Berlin region. The incursions were followed by a rapid retreat. The Baltic Ice Stream occupied a broad trough, well below the water level and underlain by Mesozoic and Paleozoic sediments which are far more susceptible to deformation than the bedrock of the Baltic Shield. It is likely, therefore, that the southwesterly advances of the Baltic Ice Stream were the result of large-scale soft-sediment deformation. It is possible that these advances were, in fact, unstable and resembled large-scale surging that could not be maintained and led to drawdown of the accumulation area.

#### *Deglaciation*

The glacial landforms covering the Baltic Shield formed diachronously by the retreating active marginal zone of the ice streams. The rapid deglaciation of the Fennoscandian Ice Sheet following the Younger Dryas led to an overall decrease in ice-stream activity. This was the result of diminishing ice fluxes as the accumulation areas shrank and the ice sheet became thinner. In south Finland this led to the dying of two ice streams (B and D) and the formation of a new one in the former interstream area. (C).

A consequence of the diminishing activity is that lineations preceding the deglaciation have a higher chance of survival in areas which were occupied by the ice sheet longest. The rapid deglaciation, especially after 9.5 ka BP, accelerated as strongly depressed areas became ice free. The marginal lakes in

the Baltic Basin became deeper and disintegration of the ice sheet was enhanced as large parts of the thinning ice sheet became buoyant.

#### *Ice-sheet-wide flow changes*

Ice-sheet-wide changes in the ice-flow pattern during the advance and retreat phases were strongly influenced by the large-scale topography of Scandinavia. This topography is dominated by the Scandinavian mountains in the west; important drains to the north (North Atlantic and Barents Sea) and south (Norwegian Channel) and the extensive plain of the Baltic Shield to the east.

The lineations resulting from flow stages preceding deglaciation have been interpreted to have been produced during the advance phase of the ice sheet. The main centres of ice growth in the initial stages were the Kebnekaise area in the north and the Jotunheimen area in the south. Initial flow in the south radiated out from the Jotunheimen area. In the north, the flow direction shifted to a NNW-SSE direction in central Finland.

Once the ice sheet expanded beyond the Scandinavian mountains, its overall growth pattern was strongly influenced by discharge of ice both towards the north, to the Barents Sea, and the south, through the Skagerrak and the Norwegian Channel. To the northeast, the advance was halted by coalescence with ice from Novaya Zemlya over Kola and the Kanin Peninsula. The only possibility for expansion was to the east and southeast. Drains to the north and south resulted in a anti-clockwise shift of the ice flow lines in the north and a clockwise shift in the south. There are no indications of ice streaming during the advance phase.

During retreat the reverse happened. Once the ice sheet withdrew on to the Shield area, the drains became less important and ablation became dominant. In the northeast, flow lines turned clockwise, in the south and southeast the shift was anti-clockwise.

The pronounced lateral variations in ice flow velocity found in this study, should make stratigraphers and geomorphologists more careful when drawing conclusions concerning the basal thermal regime of former ice sheets from data collected in limited study areas.

## 9.2 Future perspective

In this study only the shield area has been investigated. Expansion of the study area into the sedimentary lowlands to the south and east would be very interesting for several reasons: a complete picture of Late Weichselian flow patterns could be obtained; the differences in ice dynamic behaviour over bedrock area compared to that over sedimentary lowland could be studied. The differences in subglacial hydrology and the possibility of large-scale sediment deformation may have important consequences for ice-sheet dynamics; the evolution of ice streams from the Late Glacial Maximum to the final deglaciation could be studied.

An area where conditions during the last glaciation were comparable to the Baltic Shield is the Canadian Shield area. Dyke and Prest (1987), have shown that the retreating ice margin displayed a strongly lobate character in both the sedimentary area to the south and the shield area itself. A new study of this region, using the same analysis techniques as used in this study would be very interesting. This would allow more general conclusions to be drawn concerning ice-dynamic behaviour and the role of ice streaming in shield areas.

The present study proves that the concentric patterns of warm- and cold-based ice produced by 3D thermo-mechanically coupled ice-sheet models are too simplistic. In these models the concentric pattern is interrupted only where major topographic features are present. What is needed is a better formulation of basal deformation/sliding and subglacial hydrology in the existing models, to produce the lateral variations in flow velocity that dominated the ice-sheet dynamics in Fennoscandia. More work should be done on the feedback processes that are active within ice sheets, and the interaction between ice sheets and their subsurface, which allows ice streaming to become independent of the mechanisms that initially triggered it.

# Appendix A

## Isostasy and relative sea level

## **Appendix A**

### **Isostasy and relative sea level**

#### **A.1 Introduction**

Sea level changes during the Quaternary are associated with the growth and decay of ice sheets over North America, northern Europe and the Barents Sea area and changes in the volume of the Antarctic and Greenland Ice Sheets. The large amount of ocean water stored in these ice sheets caused the global sea level to drop by 100-130 m during the Late Weichselian Maximum. The major contributors to the Late Weichselian fall in eustatic sea level were West Antarctica ( $\pm 15\%$ ), Eurasia ( $\pm 15\%$ ) and the Laurentide Ice Sheet over North America ( $\pm 65\%$ ) (Budd, 1979). The contribution to the global sea-level change from mountain glaciation and the Greenland Ice Sheet was, although important on a regional scale, relatively minor.

Relative sea level (RSL) change is the change in sea level measured relative to a point on land. The land itself may undergo vertical movements: relative sea level therefore measures the difference in vertical displacement between the local sea surface and the local land surface. RSL data can be used for the reconstruction of conditions at the ice-sheet margin, which may have influenced the behaviour of the ice sheet. Most notably it enables us to differentiate between areas that were dry land and those that were submerged. In the Baltic area, for example, the changing balance between retreat of the ice margin; isostatic recovery; eustatic sea-level change; changes in the geoid; and local tectonic activity resulted in the formation of vast fresh water lakes at the margin of the ice sheet (Eronen, 1983).

This Appendix, offers an introduction to the collection of RSL data and the uncertainties and errors involved in data collection and interpretation. This is followed by a discussion of the effects of crustal loading on the relative sea level around the globe. Finally all the RSL curves that were used in this study are shown in section A.4.

## A.2 Reconstruction of relative-sea-level history: methods and problems

There is abundant morphological and biostratigraphical evidence recording sea-level changes since the last glacial maximum. There are also a wide variety of sea-level indicators representing very diverse palaeo-environments: carbonates (shells, coral reefs) in marine and brackish environments; marine sediments inter-bedded with freshwater biogenic deposits (organic muds, peat); beach sediments; wave-cut rock platforms and planation surfaces; and marine notches can all be used as sea-level indicators (Tooley, 1978; Kidson, 1982). A method frequently used in glacially scoured terrain which has been subjected to uplift, is that of lake-basin isolation. The biostratigraphic sequence records the change from a marine to a freshwater environment when the basin is lifted above sea level (Devoy, 1987). All these methods can be used to reconstruct the sea-level history of specific sites. The use of evidence from such a variety of palaeo-environments causes many methodological problems. It has been noted that comparing sea-level curves derived by using different indicators may cause significant discrepancies, even for adjacent areas (Tooley, 1978; Kidson, 1982). Some of the problems involved in relating morphological and biostratigraphical markers to palaeo-sea levels and the difficulties in accurately dating them, will be discussed in this section.

Often, the exact relation of the indicators to the sea level, or more precisely the tidal range, is open to debate. Peats intercalated with marine, estuarine or terrestrial deposits give information about whether a regression (fall in relative sea level) or a transgression (rise in relative sea level) occurred. The altitudinal range of peat-forming plant communities above the tidal zone complicates the interpretation of the exact palaeo-sea level (Jelgersma, 1966). Although most researchers seem to agree that the transition from a saltmarsh to freshwater peat takes place near the Mean High Water level, Tooley (1978) argued that local factors could strongly distort any general relationship. Beach deposits present similar difficulties because they may have formed during exceptional conditions, such as storm surges, which are not typical of mean sea level at all (Tooley, 1978). The best indicators for sea level are organic remains in growth position, where the relation to sea level or ground-water level can be established within reasonable limits (Kidson, 1982). Because these are not

always available, indicators that provide less precise evidence of the sea level often have to be used.

To establish the relationship of organic deposits to the mean sea level it is obviously important that variations in tidal range are taken into account. The tidal range is dependent on sea depth and coastal configuration. During the Late Weichselian and Holocene eustatic sea-level rise, tidal ranges along the coasts most probably changed. In estuarine areas, where the tidal amplitude can vary considerably over a short distance, it is important to reconstruct the coastline and water depth for that particular period to enable the tidal effects to be modelled (Devoy, 1987).

After deposition, sediments undergo compaction, the rate of which is dependent on time, loading, sediment characteristics and drainage. Peat can be compacted by as much as 90% of the original thickness, whereas sandy deposits compact very little. Compaction rates vary locally as well as for different positions in a sequence. This effect can introduce large errors in the height of the reconstructed sea level. Jelgersma (1966) argued that therefore only peaty sediment on top of stable sandy deposits should be used for reconstruction purposes.

At present there are a number of dating techniques that are used for sea-level dating. Radiometric methods (radiocarbon and uranium series), biochemical methods (*e.g.* amino-acid diagenesis) and paleontological methods (pollen analysis and beetle studies). The best results are obtained when two independent methods are used together.

C<sup>14</sup> dating is the main technique used in the study of sea-level changes during the past 20,000 years, therefore some of the problems associated with this method will now be discussed. Terrestrial plants are in equilibrium with the atmospheric concentrations of radiocarbon. Thus, if no contaminants are present, the measured radiocarbon activity is related to the time that has passed since the death of the organisms. However, contaminants are often present in the samples, these have to be recognised and removed if possible. Contamination of samples may be caused by younger plant roots; organic acids

circulating with the ground water; and secondary carbonate deposits (Sutherland, 1987).

While the atmospheric radiocarbon cycle is very rapid and any changes are fed through the system in about a decade, the oceanic  $C^{14}$  cycle is much slower. Marine organisms will therefore incorporate radiocarbon that is 'older'. This results in the so-called "reservoir" or "apparent-age" effect. The reservoir age depends on the mixing characteristics of the environment. Organisms in zones of upwelling, where 'older' water reaches the surface, will have an older apparent age than organisms in a shallow coastal setting.

This effect is counteracted by isotopic fractionation (different isotopes are preferred or discriminated against depending on their atomic mass) which gives marine carbonates a  $\pm 5\%$  higher radiocarbon activity compared to terrestrial organisms.

Finally, natural radiocarbon production has not been constant throughout the last 20,000 years and consequently the original radiocarbon activity in organisms varied. This leads to a discrepancy between sidereal and radiocarbon dates. Ammann and Lotte (1989) have found evidence in Swiss lake basins for the existence of two distinct plateaux of constant radiocarbon dates. The plateaux occur at 12,700 and 10,000 BP. These plateaux of constant radiocarbon age are probably related to a decrease of atmospheric  $C^{14}$  during these periods. The result is that the exact time-depth relationship of deposits from these periods cannot be established because the  $C^{14}$  dates tend to group together.

Errors in relative-sea-level curves are the result of the problems concerned with establishing the exact relationship between the morphological and biostratigraphical indicators and the palaeo-sea level, and of errors resulting from dating. Errors can be especially large during periods of rapid sea-level change, *e.g.* immediately following deglaciation in formerly glaciated areas. Because of the high rates of uplift a small error in the dating can result in a substantial over- or under-estimate of relative sea level. It is evident that the plateaux of constant  $C^{14}$  dates (Ammann and Lotte, 1989) result in a large error margin in estimating the relative sea level for these periods.

It is, however, very difficult to quantify the error margins. Sea-level researchers do often not state explicitly which corrections they have used in relating sea-level indicators to a mean palaeo-sea level. Although most radiocarbon dates include a standard deviation, this only reflects the accuracy of the laboratory radioactivity count. It does not provide information on the degree of contamination or the likelihood of reservoir effects that may also have affected the outcome.

### A.3 The earth's response to changes in surface loading

#### A.3.1 Different components of response

The Sixties and early Seventies were dominated by the search for a true 'eustatic' sea-level curve (Fairbridge, 1961; Jelgersma, 1966; Mörner, 1969). Although researchers realised that the curves they produced were relative-sea-level curves, because of the occurrence of vertical land movements, many tried to correct for these movements and thus produce a curve that would show the global sea-level change. Figure A.1 gives examples of these eustatic sea-level curves. It became clear that sea-level curves from the same region often showed a strong similarity but curves from different parts of the world almost invariably showed large differences.

The theoretical concepts of glacio- and hydro-isostasy demonstrated that eustatic sea-level change, while affecting the entire world, does not produce relative-sea-level records that are similar in different parts of the earth. Clark *et al.* (1978) developed a model for a spherical visco-elastic earth and modelled the earth's response to the changes in surface loading such as occurred during a deglaciation. They distinguished several zones, each having a very distinct relative-sea-level history in response to the melting of the mid-latitude ice sheets. This response is the result of the interplay between glacio-isostatic uplift or subsidence; hydro-isostatic uplift or subsidence; and the eustatic sea-level rise. The adjustment of the hydrosphere, cryosphere and asthenosphere during and after deglaciation has left no place on earth unaffected.

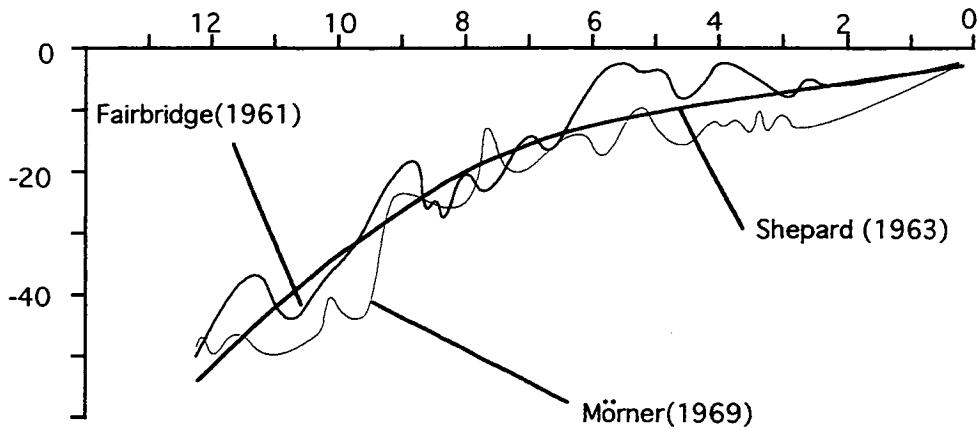


Fig. A.1 Different proposed eustatic sea level-curves.

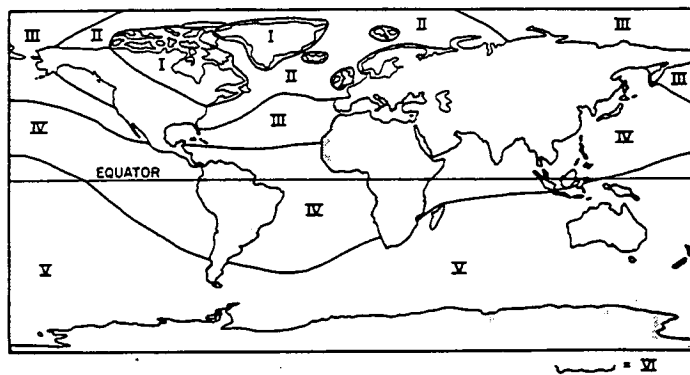


Fig. A.2 Zonal distribution of predicted sea-level response. (From Clark, 1980).

In the following section, the processes operating upon the earth's surface during this large-scale surface mass transfer will be discussed in more detail. The word eustatic refers to a world-wide fluctuation in sea level caused by a change in the total water quantity in the ocean basins. This is the result of a net change in the mass of oceanic water (change in global ice volume) or of a change in the volume of the oceans as a result of density changes caused by thermal or salinity changes (so-called steric effects, Peltier, 1987).

#### *Glacio-isostasy*

The loading of the earth's crust by the growth of an ice sheet will disturb the isostasy, which is the balance that exists between the rigid lithospheric plate floating on the denser, viscous mantle. Mantle material will flow outwards from the centre of the ice sheet towards the periphery. Maximum subsidence will occur underneath the centre of the ice sheet and diminish towards the margins (Walcott, 1972; Mörner, 1979; Peltier and Andrews, 1976). As a consequence of the crustal rigidity, the bending of the lithosphere will result in a 20-30m high forebulge near the margin of the ice sheet .

During the last glaciation complete isostatic equilibrium may have never been established because the maximum extent of the ice sheet lasted only a short time. Mörner (1979) claims that the uplift of Scandinavia since the Late Weichselian glaciation can be represented by an uplift cone of 830 m high, surrounded by a subsidence trough of at most 170 m deep. Only the last part of the uplift history is recorded by raised shorelines and marine deposits: uplift started as soon as the ice sheet started to thin, while deposits can survive only after deglaciation of an area.

#### *Hydro-isostasy*

The increase in total mass of ocean water as a result of the disappearance of the mid-latitude ice sheets and the contraction of Antarctica and Greenland resulted in extra loading on the ocean floor. This extra loading caused the sea floor to subside (Walcott, 1972; Chappell, 1974 ; Farrell and Clark, 1976 ). In coastal areas this resulted in hydrostatic warping that may have introduced differences of up to 30 % in estimates of marine transgression rates between oceanic islands (which subsided with the oceanic plate) and the continental coasts (which rose as a result of hydro-isostatic warping).

### *Changes in geoid configuration*

Another factor that should be taken into account is that of geoidal changes. The geoid is the equipotential surface of the earth's gravity field, i.e. the surface which the sea level would occupy if temperature, salinity and air pressure were distributed uniformly. The earth's gravity field is determined by the structure, density, rheology and rotation of the earth, and by the astronomic gravity. Differences in the earth's density and internal flow patterns mean that the geoid, and thus sea level, is not parallel to the earth's crust but has an irregular configuration (Mörner, 1976). The present geoid pattern of the earth shows huge differences in relatively nearby areas. Between the New Guinea High and the Maldives Low there is a difference of 180 m. Mörner argues that mass redistribution, leading to geoidal changes in the order of hundreds of metres, can be generated by the hydrosphere, asthenosphere and the core/mantle interface.

The differences in response time between melting of the ice sheet and the subsequent uplift of the deglaciated area, give rise to substantial mass deficits over the ice-free areas. This causes a decrease in the geoid (and thus also sea level) over this area. The relative-sea-level curves have to be corrected for these effects if we want to use them to study the rheology of the earth. Models that do just this have been developed by Farrell and Clark (1976) and Peltier and Andrews (1976).

In addition to the earth's response to surface mass transfer, tectonics and basin subsidence are also active on a variety of scales. Sediment loading in many coastal areas has caused increased subsidence. These factors greatly increase the complexity of the problems because the different processes are often impossible to separate.

#### A.3.2 Zonal distribution of response

Clark *et al.* (1978) developed a numerical model that simulates sea-level changes over the earth, which is considered to be a spherically symmetric, radially stratified Maxwell visco-elastic body. In a Maxwell visco-elastic body,

the initial reaction to applied shear stress is elastic, whereas the final response is viscous. Viscosity is a function of depth only. Thus, during deglaciation, there will be an accompanying elastic deformation of the entire globe.

After this initial response, the long-term deformation resulting from eustatic changes and postglacial rebound are described by relaxation models, which assume a relatively thin, viscous, asthenosphere overlain by a rigid lithosphere (Walcott, 1972; Peltier and Andrews, 1976; Clark *et al.*, 1978; Peltier, 1987). The models use relative-sea-level curves to calibrate their earth response parameters. These parameters include viscosity of the upper and lower mantle and the thickness of the lithosphere. Although a considerable mismatch between the predicted and the recorded sea level response remains, the models have enabled researchers to analyse the different processes that are operating. Models incorporating glacio-isostasy, hydro-isostasy and geoidal eustasy combined with realistic ice-sheet and deglaciation models predict that the combined effect of all these processes is to produce unique signals at different places on earth (Devoy, 1987).

Fig. A.2 shows the zonal distribution of sea-level recovery as predicted by the Clark *et al.* (1978) model. Each zone has its own distinct pattern of sea-level recovery.

- Zone I : Relative land emergence
- Zone I/II : Initial relative emergence followed by submergence
- Zone III : Continued land submergence
- Zone IV : Land submergence, followed by Late Holocene emergence (continental shorelines)

*Zone I* is dominated by glacio-isostatic crustal uplift. The rate of uplift depends on the thickness of the ice that originally covered the area, its deglaciation history and local tectonic activity (Devoy, 1987).

*Zone I/II* is dominated by the interaction of the migration and collapse of the forebulge with glacio-isostatic and eustatic factors (Clark *et al.*, 1978). In this zone, initial emergence will be followed by subsidence. The forebulge is thought

to migrate inwards as the of ice sheet retreats. While the bulge passes an area, this area is uplifted until it has passed or collapsed. From then on subsidence will dominate. Areas to which this pattern of relative-sea-level history is applicable are the northeast of the United States, the Atlantic coast of Canada and the area on the periphery of the Fennoscandian Ice Sheet.

*Zone II* is dominated by submergence throughout the Late Glacial and Holocene. The combined effects of the collapse of the forebulge and the rise in eustatic sea level result in strong subsidence rates. The area around the southern North Sea is a good example of this zone. Subsidence in southeast England, the Netherlands and North Germany is continuing up to the present. On the basis of geological and geophysical data, Mörner (1979) estimates that the maximum absolute subsidence that the region underwent was 170m. Jansen (1976) gives a minimum absolute subsidence of 25m for the northern parts of the North Sea.

*Zone III* shows initial submergence followed by limited emergence to a maximum of 0.75 m in the last 4000 years. The collapse of the forebulge is felt in this region, but very faintly. When the eustatic sea level stabilised, after 6000 years BP, the hydro-isostatic depression of the ocean floor and the subsequent tilting of the continental margin resulted in emergence of these coasts. An examples of this zone is the southern Atlantic Ocean. However, contrary to theoretical prediction, most of these coasts showed continued submergence throughout the Holocene. The most likely reason for this discrepancy is the continued subsidence of these margins as a result of the sinking of the cooling oceanic plates and sedimentary loading.

#### A.4 Relative-sea-level curves used in this study

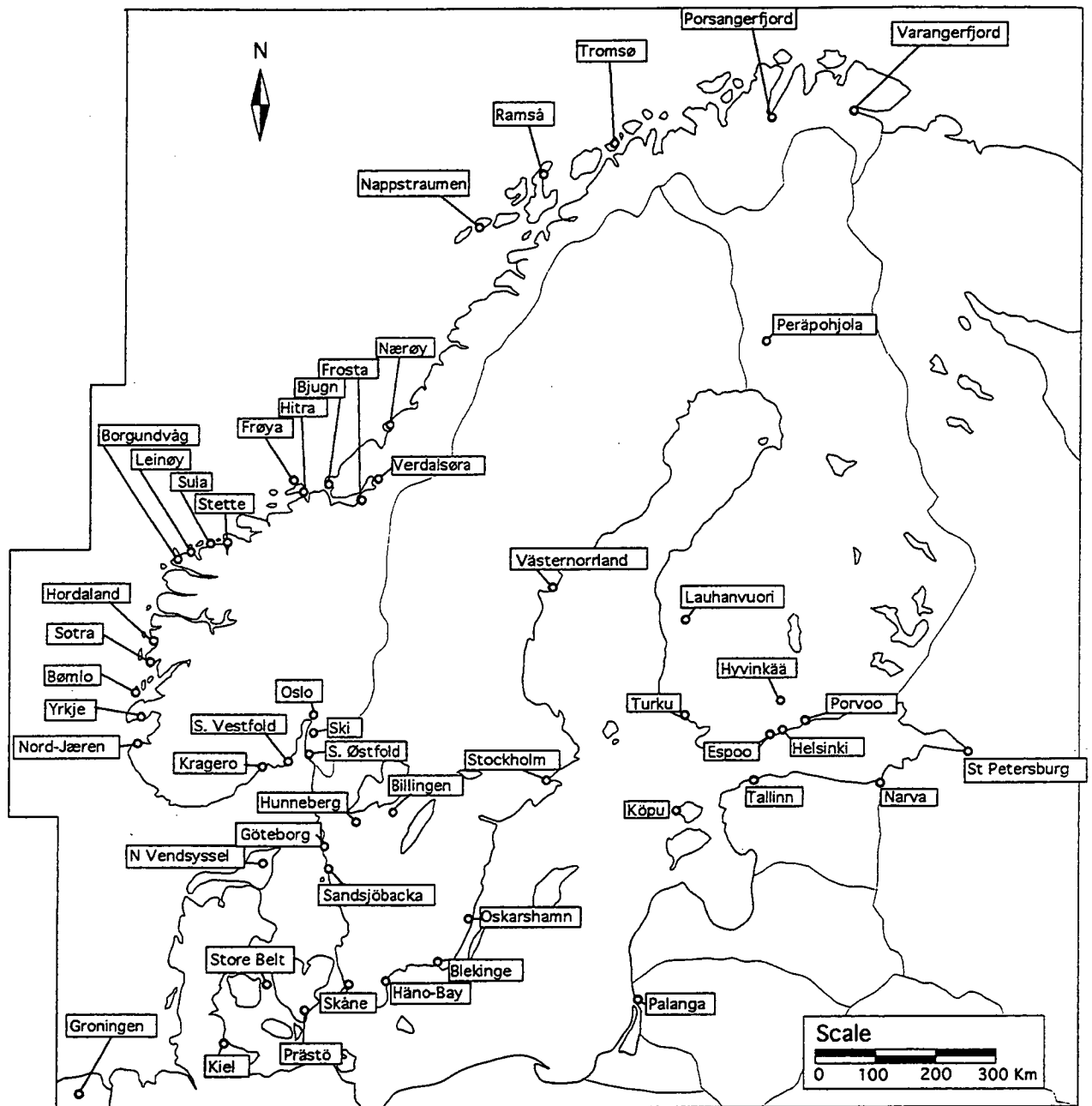
In this final section of Appendix A, all the relative-sea-level curves that have been used in this study are shown.

## List of figures

A.3	Location map of relative-sea-level curves	191
A.4	RSL curves of Kiel (Winn <i>et al.</i> , 1986) and Groningen (Jelgersma, 1980)	192
A.5	RSL curves of N.Vendsyssel (Petersen, 1984), Store Belt (Krog, 1960) and Prästö (Mikkelsen, 1949)	192
A.6	RSL curve of Häno-Bay (Björck and Dennegård, 1988)	192
A.7	RSL curve of Blekinge (Björck, 1979)	192
A.8	RSL curves of Oskarshamn (Svensson, 1985) and Skåne (Digerfeldt, 1975)	192
A.9	RSL curves of Billingen (Björck and Digerfeldt, 1986), Hunneberg (Björck and Digerfeldt, 1982), Göteborg (Bergsten and Dennegård, 1988) and Sandsjöbacka (Pässe, 1987)	192
A.10	RSL curves of Oslo (Hafsten, 1956), S.Vestfold (Henningsmoen, 1979) and Kragero (Stabell, 1980)	193
A.11	RSL curves of Ski (Sørensen, 1979) and S.Østfold (Danielsen, 1970)	193
A.12	RSL curves of Yrkje (Anundsen, 1980), Nord-Jaeren (Thomsen, 1981) and Bømlø (Fægri, 1944)	193
A.13	RSL curves of Sotra (Krzywinski & Stabell, 1978) and Hordaland (Kaland, 1984)	193
A.14	RSL curves of Stette (Svendsen & Mangerud, 1987), Sula (Lie <i>et.al.</i> , 1983), Leinøy (Svendsen, 1985) and Borgundvåg (Longva <i>et.al.</i> , 1983)	193
A.15	RSL curves of Frosta (Kjemperud, 1981), Bjugn (Kjemperud, 1986), Hitra (Kjemperud, 1986) and Frøya (Kjemperud, 1986)	194
A.16	RSL curves of Verdalsøra (Sveian & Olsen, 1984) and Nærøy (Ramfjord, 1982)	194
A.17	RSL curves of Tromsø (Hald & Vorren, 1983), Nappstraumen (Møller, 1984) and Ramså (Møller, 1986)	194
A.18	RSL curves of Varangerfjord (Donner <i>et. al.</i> , 1977) and Porsangerfjord (Donner <i>et. al.</i> , 1977)	194

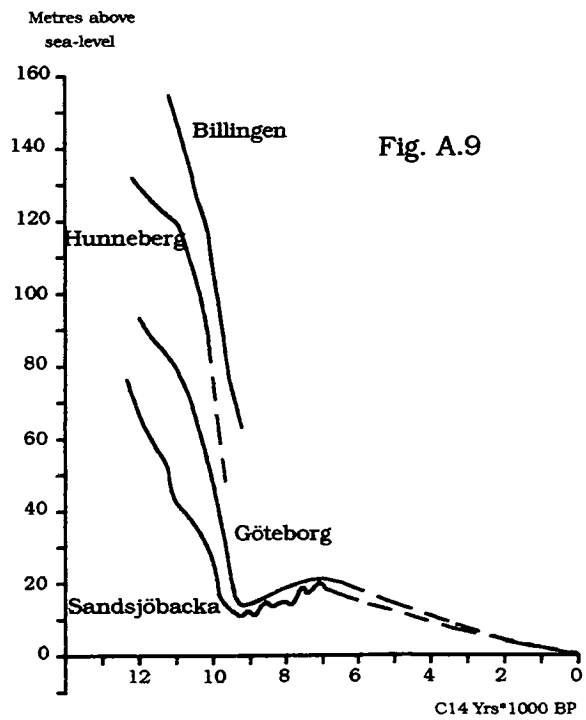
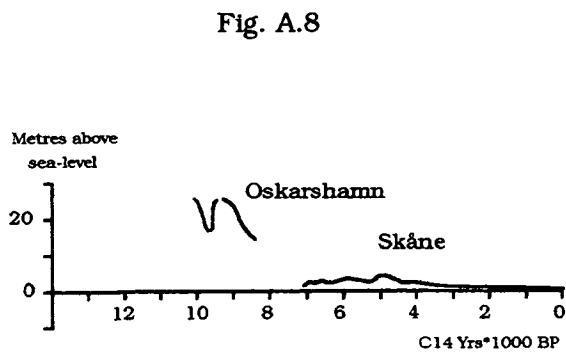
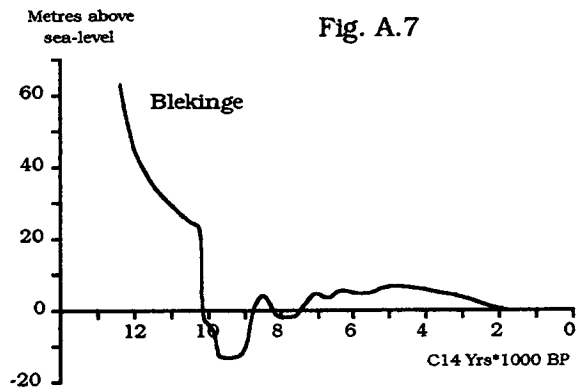
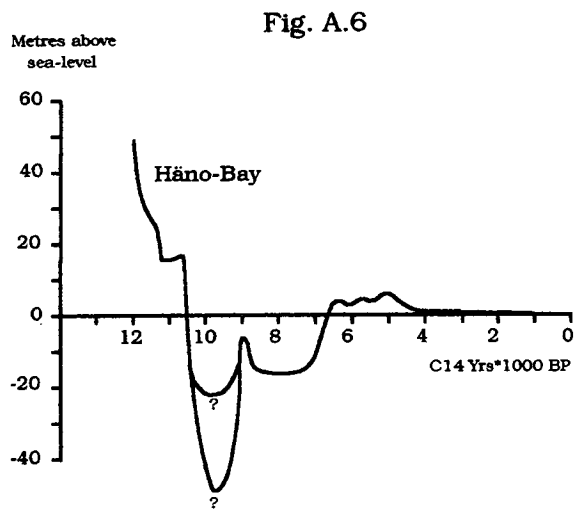
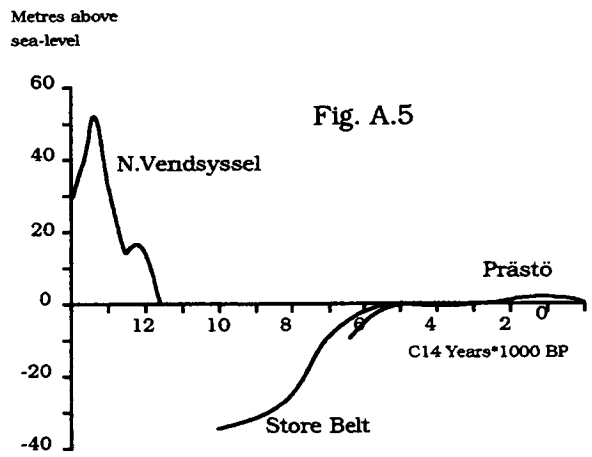
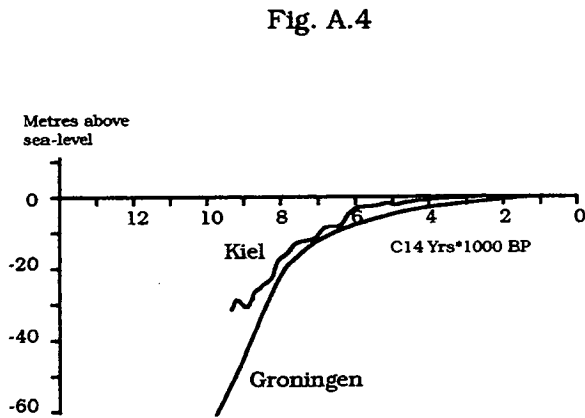
A.19	RSL curves of Peräpohjola (Saarnisto, 1981), Hyvinkää (Synge, 1982) and Porvoo (Eronen, 1983)	195
A.20	RSL curves of Västernorrland (Miller & Robertsson, 1979) and Stockholm (Åse & Bergström, 1982)	195
A.21	RSL curves of Lauhanvuori (Salomaa, 1982), Turku (Glückert, 1976) and Espoo (Hyvarinen, 1980)	195
A.22	RSL curve of Helsinki (Hyvarinen, 1980)	195
A.23	RSL curves of Köpu (Kessel & Raukas, 1979), Tallinn (Kessel & Raukas, 1979) and Narva (Kessel & Raukas, 1979)	196
A.24	RSL curve of Palanga (Gudelis, 1979)	196
A.25	RSL curve of St Petersburg (Dolukhanov, 1979)	196

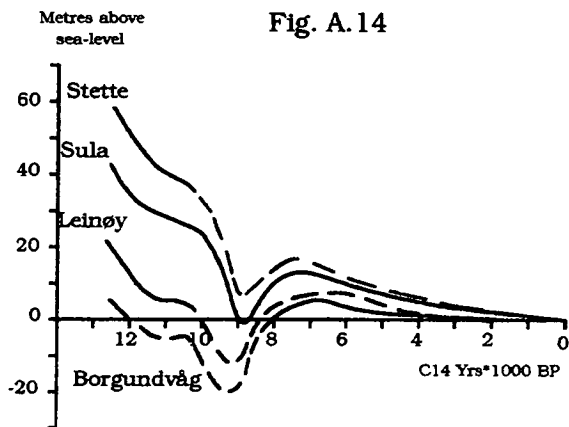
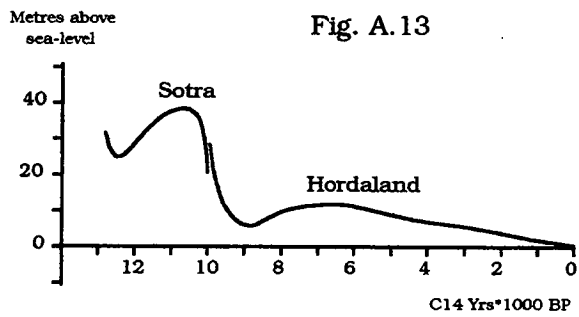
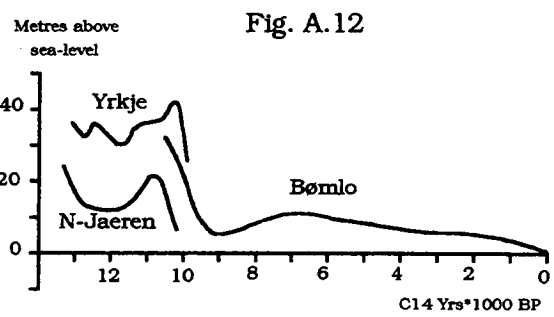
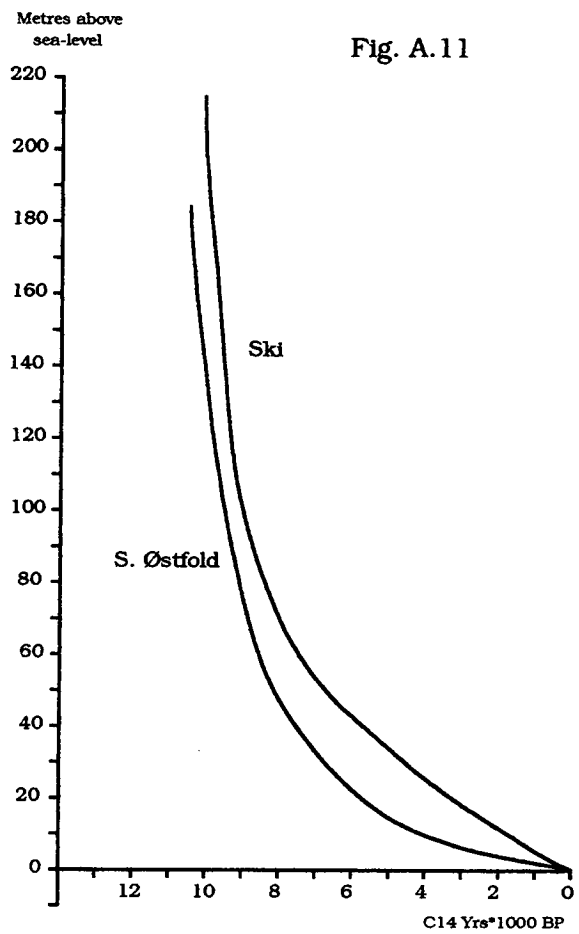
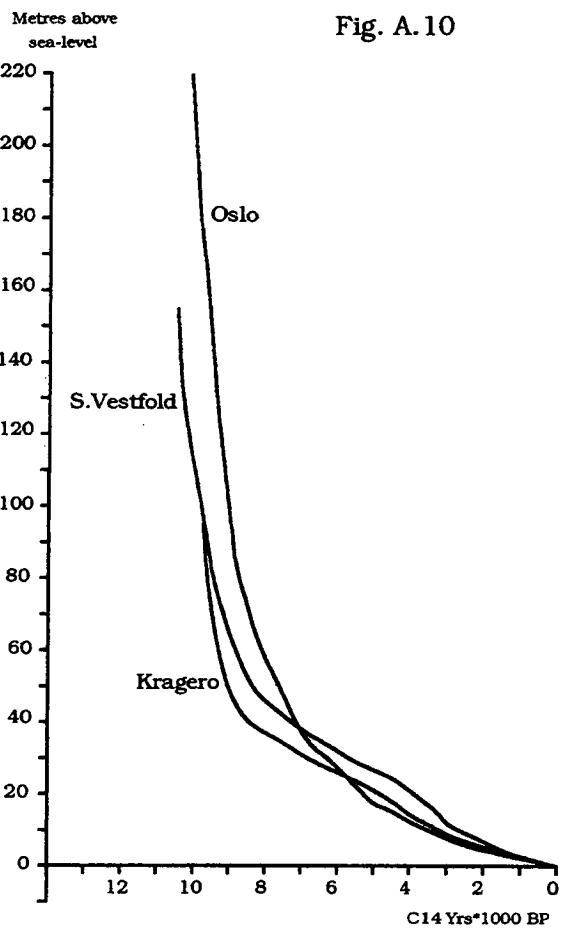
## Locations of relative sea-level curves

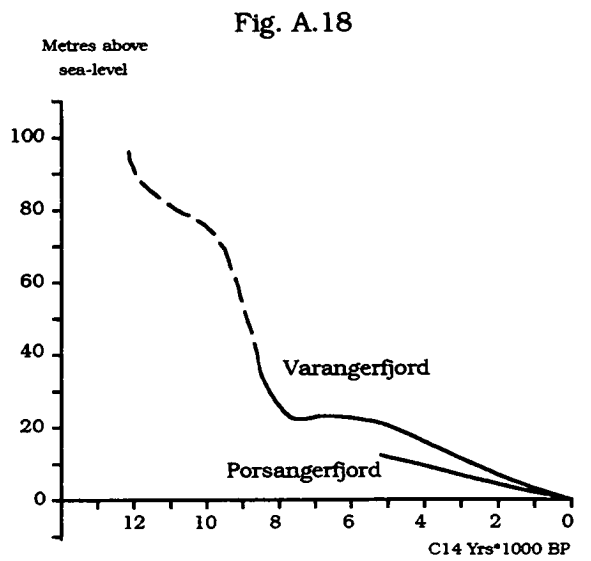
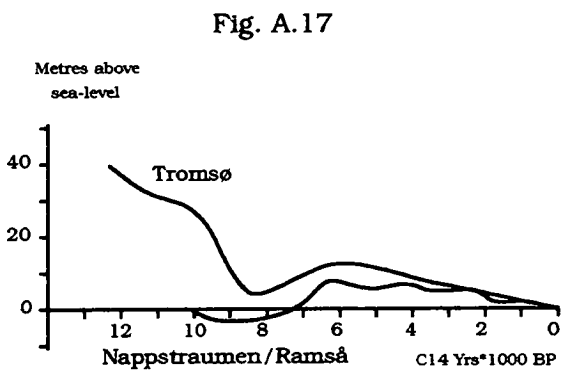
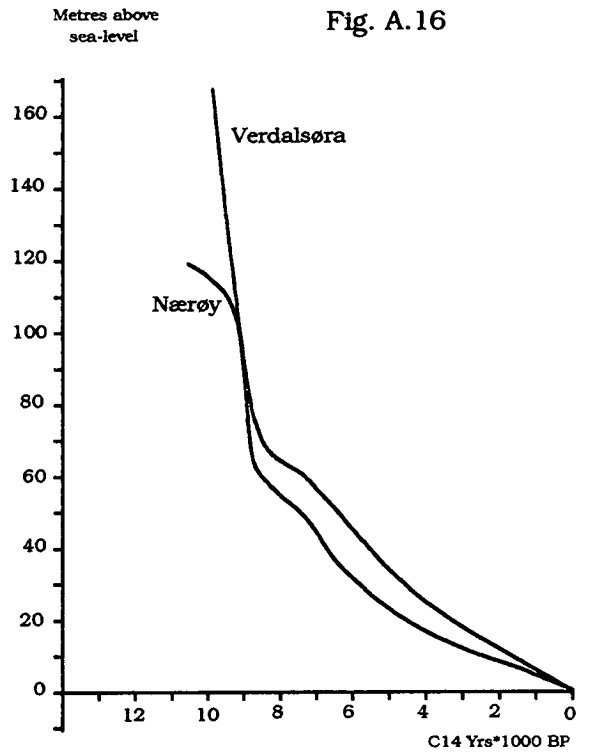
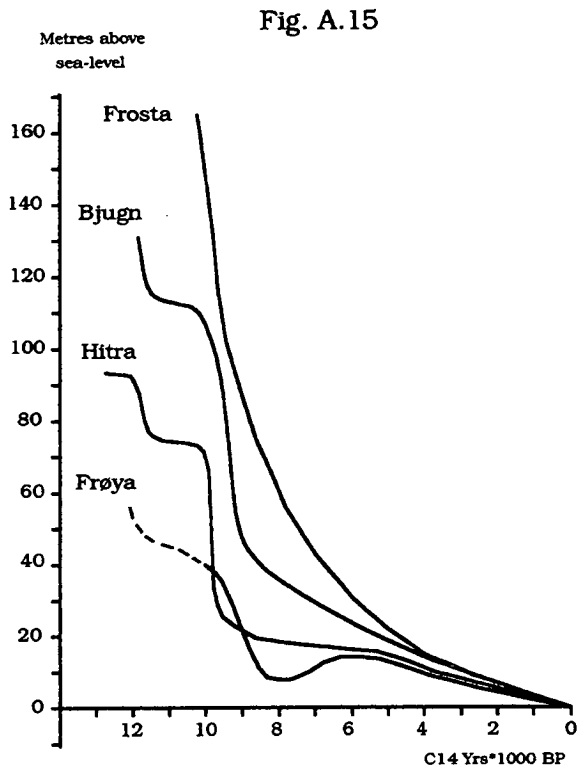


**Fig. A.3** Location map of relative sea-level curves

Porsangerfjord (Donner et al., 1977), Varangerfjord (Donner et al., 1977), Tromsø (Hald & Vorren, 1983), Ramså (Møller, 1986), Nappstraumen (Møller, 1984), Nærøy (Ramfjord, 1982), Verdalesøra (Sveian & Olsen, 1984), Frosta (Kjemperud, 1981), Bjugn (Kjemperud, 1986), Frøya (Kjemperud, 1986), Hitra (Kjemperud, 1986), Stette (Svendsen & Mangerud, 1987), Sula (Lie et al., 1983), Leinøy (Svendsen, 1985), Borgundvåg (Longva et al., 1983), Hordaland (Kaland, 1984), Sotra (Krzywinski & Stabell, 1978), Bømlo (Fægri, 1944), Yrkje (Anundsen, 1980), Nord-Jæren (Thomsen, 1981), Kragero (Stabell, 1980), S. Vestfold (Henningsmoen, 1979), Oslo (Hafsten, 1956), Ski (Sørensen, 1979), S. Østfold (Danielsen, 1970), Billingen (Björck & Digerfeldt, 1986), Hunneberg (Björck & Digerfeldt, 1982), Göteborg (Bergsten & Dennegård, 1988), Sandsjöbacka (Pässe, 1987), Skåne (Digerfeldt, 1975), Häno-Bay (Björck & Dennegård, 1988), Blekinge (Björck, 1979), Oskarshamn (Svensson, 1985), Stockholm (Åse & Bergström, 1982), Västernorrland (Müller & Robertsson, 1979), Peräpohjola (Saarnisto, 1981), Lauhanvuori (Salomaa, 1982), Turku (Glückert, 1976), Espoo (Hyvarinen, 1980), Helsinki (Hyvarinen, 1980), Porvoo (Eronen, 1983), Hyvinkää (Synge, 1982), St Petersburg (Dolukhanov, 1979), Köpu (Kessel & Raukas, 1979), Tallinn (Kessel & Raukas, 1979), Narva (Kessel & Raukas, 1979), Palanga (Gudelis, 1979), N Vendsyssel (Petersen, 1984), Store Belt (Krog, 1960), Prästö (Mikkelsen, 1949), Kiel (Winn et al., 1986), Gröningen (Jelgersma, 1980).







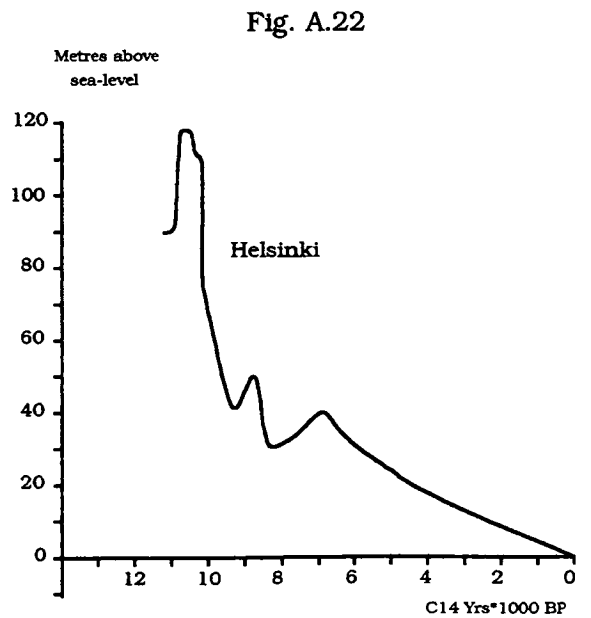
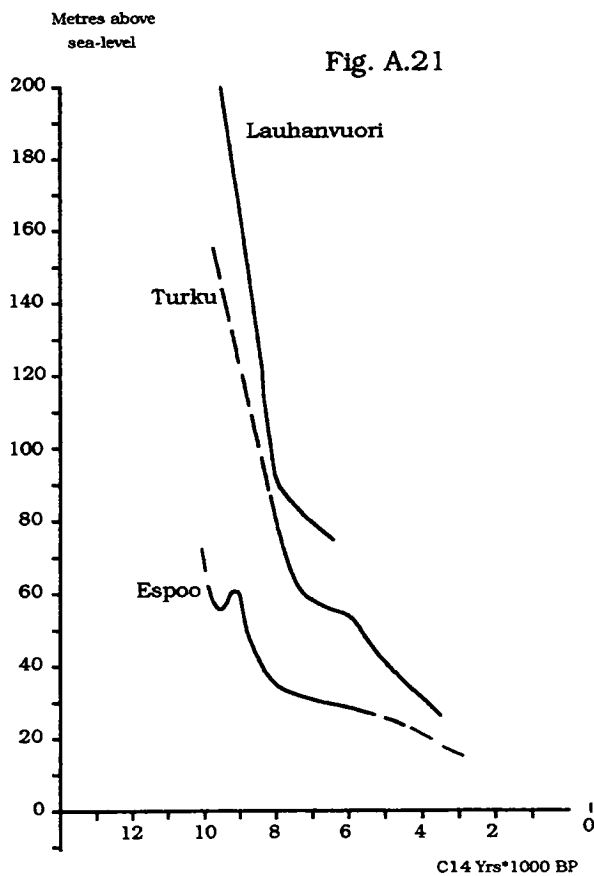
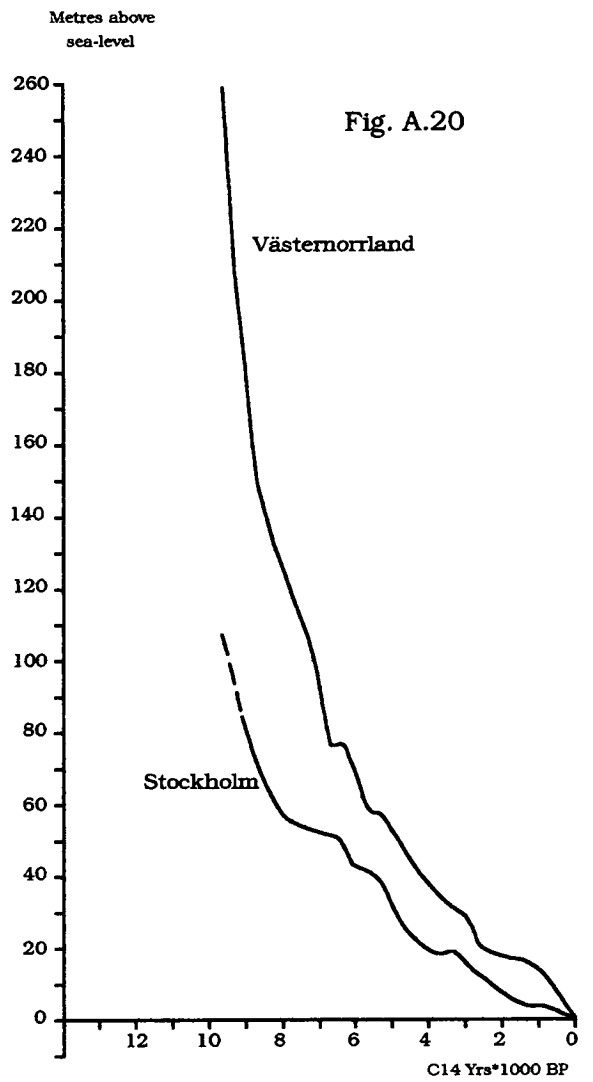
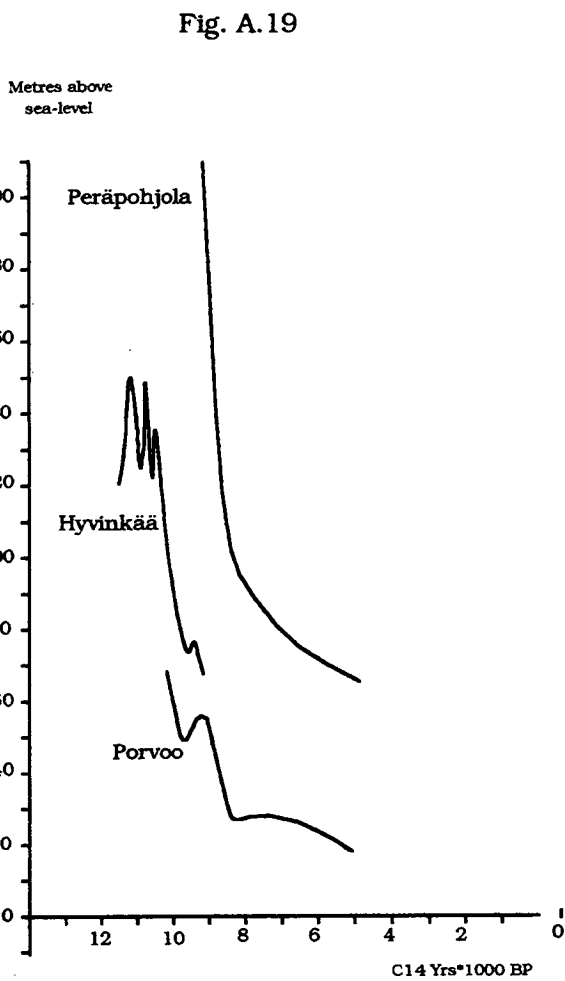


Fig. A.23

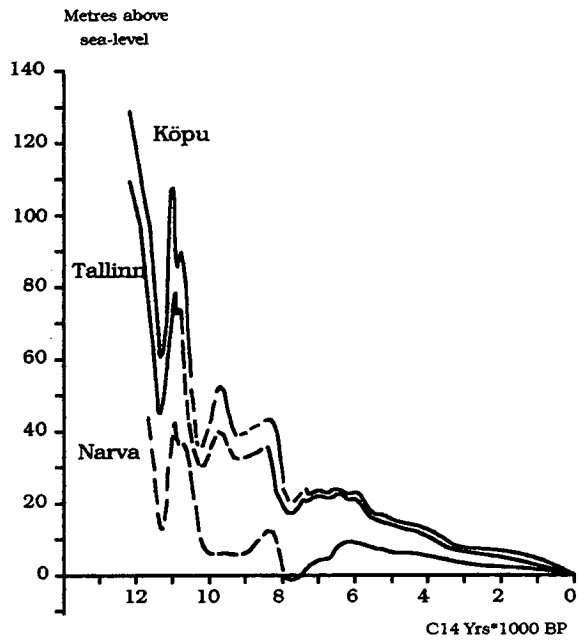


Fig. A.24

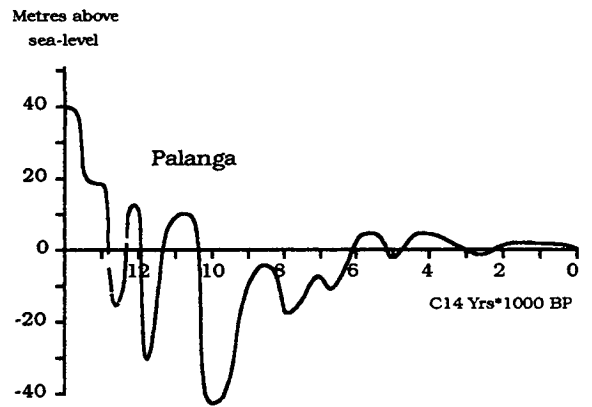
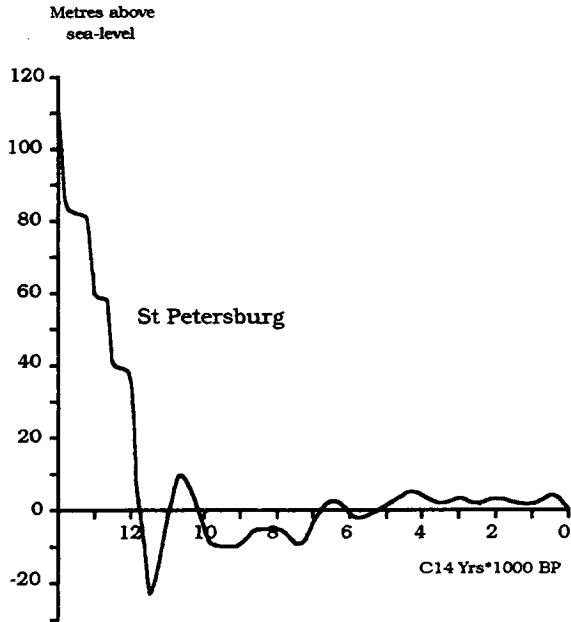


Fig. A.25



## **Appendix B**

**First- and second-order interpretations  
of Landsat MSS satellite images**

## **Appendix B**

### **First- and second-order interpretations of Landsat MSS satellite images**

In Appendix B the first- and second-order interpretations of all the Landsat MSS images are shown. Some of the satellite images have been shown already (Chapter 5), but they are included for the sake of clarity. The interpreted Landsat mosaics have been shown and described in the thesis itself and are not included. The Landsat TM images cover the same area as MSS sheets F15, F17, F18 and F19. The Landsat TM and the aerial photograph interpretations are not available in a format comparable to the Landsat MSS interpretations. Therefore, it was decided not to include them in this Appendix.

## List of figures

B.1	Legend used for interpretation of satellite images	200
B.2	Locations of Landsat MSS and TM images in Finland	201
B.3	First- and second-order interpretation of sheet F2	202
B.4	First- and second-order interpretation of sheet F3	203
B.5	First- and second-order interpretation of sheet F4	204
B.6	First- and second-order interpretation of sheet F6	205
B.7	First- and second-order interpretation of sheet F7	206
B.8	First- and second-order interpretation of sheet F8	207
B.9	First- and second-order interpretation of sheet F10	208
B.10	First- and second-order interpretation of sheet F10b	209
B.11	First- and second-order interpretation of sheet F11	210
B.12	First- and second-order interpretation of sheet F12	211
B.13	First- and second-order interpretation of sheet F13	212
B.14	First- and second-order interpretation of sheet F13b	213
B.15	First- and second-order interpretation of sheet F14	214
B.16	First- and second-order interpretation of sheet F15	215
B.17	First- and second-order interpretation of sheet F16	216
B.18	First- and second-order interpretation of sheet F17	217
B.19	First- and second-order interpretation of sheet F18	218
B.20	First- and second-order interpretation of sheet F19	219
B.21	First- and second-order interpretation of sheet F19b	220
B.22	First- and second-order interpretation of sheet F20	221
B.23	First- and second-order interpretation of sheet F21	222
B.24	First- and second-order interpretation of sheet F22	223
B.25	First- and second-order interpretation of sheet F23	224
B.26	First- and second-order interpretation of sheet F25	225
B.27	First- and second-order interpretation of sheet F26	226
B.28	First- and second-order interpretation of sheet F27	227
B.29	First- and second-order interpretation of sheet K1	228
B.30	First- and second-order interpretation of sheet K2	229
B.31	First- and second-order interpretation of sheet K3	230
B.32	First- and second-order interpretation of sheet K4	231

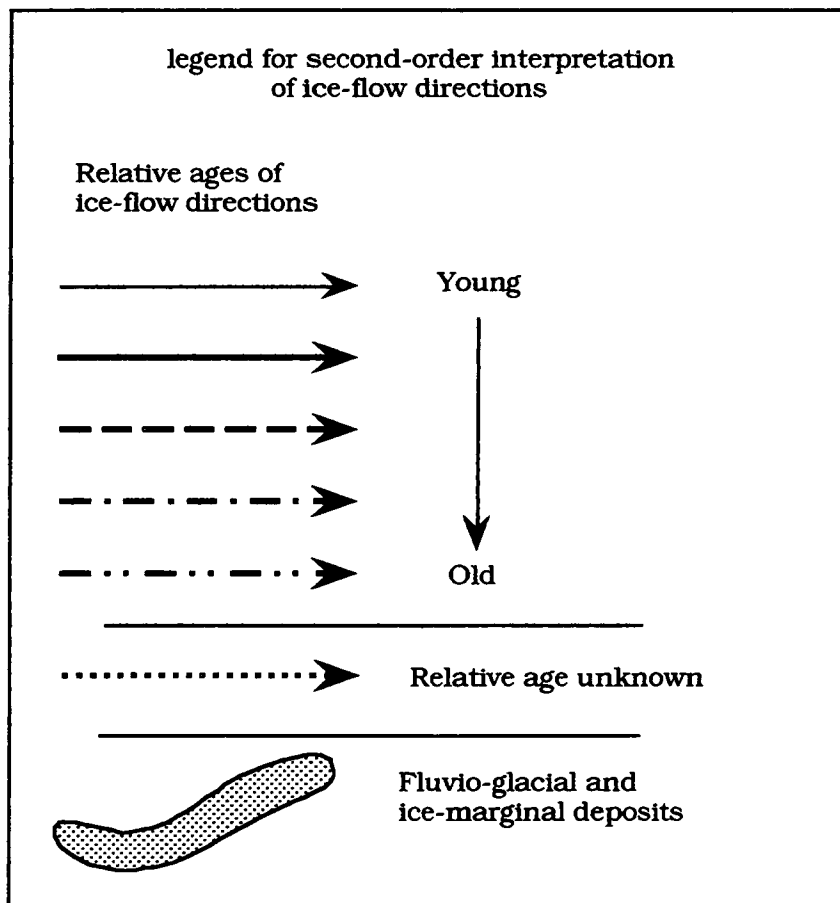
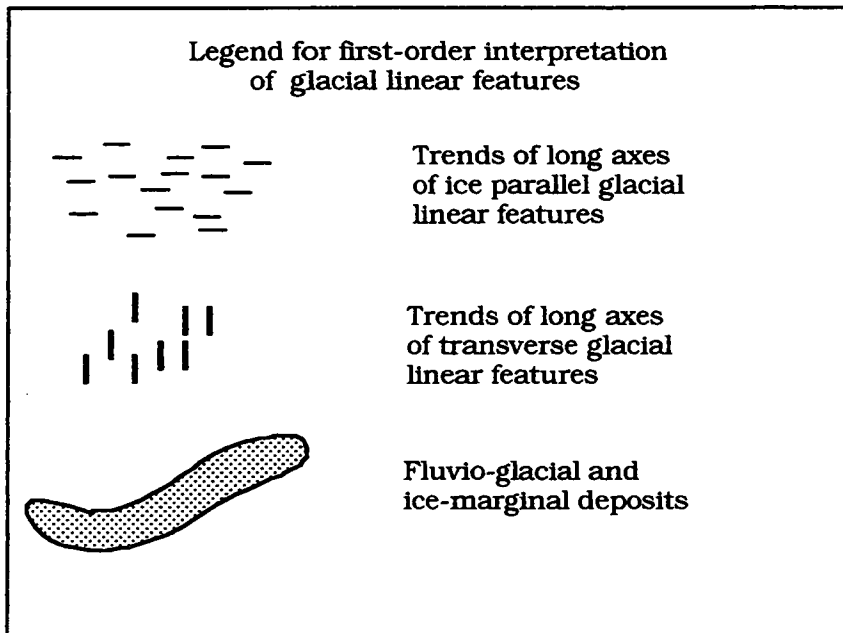


Fig. B.1 Legend used for interpretation of satellite images.

Fig. B.2 Locations of Landsat MSS and TM images in Finland, Russian Karelia and the Kola peninsula.

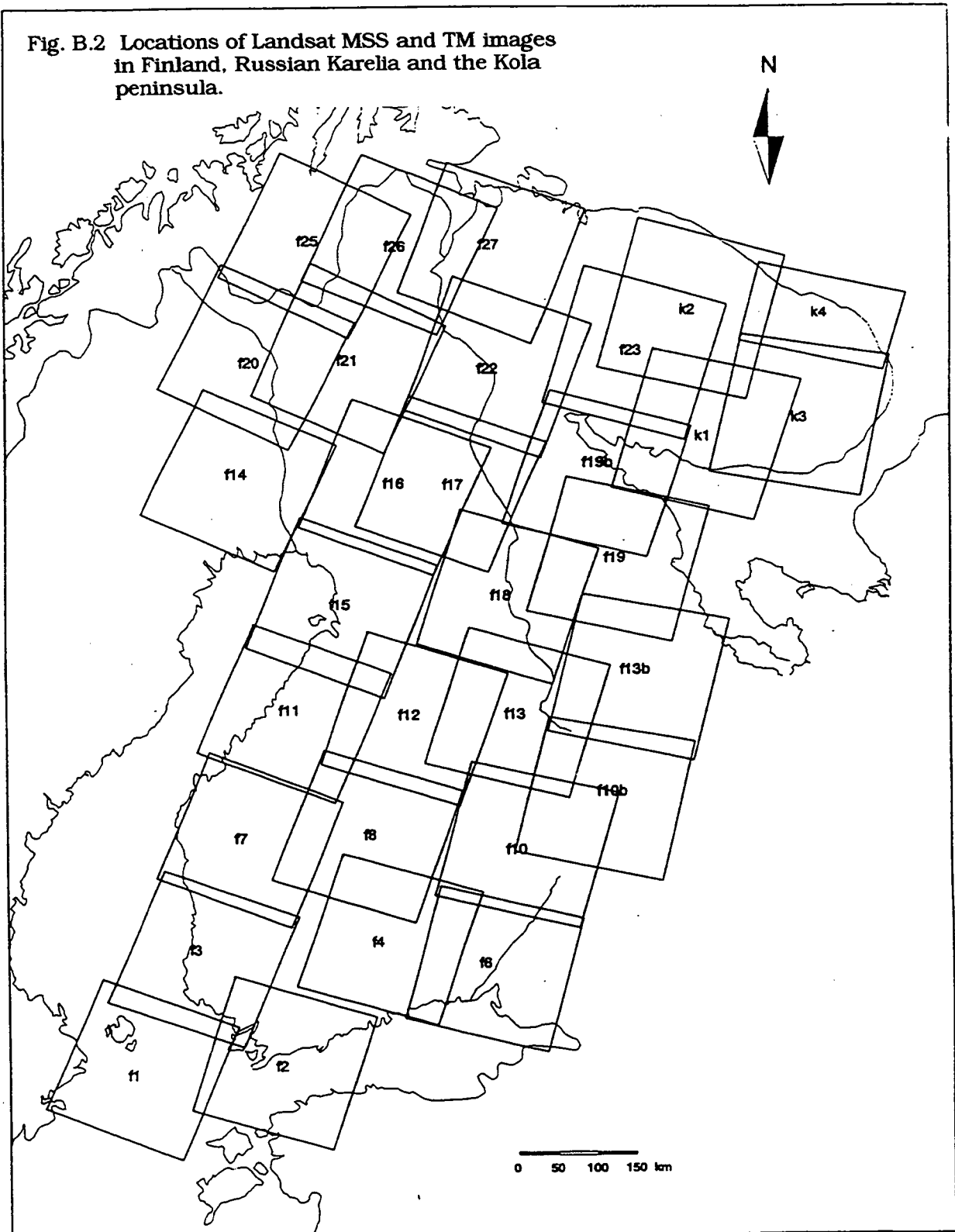


Fig. B.3

Interpretation of glacial linear features and iceflow directions (Landsat image F 2)

Scale (Km) 0 40

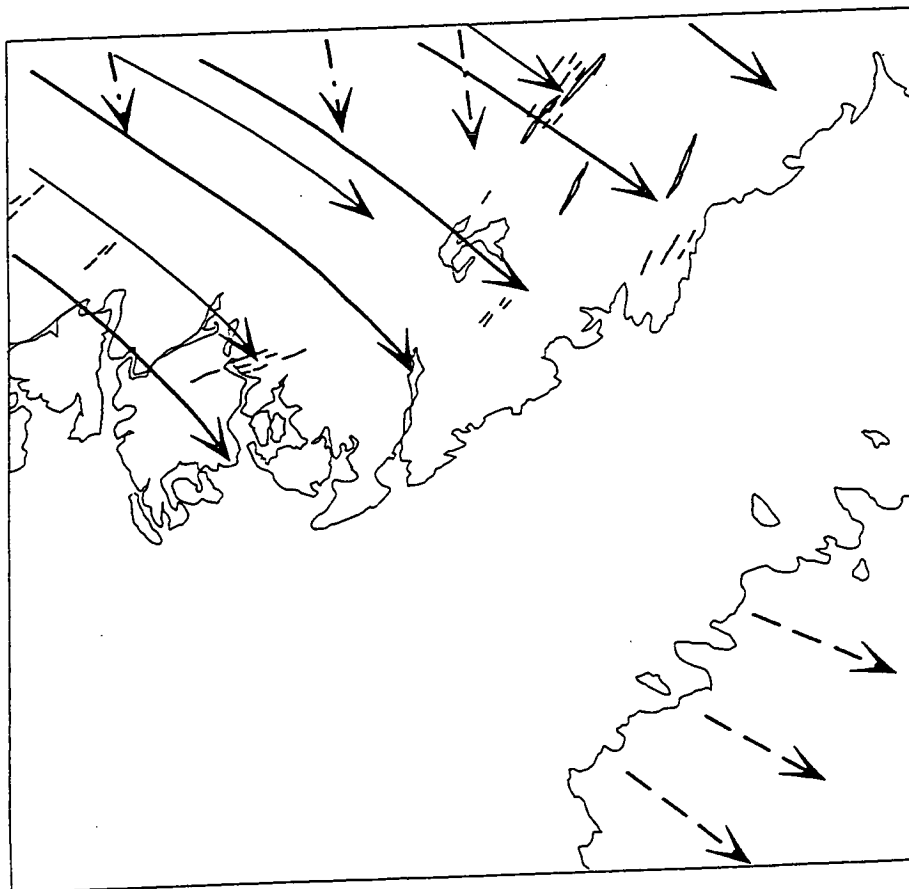
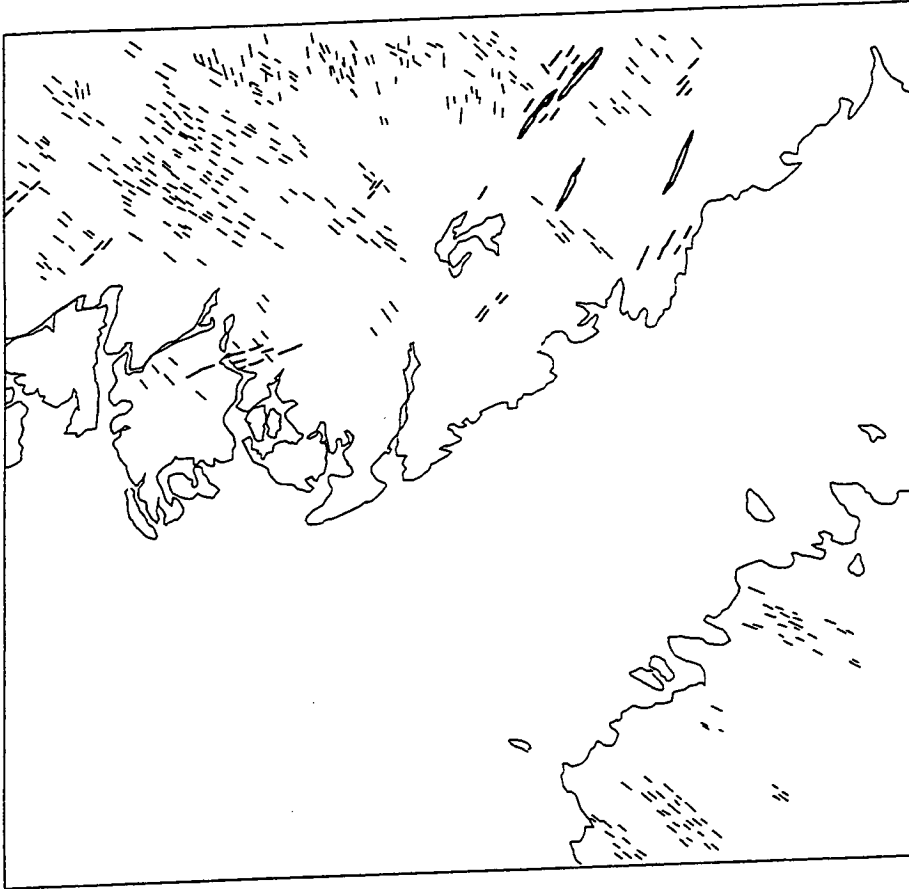


Fig. B.4 Interpretation of glacial linear features and iceflow directions (Landsat image F3)

Scale (Km) 0 40

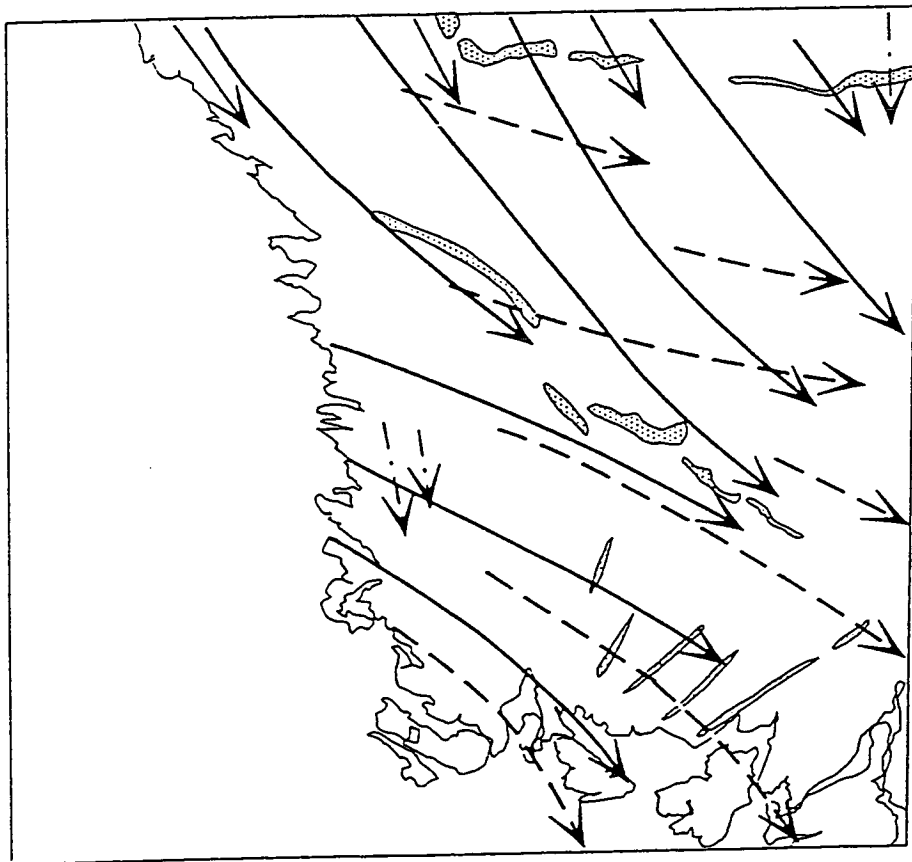
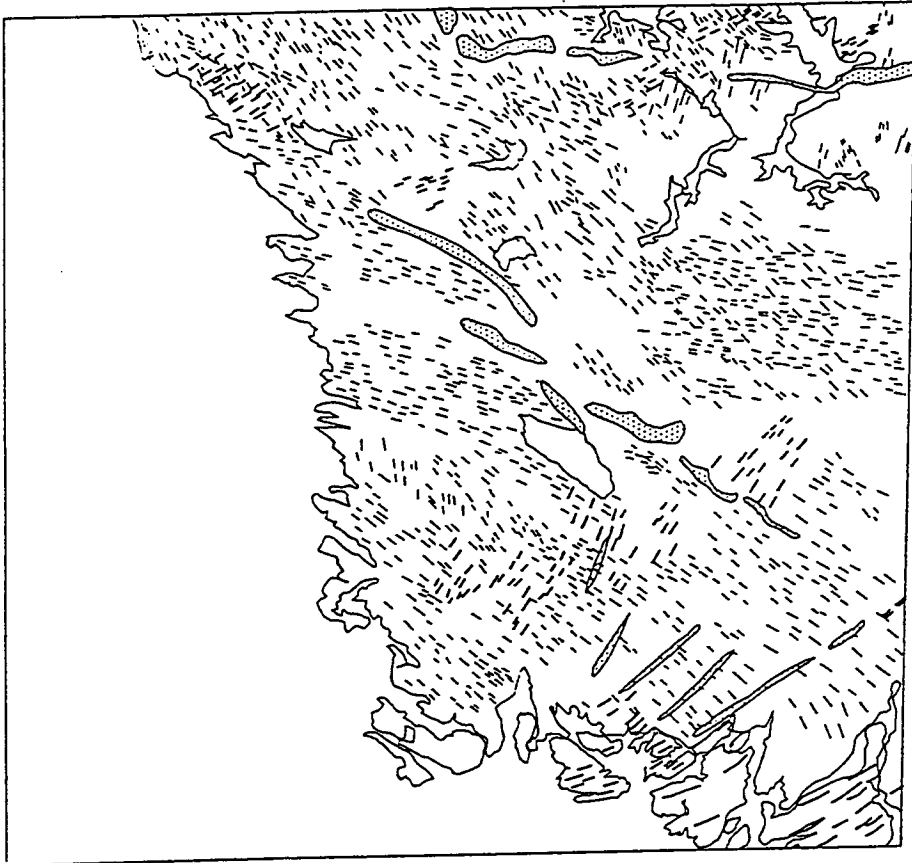


Fig. B.5 Interpretation of glacial linear features and iceflow directions (Landsat image F4)

Scale (Km) 0 40

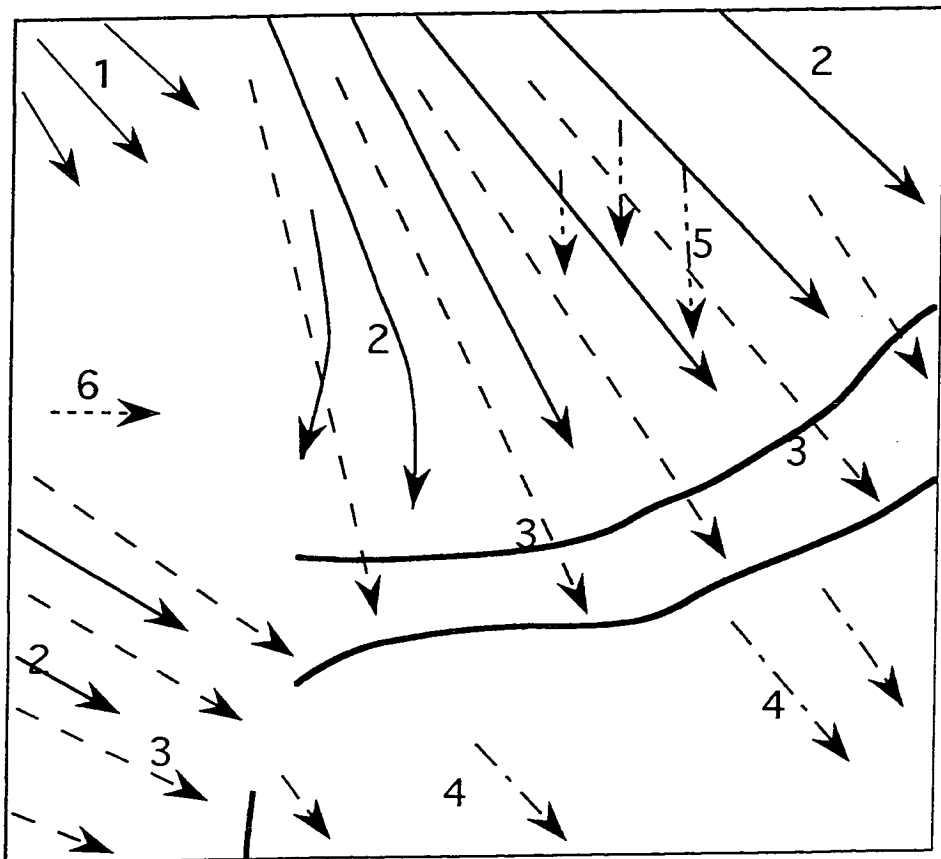
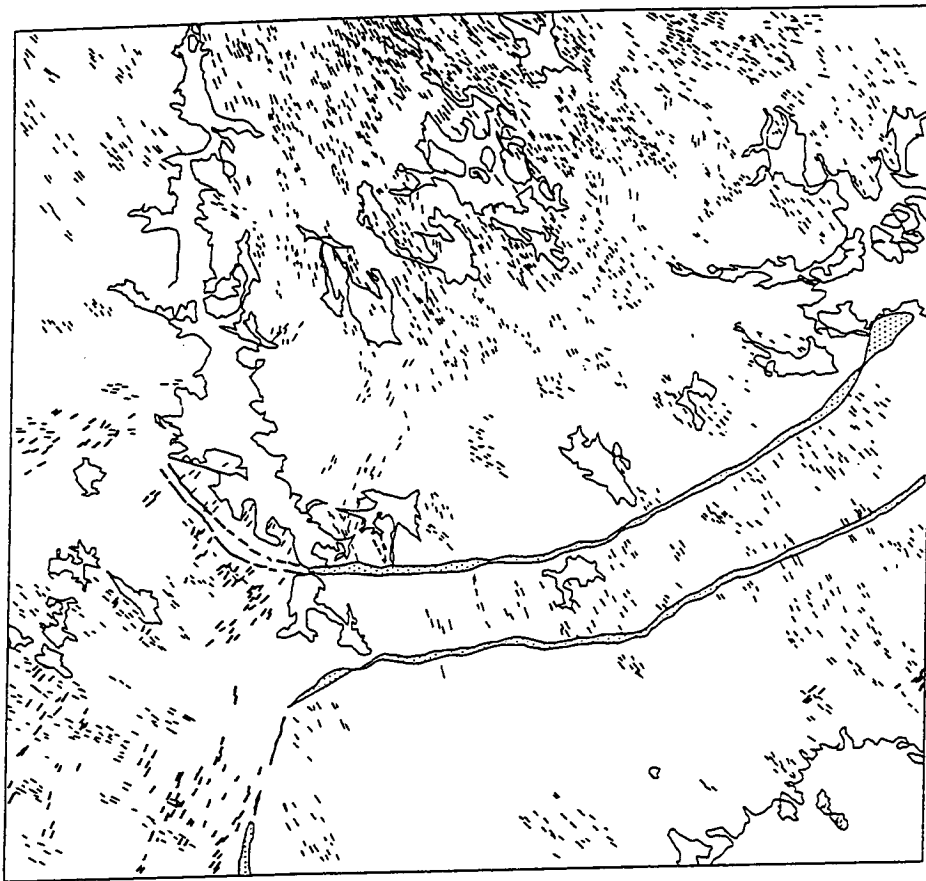


Fig. B.6 Interpretation of glacial linear features and iceflow directions (Landsat image F6)

Scale (Km) 0 40

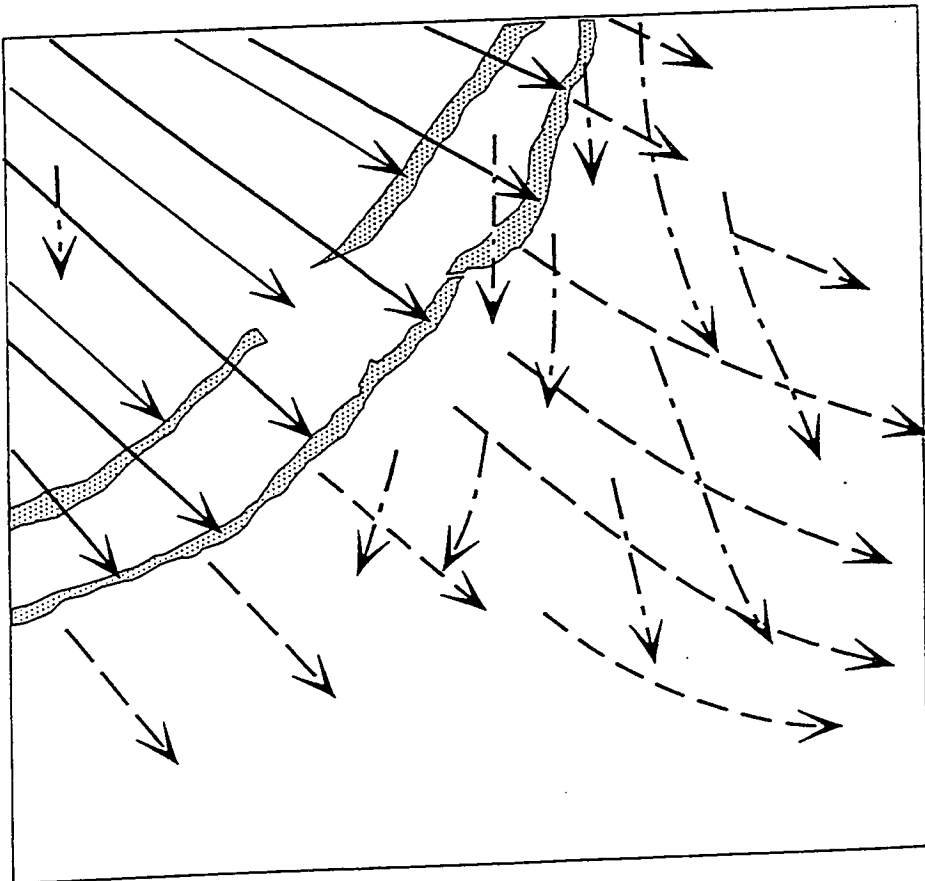
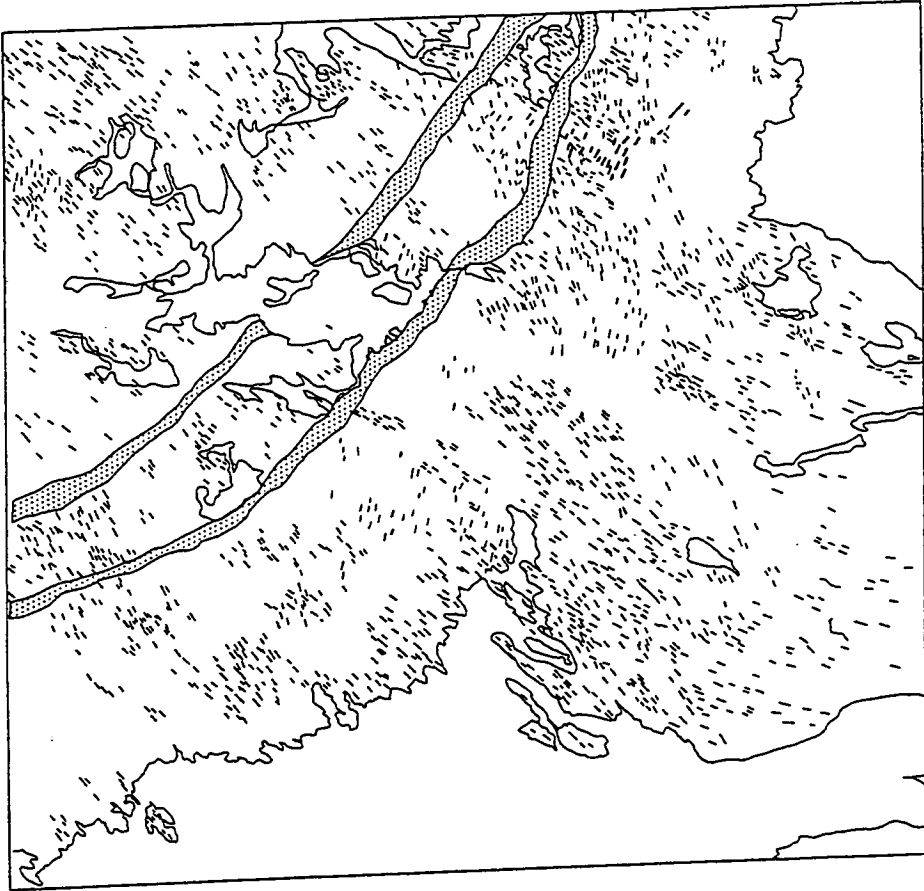


Fig. B.7 Interpretation of glacial linear features and iceflow directions (Landsat image F7)

Scale (Km) 0 40

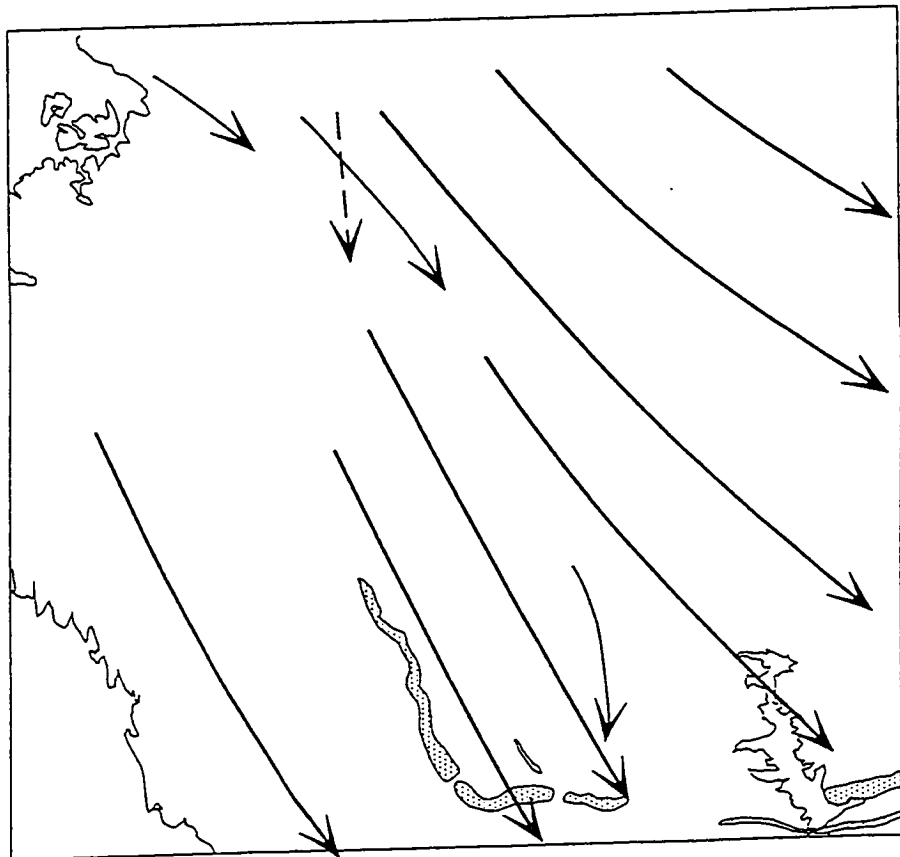
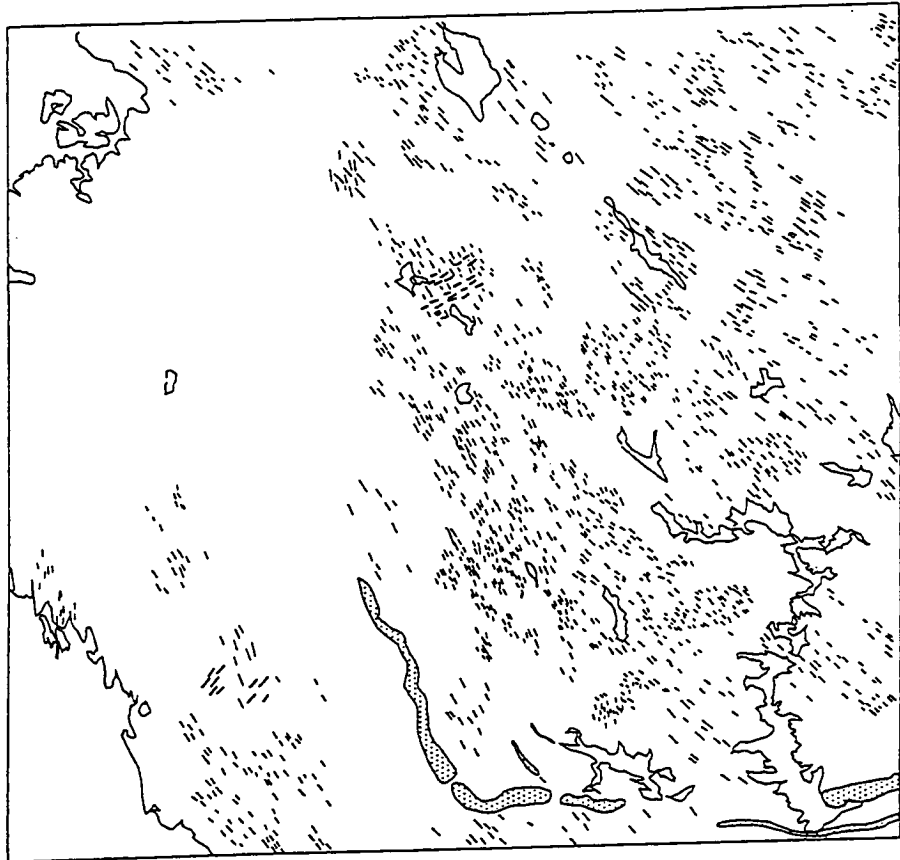


Fig. B.8 Interpretation of glacial linear features and iceflow directions (Landsat image F8)

Scale (Km) 0 40

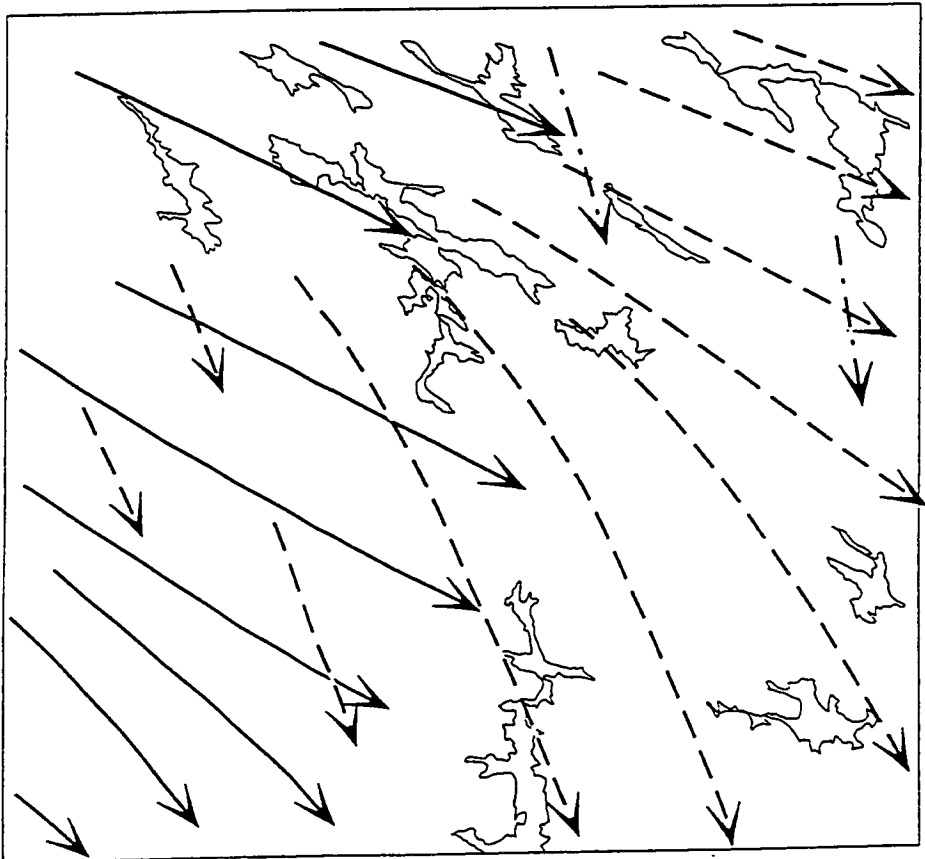
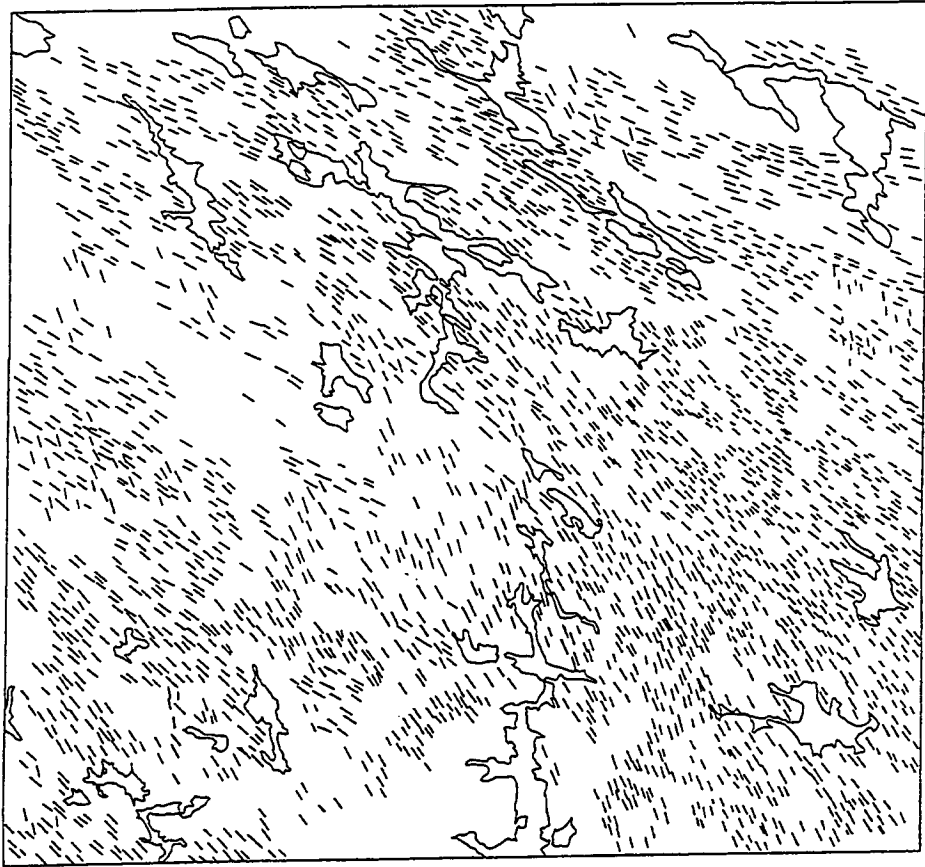
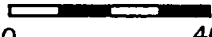


Fig. B.9 Interpretation of glacial linear features and iceflow directions (Landsat image F10)

Scale (Km)  0 40

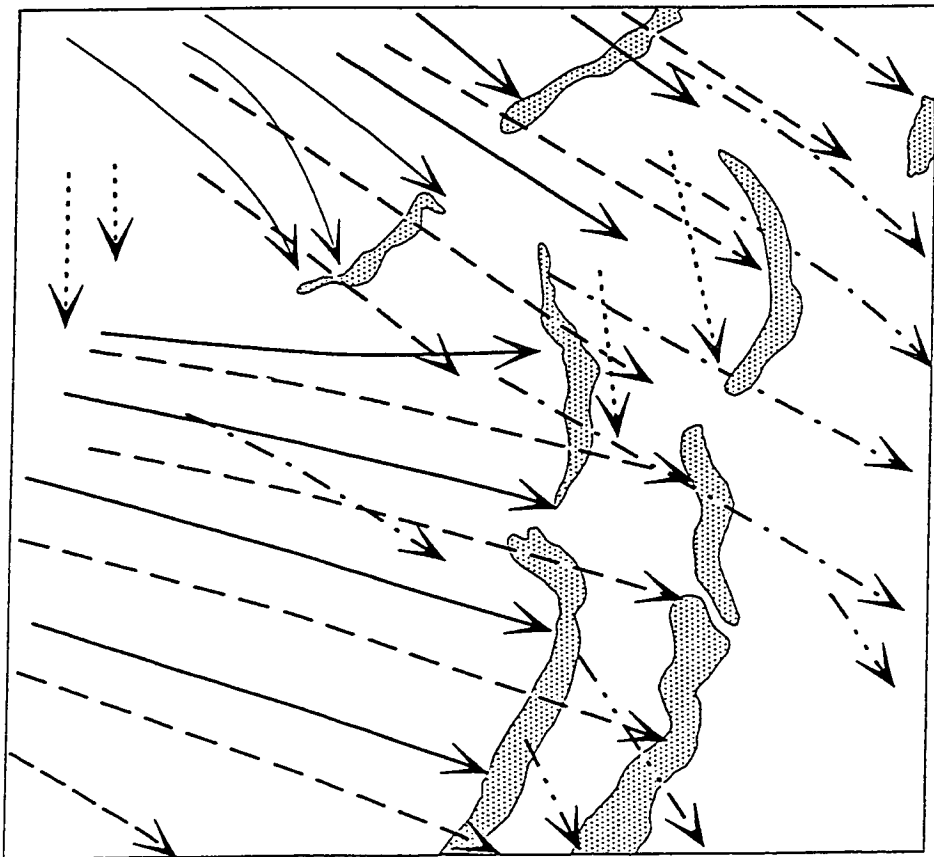
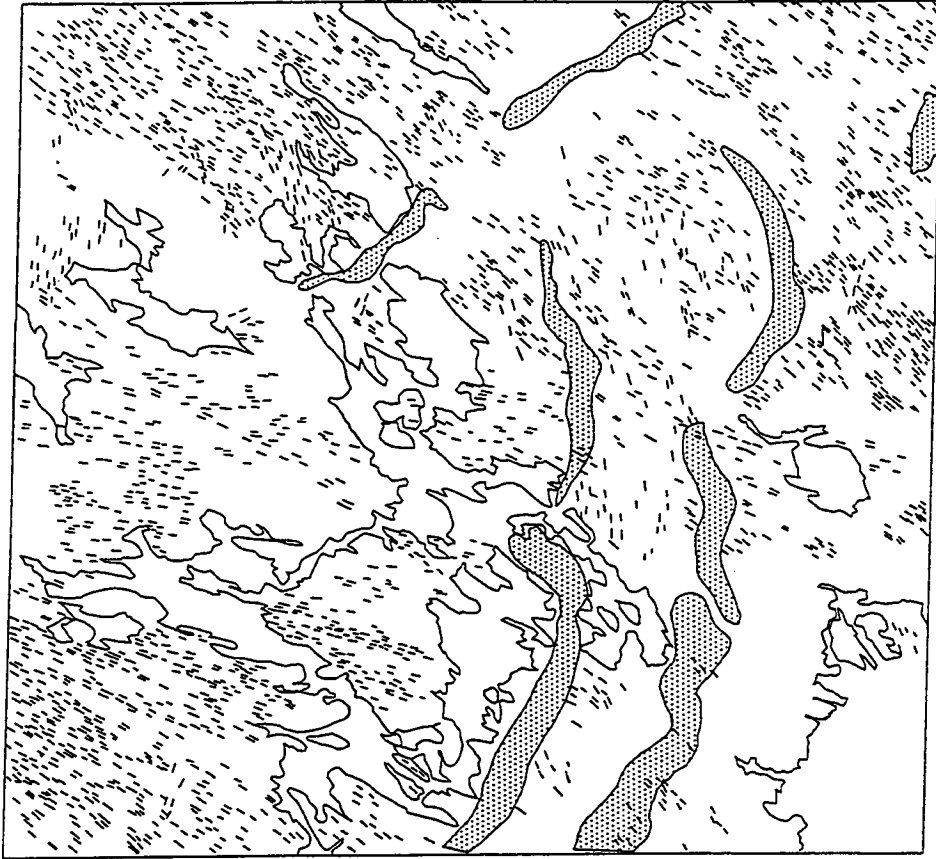


Fig. B.10 Interpretation of glacial linear features and iceflow directions (Landsat image F10b)

Scale (Km) 0 40

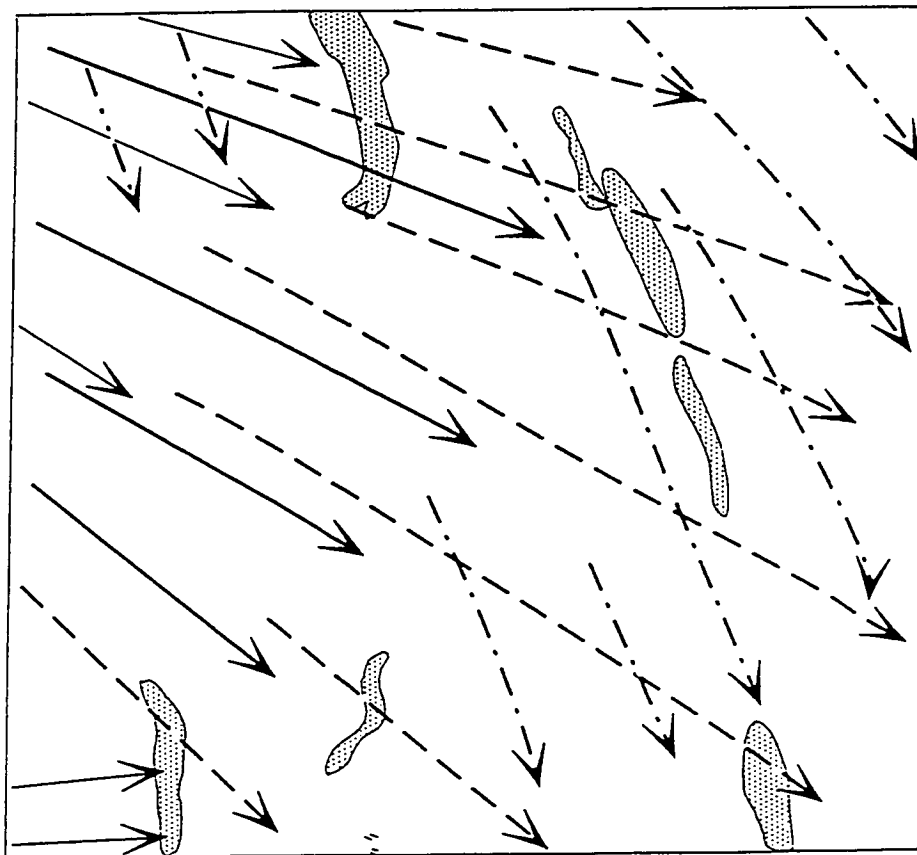



Fig. B.11 Interpretation of glacial linear features and iceflow directions (Landsat image F 1 1)

Scale (Km)  0 40

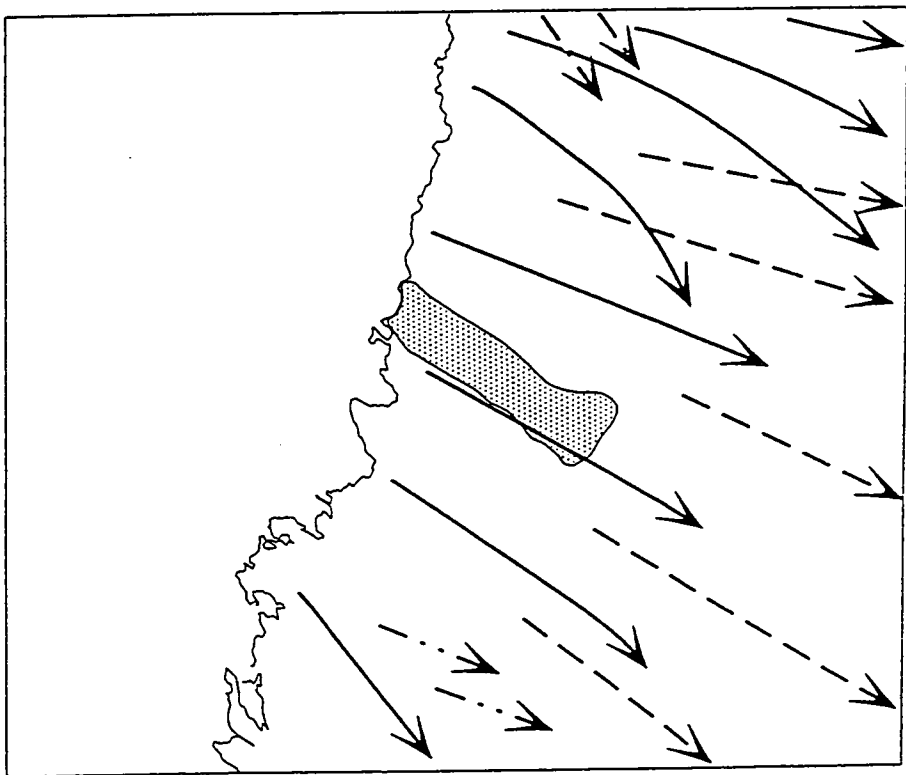
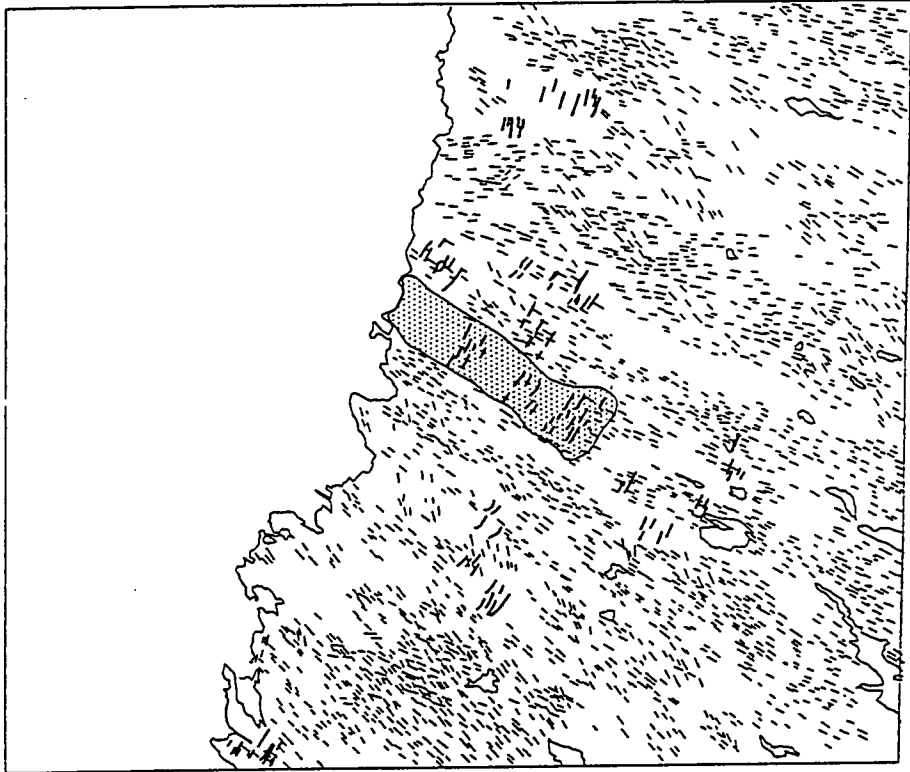


Fig. B.12 Interpretation of glacial linear features and iceflow directions (Landsat image F12)

Scale (Km) 0 40

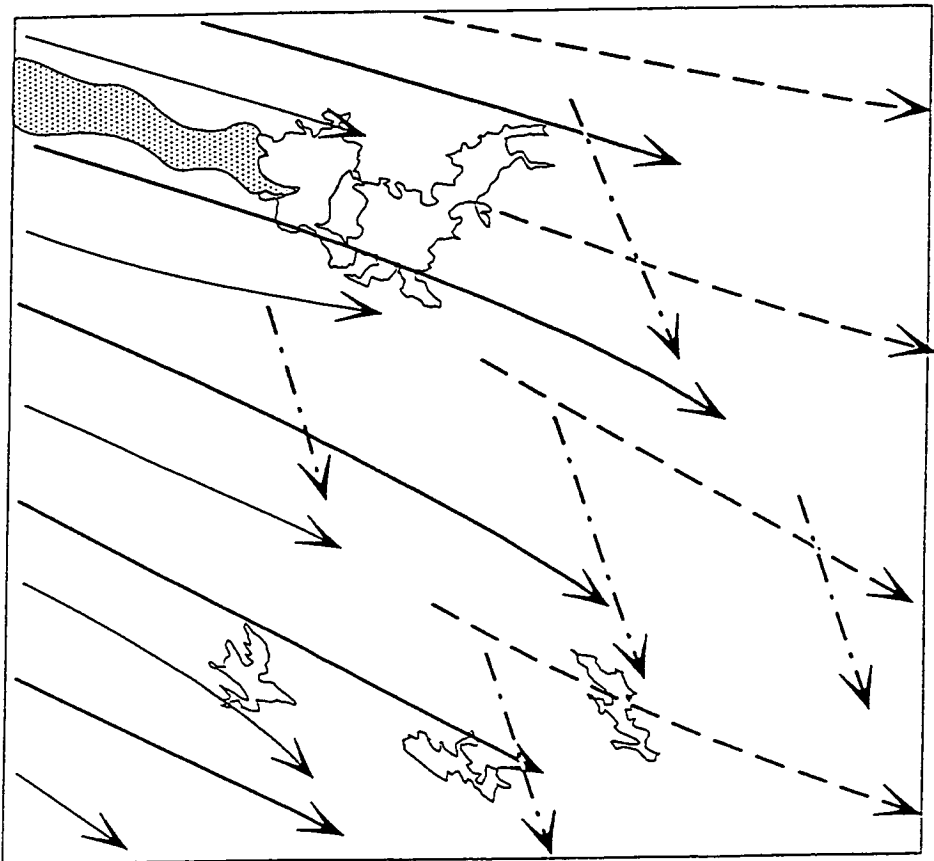
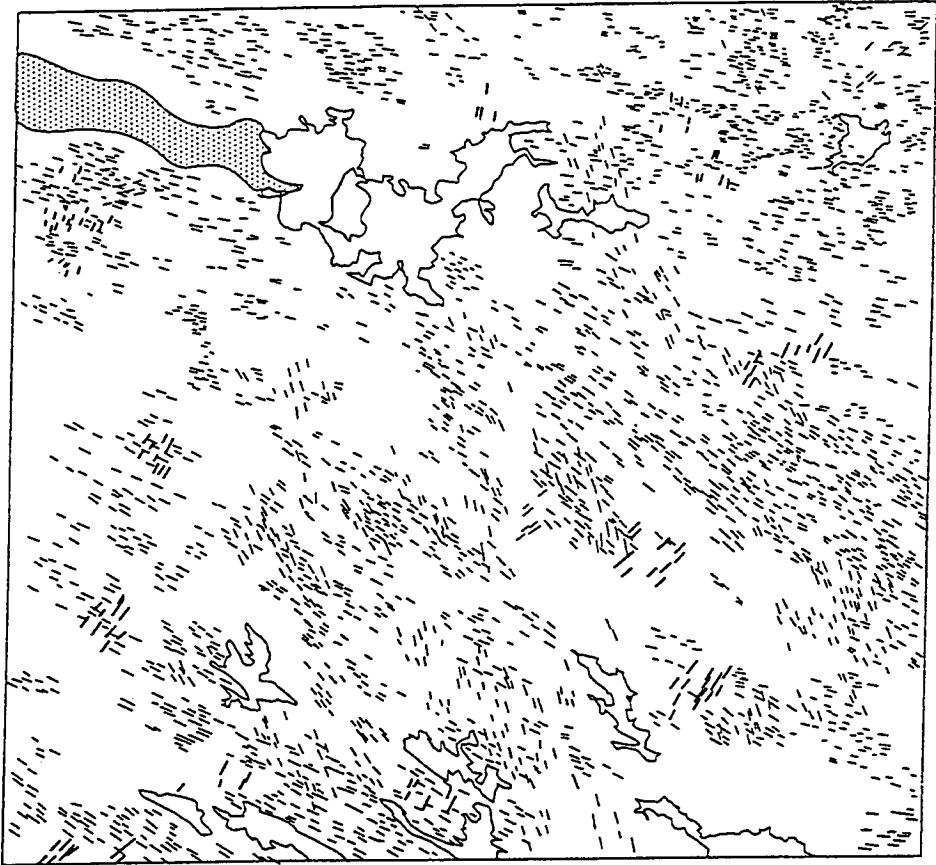


Fig. B.13 Interpretation of glacial linear features and iceflow directions (Landsat image F 13)

Scale (Km) 0 40

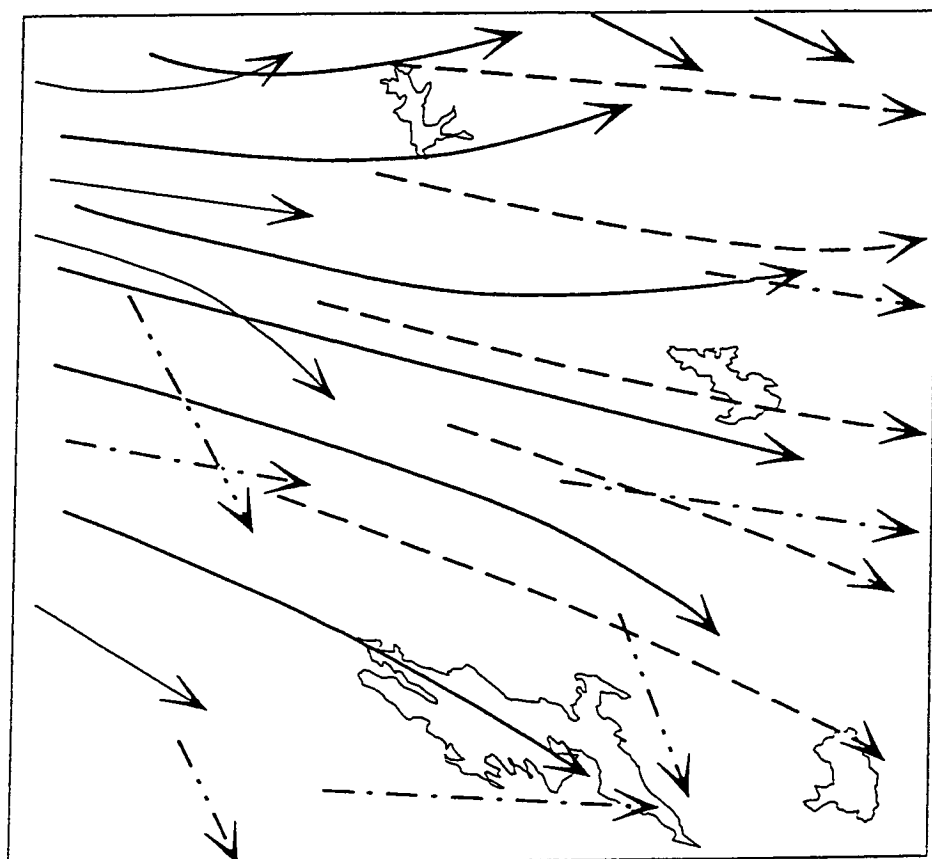
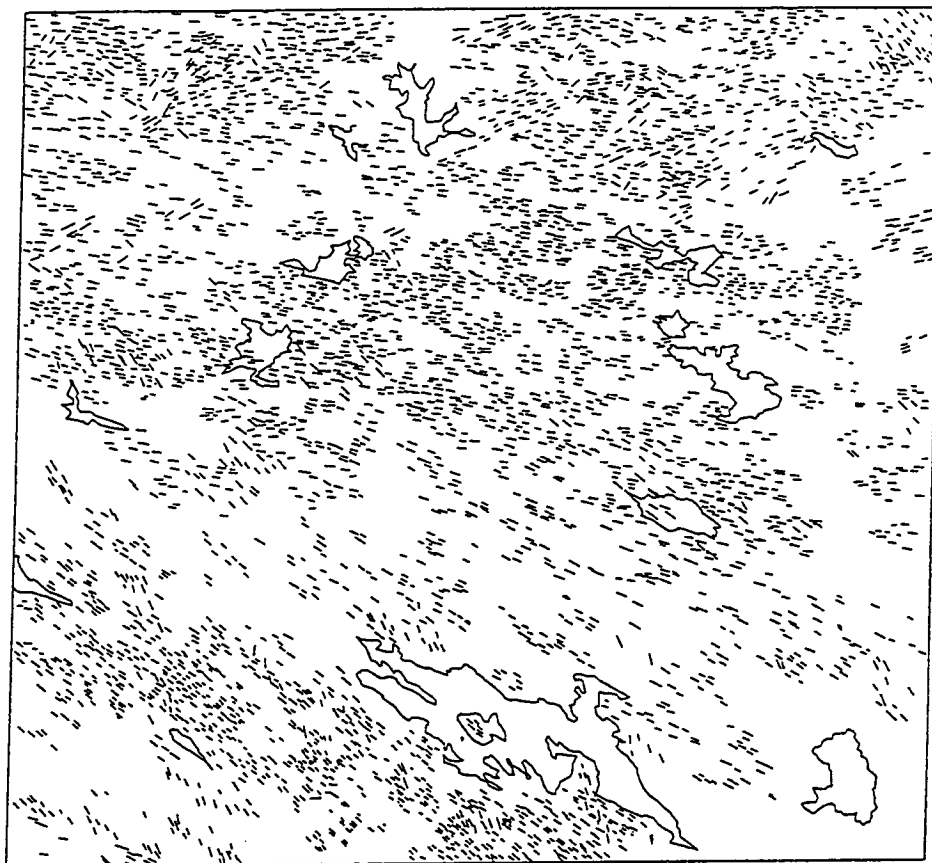


Fig. B.14 Interpretation of glacial linear features and iceflow directions (Landsat image F13b)

Scale (Km) 0 40

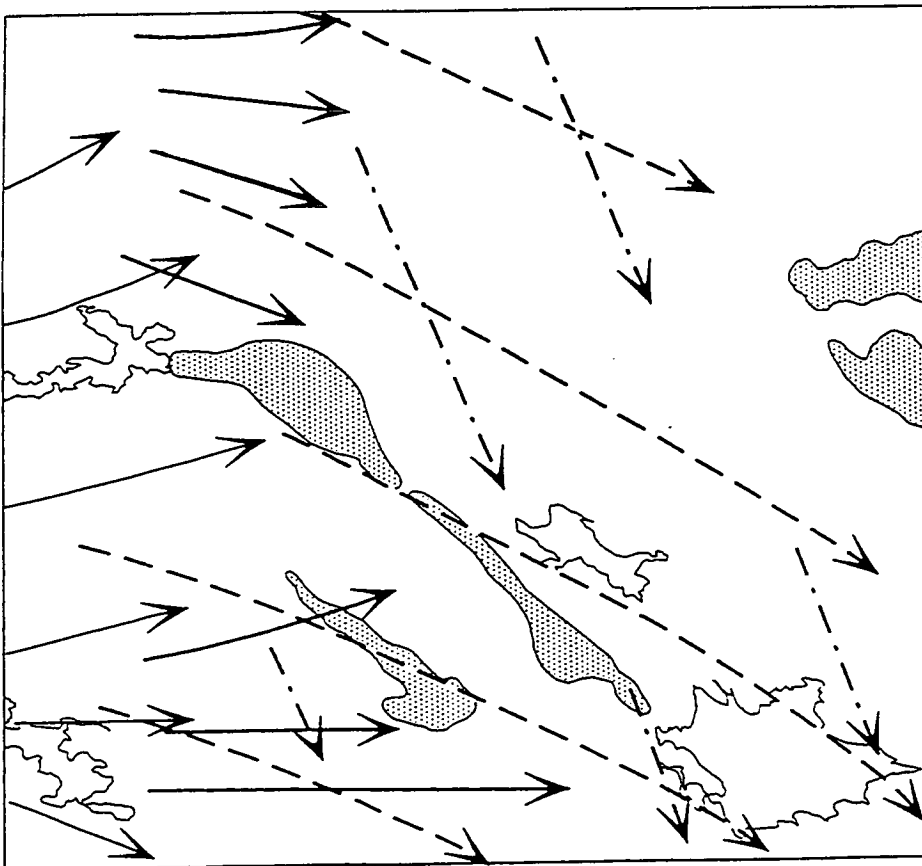
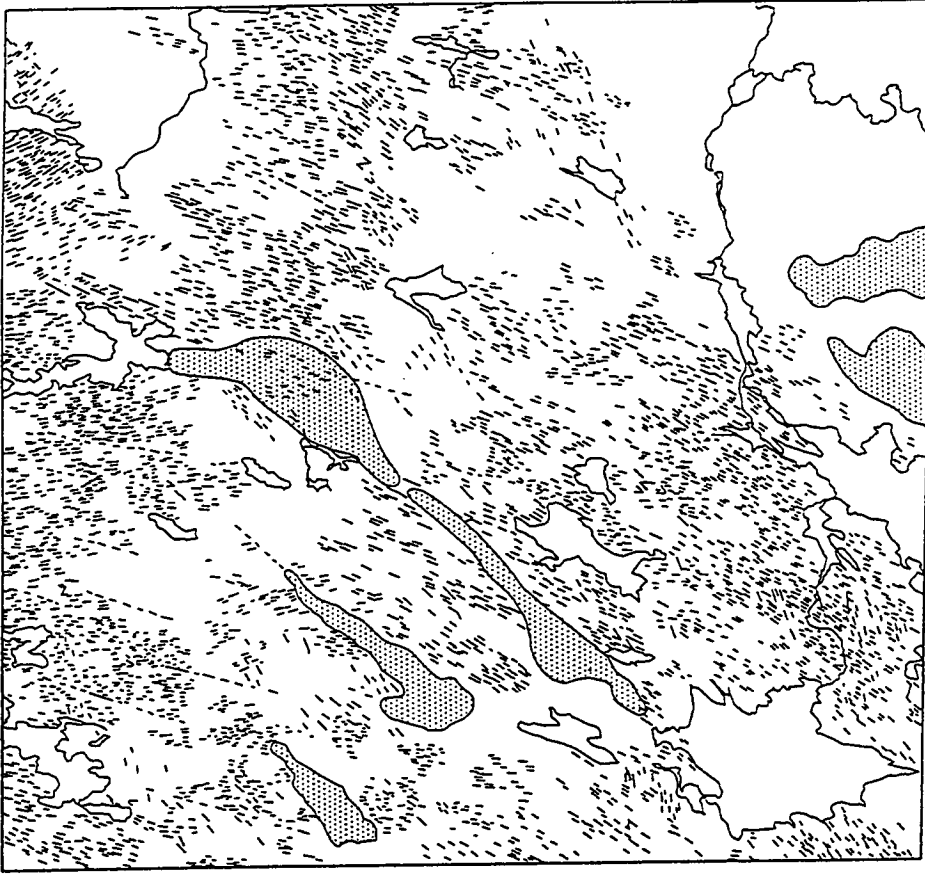


Fig. B.15 Interpretation of glacial linear features and iceflow directions (Landsat image F 1 4)

Scale (Km) 0 40

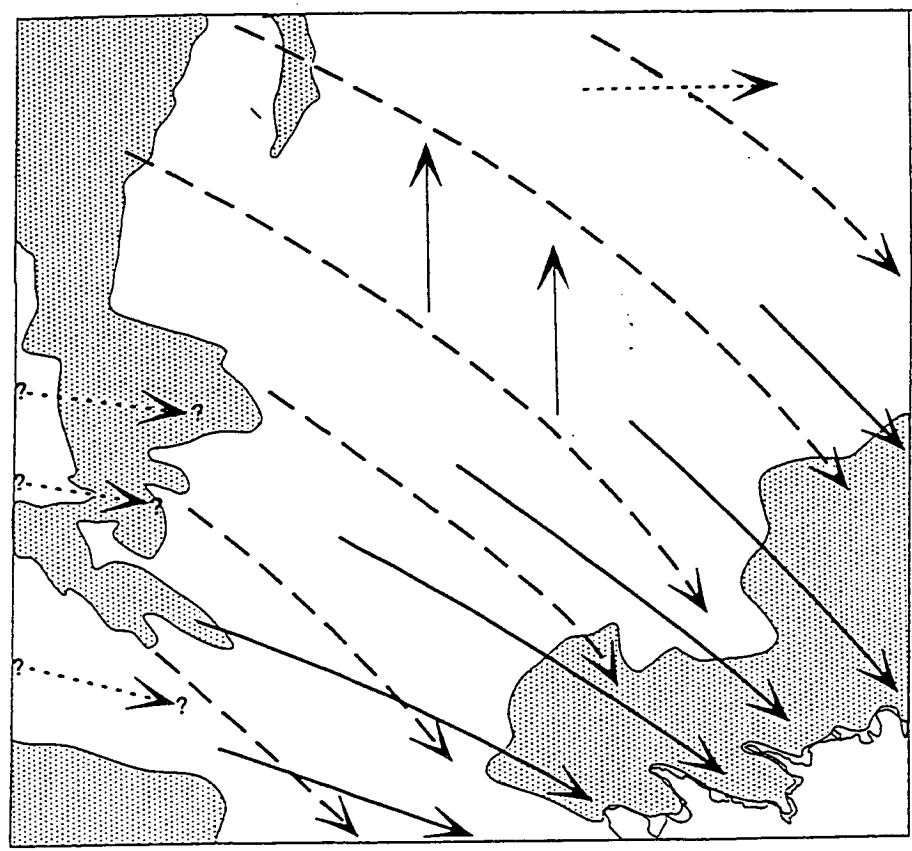


Fig. B.16 Interpretation of glacial linear features and iceflow directions (Landsat image F 1 5)

Scale (Km) 0 40

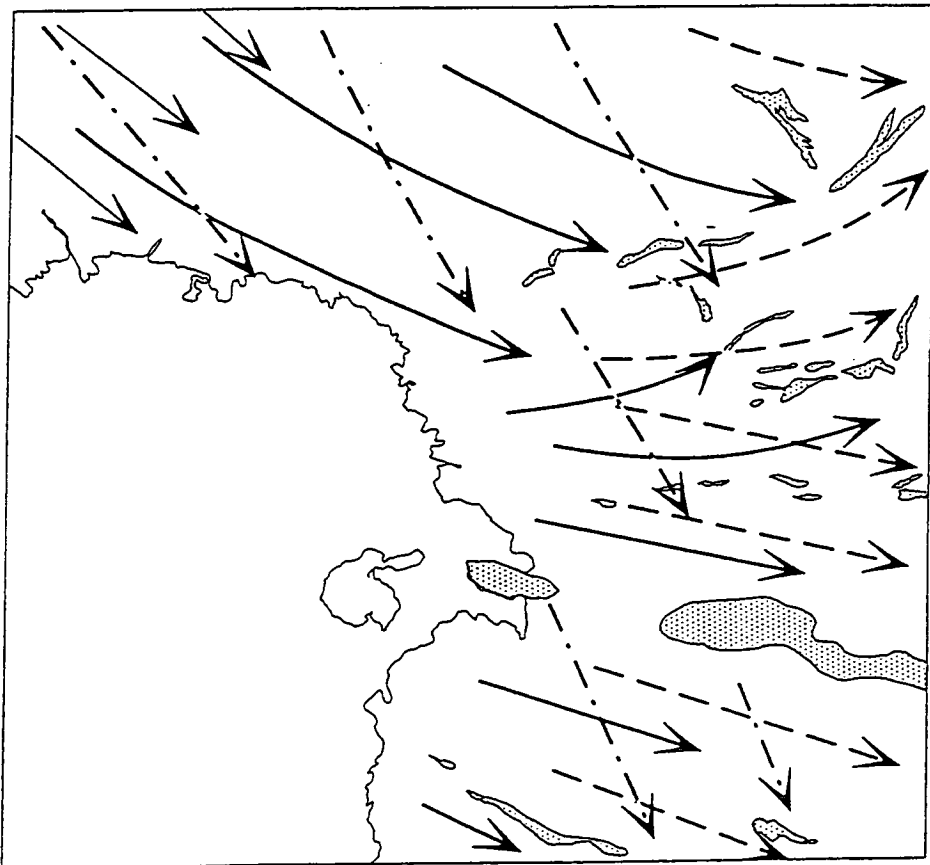


Fig. B.17 Interpretation of glacial linear features and iceflow directions (Landsat image F16)

Scale (Km) 0 40

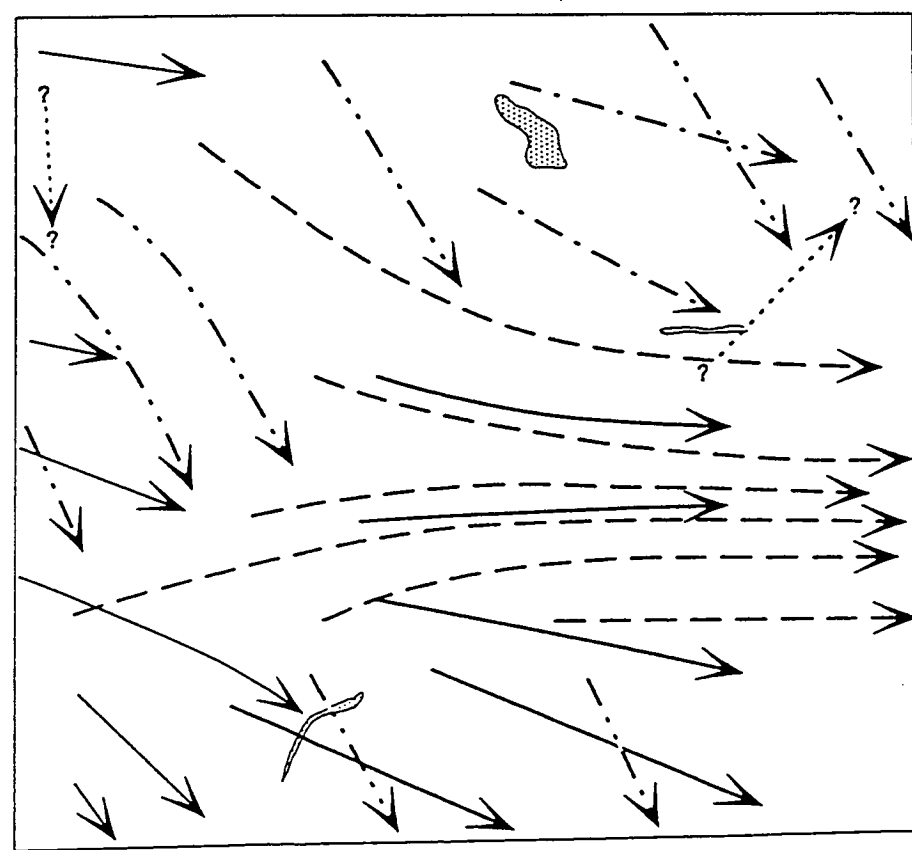
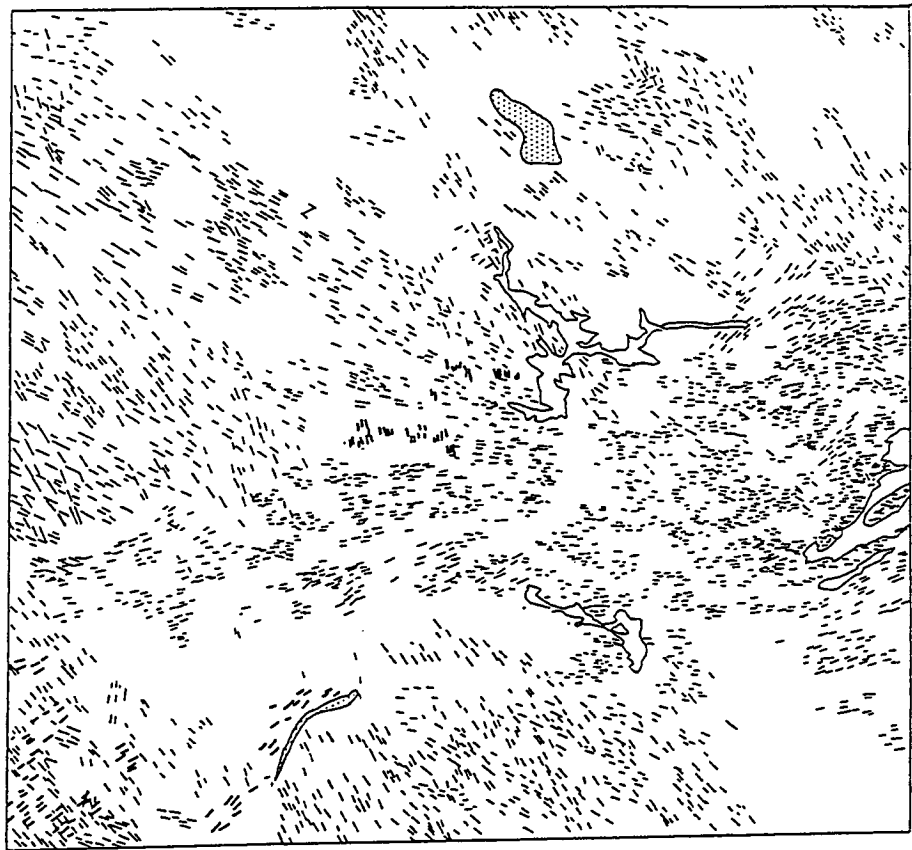


Fig. B.18 Interpretation of glacial linear features and iceflow directions (Landsat image F 17)

Scale (Km) 0 40

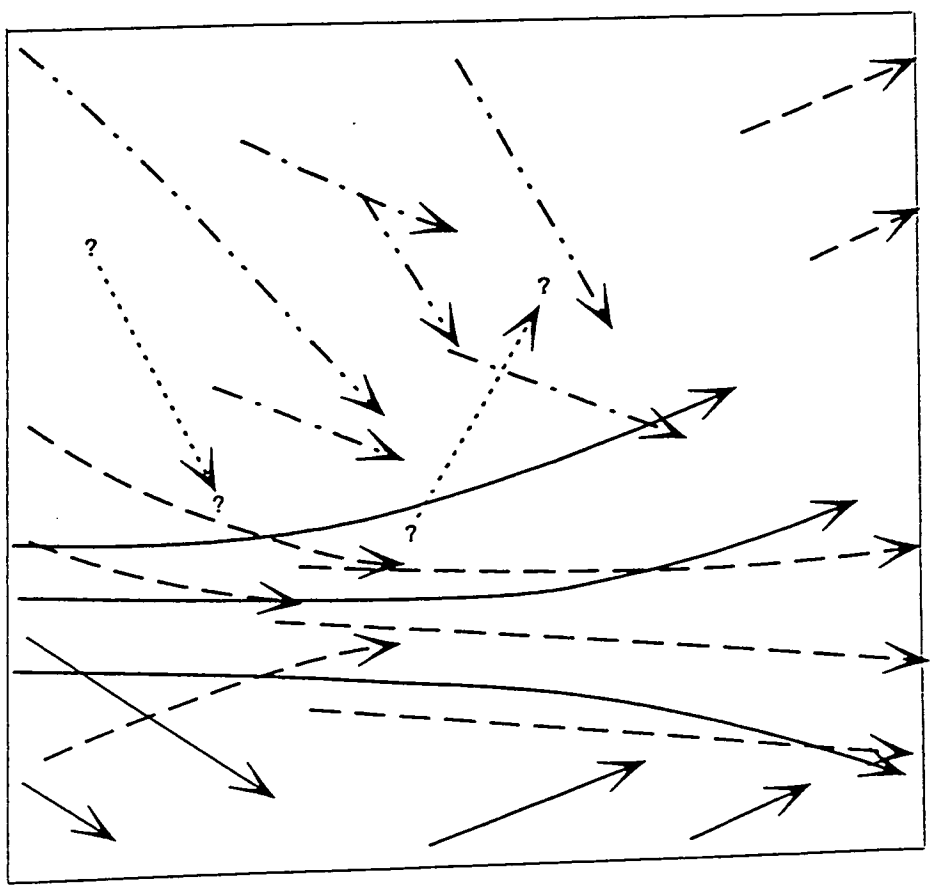
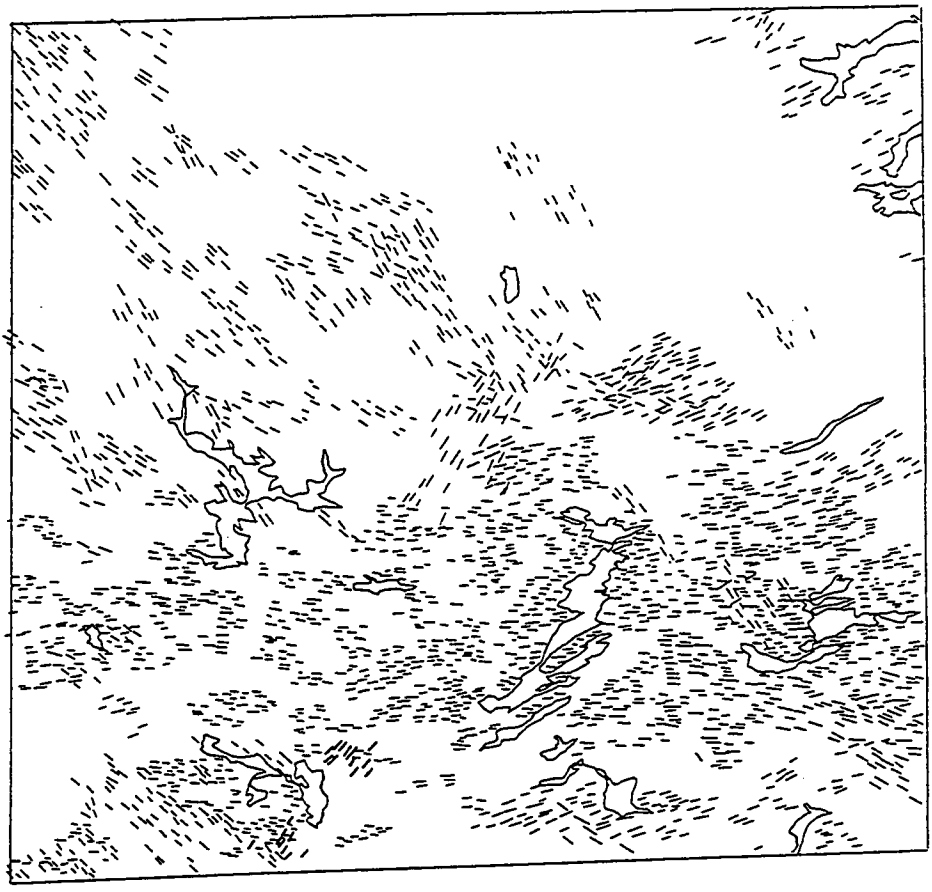


Fig. B.19 Interpretation of glacial linear features and iceflow directions (Landsat image F18)

Scale (Km) 0 40

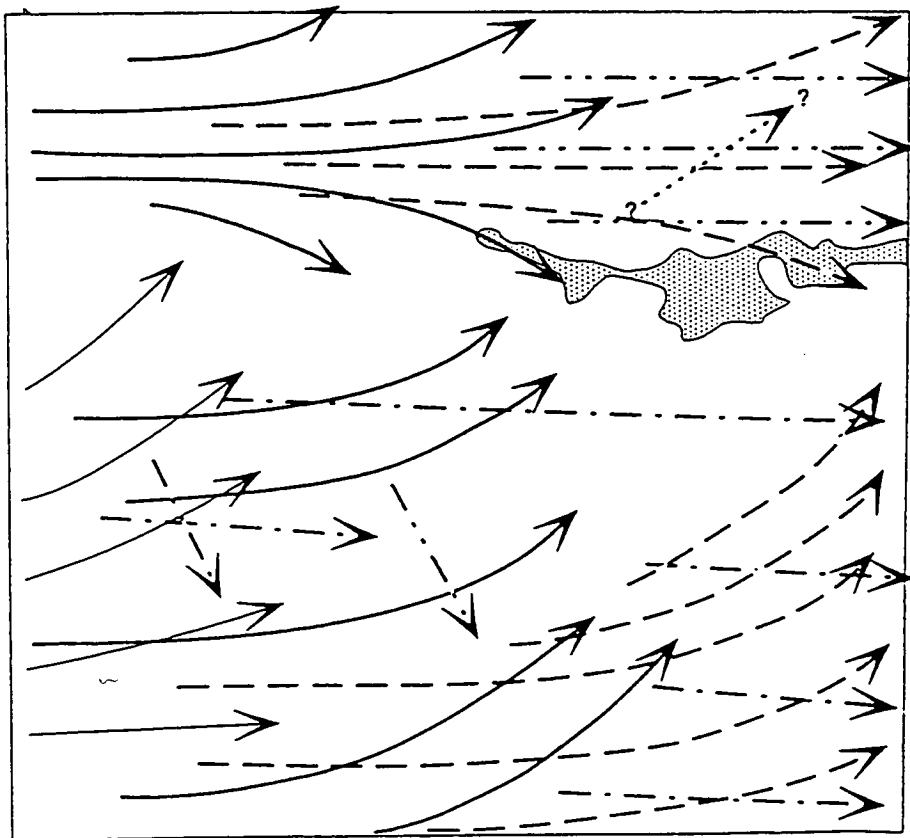
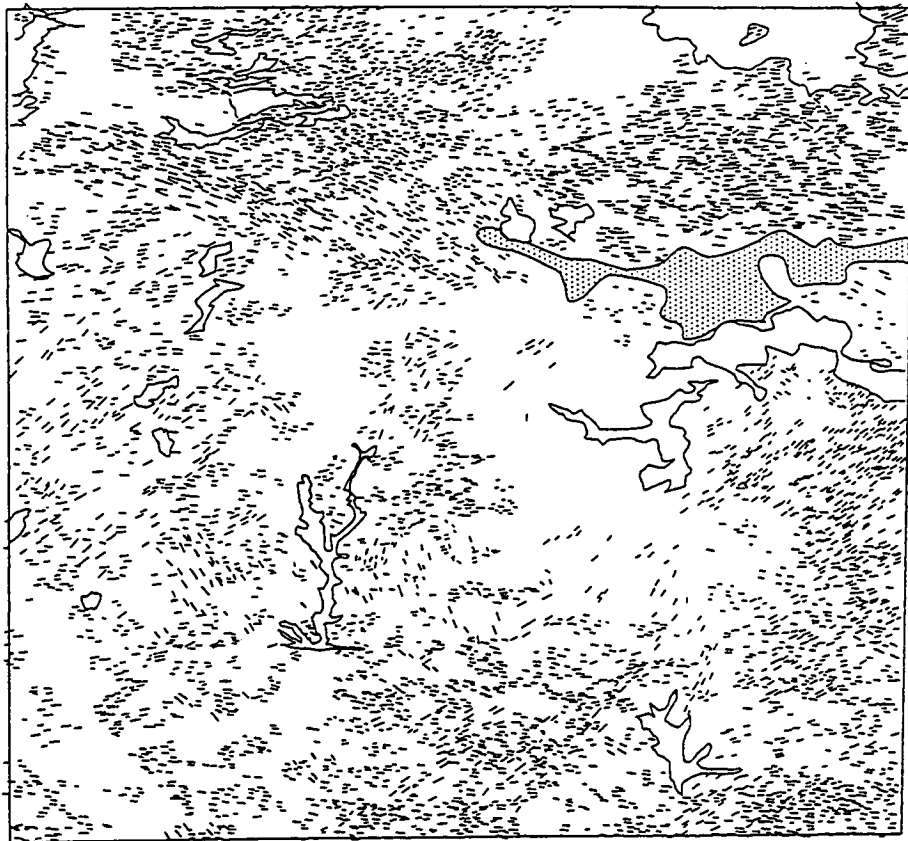


Fig. B.20 Interpretation of glacial linear features and iceflow directions (Landsat image F 1 9)

Scale (Km) 0 40

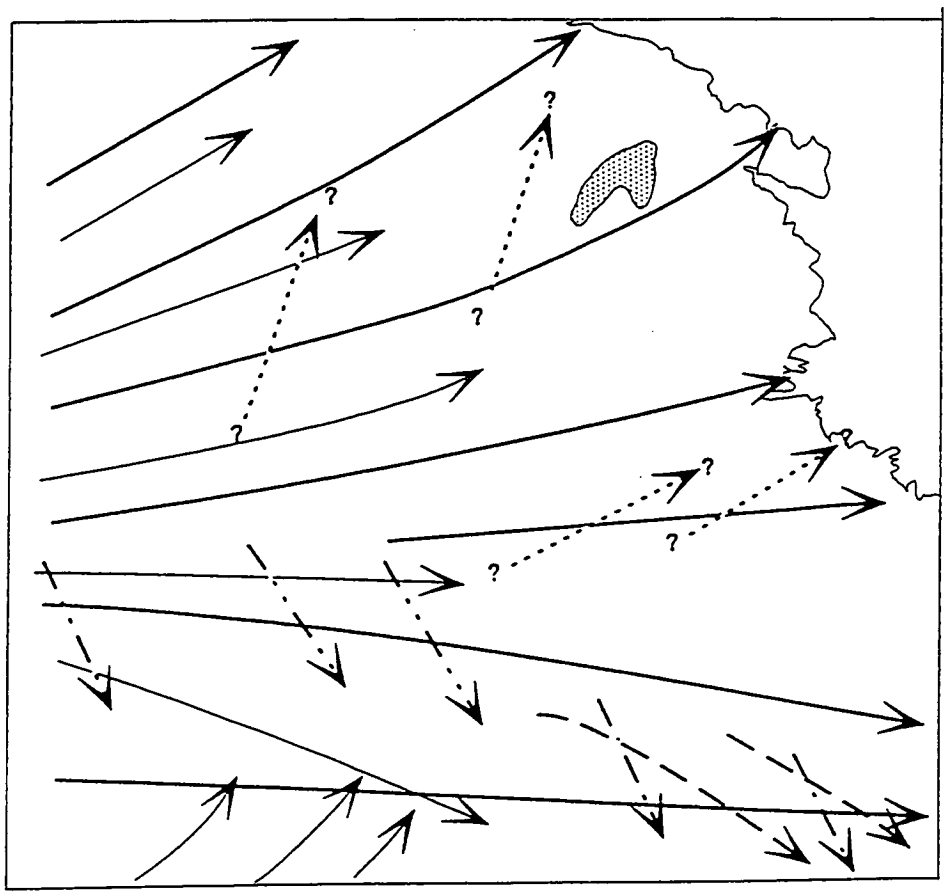


Fig. B.21 Interpretation of glacial linear features and iceflow directions (Landsat image F 1 9 b)

Scale (Km) 0 40

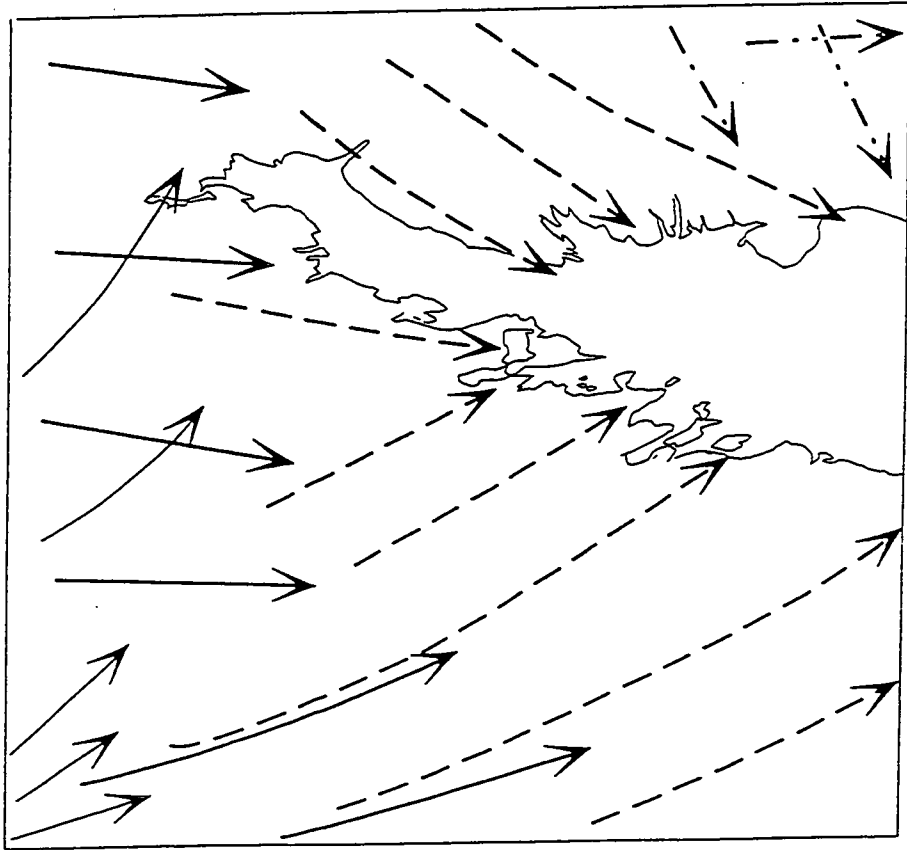


Fig. B.22 Interpretation of glacial linear features and iceflow directions (Landsat image F20)

Scale (Km) 0 40

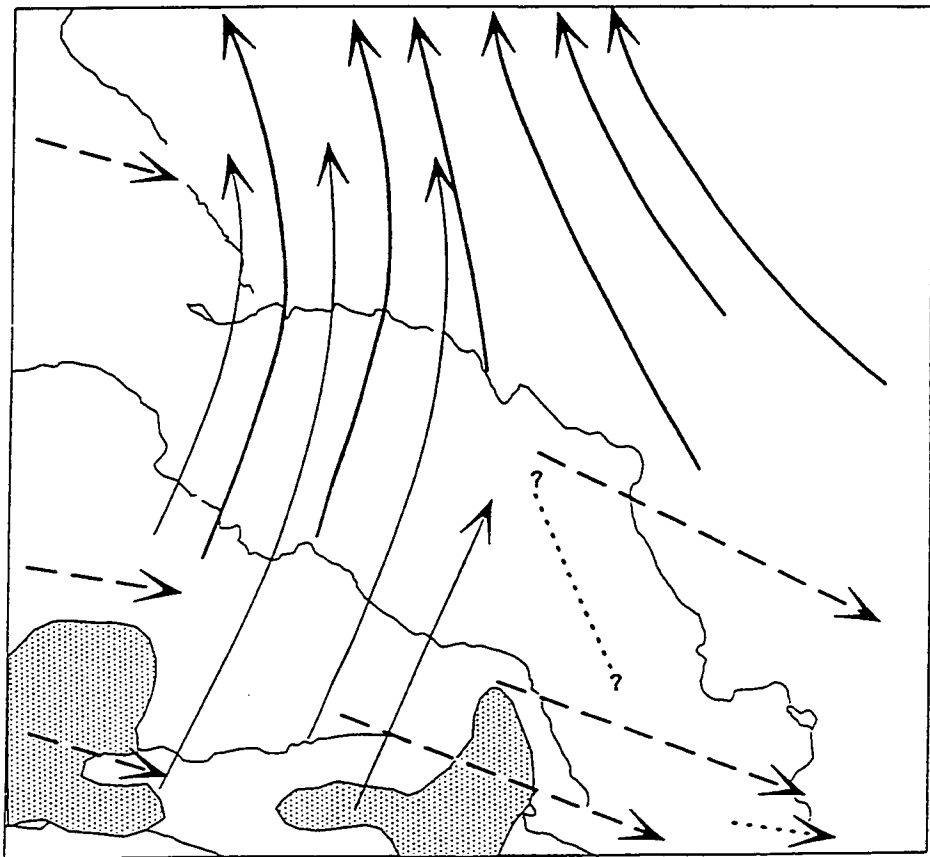
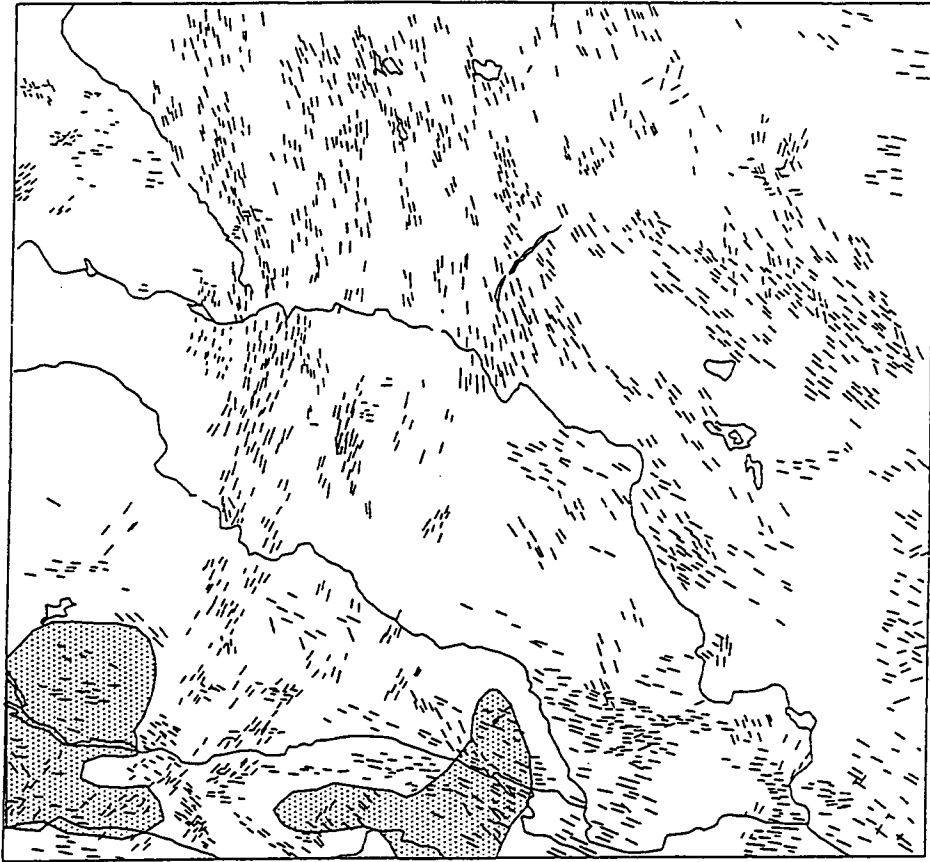


Fig. B.23 Interpretation of glacial linear features and iceflow directions (Landsat image F 2 1)

Scale (Km) 0 40

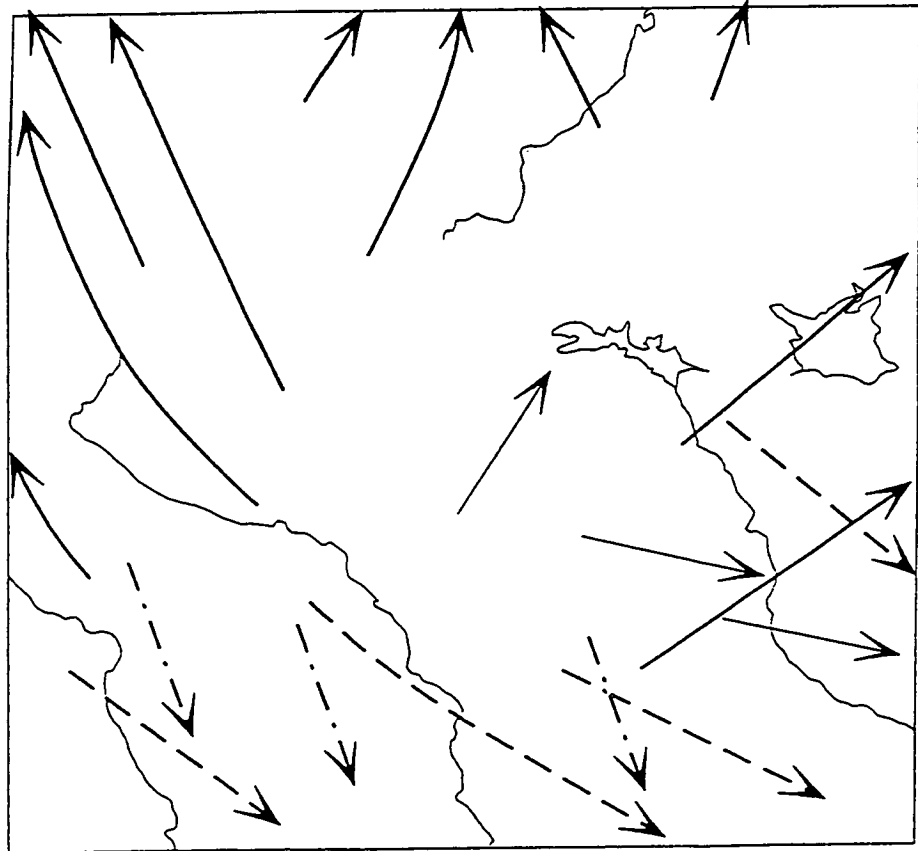
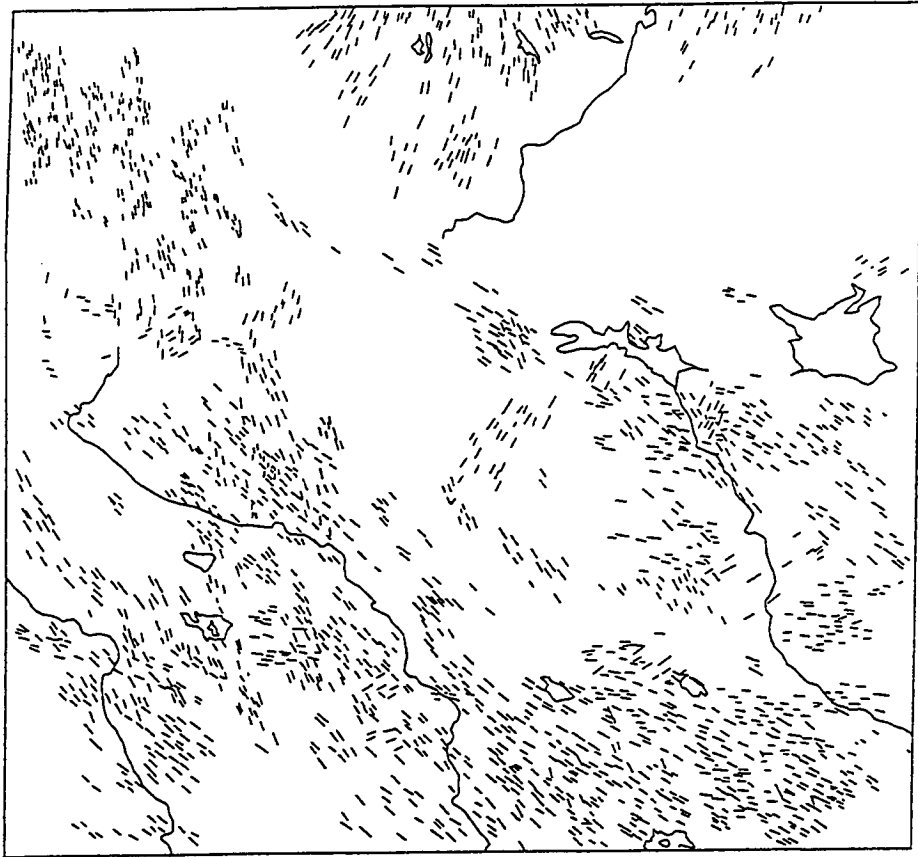


Fig. B.24 Interpretation of glacial linear features and iceflow directions (Landsat image F 2 2)

Scale (Km) 0 40

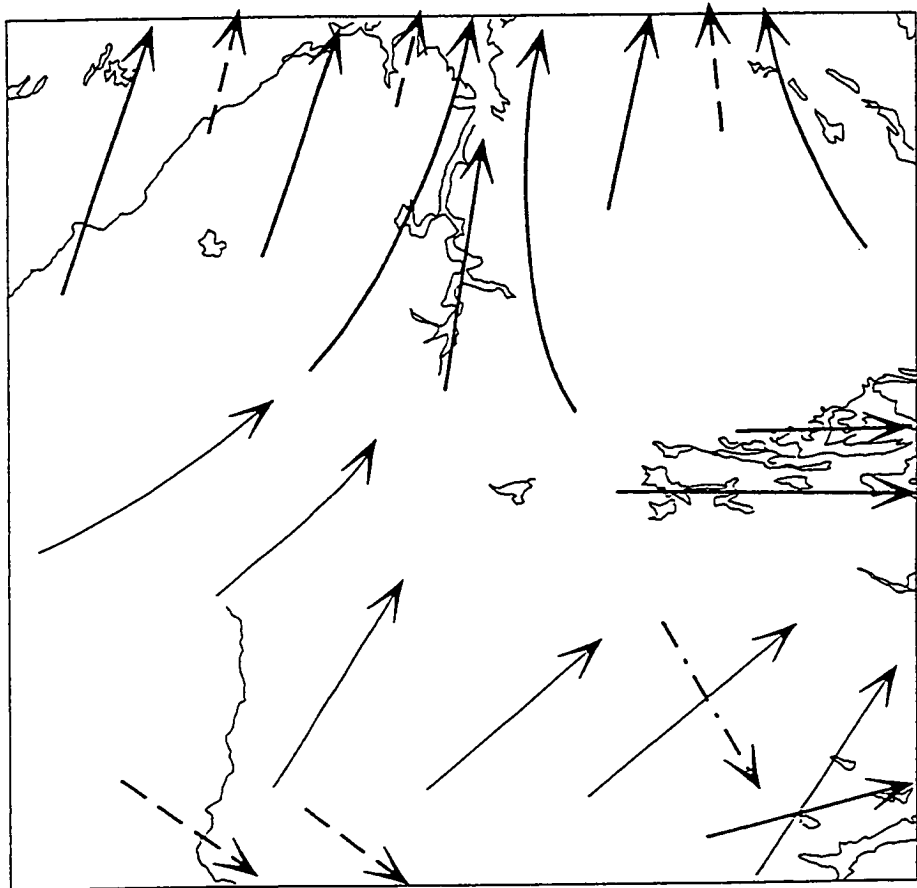



Fig. B.25 Interpretation of glacial linear features and iceflow directions (Landsat image F 2 3)

Scale (Km)  0 40

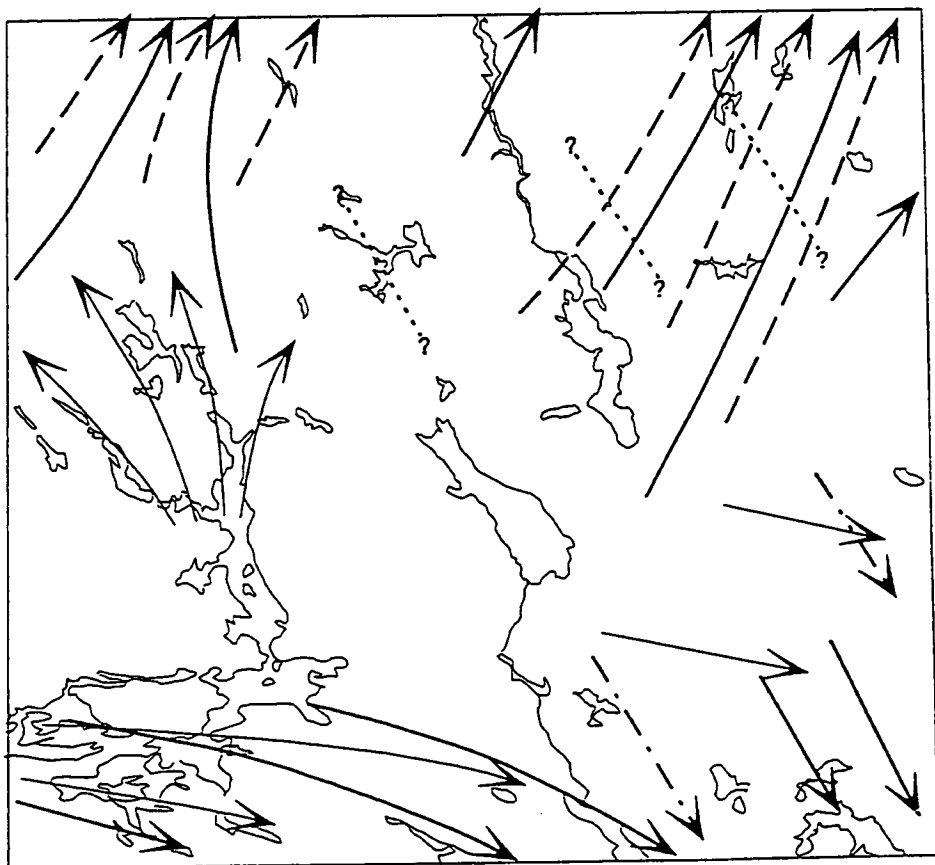
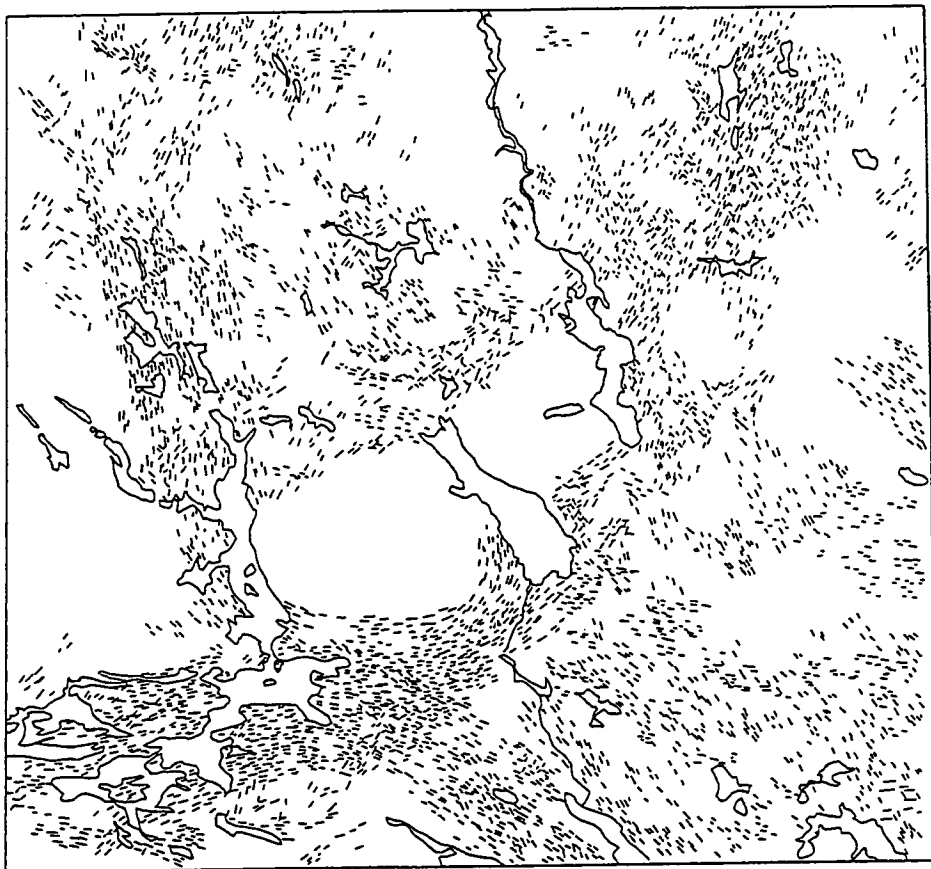


Fig. B.26 Interpretation of glacial linear features and iceflow directions (Landsat image F25)

Scale (Km) 0 40

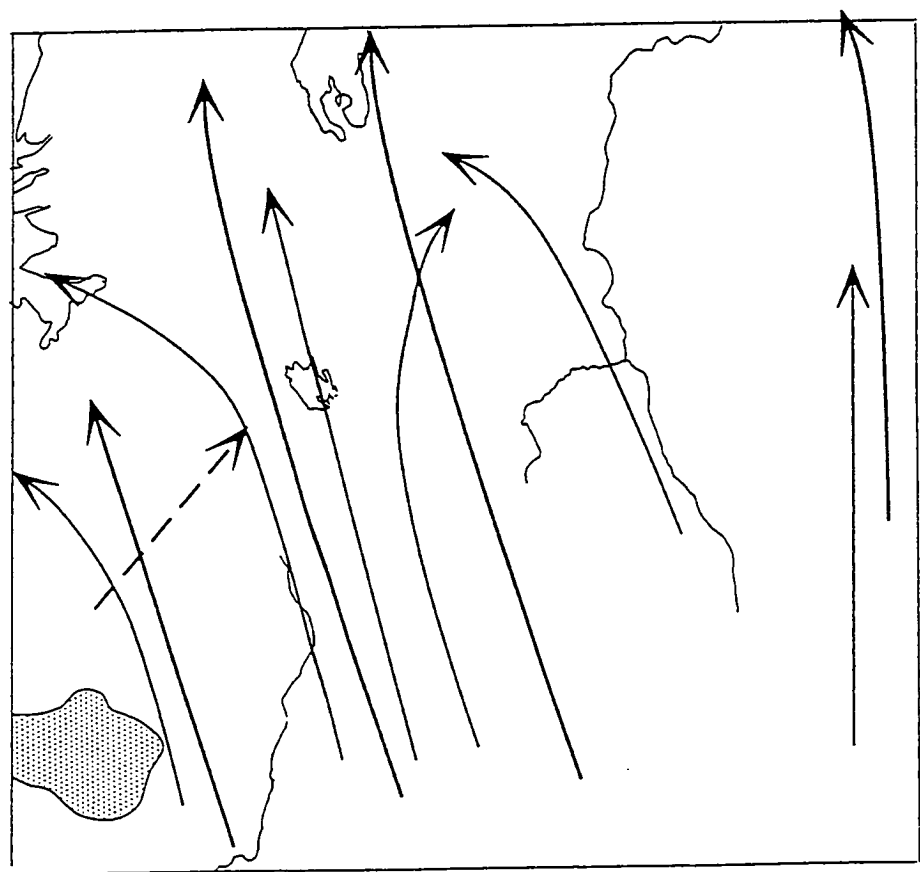
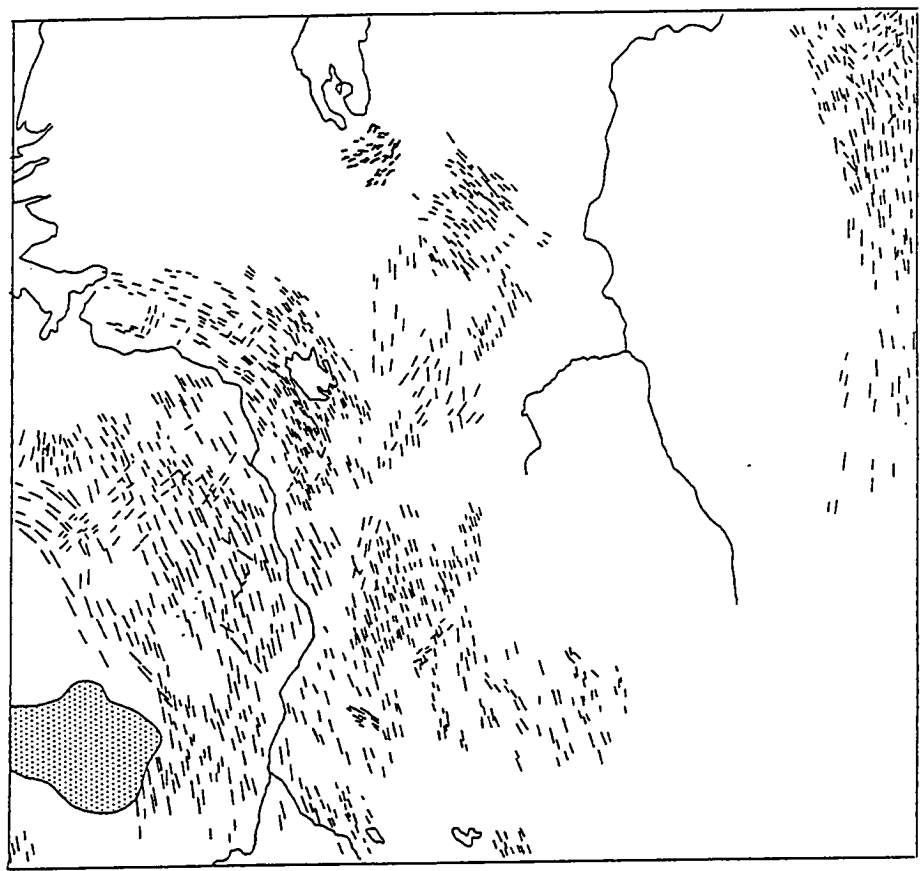


Fig. B.27 Interpretation of glacial linear features and iceflow directions (Landsat image F26)

Scale (Km) 0 40

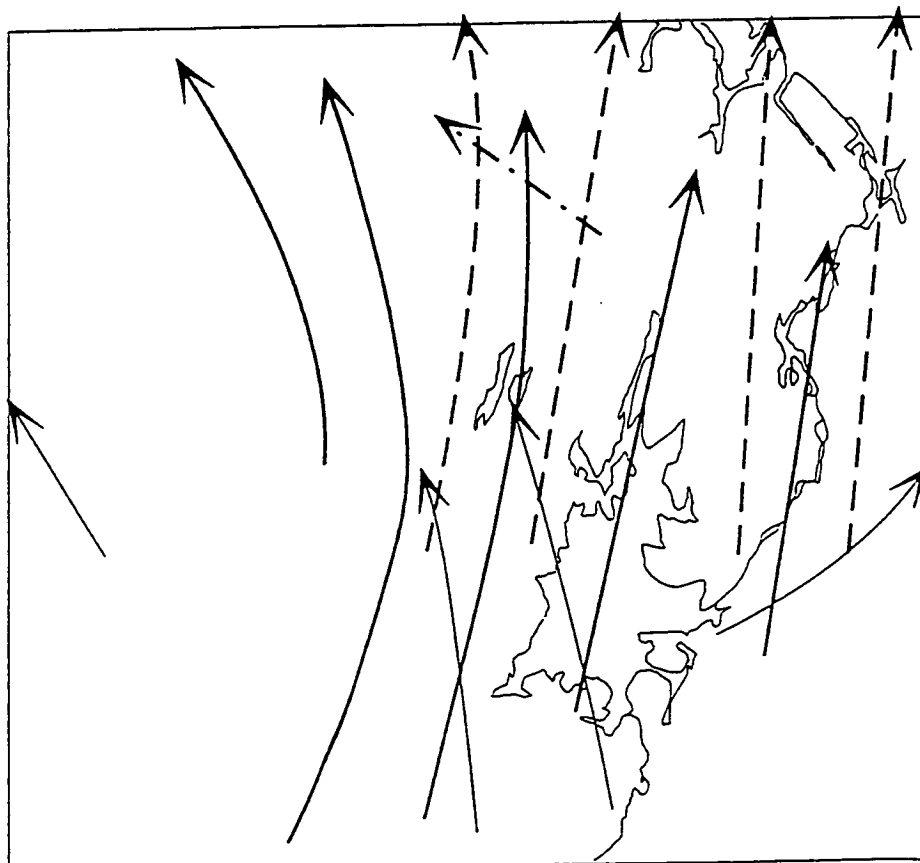
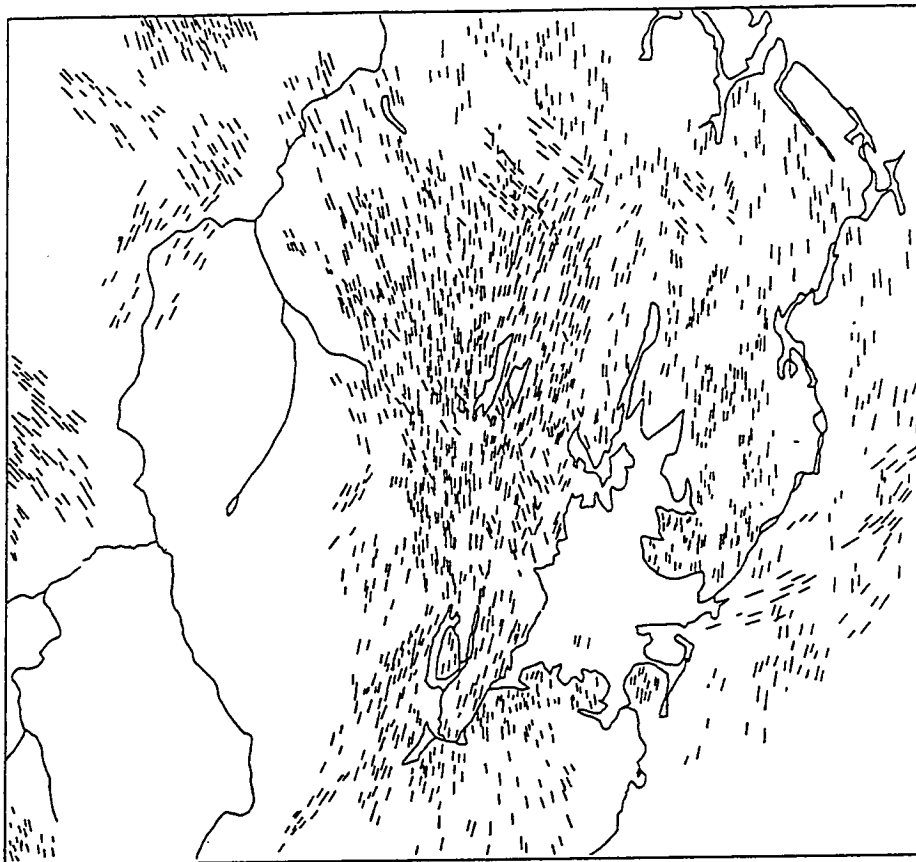


Fig. B.28 Interpretation of glacial linear features and iceflow directions (Landsat image F 2 7)

Scale (Km) 0 40

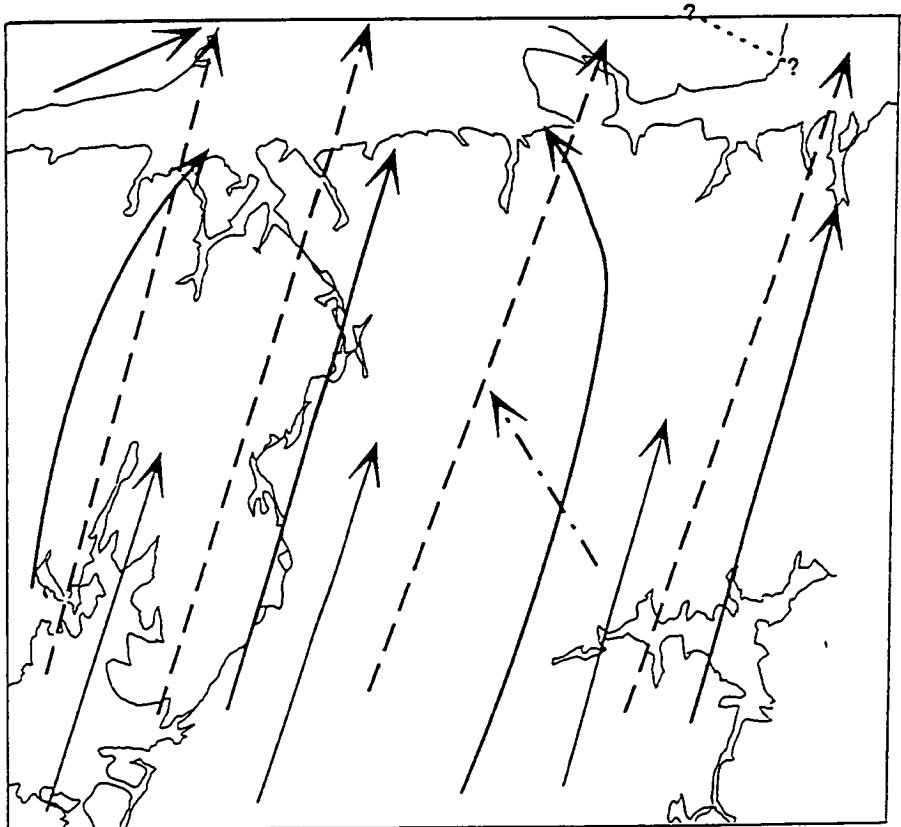
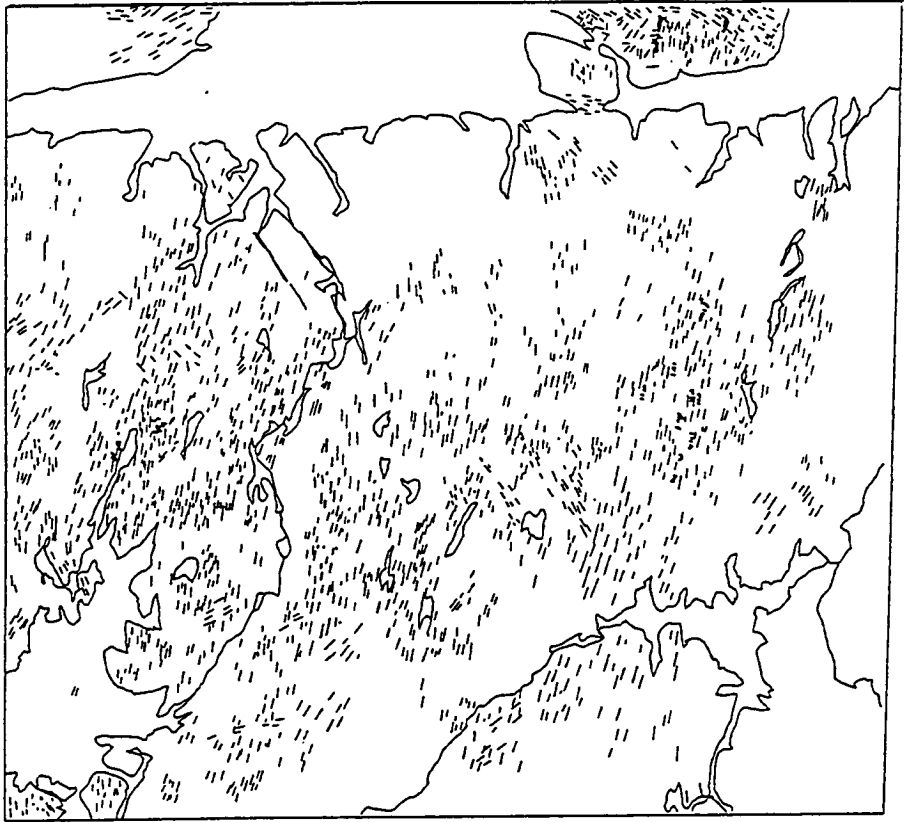


Fig. B.29 Interpretation of glacial linear features and iceflow directions (Landsat image K1)

Scale (Km) 0 40

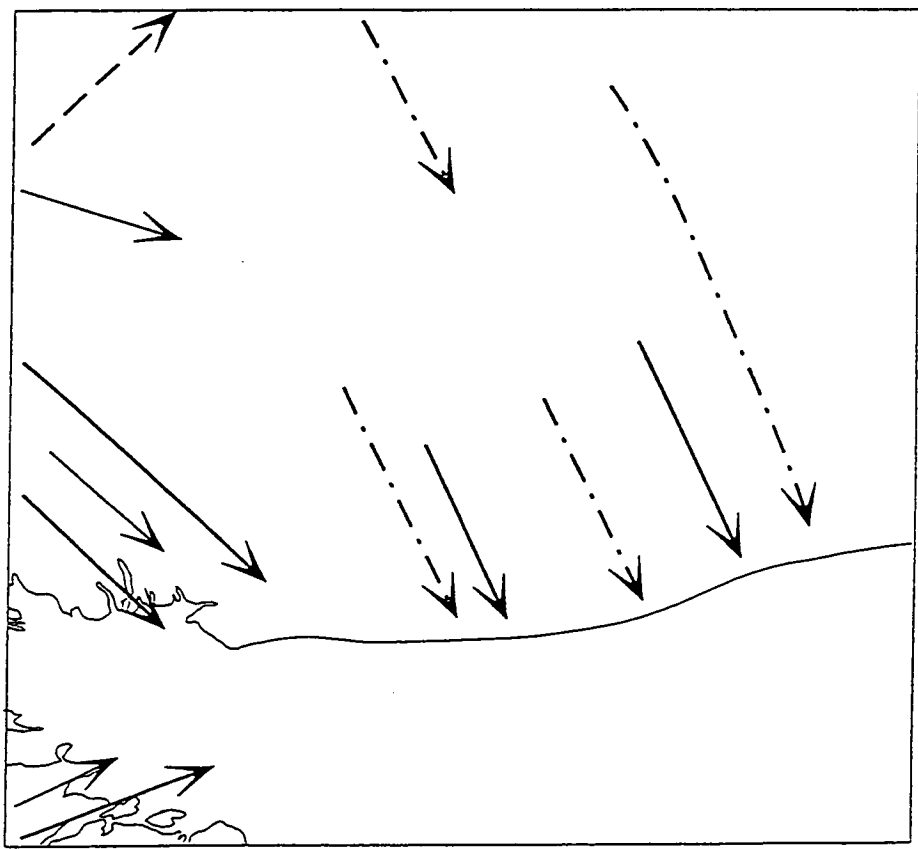


Fig. B.30 Interpretation of glacial linear features and iceflow directions (Landsat image K 2)

Scale (Km) 0 40

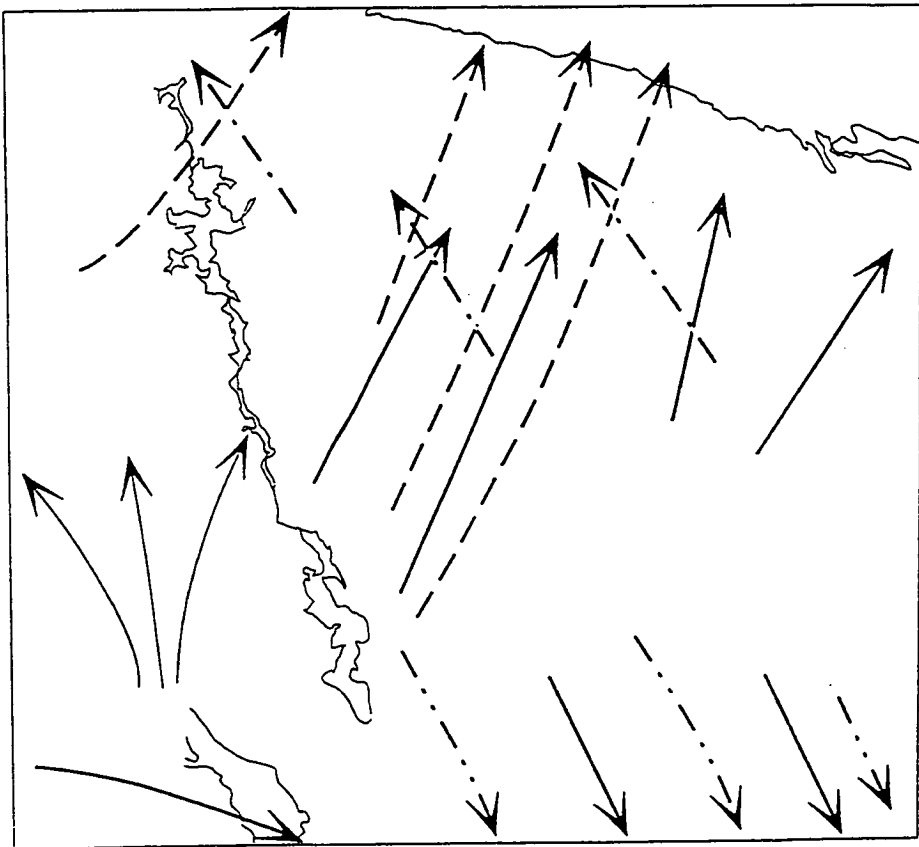
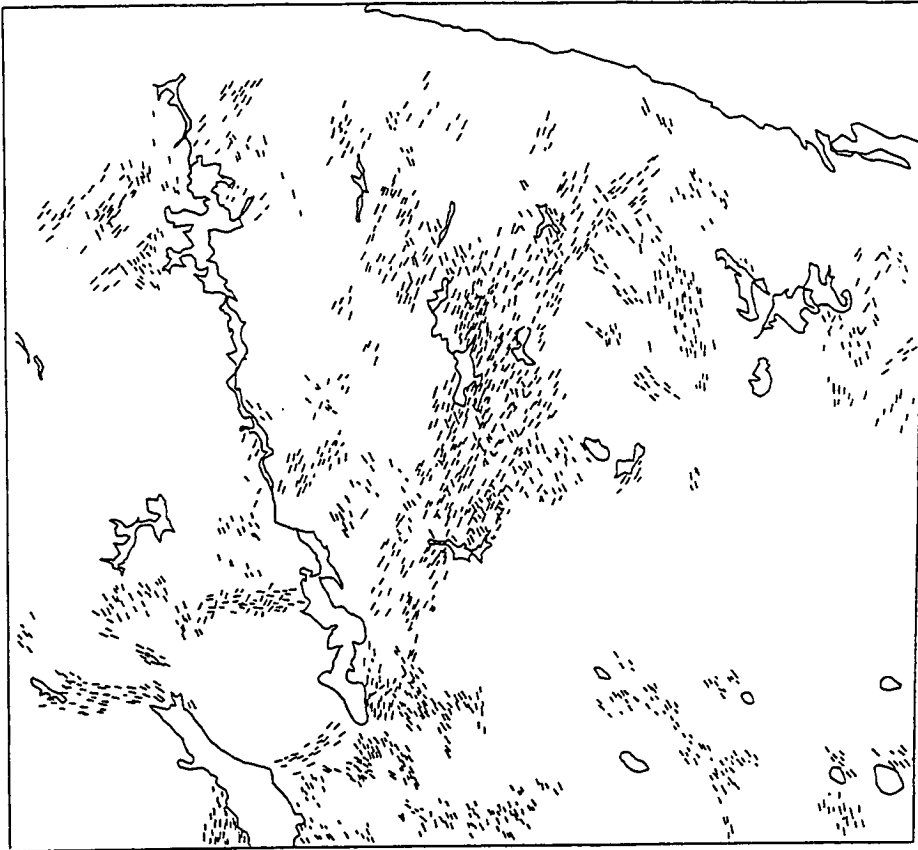


Fig. B.31 Interpretation of glacial linear features and iceflow directions (Landsat image K 3)

Scale (Km) 0 40

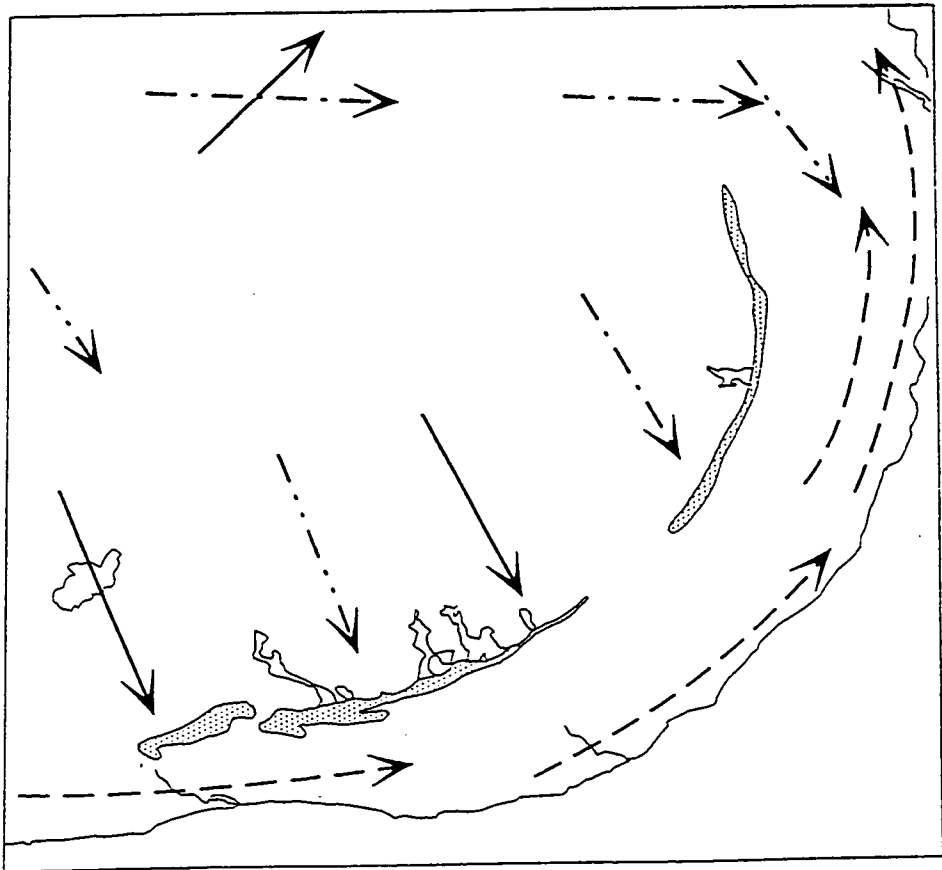

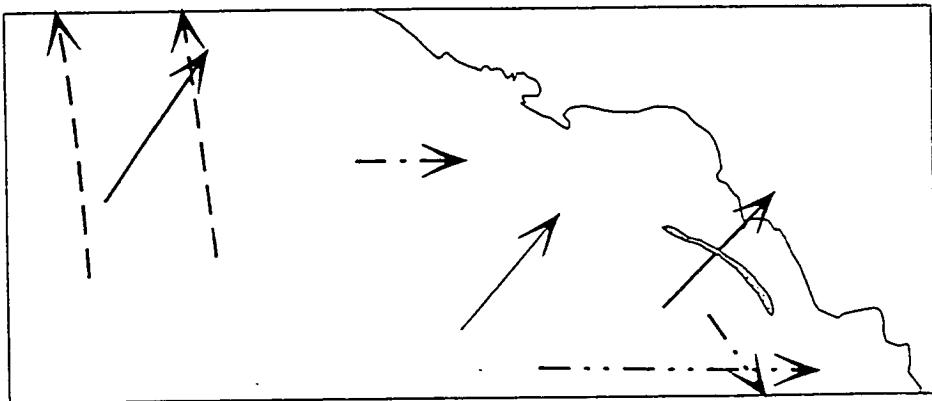
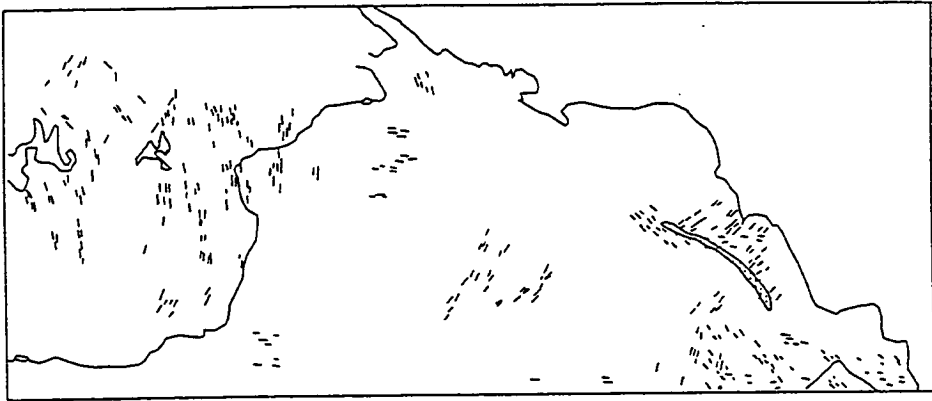


Fig. B.32 Interpretation of glacial linear features and iceflow directions (Landsat image K4)

Scale (Km)  0 40



## References

- Aario, R.**, 1977. Classification and terminology of morainic landforms in Finland. *Boreas*, 6, pp.67-100.
- Aario, R.**, 1987. Drumlins of Kuusamo and Rogen-ridges of Ranua, northeast Finland. In: Drumlin symposium, J.Menzies and J.Rose (eds). Balkema, Rotterdam, pp. 87-102
- Ager, D. V.**, 1980. The Geology of Europe. McGraw-Hill Book Company Ltd, UK, 535 p.
- Agrell, H.**, 1979. The Quaternary history of the Baltic, Sweden. In: *The Quaternary history of the Baltic*, V. Gudelis and L.-K. Köningsson (eds). Acta Univ. Ups. Ann. Quing. Cel 1, Uppsala, pp. 219-239.
- Alhonen, P.**, 1979. The Quaternary history of the Baltic, Finland. In: *The Quaternary history of the Baltic*, V. Gudelis and L.-K. Köningsson (eds). Acta Univ. Ups. Ann. Quing. Cel 1, Uppsala, pp. 240-261.
- Alley, R. B.**, 1993. In search of ice-stream sticky spots. *Journal of Glaciology*, Vol. 39, pp. 447-456.
- Alley, R. B., Blankenship, D. D., Bentley, C. R. and Rooney, S. T.**, 1987a. Till beneath Ice Stream B 3. Till deformation: evidence and implications. *Journal of Geophysical Research*, 92, pp. 8921-8929.
- Alley, R. B., Blankenship, D. D., Rooney, S. T. and Bentley, C. R.**, 1987b. Till beneath Ice Stream B 4. A coupled ice-till flow model. *Journal of Geophysical Research*, 92, pp. 8931-8940.
- Ammann, B. and Lotte, A. F.**, 1989. Late-Glacial radiocarbon and palynostratigraphy on the Swiss Plateau. *Boreas* 18, pp.109-126.
- Anundsen, K.**, 1980. Quaternary geological studies in Sunnhordland and Nord-Rogaland, southwest Norway. Dr. philos. *Thesis Bergen Univ.*
- Åse, L-E. and Bergström, E.**, 1982. The ancient shorelines of the Uppsala esker around Uppsala and the shoreline displacement. *Geografiska Annaler*, Vol. 64A, pp.229-244.
- Banerjee, I and McDonald, B. C.**, 1975. Nature of esker sedimentation. In: *Glaciofluvial and glaciolacustrine sedimentation*. A. V. Jopling and B. C. McDonald (eds), Society of Economic Paleontologists and Mineralogists, Special Publication 23, pp. 132-154.
- Basalykas, A. and Gudelis, V.**, 1977. Charakter und Verlauf des Eisaufbaues während der Weichselvereisung in Litauen. *Zeitschrift für Geomorphologie*, 27, pp. 59-67.
- Behre, K. E. & Lade, U.**, 1986. Eine Folge von Eem und 4 Weichselnterstadialen in Oerel/Niedersachsen und ihre Vegetationsablauf. *Eiszeitalter und Gegenwart* 36, 11-36.
- Bentley, C. R.**, 1987. Antarctic ice streams: a review. *Journal of Geophysical Research*, 92, B9, 8843-8858.

**Bergsten, H., & Dennegård, B.,** 1988. Late Weichselian-Holocene foraminiferal stratigraphy and palaeohydrographic changes in the Gothenburg area, southwestern Sweden. *Boreas*, Vol.17, pp.229-242.

**Björck, S.,** 1979. Late Weichselian stratigraphy and chronology of Blekinge in SE Sweden in the light of water level changes in the Baltic Ice Lake. University of Lund, Department of Quaternary Geology, *Thesis* 7, 248pp.

**Björck, S & Dennegård, B.,** 1988. Preliminary stratigraphic studies on the Late Weichselian and Holocene development of the Håno Bay, southeastern Sweden. *Geographica Polonica*, Vol.55, pp.51-62.

**Björck, S & Digerfeldt, G.,** 1982. Late Weichselian shore displacement at Hunneberg, southern Sweden, indicating complex uplift. *Geologiska Föreningens i Stockholm Förhandlingar*, Vol.104, 132-155.

**Björck, S & Digerfeldt, G.,** 1986. Late Weichselian-Early Holocene shore displacement west of Mt. Billingen, within the Middle Swedish end-moraine zone. *Boreas*, Vol.15, 1-18.

**Bond, G., Broecker, W., Johnsen, S., McManus, J., Labeyrie, L., Jouzel, J. and Bononi, G.,** 1993. Correlations between climate records from North Atlantic sediments and Greenland ice. *Nature* 365, pp. 143-147.

**Boulton, G.S.,** 1987. A theory of drumlin formation by subglacial sediment deformation. In: *Drumlin symposium*, J.Menzies and J.Rose (eds). Balkema, Rotterdam, pp.25-80.

**Boulton, G.S. and Clark, C.D.,** 1990. The Laurentide ice sheet through the last glacial cycle: the topology of drift lineations as a key to the dynamic behaviour of former ice sheets. *Transactions of the Royal Society of Edinburgh, Earth Sciences*, 81, pp.327-347.

**Boulton, G.S. and Hindmarsh, R.C.A.,** 1987. Sediment deformation beneath glaciers: rheology and geological consequences. *Journal of Geophysical Research*, 92, pp. 9059-9082.

**Boulton, G. S. and Jones, A. S.,** 1979. Stability of temperate ice caps and ice sheets resting on beds of deformable sediment. *Journal of Glaciology* 24, pp. 29-43.

**Boulton, G. S. and Payne, A.,** 1994. Mid-latitude ice sheets through the last glacial cycle: glaciological and geological reconstructions. In: *Long term climatic variations*, J-C. Duplessey and M-T. Spyridakis (eds). NATO ASI Series I 22, pp. 177-212.

**Boulton, G.S., Smith, G.D., Jones, A.S. and Newsome, J.,** 1985. Glacial geology and glaciology of the last mid-latitude icesheets. *Journal of the Geological Society of London*, 142, pp.447-474.

**Böse, M.,** 1989. Methodisch-stratigraphische Studien und paläomorphologische Untersuchungen zum Pleistozän südlich der Ostsee. *Berliner Geographische Abhandlungen*, 51, 114 p.

**Böse, M.,** 1990. Reconstruction of ice flow directions south of the Baltic Sea during the Saalian and Weichselian glaciations, *Boreas*, Vol. 19, pp.217-226.

**Budd, W. F.**, 1979. The importance of ice sheets in long term changes of climate and sea level. In: *Sea level, Ice and Climate Changes*, proceedings of the Canberra Symposium, Dec. 1979.

**Budd, W. F., Jensen, D. and Radok, U.**, 1970. The extent of basal melting in Antarctica. *Polarforschung*, 6 (39), pp.293-306.

**Cato, J.**, 1985. The definitive connection of the Swedish time scale with the present, and the new date of the zero year in Döviken, northern Sweden. *Boreas*, 14, pp. 117-122.

**Chappell, J.**, 1974. Late Quaternary glacio- and hydro-isostasy, on a layered earth. *Quaternary Research* 4, pp. 429-440.

**Clark, C. D.**, 1990. Reconstruction of the behaviour of the Laurentide Ice Sheet using satellite imagery. *Unpublished PhD Thesis*, University of Edinburgh.

**Clark, J. A.**, 1980. A numerical model of worldwide sea-level changes in a viscoelastic earth. In: *Earth Rheology, Isostasy and Eustasy*, N.-A. Mörner (ed), Chichester: John Wiley and Sons, pp. 525-534.

**Clark, J. A., Farrell, W. E. and Peltier, W. R.**, 1978. Global changes in postglacial sea level: A numerical calculation, *Quaternary Research* 9, pp. 265-287.

**Clarke, K. C.**, 1987. Fast glacier flow: ice streams, surging and tidewater glaciers. *Journal of Geophysical Research* 92, pp. 8835-8841.

**Clark, P. U.**, 1994. Unstable behaviour of the Laurentide Ice Sheet over Deforming Sediment and its implications for Climate Change. *Quaternary Research* 41, pp.19-25.

**Clark, P. U., Clague, J. J., Curry, B. B., Dreimanis, A., Hicock, S. R., Miller, G. H., Berger, G. W., Eyles, N., Lamothe, M., Miller, B. B., Mott, R. J., Oldale, R. N., Stea, R. R., Szabo, J. P., Thorleifson, L. H. and Vincent, J.-S.**, 1993. Initiation and Development of the Laurentide and Cordilleran Ice Sheets following the Last Interglaciation. *Quaternary Science Reviews*, 12, pp. 56-87.

**Dahl-Jensen, D.**, 1989. Steady thermomechanical flow along two-dimensional flow lines in large grounded ice sheets. *Journal of Geophysical Research*, 94, pp. 10355-10362.

**Danielsen, A.**, 1970. Pollen-analytical Late-Quaternary studies in the Ra district of Østfold, southeast Norway. Univ. Bergen *Årb. Mat-naturvitensk. Ser.* 1969, Vol.14, 146pp.

**Denton, G. H. and Hughes, T. J.**, 1981 (eds) *The Last Great Ice Sheets*, Wiley, New York, 484p.

**Devoy, R. J. N.**, 1987. Sea-level changes during the Holocene: The North Atlantic and Arctic Oceans. In: *Sea Surface Studies: A global view*, R. J. N. Devoy (ed) Croom Helm, London, pp. 295-347.

**Digerfeldt, G.**, 1975. A standard profile for Littorina transgressions in western Skåne, South Sweden. *Boreas*, Vol.4, pp.125-142.

**Dolukhanov, P. M.** 1979. The Quaternary History of the Baltic, Leningrad and Soviet Karelia. In: *The Quaternary History of the Baltic*. V. Gudelis and L.-K. Königsson (eds), Acta Univ. Ups. Symp. Univ. Ups. Ann. Quing. Cel.:1. pp.115-125.

**Donner, J.** 1969. Land/sea level changes in southern Finland during the formation of the Salpausselkä endmoraines. *Bull. Geol. Soc. Finl.* 41, pp. 135-150.

**Donner, J.** 1983. The identification of Eemian interglacial and Weichselian interstadial deposits in Finland. *Ann. Acad. Scient. Fenn. Ser. A* 136, 1-138.

**Donner, J., Eronen, M. and Jungner, H.,** 1977. The dating of the Holocene relative sea-level changes in Finnmark, North Norway. *Norsk Geografisk Tidsskrift*, Vol.31, pp.103-128.

**Donner, J., Junger, H. and Kurtén, B.,** 1979. Radiocarbon dates of mammoth finds in Finland compared with radiocarbon dates of Weichselian and Eemian deposits. *Bull. Geol. Soc. Finland* 51, 45-54.

**Duplessey, J. C., Delibras, G., Tesron, J. L., Pujol, C. and Duprat, J.,** 1981. Deglacial warming of the northeastern Atlantic Ocean: Correlation with the paleoclimatic evolution on the European continent. *Paleogeography, Paleoclimatology, Paleoecology*, 35, 121-144.

**Dyke, A. S. and Prest, V. K.,** 1987. Late Wisconsinan and Holocene history of the Laurentide Ice Sheet, *Geographie Physique et Quaternaire*, 41, pp. 237-263.

**Ehlers, J.,** 1990. Reconstruction of the dynamics of the North-West European Pleistocene ice sheets. *Quaternary Science Reviews* 9, pp. 71-83.

**Ehlers, J.,** 1992. Origin and distribution of red tills in North Germany. *Geologiska Undersökning*, Ser. Ca. 81, pp.97-105.

**Elverhøi, A., Solheim, A., Nyland-Berg, M. and Russwurm, L.,** 1992. Last interglacial-glacial cycle, West Barents Sea. *Lunqua Report*, Vol. 35, 17-24.

**Elverhøi, A., Nyland-Berg, M., Russwurm, L., Solheim, A., and Vulstad, A. A.,** 1990. Late Weichselian ice recession in the central Barents Sea. *Proceedings of the advanced research workshop on the "Geologic History of the Polar Oceans: Arctic versus Antarctic"*. Bremen, Germany, October 10-14.

**Eronen, M.,** 1976. A radio-carbon dated *Ancylus* transgression site in south-eastern Finland. *Boreas* 5, pp. 65-76.

**Eronen, M.,** 1983. Late Weichselian and Holocene shore displacement in Finland. In: *Shoreline and Isostasy*, D. E. Smith & A. G. Dawson (eds), Academic Press, London, pp. 183-207.

**Eronen, M and Haila, H.,** 1982. Shore displacement during the *Ancylus* Lake stage near Helsinki, South Finland. *Annales Academiae. Scientiarum Fennicae*, A III, 134, pp. 111-137

**Fægri, K.,** 1944. Studies on the Pleistocene of western Norway, III, Bømlo. *Bergens Mus. Årb.* 1943, Naturvitens. R. 8, 100pp.

**Fairbridge, R.W.,** 1961. Eustatic changes in sea level. *Physics and Chemistry of the Earth*, 5, pp. 99-185.

**Farrell, W. E. and Clark, J.A.,** 1976. On postglacial sea level. *Geophysical Journal of the Royal Astronomical Society*, 46, pp. 647-667.

**Fowler, A. C.,** 1987a. Sliding with cavity formation. *Journal of Glaciology*, 33, pp.255-267.

**Fowler, A. C.,** 1987b. A theory of glacier surges. *Journal of Geophysical Research*, 92, pp.9111-9120.

**Glückert, G.,** 1973. Two large drumlin fields in central Finland. *Fennia* 120. 37pp.

**Glückert, G.,** 1974. Map of glacial striation of the Scandinavian Ice Sheet during the last (Weichsel) Glaciation of northern Europe. *Bulletin of the Geological Society of Finland* 46, pp. 1-8.

**Glückert, G.,** 1976. Post-glacial shore-level displacement of the Baltic in SW Finland. *Annales Academiae Scientiarum Fennicae, Ser.A, III*, 92pp.

**Glückert, G.,** 1977. On the Salpausselkä ice-marginal formations in southern Finland. *Zeitschrift für Geomorphologie*, 27, 79-88.

**Glückert, G. and Ristaniemi, O.,** 1982. The Ancylus transgression west of Helsinki, south Finland. *Annales Academiae Scientiarum Fennicae, A III*, 134, pp. 99-110.

**Gudelis, V.,** 1979. The Quaternary History of the Baltic, Lithuania. In: *The Quaternary History of the Baltic*, V. Gudelis and L.-K. Königsson (eds), . Acta Univ. Ups. Symp. Univ. Ups. Ann. Quing. Cel.:1. pp.148-179.

**Haavisto-Hyvärinen, M., Kielosto, S. and Niemelä, J.,** 1989. Precrags and drumlin fields in Finland. *Sedimentary Geology*, 62, pp.337-348.

**Hafsten, U.,** 1956. Pollen-analytic investigations on the Late Quaternary development in the inner Oslofjord area. *Univ. Bergen Årb.* 1956, Naturvitensk. R. 8, 161pp.

**Hald, M. and Vorren, T. O.,** 1983. A shoreline displacement curve from the Tromsø district, North Norway. *Norsk Geologisk Tidsskrift*, Vol.63, pp.103-110.

**Heikkinen, O. and Tikkanen, M.,** 1989. Drumlins and flutings in Finland: their relationships to ice movement and to each other. *Sedimentary Geology*, 62, pp.349-356.

**Heinrich, H.,** 1988. Origin and consequences of cyclic ice-rafting in the north-east Arctic Ocean during the past 130.000 years. *Quaternary Research* 29, pp. 141-152.

**Helle, M., Sønstegaard, E., Coope, R.G., and Rye, N.** 1981. Early Weichselian peat at Brumunddal, southeastern Norway. *Boreas* 10, pp. 369-379

**Henningsmoen, K. E.,** 1979. en karbon-datert strandforskyvningskurve frå søndre Vestfold. In: Nydal R., Westin S., Hafsten U, & Gulliksen, S.; *Fortiden i søkelyset*. Trondheim (Univ.forl.).

- Hirvas, H.**, 1991. Pleistocene stratigraphy of Finnish Lapland. *Geological Survey of Finland, bull.* 354, 123p.
- Hirvas, H. and Kujansuu, R.**, 1979. On glacial, interglacial and interstadial deposits in Northern Finland. *IGCP, Project 71/1/24 'Quaternary Glaciations in the Northern Hemisphere'. Report 5*, 146-164 Prague.
- Hirvas, H. & Nenonen, K.**, 1987. The till stratigraphy of Finland. In: *INQUA till symposium Finland 1985*. R. Kujansuu & M. Saarnisto (eds), M. Geological Survey of Finland. Special Paper 3. pp. 49-63.
- Hirvas, H., Korpela, K & Kujansuu, R.**, 1981. Weichselian in Finland before 15,000 BP. *Boreas*, 10, pp. 423-431.
- Hoppe, G. and Schytt, V.**, 1953. Some observations on fluted moraine surfaces. *Geografisker Annaler*, 33, pp.105-115.
- Houmark-Nielsen, M.**, 1983. Glacial stratigraphy and morphology of the northern Baelthav region. In: *Glacial Deposits in North-West Europe*, J. Ehlers (ed), Balkema Publishers, Rotterdam, pp. 211-217.
- Houmark-Nielsen, M.**, 1987. Pleistocene stratigraphy and glacial history of the central part of Denmark. *Bulletin of the Geological Society of Denmark* 36, pp. 1-189.
- Huybrechts, P.**, 1990a. A 3-D model for the Antarctic Ice Sheet: a sensitivity study on the glacial-interglacial contrast. *Climate Dynamics*, 5, pp. 79-92.
- Huybrechts, P.**, 1990b. The Antarctic Ice Sheet during the last glacial-interglacial cycle: a three-dimensional experiment. *Annals of Glaciology*, 14, pp. 115-119.
- Huybrechts, P. and Oerlemans, J.**, 1990. Response of the Antarctic ice Sheet to future greenhouse warming. *Climate Dynamics* 5, pp. 93-102.
- Huybrechts, P. and T'siobbel, S.**, 1995. Thermomechanical modelling of northern hemisphere ice sheets with two-level mass-balance parameterisation. *Annales of Glaciology* 21, pp. 111-116.
- Hyvärinen, H.**, 1980. Relative sea-level changes near Helsinki, southern Finland, during early Litorina times. *Bulletin Geological Society of Finland*, Vol. 52, pp.207-219.
- Hyvärinen, H.**, 1982. Holocene sea level changes in Helsinki area, *Annales Academiae Scientiarum Fennicae*, A III, 134, 139-149.
- Ignatius, H., Korpela, K. and Kujansuu, R.**, 1980. The deglaciation of Finland after 10,000 BP. *Boreas*, 9, pp. 217-228.
- Iken, A. and Bindshadler, R. A.**, 1986. Combined measurements of subglacial water pressure and surface velocity of Findelengletscher, Switzerland: conclusions about drainage system and sliding mechanisms. *Journal of Glaciology*, 32, pp. 101-119.
- Jansen, H. L. F.**, 1976. Late Pleistocene and Holocene history of the northern North Sea, based on acoustic reflection records, *Netherlands Journal of Sea Research*, 10, pp. 1-43.

- Jelgersma, S.**, 1966. Sea-Level changes during the last 10.000 years. *Royal Meteorological Society Proceedings of Symposium on World Climate 8000-0 B.C.* pp.54-71.
- Jelgersma, S.**, 1980. Late Cenozoic sea-level changes in the Netherlands and adjacent North Sea basin. In: *Earth rheology, isostasy and eustasy*, N.-A. Mørner (ed), John Wiley, pp.435-447.
- Jones, G. A. and Keigwin, L. D.**, 1988. Evidence from Fram Strait (78°N) for early deglaciation. *Nature*, 336, pp.56-59.
- Kaland, P. E.**, 1984. Holocene shore displacement and shorelines in Hordaland, western Norway. *Boreas*, Vol.13, pp.203-242.
- Kamb, B.**, 1987. Glacier surge mechanism based on linked cavity configuration of the basal water conduit system. *Journal of Geophysical Research*, 92, pp. 9083-9100.
- Kessel, H. and Raukas, A.**, 1979. The Quaternary History of the Baltic, Estonia. In: *The Quaternary History of the Baltic*, V. Gudelis and L.-K. Königsson (eds), Acta Univ. Ups. Symp. Univ. Ups. Ann. Quing. Cel.:1. pp.127-146.
- Kidson, C.**, 1982. Sea level changes in the Holocene. *Quaternary Science Reviews* 1, pp.121-151.
- Kjemperud, A.**, 1981. A shoreline displacement investigation from Frosta in Trondheimsfjorden, Nord-Trøndelag, Norway. *Norsk Geologisk Tidsskrift*, Vol.61, pp.1-15.
- Kjemperud, A.**, 1986. Late Weichselian and Holocene shoreline displacement in the Trondheim area, central Norway. *Boreas*, Vol.15, pp.61-82.
- Kleman, J.**, 1990. On the use of glacial striae for reconstructions of paleo-ice sheet flow patterns. *Geografisker Annaler*, 72A, pp.217-236.
- Krog, H.**, 1960. Post-glacial submergence of the Great Belt dated by pollen-analysis and radiocarbon. *Rep. Int. Geol. Congr.*; XXI sess., Norden, 1960, Part IV, Chronology and Climatology of the Quaternary, pp.127-133.
- Krzywinski, K. and Stabell, B.**, 1978. Senglaciale undersøkelser på Sorta. *Arkeo*, Vol.1, pp.27-31.
- Kujansuu, R.** 1976. Glaciogeological surveys for oreprospecting purposes in northern Finland. In: *Glacial Till*, R. F. Legget (ed), The Royal Society of Canada. Special Publications 12, 225-239.
- Kujansuu, R.**, 1990. Glacial flow indicators in air photographs. In: *Glacial Indicator Tracing*, R. Kujansuu & M. Saarnisto (eds). Balkema, Rotterdam, 1990, pp. 71-86.
- Kujansuu, R. and Niemelä, J.** (eds), 1984. Quaternary Deposits of Finland. 1:1,000,000, Geological Survey of Finland, Helsinki.
- Lagerbäck, R.** 1988. The Veiki moraines in northern Sweden - widespread evidence of Early Weichselian deglaciation. *Boreas*, 17, pp. 469-486)

- Lagerbäck, R. & Robertsson, A.M.**, 1988. Kettle holes-stratigraphical archives for Weichselian geology and paleoenvironment in northernmost Sweden. *Boreas* 17, 439-468.
- Lagerlund, E.**, 1987. An alternative Weichselian glaciation model, with special reference to the glacial history of Skåne, South Sweden. *Boreas* 16, pp. 433-459.
- Lauritzen, S-E.**, 1984. Speleothem dating in Norway: an interglacial chronology. *Norsk Geografisk Tidsskrift* 38, pp. 138-142.
- Lie, S. E., Stabell, B. and Mangerud, J.**, 1983. Diatom stratigraphy related to Late Weichselian sea-level changes in Sunnmøre, western Norway. *Norges geologiske Undersøkelse*, Vol 380, pp.203-219.
- Liivrand, E.**, 1991. Biostratigraphy in the Pleistocene deposits in Estonia and correlations in the Baltic region. *Department of Quaternary Research, University of Stockholm, Report* 19, 1-114 p.
- Liivrand, E.**, 1992. Problems of reconstructing Pleistocene stratigraphy in Estonia. *Sveriges Geologiska Undersökning Serie Ca* 81, pp. 171-176.
- Lillesand, T. M. and Kiefer, R. M.**, 1987. Remote sensing and image interpretation. John Wiley & Sons, 721 p.
- Ljunger, E.**, 1949. East-West Balance of the Quaternary Ice Caps in Patagonia and Scandinavia. *Bulletin of the Geological Institution of the University of Upsala*, 33, 95p.
- Longva, O., Larsen, E. and Mangerud, J.**, 1983. Stad. Skildring av Kvartærgeologisk kart 1019 II-M 1:5000. *Norges geologiske Undersøkelse*, Vol. 393, pp.1-66.
- Lundqvist, J.**, 1967. Submörena sediment i Jämtland län. *Sveriges Geologiska Undersökning*, C 618, 267 p.
- Lundqvist, J.**, 1981. Weichselian in Sweden before 15,000 B.P. *Boreas* 10, 395-402.
- Lundqvist, J.**, 1986. Stratigraphy of the central area of the Scandinavian glaciation. *Quat. Sci. Rev.* 5, pp 251-268.
- Lundqvist, J.**, 1990. Glacial morphology as an indicator of the direction of glacial transport. In: *Glacial Indicator Tracing*, R. Kujansuu & M. Saarnisto (eds). Balkema, Rotterdam, 1990, pp. 61-70.
- Mangerud, J.**, 1991. The last ice age in Scandinavia. In: *Late Quaternary Stratigraphy in the Nordic Countries 150,000-15,000 B.P.*, B. G. Andersen and L-K. Königsson (eds), *Striae* 34, 15-30. Uppsala.
- Mangerud, J., Gulliksen, S., Larsen, E., Longva, O., Miller, G., Sejrup, H-P., and Sønstegeard, E.**, 1981. A Middle Weichselian ice-free period in Western Norway: the Alesund Interstadial, *Boreas* 10, pp. 447-462.
- Martinson, D. G., Pisias, N. G., Hays, J. D., Imbrie, J., Moore, T. C. & Shackleton, N. J.**, 1987. Age dating and orbital theory of the ice ages: development of a high resolution 0 to 300,000-year chronostratigraphy. *Quat. Res.* 27, 1-29.

- McIntyre, N. F.**, 1985. The dynamics of ice sheet outlets, *Journal of Glaciology* 31, pp. 99-107.
- Menzies, J.**, 1989. Subglacial hydraulic conditions and their possible impact upon subglacial bedformation. *Sedimentary Geology*, 62, pp.125-150.
- Menzies, J. and Rose, J.**, 1987. (eds) *Drumlin symposium*. Balkema, Rotterdam, 360 p.
- Mikkelsen, V.**, 1949. Prästö Fjord. The development of the Post-glacial vegetation and a contribution to the history of the Baltic Sea. *Dansk bot. Ark.* Vol. 13, no. 5, 171 pp.
- Miller, U.**, 1982. Relative sea level curve from Vasternorrland, northern Sweden. *Annales Academiae Scientiarum Fennicae, A III*, 134. pp. 185-211.
- Miller, U. and Robertsson, A-M.**, 1979. Biostratigraphical investigations in the Anundsjö region, Ångermanland, northern Sweden. *Kungl. Vittern. Hist. Antikr. Akad.* Early Norrland 12.
- Miller, G. H., Sejrup, H-P., Mangerud, J. and Andersen, B. G.**, 1983. Amino acid ratios in Quaternary molluscs and foraminifera from western Norway: correlations, geochronology and paleotemperatures estimates. *Boreas* 12, pp. 107-124.
- Mojski, J. E.**, 1982. Outline of the Pleistocene stratigraphy in Poland. *Biuletyn Instytutu Geologicznego* 343. pp. 9-29.
- Møller, J. J.**, 1984. Holocene shore displacement at Nappstraumen, Lofoten, North Norway. *Norsk Geologisk Tidsskrift*, Vol. 64, pp.1-5.
- Møller, J. J.**, 1986. Holocene transgression maximum about 6000 years at Ramså, Vesterålen, North Norway. *Norsk Geologisk Tidsskrift*, Vol.40, pp. 77-84.
- Mörner, N-A.**, 1969. The Late Quaternary history of the Kattegatt Sea and the Swedish West Coast; deglaciation, shorelevel displacement, chronology, isostasy and eustasy. *Sveriges Geologiska Undersökning C-640*, pp. 1-487.
- Mörner, N-A.**, 1976. Eustasy and geoid changes. *The Journal of Geology*, 2, pp.123-151.
- Mörner, N-A.**, 1979. The Fennoscandian Uplift: Geological Data and their Geodynamical Implication. In: *Earth Rheology, Isostasy and Eustasy*, N.-A. Mörner (ed) Chichester: John Wiley and Sons, pp. 251-283.
- Mott, R. J. and DiLabio, N. W.**, 1990. Paleoecology of organic deposits of probable last interglacial age in northern Ontario. *Geographie Physique et Quaternaire* 44:3, pp. 309-318.
- Nordkalott Project**, 1986a. Map of Quaternary Geology, sheet 2; Glacial Geomorphology, Northern Fennoscandia, 1:1.000.000. *Geological Surveys of Finland, Norway and Sweden*.
- Nordkalott Project**, 1986b. Map of Quaternary Geology, sheet 3; Ice Flow Indicators, Northern Fennoscandia, 1:1.000.000. *Geological Surveys of Finland, Norway and Sweden*.

**Nordkalott Project**, 1986c. Map of Quaternary Geology, sheet 4; Quaternary Stratigraphy, Northern Fennoscandia, 1:1.000.000. *Geological Surveys of Finland, Norway and Sweden*.

**Nordkalott Project**, 1986d. Map of Quaternary Geology, sheet 5; Ice Flow Directions, Northern Fennoscandia, 1:1.000.000. *Geological Surveys of Finland, Norway and Sweden*.

**Oerlemans, H. and van der Veen, C. J.**, 1984. Ice sheets and climate. Reidel, Dordrecht, 217p.

**Okko, V.**, 1964. Maaperä. In: *Suomen Geologia*, K. Rankama (ed), Kirjayhtymä, Helsinki, pp. 239-332.

**Paterson, W. S. B.**, 1994. The Physics of glaciers. Pergamon. 480 p.

**Påsse, T.**, 1987. Shore displacement during the Late Weichselian and Holocene in the Sandsjöbacka area, SW Sweden. *Geologiska Föreningens i Stockholm Förhandlingar*, Vol.109, pp.197-210.

**Payne, A. J.**, 1995. Limit cycles in the basal thermal regime of ice sheets. *Journal of Geophysical Research* 100, pp. 4249-4263.

**Peltier, W. R.**, 1987. Mechanisms of relative sea-level change and the geophysical responses to ice-water loading. In: *Sea Surface Studies: A global view*, R. J. N. Devoy (ed) Croom Helm, London, pp.57-94.

**Peltier, W. R. and Andrews, J. T.**, 1976. Glacial isostatic adjustment I: The forward problem. *Geophysical Journal of the Royal Astronomical Society*, 46, pp. 605-646.

**Petersen, K. S.**, 1984. Late Weichselian sea-levels and fauna communities in northern Vendsyssel, Jutland, Denmark. In: *Climatic changes on a yearly to millennial basis*, N.-A. Mörner and W. Karlén (eds), Reidel Publishing Company, 63-68.

**Prest, V.K.**, 1968. Nomenclature of moraines and ice flow features as applied to the glacial map of Canada. *Geological Survey Papers Canada*, 67-57, 32 p.

**Prest, V. K.**, 1969. Retreat of the Wisconsin and Recent ice in North America, *Geological Survey of Canada*, map 1257A, scale 1:500.00.

**Punkari, M.**, 1980. The ice lobes of the Scandinavian ice sheet during the deglaciation of Finland. *Boreas* 9, 307-310.

**Punkari, M.**, 1982. Glacial geomorphology and dynamics in the eastern parts of the Baltic Shield interpreted using Landsat imagery. *The Photogrammetric Journal of Finland* 9, pp. 77-93.

**Punkari, M.**, 1984. The relations between glacial dynamics and tills in the eastern parts of the Baltic Shield. *Striae* 20, 49-54.

**Punkari, M.**, 1985. Glacial geomorphology and dynamics in Soviet Karelia interpreted by means of satellite imagery. *Fennia* 163, 113-153.

- Punkari, M.**, 1989. Glacial dynamics and related erosion-deposition processes in the Scandinavian ice sheet in south-western Finland. *Final report, Project 01/663, Research Council for the Natural Sciences, Academy of Finland*, pp. 86.
- Punkari, M.**, 1991. Old organic matter inside glacial deposits in Finland: sedimentation models. Late Quaternary stratigraphy in the Nordic countries 150.000-15.000 BP. *Striae* 34, pp. 77-83.
- Punkari, M.**, 1993. Modelling of the dynamics of the Scandinavian Ice Sheet using Remote Sensing and GIS methods. In: *Glaciotectonics and Mapping Glacial Deposits*, J. S. Aber (ed), Canadian Plain Research Center, University of Regina. pp. 233-251.
- Punkari, M., and Forsström, L.**, 1995. Organic remains in Finnish subglacial sediments, *Quaternary Research* 43, pp. 414-425.
- Rainio, H. & Lahermo, P.**, 1976. Observations on dark grey basal till in Finland. *Bull. Geol. Soc. Finland* 48, 137-152.
- Ramfjord, H.**, 1982. On the Late Weichselian and Flandrian shoreline displacement in Nærøy, Nord-Trøndelag, Norway. *Norsk Geologisk Tidsskrift*, Vol.62, pp.191-205.
- Raukas, A.**, 1977. Ice-marginal formations and the main regularities of the deglaciation in Estonia, 1977. *Zeitschrift für Geomorphologie*, 27, pp. 68-78.
- Raukas, A and Gaigalas, A.**, 1993. Pleistocene glacial deposits along the eastern periphery of the Scandinavian ice sheets - an overview. *Boreas*, Vol.22. pp. 214-222.
- Ringberg, B.**, 1988. Late Weichselian geology in southernmost Sweden. *Boreas*, 17, pp.243-263.
- Robersson, A-M. and Rohde, L.**, 1988. A Late Pleistocene sequence at Eitevare, Swedish Lapland. *Boreas* 17. pp 501-509.
- Rose, J.**, 1987. Drumlins a part of a glacier bedform continuum. In: *Drumlin Symposium*, J. Menzies and J. Rose, Balkema (eds) , Rotterdam, pp.103-118.
- Rose, J.**, 1989. Glacier stress pattern and sediment transfer associated with the formation of superimposed flutes. *Sedimentary Geology*, 62, pp.151-176.
- Röthlisberger, H.**, 1972. Water pressure in intra- and subglacial channels. *Journal of Glaciology*, 11, pp.177-203.
- Saarnisto, M.**, 1981. Holocene emergence history and stratigraphy in the area North of the Gulf of Bothnia. *Annales Academiae Scientiarum Fennicae*, Ser.A, III, 130, pp. 42-59.
- Saarnisto, M.**, 1982. Ice retreat and the Baltic Ice Lake in the Salpausselkä zone between Lake Päijänne and Lake Saimaa. *Annales Academiae Scientiarum Fennicae*, Ser.A, III, 134, pp. 61-79.
- Saarnisto, M. and Tamminen, E.**, 1987. Placer gold in Finnish Lapland. In: *INQUA Till symposium*, Finland, 1985, R. Kujansuu and M. Saarnisto (eds). Geological Survey of Finland. Special Paper 3, pp. 181-194.

- Salomaa, R.**, 1982. Post-glacial shoreline displacement in the lauhanvuori area, western Finland. *Annales Academiae Scientiarum Fennicae*, Ser.A, III, 51, 522 p.
- Sauramo, M.**, 1958. Die Geschichte der Ostsee, *Annales Academiae Scientiarum Fennicae*, Ser.A, III, Vol.134
- Sejrup, H-P.** 1987. Molluscan and foraminiferal biostratigraphy of an Eemian-Early Weichselian section on Karmøy, southwestern Norway. *Boreas* 16, pp. 27-42.
- Shabtaie, S. and Bentley, C. H.**, 1987. West Antarctic icestreams draining into the Ross Iceshelf: configuration and mass balance. *Journal of Geophysical Research*, 92, pp.1311-1336.
- Shabtaie, S., Whillans, I. M. and Bentley, C. H.**, 1987. The morphology of icestreams A, B and C, West Antarctica, and their environs. *Journal of Geophysical Research*, 92, B9, 8865-8883.
- Sharpe, D.R.**, 1987. The stratified nature of drumlins from Victoria Island and Southern Ontario. In: *Drumlin Symposium*, J. Menzies and J. Rose (eds) , Balkema, Rotterdam, pp.185-214.
- Shaw, J.**, 1983. Drumlin formation related to inverted erosion marks, *Journal of Glaciology*, 29, pp.461-479.
- Shepard, F. P.**, 1963. 'Thirty-five thousand years of sea level', In: *Essays in marine geology in honor of K. O. Emery*, T. Clemens (ed.), Los Angeles, Univ. Southern California Press, pp. 1-10.
- Shilts, W. W.**, 1980. Flow patterns in the central North American Ice Sheet. *Nature*, 286, pp. 213-218.
- Shoemaker, E.M.**, 1986. Subglacial hydrology for an ice sheet resting on a deformable aquifer. *Journal of Glaciology*, 32, pp.20-30.
- Shreve, R. L.**, 1972. Movement of water in glaciers. *Journal of Glaciology*, Vol. 11, No. 62, pp. 205-214.
- Simonen, A.**, 1980. The Precambrian in Finland. *Geological Survey of Finland*, Bull. 304. 58 p.
- Solheim, A., Russwurm, L., Elverhøi, A. and Nyland-Berg, M.**, 1990. Glacial geomorphic features in the northern Barents Sea: direct evidence for grounded ice and implications for the pattern of deglaciation and late glacial sedimentation. In: *Glacimarine Environments: Processes and Sediments*, J. A. Dowdeswell and J. D. Scourse (eds), Geological Society Special Publication, 53, pp. 253-268.
- Sjørring, S.**, 1983. The glacial history of Denmark. In: *Glacial Deposits in North-West Europe*, J. Ehlers (ed). Balkema, Rotterdam , pp. 163-179.
- Sørensen, R.**, 1979. Late Weichselian deglaciation in the Oslofjord area, South Norway, *Boreas*, Vol. 8, pp.241-246.
- Stea, R. R. and Brown, Y.**, 1989. Variation in drumlin orientation, form and stratigraphy relating to successive ice flows in southern and central Nova Scotia. *Sedimentary Geology*, 62, pp.223-240.

**Sugden, D. E.**, 1977. Reconstruction of the morphology, dynamics and thermal characteristics of the Laurentide Ice Sheet at its maximum. *Arctic and Alpine Research*, 9, pp. 21-47.

**Sugden, D. E. and John, B. S.**, 1976. *Glaciers and Landscape*, Edward Arnold, London, 376 p.

**Sutherland, D G.**, 1987. Dating and associated methodological problems in the study of Quaternary sea level changes. In: *Sea Surface Studies: A global view*, R. J. N. Devoy (ed) Croom Helm, London, pp.57-94.

**Stabell, B.**, 1980. Holocene shorelevel displacement in Telemark, southern Norway. *Norsk Geologisk Tidsskrift*, Vol 60, pp.71-80.

**Sveian, H. and Olsen, L.**, 1984. En strandforskyvningskurve fra Verdalsøra, Nord-Trøndelag. *Norsk Geologisk Tidsskrift*, Vol. 64, pp.27-38.

**Svendson, J. I.**, 1985. Strandforskyvning på Sunnmøre. Bio- og litostratigrafiske undersøkelser på Gurskøy, Leinøy og Bergsøy. *Unpubl. Thesis*. University of Bergen.

**Svendson, J. I. and Mangerud, J.**, 1987. Late Weichselian and Holocene sea-level history for a cross-section of western Norway. *Journal of Quaternary Science*, Vol.2, pp.113-132.

**Svensson, N-O.**, 1985. Some preliminary results on the early Holocene shore displacement in the Oskarshamn area, southeastern Sweden. *Eiszeitalter u. Gegenwart*, Vol. 35, pp.119-133.

**Swain, P. H. and Davis, S. M.**, 1978. *Remote Sensing: The Quantitative Approach*, Mcgraw-Hill, New York.

**Synge, F. M.**, 1980. A morphometric comparison of raised shorelines in Fennoscandia, Scotland and Ireland. *Geologiska Föreningens i Stockholm Förhandlingar*, 102, pp. 235-249.

**Synge, F. M.**, 1982. A new shoreline chronology for the Salpausselkäs, *Annales Academiae Scientiarum Fennicae*, Ser. A. III. Vol.134, pp.29-60.

**Thomsen, H.**, 1981. Late Weichselian shore-level displacement on Nord-Jæren, south-west Norway. *Geologiska Föreningens i Stockholm Förhandlingar*, Vol.103, pp. 447-468.

**Tooley, M. J.**, 1978. *Sea-level changes: North-west England during the Flandrian stage*. Oxford: Clarendon Press. 215 p.

**Tynni, R.**, 1982. The reflection of geological evolution in Tertiary and interglacial diatoms and silico-flagelletes in Finnish Lapland. *Geological Survey of Finland. Bulletin* 320, 40 p.

**Walcott, R.I.**, 1972. Past sea levels, Eustasy and Deformation of the Earth. *Quaternary Research* 2, pp.1-14.

**Walder, J. S.**, 1986. Hydraulics of subglacial cavities. *Journal of Glaciology*, 32, pp. 439-445.

**Walder, J. S. and Fowler, A. C.,** 1994. Channelized subglacial drainage over a deformable bed. *Journal of Glaciology*, 40, pp. 3-15.

**Whillans, I. M., Bolzan, J. and Shabtaie, S.,** 1987. Velocity of ice streams B and C, Antarctica, *Journal of Geophysical Research* 92, pp. 8895-8902

**Winn, K., Averdieck, F.-R., Erlenkeuser, H. & Werner, F.,** 1986. Holocene sea level rise in the western Baltic and the question of isostatic subsidence. *Meyniana*, Vol.38, pp.61-80.

**Ziegler, P.,** 1990. Geological Atlas of Western and Central Europe. Verwey BV, Mijdrecht (NL) 235 p.